Time-Dependent Density Functional Theory for Open Quantum Systems and Quantum Computation

Dissertation advisor

Alán Aspuru-Guzik

Author

David Gabriel Tempel

Time-Dependent Density Functional Theory for Open Quantum Systems and Quantum Computation

Abstract

First-principles electronic structure theory explains properties of atoms, molecules and solids from underlying physical principles without input from empirical parameters. Time-dependent density functional theory (TDDFT) has emerged as arguably the most widely used first-principles method for describing the time-dependent quantum mechanics of many-electron systems. In this thesis, we will show how the fundamental principles of TDDFT can be extended and applied in two novel directions: The theory of open quantum systems (OQS) and quantum computation (QC).

In the first part of this thesis, we prove theorems that establish the foundations of TDDFT for open quantum systems (OQS-TDDFT). OQS-TDDFT allows for a first-principles description of non-equilibrium systems, in which the electronic degrees of freedom undergo relaxation and decoherence due to coupling with a thermal environment, such as a vibrational or photon bath. We then discuss properties of functionals in OQS-TDDFT and investigate how these differ from functionals in conventional TDDFT using an exactly solvable model system. Next, we formulate OQS-TDDFT in the linear-response regime, which gives access to environmentally broadened excitation spectra. Lastly, we present a hybrid approach in which TDDFT can be used

to construct master equations from first-principles for describing energy transfer in condensed phase systems.

In the second part of this thesis, we prove that the theorems of TDDFT can be extended to a class of qubit Hamiltonians that are universal for quantum computation. TDDFT applied to universal Hamiltonians implies that single-qubit expectation values can be used as the basic variables in quantum computation and information theory, rather than wavefunctions. This offers the possibility of simplifying computations by using the principles of TDDFT similar to how it is applied in electronic structure theory. Lastly, we discuss a related result; the computational complexity of TDDFT.

Contents

Citations to previously published work

"Time-dependent density functional theory for open quantum systems with unitary propagation," Joel Yuen-Zhou, David G. Tempel, Cesar Rodríguez-Rosario and Alán Aspuru-Guzik, *Phys. Rev. Lett.* **104**, 043001 (2010). Preprint: arXiv:0902.4504

"Time-dependent density functional theory of open quantum systems in the linear-response regime," David G. Tempel, Mark A. Watson, Roberto Olivares-Amaya and Alán Aspuru-Guzik, *J. Chem. Phys.* **134**, 074116 (2011). Preprint: arXiv:1004.0189

"Relaxation and dephasing in open quantum systems time-dependent density functional theory: Properties of exact functionals from an exactly-solvable model system," David G. Tempel and Alán Aspuru-Guzik, *Chem. Phys.* **391**, 130 (2011). Preprint: arXiv:1101.0141

"Open quantum systems: Density matrix formalism and applications," David G. Tempel, Joel Yuen-Zhou and Alán Aspuru-Guzik, In *Fundamentals of Time-Dependent Density Functional Theory*, edited by Miguel A.L. Marques, Neepa T. Maitra, Fernando M.S. Nogueira, E.K.U. Gross, and Angel Rubio, **837**, 211229. Berlin, Heidelberg: Springer Berlin Heidelberg, (2012)

"Quantum computing without wavefunctions: Time-dependent density functional theory for universal quantum computation," David G. Tempel and Alán Aspuru-Guzik, *Sci. Rep.* **2**, 391 (2012). Preprint: arXiv:1108.0097.

"Exciton coherence lifetimes from electronic structure," John Parkhill, David G. Tempel and Alán Aspuru-Guzik, *J. Chem. Phys.* **136**, 104510 (2012). Preprint: arXiv:1112.1665

"Introduction to quantum algorithms for physics and chemistry," Man-Hong Yung, James D. Whitfield, Sergio Boixo, David G. Tempel and Alán Aspuru-Guzik, *Adv. Phys. Chem.* (2012). In Press. Preprint: arXiv:1203.133

Acknowledgments

I have been very lucky to have had Alán Aspuru-Guzik as an advisor, mentor and also a friend. Alán gave me the perfect mixture of guidance and support when I needed it, but also freedom to tap into my own interests and creativity. His enthusiasm and excitement for our work kept me motivated and going strong throughout the Ph.D. The work in this thesis is the culmination of many inspiring discussions and blackboards filled with diagrams and equations in Alán's office. Perhaps most importantly, Alán always kept an open ear and I knew I could count on his support and guidance, whether it be about science or simply life in general.

I have also had the pleasure of having many discussions and collaborations with other members of the Aspuru-Guzik group, which have contributed greatly to the work presented in this thesis. In particular, I would like to thank John Parkhill, Joel Yuen-Zhou, James Whitfield, Man-Hong Yung and Sergio Boixo for their collaboration.

I owe special gratitude to Neepa Maitra, whose mentorship and friendship gave me my start and inspired me to pursue a Ph.D. in theoretical physics in the first place. Neepa patiently taught me basic quantum mechanics, while at the same time introducing me to scientific research and teaching me what it meant to be a scientist at a very early stage in my career. I would also like to thank Rick Heller, who's brilliant intuition and unique way of approaching problems in physics has taught me to think critically and Adam Cohen, who has been an inspirational figure throughout my Ph.D.

I thank my family, without whom my success up to this point would not have been possible. I thank my mother for always listening to me and her encouragement throughout, which kept me going strong. Also, for her helpful advice many times as she herself completed a Ph.D. and understands what it entails. My father instilled in me a thirst for knowledge and a desire to try to "know everything", although I now know that "everything" is uncountably infinite. I still remember our long walks together when I was a kid, in which our discussions taught me so much. I thank my love, Anna, for bringing happiness into my life, and with it productivity; I could not have completed this thesis without her support and advice. Lastly, I dedicate this thesis to my grandmother Lillian, whose love and strong belief in education were instrumental in shaping my outlook. Many of my early scientific memories are of reading her chemistry textbooks and playing with the chemistry set she bought me at her bungalow in Far Rockaway. I know that it would have made her very proud to see me complete my Ph.D.

Chapter 1

Introduction

Time-dependent density functional theory (TDDFT) has enjoyed an exponentially growing number of applications in chemistry, materials science and solid-state physics, as evidenced by the number of TDDFT-related publications in recent years (see Figure 1.1). Often, TDDFT is simply viewed as an efficient computational method for calculating dynamic properties of many-electron systems evolving under the time-dependent Schrödinger equation (TDSE). However, at the most basic level, TDDFT is not simply another computational method, but rather is a formally exact reformulation of time-dependent quantum mechanics, which uses single-particle probability densities as the basic variables rather than wavefunctions [201, 247]. When viewed in this context, there is no reason that the application of TDDFT needs to be restricted to many-electron systems evolving under the TDSE and one can ask the following question: Are there other systems described by time-dependent quantum mechanics, where the basic principles of TDDFT can be applied? In this thesis, we will explore this question in great detail and show that for two particular classes of systems, the

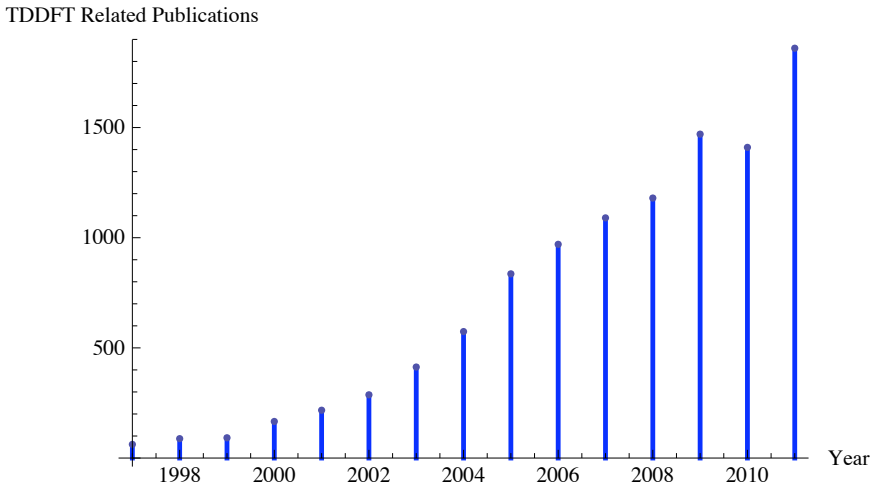

Figure 1.1: The number of TDDFT-related publications from 1997 through 2011, displaying an exponential growth curve.

answer is in fact yes.

In the first part of the thesis, we will show that the principles of TDDFT can be extended to many-electron systems, which are no longer described by the TDSE, but whose evolution is instead governed by a master equation at finite temperature. This is a very relevant problem for describing dynamics in condensed phase chemistry and solid-state physics, since the electronic degrees of freedom are not isolated, but must interact with nuclei and externally applied electromagnetic fields. For instance, in considering single-molecule transport between metallic leads, it is often important to take into account dissipation due to coupling of electronic degrees of freedom to phonons in the leads [38, 69, 70]. In linear and non-linear electronic spectroscopy of molecules, absorption spectra are broadened and shifted due to coupling to molecular vibrations as well as solvent molecules in the sample [162, 161, 2]. Additionally, one must also take into account spontaneous and stimulated emission of electronic

excitations due to coupling with the electromagnetic field [4, 6, 162, 48]. This coupling is often particularly relevant in strong-field experiments, where laser fields can no longer be considered as weak perturbations and may induce relaxation and dephasing of electronic degrees of freedom [157].

In these situations, in principle it is possible to use conventional TDDFT by propagating the coupled electron-nuclear dynamics using semi-classical methods [213], surface hopping techniques [50] or a multicomponent TDDFT scheme [41], or by treating the coupled electron-photon field using quantum electrodynamics [48]. However, often this is not computationally feasible or conceptually useful and it is convenient to treat the nuclei and/or electromagnetic field as an external environment. By using the theory of open quantum systems (OQS), we can avoid explicitly treating the environmental degrees of freedom, by taking them into account via an effective dynamics of the electrons alone. This is done by associating a finite temperature and entropy with the electronic degrees of freedom and then propagating the non-equilibrium dynamics according to a master equation [156, 170]. As the electronic system evolves in the presence of its environment, it undergoes relaxation and decoherence, which are approximately taken into account using system-bath models of varying degrees of sophistication. Even with simple system-bath models, the reduced dynamics of a many-electron system in the presence of an environment is computationally intractable. By treating the electronic degrees of freedom using TDDFT (OQS-TDDFT), one arrives at a computationally useful scheme for describing many-electron open quantum systems.

In the second part of the thesis, we will show how TDDFT can be used to describe

the time-dependent quantum mechanics of entangled 2-level systems (qubits), which naturally leads us to a discussion of the connections between TDDFT and quantum computation and information theory. Here, we will stray far from the traditional view of TDDFT as a computational method for obtaining the dynamics of many-electron systems in quantum chemistry and solid-state physics. Rather, we will view TDDFT as an exact reformulation of time-dependent quantum mechanics, which enables quantum simulation to be performed using single-qubit probabilities as the basic variables in quantum computation and information theory, rather than wavefunctions. When seen in this context, approximate TDDFT calculations can be viewed as a means of efficiently simulating quantum systems on classical computers.

In Chapter 9, we will prove that the theorems of TDDFT hold for a class of Hamiltonians that are "universal" for quantum computation. This in turn means that in principle, TDDFT can be used to efficiently simulate any system that can be simulated on a quantum computer. This concept leads naturally into Chapter 10, where we discuss the computational complexity of TDDFT. Interestingly, we will conjecture that TDDFT is in a simpler complexity class than ground state DFT. Although this might appear counterintuitive, it is a sensible result since time evolution can be performed efficiently on quantum computers, while finding ground states of arbitrary Hamiltonians cannot be done efficiently.

Although the two parts of this thesis might appear disjoint at a first glance, they are actually intimately related. In a first approximation, quantum computation and information theory is applied to isolated systems undergoing unitary dynamics. However, any realistic quantum computing device necessarily interacts with its en-

vironment and undergoes relaxation and decoherence. In fact, the main obstacle to constructing large-scale quantum computers is that the decoherence induced by the surrounding environment will quickly cause them to become classical computing devices. As a result, much of the theory of open quantum systems is concerned with problems in quantum computation and information theory. In this thesis, we apply the principles of TDDFT separately to open electronic systems and closed systems of qubits in parts 1 and 2 respectively. A natural unification of these two parts would apply OQS-TDDFT to systems of entangled qubits, which could be used to address problems of decoherence in quantum computation and information theory. In fact, a recent publication took a first step in this direction [56] and hopefully the concepts introduced in this thesis will be continued further by other researchers as well.

Part I: Time-dependent density functional theory for open quantum systems

The first step in extending TDDFT to OQS is to prove that the relevant theorems of TDDFT can be extended to electronic systems described by master equations. In Chapter 4, we prove the relevant theorems carefully and discuss their implications. Naturally, the density functionals in OQS-TDDFT will be very different than in conventional TDDFT. We explore properties of OQS-TDDFT functionals in Chapter 5, by studying a simple model system. We then focus on applications of TDDFT for OQS. In Chapter 6, we extend the formalism of TDDFT linear response theory to OQS to obtain environmentally broadened linear absorption spectra. In Chapter

7, we explore how TDDFT can be used to construct master equations for describing coherent energy transport in excitonic systems. Below, we provide a more detailed outline of the chapters in Part 1 of the thesis.

Chapters 2 and 3

Chapters 2 and 3 are background chapters which introduce the reader to time-dependent density functional theory and the theory of open quantum systems respectively. They are by no means intended to exhaustively review these fields, but provide the reader with the tools needed to understand the research presented in this thesis and make it self contained.

In Chapter 2, we review the fundamental theorems of conventional TDDFT, which will later be extended to OQS-TDDFT in Chapter 4. We then discuss the linear response formulation of TDDFT which is later applied to OQS-TDDFT in Chapter 6 and conclude with a discussion of commonly used functional approximations.

In Chapter 3, we review OQS within the master equation approach, with the emphasis on the microscopic derivation of master equations starting from first-principles. Such a formulation of master equations without empirical parameters is particularly amenable to a first-principles electronic structure theory such as TDDFT. We present the Born-Markov approximation as well as the Lindblad and Redfield master equations, which will be used in later chapters. We do not discuss specific non-Markovian master equations, which although very important, are not used in this thesis. Parts of Chapter 3 were published in [227].

Chapter 4

In Chapter 4, concepts from Chapters 2 and 3 are unified and the foundations of OQS-TDDFT are established. Large portions of Chapter 4 were published in ref. [227] with minor modifications. We begin the chapter by proving the van Leeuwen construction for OQS-TDDFT, which establishes it as a formally exact theory. We then discuss two different computational schemes that can be used in OQS-TDDFT and discuss their usefulness. We also prove the counterintuitive fact that the density evolution of an open quantum system can be reproduced with a closed auxiliary system. Lastly, we discuss the "double adiabatic connection", which allows for a generalization of perturbation theory techniques used in conventional TDDFT.

Chapter 5

Chapter 5 investigates exact properties of functionals in OQS-TDDFT, specifically for the computational scheme in which the density evolution of an open system is reproduced with a closed auxiliary system. We construct the exact functional for an exactly solvable model system: one-electron in a harmonic potential evolving under the Lindblad master equation. By focusing on this simple system, we are able to deduce exact conditions that approximate functionals for many-electron systems should satisfy. We examine the functional for two representative limits of the Lindblad equation: Pure dephasing and relaxation with no pure dephasing. We find a number of parallels between the exact OQS-TDDFT functional and existing approximate functionals in time-dependent current density functional theory (TDCDFT). We also

compare our exact solution with an approximate "Markovian bath functional" we proposed in ref. [278]. With minor modifications, Chapter 5 was published in ref. [224].

Chapter 6

Chapter 6 presents the linear response formulation of OQS-TDDFT, which allows for a first-principles description of environmentally broadened absorption spectra. This is in contrast to conventional linear response TDDFT, in which spectra are always calculated without broadening. With minor modifications, Chapter 6 was published in [226].

The chapter begins with a general formulation of OQS-TDDFT linear response theory, which is applicable to any electronic system interacting with an arbitrary and even non-Markovian environment. We then focus specifically on the Redfield master equation and formulate a computationally useful "Kohn-Sham-Redfield" master equation for many-electron non-equilibrium systems. This is followed by a derivation of matrix equations (Casida-like equations) which can readily be implemented in quantum chemical packages and whose solutions yield environmentally broadened absorption spectra. We then solve these equations numerically to obtain the absorption spectrum of a C^{2+} atom interacting with the vacuum modes of the electromagnetic field, which are collectively treated as an environment in our formalism. We solve these equations using a variety of approximations from conventional TDDFT and discuss the shortcomings of using these approximations in OQS-TDDFT. Finally, we derive an approximate frequency-dependent correction to the adiabatic approximation which fixes some of these shortcomings and we then discuss future challenges.

Chapter 7

Chapter 7 presents a study of the coherence lifetimes of three excitonic dimers, using TDDFT to calculate the vibrational correlation functions as input to a Redfield-type master equation. Although we do not directly use the rigorous theory of OQS-TDDFT presented in previous chapters, the approach used in Chapter 7 is closely related. We use TDDFT to construct the parameters of the dissipative superoperator in the master equation and then treat the Kohn-Sham reduced 1-particle density matrix (1-RDM) as an approximation to the true 1-RDM. Solvent effects are taken into account by using localized diabatic Kohn-Sham orbitals that minimize the system-bath coupling, rather than than the usual adiabatic states. We find qualitative agreement with experiment, however as we discuss in detail, quantitative agreement requires a more rigorous treatment of the system-bath coupling. Large portions of Chapter 7 were published in [173]

Part II: Time-dependent density functional theory for quantum computation

In Part 2 of this thesis, we apply the principles of TDDFT to quantum computation and information theory. Our central result is to prove in Chapter 9 that the fundamental theorems of TDDFT hold for a certain class of spin Hamiltonians that are universal for quantum computation. Traditionally, in quantum computation and information theory, the wavefunction has played a central role. The theorems we

prove establish that the spin density of a universal Hamiltonian can actually be considered as the basic variable, rather than the wavefunction. We also outline a proof that TDDFT is in the complexity class "BQP" (bounded-error quantum polynomial), which is actually a simpler complexity class than "QMA" (quantum Merlin-Arthur) in which ground state DFT lies. Below, we provide a more detailed outline of the chapters in Part 2 of the thesis.

Chapter 8

Chapter 8 serves as a brief overview of topics in quantum computation and information theory that will be relevant in later chapters. We begin by introducing the circuit model of quantum computation and discuss the concept of a set of universal single-qubit and two-qubit quantum gates. We then introduce a particular class of universal spin Hamiltonians that we will apply TDDFT to in Chapter 9. Finally, we discuss two measures of entanglement: The von Neumann entropy and the concurrence.

Chapter 9

In Chapter 9, we prove the two fundamental theorems of TDDFT (the Runge-Gross (RG) and van Leeuwen (VL) theorems) for the universal spin Hamiltonians presented in Chapter 8. We begin with an overview of the main results and implications of TDDFT applied to these universal Hamiltonians. Generally speaking, the theorems we prove demonstrate that quantum computations can in principle be

performed using single-qubit expectation values (densities) rather than wavefunctions. We then provide a detailed proof of the theorems, followed by a discussion how to construct entanglement as a density functional. Finally, we present a numerical demonstration of the qubit VL theorem for a system of three qubits. With very minor modifications, Chapter 9 was published in ref. [223].

Chapter10

In Chapter 10, we outline a proof that TDDFT is in the quantum computational complexity class "BQP" (bounded-error quantum polynomial). We begin with a general overview of quantum complexity theory and its connections to methods in computational physics and chemistry. We next precisely define the problem of "finding the complexity of TDDFT" and we outline an algorithm to be performed on a quantum computer which solves this problem. We then proceed to bound the errors in the algorithm and show that these errors increase only polynomially in the number of computational resources required, thus completing the proof. We also provide a conclusion and conjecture that TDDFT is not only in BQP, but it is also "BQP Complete." [1]

[1] "Completeness" means that a computational problem is not only within the given complexity class, but it is at least as difficult to solve as any other problem in the complexity class.

Part I

Time-dependent density functional theory for open quantum systems

Chapter 2

Time-dependent density functional theory

2.1 Introduction

TDDFT is a formally exact method for treating time-dependent many-electron quantum mechanics, which has become widely used in quantum chemistry and solid-state physics due to it's practical balance between computational accuracy and efficiency [201, 153, 190, 38]. The time-dependent many-electron problem encompasses diverse physical phenomena, ranging from optical response properties of atoms, molecules and solids, to strong-field ionization physics and quantum optimal control theory. In all of these applications, a full solution of the correlated time-dependent many-electron Schrödinger equation is computationally intractable for more than a few electrons and one must resort to approximate methods.

TDDFT has become a popular method, particularly in quantum chemistry and electronic structure theory for several reasons. Firstly, it is a formally exact theory based on rigorous mathematical theorems [201, 247]. This feature of TDDFT allows

one to develop better approximate functionals by studying simple model problems in which exact solutions are known, with the hope of incorporating more exact conditions into the approximations [92, 144, 91, 238]. Ground state DFT, which is a much more mature theory than TDDFT, has enjoyed tremendous success due to exact conditions obtained from the uniform electron gas paradigm using quantum monte carlo methods [45]. Such a universal exactly-solvable model system does not yet exist for TDDFT and understanding properties of exact TDDFT functionals is a very active area of research [92, 37]. In this thesis, we will discuss a variety of exact conditions obtained from exactly solvable model systems in the context of TDDFT for open quantum systems (OQS-TDDFT) [278, 277, 226, 224] and TDDFT for qubit systems in quantum computation theory (QC-TDDFT) [223]. Secondly, practical applications of TDDFT utilize a non-interacting reference system of electrons, known as the "Kohn-Sham" system [115], whose effective single-particle orbital equations can be solved with a modest computational scaling (typically $\sim N^2$ or N^3, with N denoting the system size [113]). Very simple approximate functionals can often be used, such as those derived from the adiabatic approximation (discussed below), which allows TDDFT to be readily implemented in quantum chemistry and electronic structure programs and applied to relatively large systems [234, 43].

In this chapter, we will provide a brief overview of the fundamentals of TDDFT in it's original formulation, as applied to many-electron systems evolving unitarily according to the time-dependent Scrödinger equation. In section 2.2, we discuss the Runge-Gross and van Leeuwen theorems which establish TDDFT as a formally exact theory, as well as the Kohn-Sham equations which are used in virtually all practical

applications. In section 2.3 we discuss the linear response formulation of TDDFT (LR-TDDFT) which is used for calculating electronic absorption spectra. We also discuss the matrix formulation of LR-TDDFT which is widely implemented in quantum chemical computer codes. Finally, in section 2.4 we discuss approximate density functionals used in practical applications of TDDFT. We will discuss the simple and ubiquitous adiabatic approximation to TDDFT (ATDDFT) as well as functionals which go beyond ATDDFT. Atomic units are used throughout this chapter.

2.2 Fundamentals of TDDFT

In this section, we discuss the fundamental theorems of TDDFT which establish it as a formally exact method as well as the time-dependent Kohn-Sham equations which are used in virtually all implementations of TDDFT. Unless otherwise stated, we will consider a system of N electrons described within the Born-Oppenheimer approximation by the Hamiltonian,

$$\hat{H}(t) = -\frac{1}{2}\sum_{i=1}^{N}\nabla_i^2 + \sum_{i<j}^{N}\frac{1}{|\mathbf{r_i}-\mathbf{r_j}|} + \sum_i v_{ext}(\mathbf{r_i},t). \tag{2.1}$$

In Eq. 2.1, $-\frac{1}{2}\nabla_i^2$ is the kinetic energy operator for the ith electron, $\frac{1}{|\mathbf{r_i}-\mathbf{r_j}|}$ is the pairwise coulomb repulsion between the ith and jth electrons, while $v_{ext}(\mathbf{r_i},t)$ is a potential external to the electrons. For atomic, molecular and solid-state systems, $v_{ext}(\mathbf{r_i},t)$ will consist of the attractive coulomb field due to the nuclei, as well as any externally applied time-dependent fields, such as a laser field.

All properties of the many-electron system described by the Hamiltonian in Eq. 2.1 can in principle be obtained from the correlated many-electron wavefunction $\psi(\mathbf{r_1},\mathbf{r_2},...\mathbf{r_N};t)$,

which is a solution to the time-dependent Schrödinger equation,

$$\imath\frac{\partial}{\partial t}\psi(\mathbf{r_1},\mathbf{r_2},...\mathbf{r_N};t)=\hat{H}(t)\psi(\mathbf{r_1},\mathbf{r_2},...\mathbf{r_N};t). \tag{2.2}$$

However, in practice, an exact solution to Eq. 2.2 is intractable for two main reasons. Firstly, the two-body coulomb repulsion $\frac{1}{|\mathbf{r_i}-\mathbf{r_j}|}$ causes Eq. 2.2 to be an *unseparable* partial differential equation, which requires an amount of computer time to solve that scales exponentially with the number of electrons in the system. Secondly, even if one could somehow obtain the many-body wavefunction $\psi(\mathbf{r_1},\mathbf{r_2},...\mathbf{r_N};t)$, it would contain far more information than one could possibly need and also would require an exponential amount of computer memory to store. For instance, a 10-electron wavefunction on a modest $10\times10\times10$ real-space grid would require a computer to store $(10\times10\times10)^{10}=10^{30}$ numbers! In electronic structure theory, one is typically interested in calculating observables that depend on one or two electron coordinates and therefore it makes sense to focus on reduced variables rather than the full wavefunction. In TDDFT, the reduced variable of interest is the time-dependent density,

$$n(\mathbf{r},t)=N\int d^3r_2...d^3r_N|\psi(\mathbf{r},\mathbf{r_2},...\mathbf{r_N};t)|^2, \tag{2.3}$$

which is obtained by squaring the wavefunction, integrating over all but one coordinate and normalizing to the number of electrons in the system. The density is a much simpler variable than the wavefunction, since it simply describes the normalized probability of finding any electron at position $\mathbf{r}$ and time t, rather than the conditional probability of finding all N electrons simultaneously at positions $\mathbf{r_1},\mathbf{r_2},...\mathbf{r_N}$ at time t. At first glance, it might appear that we have lost a great deal of information in

replacing the wavefunction with the density as the basic variable, since N-1 electron coordinates have been integrated over. However, the Runge-Gross theorem which we now discuss, establishes the remarkable fact that the density in principle contains the same information as the many-body wavefunction and therefore observables can be directly calculated from the density without requiring access to the wavefunction.

The Runge-Gross theorem

The Runge-Gross (RG) theorem [201, 83] can be stated follows: *The densities* $n(\mathbf{r},t)$ *and* $n'(\mathbf{r},t)$ *evolving from a common initial state* $\psi_0 \equiv \psi(\mathbf{r_1},\mathbf{r_2},...\mathbf{r_N};t_0)$ *evolving under the influence of two different potentials* $v_{ext}(\mathbf{r},t)$ *and* $v'_{ext}(\mathbf{r},t)$ *(both Taylor expandable around the initial time* t_0*) are always different provided that the potentials differ by more than a purely time-dependent (*$\mathbf{r}$*-independent) function. i.e.*

$$v_{ext}(\mathbf{r},t) \neq v'_{ext}(\mathbf{r},t) + c(t). \tag{2.4}$$

The purely time-dependent function $c(t)$ corresponds to a trivial global phase in the wavefunction that does not affect the expectation values of any observables. Thus, for a given initial state ψ_0 the RG theorem establishes a one-to-one mapping between the time-dependent density and the external potential acting on the system:

$$\psi_0 : n(\mathbf{r},t) \leftrightarrow v_{ext}(\mathbf{r},t). \tag{2.5}$$

However, $v_{ext}(\mathbf{r},t)$ is the only part of the Hamiltonian in Eq. 2.1 that is non-universal. i.e. $-\frac{1}{2}\sum_{i=1}^{N}\nabla_i^2 + \sum_{i<j}^{N}\frac{1}{|\mathbf{r_i}-\mathbf{r_j}|}$ is the *same* operator for each electronic system, while $v_{ext}(\mathbf{r},t)$ is different, depending on the configuration of the nuclei or the type of laser

field applied etc. This means that $v_{ext}(\mathbf{r}, t)$ determines the Hamiltonian in Eq. 2.1, and since the solution to Eq. 2.2 is unique, we have a one-to-one mapping between the external potential and the many-body wavefunction:

$$\psi_0 : v_{ext}(\mathbf{r}, t) \leftrightarrow \psi(\mathbf{r_1}, \mathbf{r_2}, ...\mathbf{r_N}; t). \tag{2.6}$$

By combining the maps in Eq 2.5 and Eq. 2.6, we see that there is in fact a one-to-one mapping between the density and the many-body wavefunction for a given initial state:

$$\psi_0 : n(\mathbf{r}, t) \leftrightarrow \psi(\mathbf{r_1}, \mathbf{r_2}, ...\mathbf{r_N}; t). \tag{2.7}$$

Eq. 2.7 forms the basis of TDDFT as an exact theory, since it implies that the time-dependent density uniquely determines the wavefunction and therefore in principle, the density contains the same information about the system as the full many-body wavefunction. Furthermore, Eq. 2.7 implies that the wavefunction is a unique functional of the density,

$$\psi(\mathbf{r_1}, \mathbf{r_2}, ...\mathbf{r_N}; t) \equiv \psi[n](\mathbf{r_1}, \mathbf{r_2}, ...\mathbf{r_N}; t), \tag{2.8}$$

and therefore any observable of the system is a unique functional of the density. i.e. the expectation value of an arbitrary Hermitian operator $\hat{A}$ is a functional of the density simply because the wavefunction is (in principle observables are also functionals of the initial state ψ_0, since this is needed as an initial condition in Eq. 2.2, but we suppress this dependence for notational simplicity):

$$\langle \hat{A} \rangle [n] = \langle \psi[n] | \hat{A} | \psi[n] \rangle. \tag{2.9}$$

This establishes that the density is a well chosen variable, and one can extract information about observables *directly* from the density without the wavefunction, provided one knows how to approximate the unknown functional $\langle \hat{A} \rangle[n]$ for a given observable A. Sometimes this is straightforward, however often it is not, especially for momentum-dependent observables [188] or observables depending on two-electron coordinates such as the pair correlation function [246].

The proof of the RG theorem begins by using the condition that the potentials v_{ext} and v'_{ext} can be expanded in a Taylor series around the initial time t_0:

$$v_{ext}(\mathbf{r}, t) = \sum_{k=0}^{\infty} \frac{1}{k!} v_{ext,k}(\mathbf{r})(t - t_0)^k \tag{2.10}$$

$$v'_{ext}(\mathbf{r}, t) = \sum_{k=0}^{\infty} \frac{1}{k!} v'_{ext,k}(\mathbf{r})(t - t_0)^k. \tag{2.11}$$

The restriction of the RG theorem to Taylor expandable potentials is somewhat restrictive, as it excludes several important situations such as potentials that are adiabatically switched on from $t = -\infty$. Attempts to extend the RG theorem beyond Taylor expandable potentials have been made in recent years [146, 248, 168]. Eq. 9.15 is equivalent to the statement that for the expansion coefficients $v_{ext,k}(\mathbf{r})$ and $v'_{ext,k}(\mathbf{r})$ there exists a smallest integer $k \geq 0$ such that

$$v_{ext,k}(\mathbf{r}) - v'_{ext,k}(\mathbf{r}) = \frac{\partial^k}{\partial t^k}(v_{ext}(\mathbf{r}, t) - v'_{ext}(\mathbf{r}, t))|_{t=t_0} \neq constant. \tag{2.12}$$

From this assumption, we will first prove that the paramagnetic current densities

$$\mathbf{j}(\mathbf{r}, t) = \langle \psi(t) | \hat{\mathbf{j}}_{\mathbf{p}}(\mathbf{r}) | \psi(t) \rangle \tag{2.13}$$

and

$$\mathbf{j}'(\mathbf{r}, t) = \langle \psi'(t) | \hat{\mathbf{j}}_{\mathbf{p}}(\mathbf{r}) | \psi'(t) \rangle \tag{2.14}$$

are different for the different potentials v_{ext} and v'_{ext}. Here,

$$\hat{\mathbf{j}}_{\mathbf{p}}(\mathbf{r}) = \frac{1}{2\imath}\sum_{j=1}^{N}(\nabla_j \delta(\mathbf{r}-\mathbf{r_j}) - \delta(\mathbf{r}-\mathbf{r_j})\nabla_j) \tag{2.15}$$

is the paramagnetic current density operator. In the next step, we will show that the densities $n(\mathbf{r},t)$ and $n'(\mathbf{r},t)$ will be different as well.

The equations of motion for the primed and unprimed current densities are

$$\frac{\partial}{\partial t}\mathbf{j}(\mathbf{r},t) = -\imath\langle\psi(t)|[\hat{\mathbf{j}}_{\mathbf{p}}(\mathbf{r}), \hat{H}(t)]|\psi(t)\rangle \tag{2.16}$$

and

$$\frac{\partial}{\partial t}\mathbf{j}'(\mathbf{r},t) = -\imath\langle\psi'(t)|[\hat{\mathbf{j}}_{\mathbf{p}}(\mathbf{r}), \hat{H}'(t)]|\psi'(t)\rangle, \tag{2.17}$$

where $\hat{H}$ and $\hat{H}'$ are Hamiltonians of the form in Eq. 2.1 with external potentials v_{ext} and v'_{ext} respectively. Since ψ and ψ' evolve from the same initial state. i.e.

$$\psi(t_0) = \psi'(t_0) = \psi_0, \tag{2.18}$$

we have

$$\frac{\partial}{\partial t}(\mathbf{j}(\mathbf{r},t)-\mathbf{j}'(\mathbf{r},t))|_{t=t_0} = -\imath\langle\psi_0|[\hat{\mathbf{j}}_{\mathbf{p}}(\mathbf{r}), \hat{H}(t_0)-\hat{H}'(t_0)]|\psi_0\rangle = -n_0(\mathbf{r})\nabla(v_{ext}(\mathbf{r},t_0)-v'_{ext}(\mathbf{r},t_0)), \tag{2.19}$$

where we have defined the initial density $n_0(\mathbf{r}) \equiv n(\mathbf{r},t_0)$. If the condition in Eq. 2.12 is satisfied for $k=0$, the right hand side of Eq 2.19 will be non-zero and the currents $\mathbf{j}$ and $\mathbf{j}'$ will be different infinitesimally later than t_0. If instead Eq. 2.12 is satisfied for some finite $k>0$, we differentiate Eq. 2.16 and Eq. 2.17 k times, take the difference and evaluate at $t=t_0$ to arrive at:

$$\frac{\partial^{k+1}}{\partial t^{k+1}}(\mathbf{j}(\mathbf{r},t)-\mathbf{j}'(\mathbf{r},t))|_{t=t_0} = -n_0(\mathbf{r})\nabla w_k(\mathbf{r}) \neq 0, \tag{2.20}$$

where

$$w_k(\mathbf{r}) = \frac{\partial^{k+1}}{\partial t^{k+1}}(v_{ext}(\mathbf{r}, t_0) - v'_{ext}(\mathbf{r}, t_0)). \tag{2.21}$$

Again, we find that the currents will eventually differ and so $\mathbf{j}(\mathbf{r}, t) \neq \mathbf{j}'(\mathbf{r}, t)$ if the external potentials differ. We now prove that the densities must also be different, by using the continuity equation,

$$\frac{\partial}{\partial t}(n(\mathbf{r}, t) - n'(\mathbf{r}, t)) = -\nabla \cdot (\mathbf{j}(\mathbf{r}, t) - \mathbf{j}'(\mathbf{r}, t)). \tag{2.22}$$

Differentiating Eq. 2.22 k times and using Eq. 2.20, we find that the densities satisfy:

$$\frac{\partial^{k+2}}{\partial t^{k+2}}(n(\mathbf{r}, t) - n'(\mathbf{r}, t)) = \nabla \cdot (n_0(\mathbf{r})\nabla w_k(\mathbf{r})). \tag{2.23}$$

In order to prove that the densities $n(\mathbf{r}, t)$ and $n'(\mathbf{r}, t)$ must become different, we must show that $\nabla \cdot (n_0(\mathbf{r})\nabla w_k(\mathbf{r})) \neq 0$. This is proven by contradiction: Assume

$$\nabla \cdot (n_0(\mathbf{r})\nabla w_k(\mathbf{r})) = 0, \tag{2.24}$$

and evaluate the integral

$$\int d^3r n_0(\mathbf{r})(\nabla w_k(\mathbf{r}))^2 = -\int d^3r w_k(\mathbf{r})\nabla \cdot (n_0(\mathbf{r})\nabla w_k(\mathbf{r})) + \oint d\mathbf{S} \cdot (n_0(\mathbf{r})w_k(\mathbf{r})\nabla w_k(\mathbf{r})), \tag{2.25}$$

which follows from Green's vector identity. The first term on the right hand side of Eq. 2.25 vanishes by assumption. For physically realistic potentials which come from finite charge distributions, the surface integral vanishes as well since $w_k(\mathbf{r})$ tends to zero at least as fast as $\frac{1}{r}$ [83]. Thus, we conclude that $\int d^3r n_0(\mathbf{r})(\nabla w_k(\mathbf{r}))^2 = 0$ and since the integrand is positive definite, we must also have that $n_0(\mathbf{r})(\nabla w_k(\mathbf{r}))^2 = 0$ or $w_k(\mathbf{r}) = \textit{constant}$, which contradicts our assumption that the Taylor coefficients

of the potentials differ by more than a constant. Therefore, we see that under the condition that the Taylor coefficients of the potentials differ at some order, Eq. 2.23 implies that the densities must differ as well. This completes the proof of the RG theorem: For a fixed initial state, no two external potentials can give rise to the same density.

The time-dependent Kohn-Sham equations

The RG theorem establishes that the density can be used in place of the wavefunction as the basic variable of interest, but the theorem doesn't give a prescription for obtaining the density other than solving Eq. 2.2, which as we discussed previously is intractable for many-electron systems. In order to obtain the density in a practical TDDFT scheme, one maps the interacting system of electrons onto a *non-interacting* system, which is described by an effective local potential $v_{ks}(\mathbf{r}, t)$ constructed to yield the same density as the true interacting system [83]. This non-interacting system is simply described by a set of single-particle orbital equations referred to as the time-dependent Kohn-Sham (KS) equations,

$$\imath\frac{\partial}{\partial t}\phi_i(\mathbf{r}, t) = \left[-\frac{1}{2}\nabla^2 + v_{ks}(\mathbf{r}, t)\right]\phi_i(\mathbf{r}, t), \tag{2.26}$$

which is the time-dependent analogue of the celebrated Kohn-Sham equations of ground state DFT [115]. Because the Kohn-Sham system is non-interacting, its wavefunction is simply a slater determinant of N occupied single-particle orbitals (we assume a fully spin-polarized system for notational simplicity) $\{\phi_1, \phi_2, ...\phi_N\}$ and

the density is obtained from the orbitals according to,

$$n(\mathbf{r},t) = \sum_{i=1}^{N} |\phi_i(\mathbf{r},t)|^2. \tag{2.27}$$

By solving the time-dependent KS equations, one is able to obtain the true density $n(\mathbf{r},t)$ of the interacting system without ever needing to calculate the many-body wavefunction ψ. Since the KS equations are single-particle equations, they can be solved on a computer with polynomial resources (typically $\sim N^2$ or N^3 scaling), thereby avoiding the exponential scaling of the full time-dependent many-body Schrödinger equation (Eq. 2.2).

Although the time-dependent KS equations can be solved efficiently on a computer, the exact KS potential $v_{ks}(\mathbf{r},t)$ is in general an unknown quantity and must be approximated in practical implementations of TDDFT. The RG theorem in the previous section was applied to a system of N interacting electrons in an external potential $v_{ext}(\mathbf{r},t)$, but it could have equally well been applied to a system of non-interacting electrons in the KS potential $v_{ks}(\mathbf{r},t)$. Thus, for a fixed initial KS slater determinant Φ_0, there is a one-to-one mapping between a given density $n(\mathbf{r},t)$ and the KS potential that yields that density. i.e.

$$\Phi_0 : n(\mathbf{r},t) \leftrightarrow v_{ks}(\mathbf{r},t). \tag{2.28}$$

This implies that like the external potential for the interacting system, the KS potential of the non-interacting system is a unique functional of the density and initial state. i.e.

$$v_{ks}(\mathbf{r},t) \equiv v_{ks}[n,\Phi_0](\mathbf{r},t). \tag{2.29}$$

Eq. 2.29 is crucial for TDDFT, since it implies that the KS potential can be approximated self-consistently as a functional of the time-dependent density and initial KS state. In the usual KS scheme used in virtually all implementations of TDDFT, the KS potential is partitioned according to

$$v_{ks}[n,\Phi_0](\mathbf{r},t) = v_{ext}[n,\psi_0](\mathbf{r},t) + v_h[n](\mathbf{r},t) + v_{xc}[n,\psi_0,\Phi_0](\mathbf{r},t). \tag{2.30}$$

Here, $v_{ext}[n,\psi_0](\mathbf{r},t)$ is the known external potential of the original interacting system and $v_h[n](\mathbf{r},t) = \int d^3r \frac{n(\mathbf{r}',t)}{|\mathbf{r}-\mathbf{r}'|}$ is the classical Hartree potential for the charge distribution $n(\mathbf{r},t)$. The remaining unknown term, $v_{xc}[n,\psi_0,\Phi_0](\mathbf{r},t)$ is the exchange-correlation potential which must be approximated reliably for TDDFT to be a practical tool for simulating electronic systems. The exchange-correlation potential of TDDFT is a much more complicated object than in ground state DFT, since not only does it depend on the entire history of the density, but it also depends on the initial states of both the interacting and KS systems [140, 142, 144]. Finding reliable approximations to v_{xc} in TDDFT is a very active area of research which we will discuss fully in section 2.4.

So far we have introduced the KS scheme of TDDFT, in which the density of an interacting system of N electrons is reproduced by a system of N noninteracting electrons moving in the potential v_{ks}. We have also shown that provided v_{ks} exists, by applying the RG theorem to the non-interacting system, v_{ks} is a unique functional of the density. However, we have not yet addressed the question of the existence of v_{ks}, i.e. given a density $n(\mathbf{r},t)$ from a many-body Hamiltonian of the form in Eq. 2.1, is it always possible to find a potential $v_{ks}[n,\Phi_0](\mathbf{r},t)$ which reproduces this density using

a non-interacting system? In the next section, we will introduce the Van Leeuwen (VL) construction [247] which proves that under certain conditions, the answer to this question is in general yes, which is obviously of crucial importance to TDDFT.

The Van-Leeuwen Construction

In order to introduce the VL construction, we write the Hamiltonian in Eq. 2.1 in the slightly more general form:

$$\hat{H}(t) = -\frac{1}{2}\sum_{i=1}^{N}\nabla_i^2 + \sum_{i<j}^{N} v_{ee}(\mathbf{r_i}, \mathbf{r_j}) + \sum_i v_{ext}(\mathbf{r_i}, t), \tag{2.31}$$

where $v_{ee}(\mathbf{r_i}, \mathbf{r_j})$ is an arbitrary (not necessarily coulomb) electron-electron interaction. The equation of motion for the density under this Hamiltonian is the continuity equation,

$$\frac{\partial}{\partial t} n(\mathbf{r}, t) = -\imath\langle\psi(t)|[\hat{n}(\mathbf{r}), \hat{H}(t)]|\psi(t)\rangle = \nabla\cdot\mathbf{j}(\mathbf{r}, t). \tag{2.32}$$

Here, $n(\mathbf{r}) = \sum_i \delta(\mathbf{r} - \hat{\mathbf{r}}_\mathbf{i})$ is the density operator whose expectation value yields the density $n(\mathbf{r}, t)$ and $|\psi(t)\rangle$ is the many-body wavefunction evolved under the Hamiltonian $\hat{H}(t)$ in Eq. 2.31 from a given initial state $|\psi(t_0)\rangle$. Now, we recall the equation of motion for the current density presented in Eq. 2.16:

$$\frac{\partial}{\partial t}\mathbf{j}(\mathbf{r}, t) = -\imath\langle\psi(t)|[\hat{\mathbf{j}}_\mathbf{p}(\mathbf{r}), \hat{H}(t)]|\psi(t)\rangle. \tag{2.33}$$

If we work out the commutator, we find that the αth cartesian component of the current density ($\alpha = x, y, z$) obeys:

$$\frac{\partial}{\partial t} j_\alpha(\mathbf{r}, t) = -n(\mathbf{r}, t)\frac{\partial}{\partial r_\alpha} v_{ext}(\mathbf{r}, t) + \mathcal{D}_\alpha(\mathbf{r}, t) + \mathcal{F}_\alpha(\mathbf{r}, t), \tag{2.34}$$

which is a local form of Newton's second law, relating the rate of change of the current density to various force densities acting on and within the electron liquid. The term $-n(\mathbf{r},t)\frac{\partial}{\partial r_\alpha}v_{ext}(\mathbf{r},t)$ is the force density due to the externally applied electric field acting on the system. The term

$$\mathcal{D}_\alpha(\mathbf{r},t) = -\frac{1}{4}\sum_{\beta=x,y,z}\frac{\partial}{\partial r_\beta}\langle\psi(t)|\sum_i\{\hat{v}_{i\beta},\{\hat{v}_{i\alpha},\delta(\mathbf{r}-\hat{\mathbf{r}}_\mathbf{i})\}\}|\psi(t)\rangle \tag{2.35}$$

is the divergence of the momentum-stress tensor, which describes internal forces in the electron liquid and we have introduced the velocity operator $\hat{v}_{i\alpha} \equiv -\imath\frac{\partial}{\partial r_\alpha}\delta(\mathbf{r}-\hat{\mathbf{r}}_\mathbf{i})$ in this expression. Finally, the term

$$\mathcal{F}_\alpha(\mathbf{r},t) = -\langle\psi(t)|\sum_i\delta(\mathbf{r}-\hat{\mathbf{r}}_\mathbf{i})\sum_{j\neq i}\frac{\partial}{\partial r_{i\alpha}}v_{ee}(\mathbf{r_i},\mathbf{r_j})|\psi(t)\rangle \tag{2.36}$$

describes the internal force density arising from the electron-electron interaction. We can use Eq. 2.22 to eliminate the current density in favor of the density $n(\mathbf{r},t)$, to arrive at an equation of motion for the second derivative of the density:

$$\frac{\partial^2}{\partial t^2}n(\mathbf{r},t) = \nabla\cdot[n(\mathbf{r},t)\nabla v_{ext}(\mathbf{r},t)] + q(\mathbf{r},t), \tag{2.37}$$

where we have defined $q(\mathbf{r},t) \equiv \sum_\alpha\frac{\partial}{\partial r_\alpha}[\mathcal{D}_\alpha(\mathbf{r},t)+\mathcal{F}_\alpha(\mathbf{r},t)]$. Eq. 2.37 is of crucial importance for the VL construction, because it directly relates the time-dependent density of a system to the external potential acting on that system.

Now, we consider an auxiliary "primed" system described by the hamiltonian,

$$\hat{H}'(t) = -\frac{1}{2}\sum_{i=1}^N\nabla_i^2 + \sum_{i<j}^N v'_{ee}(\mathbf{r_i},\mathbf{r_j}) + \sum_i v'_{ext}(\mathbf{r_i},t), \tag{2.38}$$

with a different electron-electron interaction v'_{ee} and a different external potential v'_{ext}. Let $|\psi'(t)\rangle$ be the wavefunction evolved from a given initial state $|\psi'(t_0)\rangle$ under

the Hamiltonian $\hat{H}'(t)$ in Eq. 2.38 and denote $n'(\mathbf{r},t)$ the corresponding density. By repeating the same steps as we did for the unprimed system, we find that the density of the auxiliary primed system obeys the equation of motion:

$$\frac{\partial^2}{\partial t^2}n'(\mathbf{r},t) = \nabla\cdot[n'(\mathbf{r},t)\nabla v'_{ext}(\mathbf{r},t)] + q'(\mathbf{r},t). \tag{2.39}$$

Here, $q'(\mathbf{r},t) \equiv \sum_\alpha \frac{\partial}{\partial r_\alpha}\left[\mathcal{D}'_\alpha(\mathbf{r},t) + \mathcal{F}'_\alpha(\mathbf{r},t)\right]$, where

$$\mathcal{D}'_\alpha(\mathbf{r},t) = -\frac{1}{4}\sum_{\beta=x,y,z}\frac{\partial}{\partial r_\beta}\langle\psi'(t)|\sum_i\{\hat{v}_{i\beta},\{\hat{v}_{i\alpha},\delta(\mathbf{r}-\hat{\mathbf{r}}_\mathbf{i})\}\}|\psi'(t)\rangle \tag{2.40}$$

and

$$\mathcal{F}'_\alpha(\mathbf{r},t) = -\langle\psi'(t)|\sum_i\delta(\mathbf{r}-\hat{\mathbf{r}}_\mathbf{i})\sum_{j\neq i}\frac{\partial}{\partial r_{i\alpha}}v'_{ee}(\mathbf{r}_\mathbf{i},\mathbf{r}_\mathbf{j})|\psi'(t)\rangle \tag{2.41}$$

are respectively the divergence of the stress-momentum tensor and internal interaction force density of the auxiliary primed system. Our goal is to construct $v'_{ext}(\mathbf{r},t)$ in such a way that $n(\mathbf{r},t) = n'(\mathbf{r},t)$ during the entire evolution. i.e. we wish to construct a local potential for the auxiliary primed system, which under a different electron-electron interaction reproduces the density of the original system we wish to study. For the particular case where $v'_{ee}(\mathbf{r},\mathbf{r}') = 0$, we would then have a system of non-interacting electrons which reproduce the density of the original interacting system and so by definition $v'_{ext}(\mathbf{r},t) \equiv v_{ks}(\mathbf{r},t)$. i.e. the auxiliary system would be the Kohn-Sham system and we would have proven the existence of the KS potential by construction.

In order to construct v'_{ext}, we will demand that $\frac{\partial^k}{\partial t^k}n'(\mathbf{r},t)|_{t=t_0} = \frac{\partial^k}{\partial t^k}n(\mathbf{r},t)|_{t=t_0}$ for all k, so that the Taylor expansion of the auxiliary system's density is equal to the Taylor expansion of the density of the original system we wish to reproduce. Because

Eq. 2.39 is a second order differential equation for the density, we must choose $|\psi'(t_0)\rangle$ such that the initial conditions

$$n'(\mathbf{r}, t_0) = \langle\psi'(t_0)|\hat{n}(\mathbf{r})|\psi'(t_0)\rangle = \langle\psi(t_0)|\hat{n}(\mathbf{r})|\psi(t_0)\rangle = n(\mathbf{r}, t_0) \tag{2.42}$$

and

$$\frac{\partial}{\partial t} n(\mathbf{r}, t)|_{t=t_0} = \langle\psi'(t_0)|\nabla \cdot \hat{\mathbf{j}}_{\mathbf{p}}(\mathbf{r})|\psi'(t_0)\rangle = \langle\psi(t_0)|\nabla \cdot \hat{\mathbf{j}}_{\mathbf{p}}(\mathbf{r})|\psi(t_0)\rangle = \frac{\partial}{\partial t} n'(\mathbf{r}, t)|_{t=t_0}, \tag{2.43}$$

are satisfied. i.e. we must choose the initial state in the primed system to reproduce the initial density and first derivative of the density. Assuming that these two conditions are satisfied, we now Taylor expand both sides of Eq. 2.39 with respect to time and arrive at,

$$n'_{k+2}(\mathbf{r}) = q'_k(\mathbf{r}) + \sum_{l=0}^{k} \binom{k}{l} \nabla \cdot \left[n'_{(k-l)}(\mathbf{r}) \nabla v'_{ext,l}(\mathbf{r}) \right], \tag{2.44}$$

where $f_k(\mathbf{r}) = \frac{\partial^k}{\partial t^k} f(\mathbf{r}, t)|_{t=t_0}$ is the kth order Taylor coefficient of an arbitrary function f. We construct the Taylor coefficients of $v'_{ext,k}(\mathbf{r})$ by *demanding* that $n'_k(\mathbf{r}) = n_k(\mathbf{r})$ for all k, which yields:

$$\nabla \cdot \left[n_{(0)}(\mathbf{r}) \nabla v'_{ext,k}(\mathbf{r}) \right] = n_{(k+2)}(\mathbf{r}) - q'_k(\mathbf{r}) - \sum_{l=0}^{k-1} \binom{k}{l} \nabla \cdot \left[n_{(k-l)}(\mathbf{r}) \nabla v'_{ext,l}(\mathbf{r}) \right]. \tag{2.45}$$

Eq. 2.45 can be solved recursively order-by-order for the Taylor coefficients $v'_{ext,k}(\mathbf{r})$, since the right hand side depends only on lower-order Taylor coefficients $v'_{ext,l}(\mathbf{r})$ where $l < k$ and known quantities. Eq. 2.45 is of the Sturm-Liouville type and has a unique solution once a suitable boundary condition is specified, which is typically taken to be $v'_{ext,k}(\mathbf{r}) \to 0$ as $r \to \infty$ [247]. In this way, the VL construction for the particular case

where $v'_{ee}(\mathbf{r}, \mathbf{r}') = 0$ proves the existence of a Kohn-Sham system which reproduces the density of a given interacting system. The VL construction assumes that the density $n(\mathbf{r}, t)$, the internal force term $q'(\mathbf{r}, t)$ and the auxiliary potential $v'_{ext}(\mathbf{r}, t)$ are all equal to their Taylor expansions with a finite radius of convergence about $t = t_0$. This is more restrictive than the RG theorem, which only assumes Taylor expandability of the potential. Extending the VL construction to non-analytic functions is an open problem and has begun to be researched [146].

2.3 TDDFT linear response theory

In section 2.2 we discussed the time-dependent Kohn-Sham equations in real-time, but we could also have formulated the discussion in the Fourier-transformed frequency domain. Since the KS orbitals reproduce the exact time-dependent density through Eq. 2.27, they also reproduce the exact density in frequency-space, and via a Fourier-transform of the KS orbitals, one can extract spectral information about the system. In this section we will review TDDFT linear response theory, which is used to extract linear absorption spectra by considering infinitesimal perturbations of the KS orbitals about their ground-state values [83, 181, 71]. We first discuss the general linear density response of an interacting electronic system [71, 185], followed by the linear density response of non-interacting KS electrons [83], and then present a derivation of the Casida equations which are implemented in virtually all quantum chemistry packages [42]. Finally, we mention two useful approximations to the Casida equations which we will use in Chapter 6 of this thesis, when we extend TDDFT

linear response theory to open quantum systems in order to obtain environmentally broadened absorption spectra.

Time-dependent linear density response

In linear response theory, we begin with a many-electron system described by the Hamiltonian in Eq. 2.1, but assume a static external potential $v_{ext}(\mathbf{r})$ for $t < t_0$, where t_0 is an arbitrary initial time. For $t < t_0$, we take the system to be in its ground-state $|\psi_0\rangle$, which is a reasonable approximation for insulators and finite systems at room temperature such as atoms and molecules, where typically $\omega_{01} \gg k_B T$ [150]. Here, ω_{01} is the lowest excitation energy, T is the temperature and k_B is Boltzmann's constant. In chapter 6 we will consider the more general situation in which one begins from a thermal density matrix at finite temperature, which is applicable to metals as well [158, 275]. At $t = t_0$, we apply an infinitesimal time-dependent perturbation $\delta v_{ext}(\mathbf{r}, t)$ to the system and let it subsequently evolve. Thus, the external potential is given by:

$$t \ < t_0, v_{ext}(\mathbf{r}, t) = v_{ext}(\mathbf{r}) \tag{2.46}$$

$$t \ > t_0, v_{ext}(\mathbf{r}, t) = v_{ext}(\mathbf{r}) + \delta v_{ext}(\mathbf{r}, t). \tag{2.47}$$

Now, if we consider the density evolution for $t < t_0$, the density is simply the static ground-state density $n_0(\mathbf{r}) = \langle\psi_0|\hat{n}(\mathbf{r})|\psi_0\rangle$. For $t > t_0$, the density will be time-dependent and given by $n(\mathbf{r}, t) = \langle\psi(t)|\hat{n}(\mathbf{r})|\psi(t)\rangle$, where $|\psi(t)\rangle$ is the solution to the time-dependent Schrödinger equation for $t > t_0$. Since we are considering an

infinitesimal perturbing potential $\delta v_{ext}(\mathbf{r},t)$, we can expand the density evolution in powers of the potential as $n(\mathbf{r},t) = n_0(\mathbf{r}) + \delta n(\mathbf{r},t) + ...$ and keep only the first-order term $\delta n(\mathbf{r},t)$. Thus, the linear density response is given by:

$$t \ < t_0, n(\mathbf{r},t) = n_0(\mathbf{r}) \tag{2.48}$$

$$t \ > t_0, n(\mathbf{r},t) = n_0(\mathbf{r}) + \delta n(\mathbf{r},t). \tag{2.49}$$

$\delta n(\mathbf{r},t)$ is related to $\delta v_{ext}(\mathbf{r},t)$ through the relation:

$$\delta n(\mathbf{r},t) = \int d^3r' \int dt' \chi_{nn}(\mathbf{r},\mathbf{r}';t-t')\delta v_{ext}(\mathbf{r}',t'), \tag{2.50}$$

where

$$\chi_{nn}(\mathbf{r},\mathbf{r}';\tau) = -\imath\Theta(\tau)\langle\psi_0|[\hat{n}(\mathbf{r},\tau),\hat{n}(\mathbf{r}')]|\psi_0\rangle, \tag{2.51}$$

is the linear density-density response function obtained from standard first-order time-dependent perturbation theory [71, 185]. Here, $\tau = t - t'$ and $\Theta(\tau)$ is the Heaviside step function which ensures that the density-density response function is causal. i.e. a perturbing potential $\delta v_{ext}(\mathbf{r}',t')$ can only give rise to a density disturbance $\delta n(\mathbf{r},t)$ at later times $t > t'$. In Eq. 2.51, $\hat{n}(\mathbf{r},t) = e^{\imath\hat{H}t}\hat{n}(\mathbf{r})e^{-\imath\hat{H}t}$ is the density operator in the Heisenberg picture with respect to the static many-body Hamiltonian $\hat{H}$ for $t < t_0$. In order to extract spectral information about the system one considers the Fourier-transform of Eq. 2.51,

$$\chi_{nn}(\mathbf{r},\mathbf{r}';\omega) = -\lim_{\epsilon\to+0}\imath\int_0^\infty dt e^{-\imath\omega t-\epsilon t}\langle\psi_0|[\hat{n}(\mathbf{r},\tau),\hat{n}(\mathbf{r}')]|\psi_0\rangle, \tag{2.52}$$

where ϵ is a convergence factor which is taken to zero after the integral in Eq. 2.52 is performed. By inserting a resolution of the identity operator in terms of a complete

set of eigenstates of $\hat{H}$, one arrives at the sum-over-states or "Lehmann" representation [124] of the density-density response function:

$$\chi_{nn}(\mathbf{r},\mathbf{r}';\omega) = \lim_{\epsilon\to+0}\sum_n \langle\psi_0|\hat{n}(\mathbf{r})|\psi_n\rangle\langle\psi_n|\hat{n}(\mathbf{r}')|\psi_0\rangle\left\{\frac{1}{\omega-\omega_{n0}+\imath\epsilon}-\frac{1}{\omega+\omega_{n0}+\imath\epsilon}\right\}. \tag{2.53}$$

Eq. 2.53 is a particularly useful representation of the density-density response function, because it directly contains all spectral information about the system. We see that excitation energies lie at the poles of χ_{nn} and oscillator strengths are obtained from the residues. The absorption spectrum is obtained by taking the imaginary part of the density-density response function in Eq. 2.53 and is given explicitly by:

$$\Im m\left[\chi_{nn}(\mathbf{r},\mathbf{r}';\omega)\right] = -\pi\sum_n \langle\psi_0|\hat{n}(\mathbf{r})|\psi_n\rangle\langle\psi_n|\hat{n}(\mathbf{r}')|\psi_0\rangle\left\{\delta(\omega-\omega_{n0})-\delta(\omega+\omega_{n0})\right\}, \tag{2.54}$$

which consists of a discrete sum of delta function peaks at the transition frequencies of the system. In Chapter 6 we will see how OQS-TDDFT enables one to obtain more realistic broadened absorption spectra by including relaxation and dephasing due to phonons or spontaneous and stimulated emission from a photon field.

Although Eq.s 2.53 and 2.54 in principle contain all spectral information about the system, they are not of much practical use because they require the many-body eigenstates and eigenenergies as input. In the next section, we will see how TDDFT linear response theory allows one to obtain the poles and residues of the density-density response function without explicitly calculating the many-body eigenstates, by considering the density response of the Kohn-Sham system and including corrections due to exchange-correlation effects.

Kohn-Sham linear density response

In the last section we discussed the linear density response of an interacting system of electrons. In this section, we will consider a fictitious system of non-interacting KS electrons which reproduce the same density response as the interacting system. In this way, it will be possible to extract the excitation energies and oscillator strengths of the interacting system of interest, by studying the density response of the simpler non-interacting KS system [83].

For $t < t_0$, we consider a system of non-interacting electrons with the *same* ground-state density $n_0(\mathbf{r})$ as the interacting system, but described by the self-consistent Kohn-Sham equations of ground-state DFT [115]:

$$\left[-\frac{1}{2}\nabla^2 + v_{ks}[n_0](\mathbf{r})\right]\phi_i(\mathbf{r}) = \epsilon_i\phi_i(\mathbf{r}), \tag{2.55}$$

where the ground-state KS potential is given by,

$$v_{ks}[n_0](\mathbf{r}) = v_{ext}[n_0](\mathbf{r}) + \int d^3r \frac{n_0(\mathbf{r}')}{|\mathbf{r}-\mathbf{r}'|} + v_{xc}[n_0](\mathbf{r}). \tag{2.56}$$

The KS ground-state wavefunction is a Slater determinant Φ_0 of N occupied orbitals and the exact ground-state density is obtained by square-summing these orbitals according to:

$$n_0(\mathbf{r}) = \sum_{i=1}^{N} |\phi_i(\mathbf{r})|^2. \tag{2.57}$$

For $t > t_0$, the perturbation $\delta v_{ext}(\mathbf{r}, t)$ is applied and the KS system subsequently evolves. The KS system reproduces the *same* density response $\delta n(\mathbf{r}, t)$ as the interacting system, but the KS electrons respond to the dressed Kohn-Sham potential,

$$\delta v_{ks}[n, \Phi_0](\mathbf{r}, t) = \delta v_{ext}[n, \psi_0](\mathbf{r}, t) + \int d^3r' \frac{\delta n(\mathbf{r}', t)}{|\mathbf{r}-\mathbf{r}'|} + \delta v_{xc}[n, \psi_0, \Phi_0](\mathbf{r}, t), \tag{2.58}$$

rather than the bare external potential $\delta v_{ext}[n,\psi_0](\mathbf{r},t)$. The density response is related to the KS potential via the relation:

$$\delta n(\mathbf{r},t) = \int d^3r' \int dt' \chi^{ks}_{nn}(\mathbf{r},\mathbf{r}';t-t')\delta v_{ks}(\mathbf{r},t'), \tag{2.59}$$

where χ^{ks}_{nn} is the density-density response function of the KS system, which in general differs from the density-density response function χ_{nn} of the interacting system. Repeating the same steps as in the previous section, but for the KS system, we arrive at the Lehmann spectral representation of χ^{ks}_{nn}:

$$\chi^{ks}_{nn}(\mathbf{r},\mathbf{r}';\omega) = \lim_{\epsilon\to+0}\sum_n \langle\Phi_0|\hat{n}(\mathbf{r})|\Phi_n\rangle\langle\Phi_n|\hat{n}(\mathbf{r}')|\Phi_0\rangle\left\{\frac{1}{\omega-\omega^{ks}_{n0}+\imath\epsilon}-\frac{1}{\omega+\omega^{ks}_{n0}+\imath\epsilon}\right\}. \tag{2.60}$$

Here, Φ_n represents an excited KS determinant of the ground state KS potential and ω^{ks}_{n0} is the corresponding KS excitation frequency. Because $\hat{n}(\mathbf{r})$ is a one-body operator, the matrix elements $\langle\Phi_0|\hat{n}(\mathbf{r})|\Phi_n\rangle$ appearing in Eq. 2.60 vanish unless Φ_n differs from Φ_0 by a single transition from an occupied orbital ϕ_k to an unoccupied orbital ϕ_j [217, 49]. For this reason, Eq. 2.60 simplifies to a sum over KS single-excitations:

$$\chi^{ks}_{nn}(\mathbf{r},\mathbf{r}';\omega) = \lim_{\epsilon\to+0}\sum_{k=0}^{N}\sum_{j=N+1}^{\infty}\left\{\frac{\phi_j(\mathbf{r})\phi^*_k(\mathbf{r})\phi^*_j(\mathbf{r}')\phi_k(\mathbf{r}')}{\omega-(\epsilon_j-\epsilon_k)+\imath\epsilon}-\frac{\phi_k(\mathbf{r})\phi^*_j(\mathbf{r})\phi^*_k(\mathbf{r}')\phi_j(\mathbf{r}')}{\omega+(\epsilon_j-\epsilon_k)+\imath\epsilon}\right\}. \tag{2.61}$$

We see that χ^{ks}_{nn} in Eq. 2.61 has poles at the bare KS single-excitations, which in general differ from the true many-body excitations of the interacting system. The true excitations will be mixtures of these KS single-excitations as well as double and higher multiple KS excitations, which are missing from χ^{ks}_{nn}. In order to extract the true excitations of the interacting system from the KS density response, we need to

relate χ_{nn} to χ^{ks}_{nn}. We do this by first noting from Eq. 2.50 that

$$\chi_{nn}(\mathbf{r},\mathbf{r}',t-t') = \frac{\delta n(\mathbf{r},t)}{\delta v_{ext}(\mathbf{r}',t')}, \tag{2.62}$$

which can be rewritten as

$$\chi_{nn}(\mathbf{r},\mathbf{r}',t-t') = \int d^3x \int d\tau \frac{\delta n(\mathbf{r},t)}{\delta v_{ks}(\mathbf{x},\tau)} \frac{\delta v_{ks}(\mathbf{x},\tau)}{\delta v_{ext}(\mathbf{r}',t')}, \tag{2.63}$$

where we have used the chain rule of functional differentiation and it is understood that all functional derivatives are evaluated at their ground-state values. Making use of the chain rule again, we can rewrite the functional derivative of the KS potential with respect to the external potential as,

$$\frac{\delta v_{ks}(\mathbf{r},t)}{\delta v_{ext}(\mathbf{r}',t')} = \delta(\mathbf{r}-\mathbf{r}')\delta(t-t') + \int d^3x \int d\tau \left\{ \frac{\delta(t-\tau)}{|\mathbf{r}-\mathbf{x}|} + \frac{\delta v_{xc}(\mathbf{r},t)}{\delta n(\mathbf{x},\tau)} \right\} \frac{\delta n(\mathbf{x},t)}{\delta v_{ext}(\mathbf{r}',t')}. \tag{2.64}$$

Inserting Eq. 2.64 into Eq. 2.63 and using Eq. 2.65 together with the relation

$$\chi^{ks}_{nn}(\mathbf{r},\mathbf{r}',t-t') = \frac{\delta n(\mathbf{r},t)}{\delta v_{ks}(\mathbf{r}',t')}, \tag{2.65}$$

one arrives at a relation between the interacting and KS density-density response functions:

$$\begin{aligned} \chi_{nn}(\mathbf{r},\mathbf{r}',t-t') &= \chi^{ks}_{nn}(\mathbf{r},\mathbf{r}',t-t') + \int d^3x \int d\tau \int d^3x' \int d\tau' \chi^{ks}_{nn}(\mathbf{r},\mathbf{x},t-\tau) \\ &\times \left\{ \frac{\delta(\tau-\tau')}{|\mathbf{x}'-\mathbf{x}|} + f_{xc}[n_0](\mathbf{x},\mathbf{x}',\tau-\tau') \right\} \chi_{nn}(\mathbf{x}',\mathbf{r}',\tau'-t'). \end{aligned} \tag{2.66}$$

Here, we have defined the exchange-correlation kernel as the functional derivative of the exchange-correlation potential evaluated on the ground-state density:

$$f_{xc}[n_0](\mathbf{r},\mathbf{r}',t-t') = \frac{\delta v_{xc}(\mathbf{r},t)}{\delta n(\mathbf{r}',t')}\Big|_{n(\mathbf{r}',t')=n_0}. \tag{2.67}$$

f_{xc} contains all of the non-trivial many-body effects and is responsible for mixing the bare KS excitations lying at the poles of χ^{ks}_{nn} to those of the true interacting system lying at the poles of χ_{nn}. Because double and higher-multiple excitations are absent from χ^{ks}_{nn}, it is the task of the exchange-correlation kernel to mix these in and generate the additional poles present in χ_{nn} [147]. As we discuss in section 2.4, constructing accurate approximations to f_{xc} is crucial for obtaining accurate spectra in TDDFT linear response theory and obtaining excitations of double and higher-multiple character is notoriously difficult.

By performing a Fourier-transform, we can write Eq. 2.66 in the frequency domain as:

$$\begin{aligned}\chi_{nn}(\mathbf{r},\mathbf{r}',\omega) &= \chi^{ks}_{nn}(\mathbf{r},\mathbf{r}',\omega) + \int d^3x \int d^3x' \chi^{ks}_{nn}(\mathbf{r},\mathbf{x},\omega) \\ &\times \left\{ \frac{1}{|\mathbf{x}'-\mathbf{x}|} + f_{xc}[n_0](\mathbf{x},\mathbf{x}',\omega) \right\} \chi_{nn}(\mathbf{x}',\mathbf{r}',\omega). \end{aligned} \tag{2.68}$$

Eq. 2.68 is reminiscent of the Dyson equation of Green's function theory, with the Hartree-exchange-correlation kernel, $\frac{1}{|\mathbf{r}'-\mathbf{r}|} + f_{xc}[n_0](\mathbf{r},\mathbf{r}',\omega)$, playing the role of the frequency-dependent self energy [63]. In principle, one can first construct χ^{ks}_{nn} from a ground-state DFT calculation and with a suitable density functional approximation to f_{xc}, one can solve Eq. 2.68 self-consistently for χ_{nn}. However, in practical quantum chemical calculations, Eq. 2.68 is usually reformulated as a non-linear eigenvalue problem in terms of matrices represented in a basis set of molecular orbitals [113]. The matrix equations representing this non-linear eigenvalue problem are referred to as the "Casida equations", whose solution yields excitation energies from the eigenvalues and oscillator strengths from the eigenvectors [42]. We now present a detailed derivation

of the Casida equations in their conventional form, which will be extended to OQS-TDDFT in Chapter 6.

The Casida equations

In this section, we derive the Casida matrix equations which are implemented in most quantum chemistry packages for obtaining excited state properties via TDDFT. These equations will be important in Chapter 6 when we generalize them to OQS-TDDFT, so we make the derivation detailed. In keeping with the original derivation by Casida [42], we introduce second quantized creation and annihilation operators, $a_i^\dagger$ and a_i, for a one-particle orbital basis. In what follows, this will be taken to be a basis of real molecular orbitals from a ground-state KS calculation, obtained by solving Eq. 2.55. An arbitrary one-particle operator $\hat{O}$ is represented in this basis as

$$\hat{O} = \sum_{ij} a_i^\dagger a_j \langle i|\hat{O}|j\rangle \equiv \sum_{ij} O_{ij} a_i^\dagger a_j. \tag{2.69}$$

The interacting density-density response function in Eq. 2.53 is given by

$$\chi_{nn}(\mathbf{r},\mathbf{r}';\omega) = \sum_{ijkl} \phi_i(\mathbf{r})\phi_j(\mathbf{r})\chi_{ijkl}(\omega)\phi_k(\mathbf{r}')\phi_l(\mathbf{r}'), \tag{2.70}$$

where the response matrix is:

$$\chi_{ijkl}(\omega) = \sum_a \left\{ \frac{\langle\psi_0|a_j^\dagger a_i|\psi_a\rangle\langle\psi_a|a_k^\dagger a_l|\psi_0\rangle}{\omega + \omega_{0a} + \imath\epsilon} - \frac{\langle\psi_0|a_k^\dagger a_l|\psi_a\rangle\langle\psi_a|a_j^\dagger a_i|\psi_0\rangle}{\omega - \omega_{0a} + \imath\epsilon} \right\}. \tag{2.71}$$

In this basis, the linear response of the interacting 1-particle reduced density matrix at frequency ω is

$$\delta\rho_{ij}(\omega) = \sum_{kl} \chi_{ijkl}(\omega)\delta v_{ext}(\omega)_{kl}, \tag{2.72}$$

and the linear density response is given by

$$\delta n(\mathbf{r},\omega) = \sum_{ij} \delta\rho_{ij}(\omega)\phi_j(\mathbf{r})\phi_i(\mathbf{r}). \tag{2.73}$$

In the KS system, the same density response is produced from

$$\delta n(\mathbf{r},\omega) = \sum_{ij} \delta\gamma_{ij}(\omega)\phi_j(\mathbf{r})\phi_i(\mathbf{r}), \tag{2.74}$$

where

$$\delta\gamma_{ij}(\omega) = \sum_{kl} \chi^{ks}_{ijkl}(\omega)\delta v_{ks}(\omega)_{kl}, \tag{2.75}$$

is the response of the KS one-particle reduced density matrix and

$$\chi^{ks}_{ijkl}(\omega) = \delta_{ik}\delta_{jl}\left\{\frac{f_j - f_i}{\omega - (\epsilon_i - \epsilon_j)}\right\}, \tag{2.76}$$

is the response matrix of the KS density-density response function in Eq. 2.61. In Eq. 2.76 $\{f_i\}$ are occupation numbers, equal to 1 for an occupied orbital and 0 for an unoccupied orbital and we have taken the limit $\epsilon \to 0$. Eq. 2.75 can then be written as

$$\delta\gamma_{ij}(\omega) = \left\{\frac{f_j - f_i}{\omega - (\epsilon_i - \epsilon_j)}\right\}(\delta v_{ext}(\omega)_{ij} + \delta v_h(\omega)_{ij} + \delta v_{xc}(\omega)_{ij}), \tag{2.77}$$

where we have explicitly written the KS potential in terms of the external, Hartree and exchange-correlation components. We now relate the response of the Hartree and exchange-correlation potentials to that of the KS density matrix via

$$\delta v_h(\omega)_{ij} + \delta v_{xc}(\omega)_{ij} = \sum_{kl} K_{ijkl}(\omega)\delta\gamma_{kl}(\omega), \tag{2.78}$$

where we have introduced the coupling matrix

$$K_{ijkl}(\omega) \equiv \int d^3\mathbf{r} \int d^3\mathbf{r}'\phi^*_i(\mathbf{r})\phi^*_j(\mathbf{r})\left\{\frac{1}{|\mathbf{r}-\mathbf{r}'|} + f_{xc}[n_0](\mathbf{r},\mathbf{r}';\omega)\right\}\phi_k(\mathbf{r}')\phi_l(\mathbf{r}'). \tag{2.79}$$

We can then re-write Eq. 2.77 as

$$\sum_{kl}^{f_k \neq f_l} \left[\delta_{ik}\delta_{jl} \frac{\omega - (\epsilon_k - \epsilon_l)}{f_l - f_k} - K_{ijkl}(\omega) \right] \delta\gamma_{kl}(\omega) = \delta v_{ext}(\omega)_{ij}. \tag{2.80}$$

We now separate particle-hole and hole-particle contributions in 2.80 as:

$$\begin{aligned} &\sum_{kl, f_k > f_l} \left[\delta_{ik}\delta_{jl} \frac{\omega - (\epsilon_k - \epsilon_l)}{f_l - f_k} - K_{ijkl}(\omega) \right] \delta\gamma_{kl}(\omega) \\ - &\sum_{kl, f_k > f_l} K_{ijlk}(\omega)\delta\gamma_{lk}(\omega) = \delta v_{ext}(\omega)_{ij} \end{aligned} \tag{2.81}$$

is the particle-hole contribution and

$$\begin{aligned} &\sum_{kl, f_k > f_l} \left[\delta_{ik}\delta_{jl} \frac{\omega - (\epsilon_l - \epsilon_k)}{f_k - f_l} - K_{jilk}(\omega) \right] \delta\gamma_{lk}(\omega) \\ - &\sum_{kl, f_k > f_l} K_{jikl}(\omega)\delta\gamma_{kl}(\omega) = \delta v_{ext}(\omega)_{ji}, \end{aligned} \tag{2.82}$$

is the hole-particle contribution. Let us recall that our goal is to formulate a matrix equation version of Eq. 2.68, whose eigenvalues yield excitation energies and whose eigenvectors yield oscillator strengths. To this end, we define the following matrices:

$$A_{ijkl}(\omega) = \delta_{ik}\delta_{jl} \frac{\epsilon_k - \epsilon_l}{f_k - f_l} - K_{ijkl}(\omega), \tag{2.83}$$

$$B_{ijkl}(\omega) = -K_{ijlk}(\omega), \tag{2.84}$$

and

$$C_{ijkl} = \frac{\delta_{ik}\delta_{jl}}{f_k - f_l}. \tag{2.85}$$

We can combine Eq. 2.81 and Eq. 2.82 into a single matrix equation,

$$\left\{ \begin{pmatrix} \bar{A} & \bar{B} \\ \bar{B} & \bar{A} \end{pmatrix} - \omega \begin{pmatrix} \bar{C} & 0 \\ 0 & \bar{C} \end{pmatrix} \right\} \begin{pmatrix} \vec{\delta\gamma}(\omega) \\ \vec{\delta\gamma}^{\,*}(\omega) \end{pmatrix} = \begin{pmatrix} \vec{\delta v_{ext}}(\omega) \\ \vec{\delta v_{ext}}^{\,*}(\omega) \end{pmatrix}, \tag{2.86}$$

or by applying the unitary transformation

$$\frac{1}{\sqrt{2}}\begin{pmatrix} 1 & 1 \\ -1 & 1 \end{pmatrix}, \tag{2.87}$$

$$\begin{pmatrix} \bar{A}+\bar{B} & \omega\bar{C} \\ \omega\bar{C} & \bar{A}-\bar{B} \end{pmatrix}\begin{pmatrix} \Re e(\vec{\delta\gamma}(\omega)) \\ -\imath\Im m(\vec{\delta\gamma}(\omega)) \end{pmatrix} = \begin{pmatrix} \Re e(\vec{\delta v_{ext}})(\omega) \\ -\imath\Im m(\vec{\delta v_{ext}}(\omega)) \end{pmatrix}. \tag{2.88}$$

These matrix equations are spanned by the set of occupied to unoccupied orbital transitions used in the calculation. Without loss of generality, we assume the applied perturbation to be real. Since the molecular orbitals are taken to be real as well, the density response can be calculated from $\Re e(\vec{\delta\gamma}(\omega))$ alone. From Eq. 2.88, we obtain

$$\left[(\bar{A}+\bar{B}) - \omega\bar{C}\left[\bar{A}-\bar{B}\right]^{-1}\omega\bar{C}\right]\Re e(\vec{\delta\gamma}(\omega)) = \Re e(\vec{\delta v_{ext}})(\omega). \tag{2.89}$$

We introduce the matrices

$$\bar{S} = -\bar{C}\left[\bar{A}-\bar{B}\right]^{-1}\bar{C}, \tag{2.90}$$

and

$$\Omega(\omega) = -\bar{S}^{-\frac{1}{2}}\left[\bar{A}+\bar{B}\right]\bar{S}^{-\frac{1}{2}}. \tag{2.91}$$

Eq. 2.89 can then be inverted to obtain

$$\Re e(\vec{\delta\gamma}(\omega)) = S^{-\frac{1}{2}}\Big\{\omega^2 - \Omega(\omega)\Big\}^{-1}S^{-\frac{1}{2}}\Re e(\vec{\delta v_{ext}})(\omega). \tag{2.92}$$

The poles of the density response, which occur at the excitation frequencies of the system, are obtained when $\Re e(\vec{\delta\gamma}(\omega))$ diverges which happens when the operator in curly brackets vanishes. Finding the frequencies at which this occurs is equivalent to solving the pseudo-eigenvalue equation,

$$\Big\{\omega^2 - \Omega(\omega)\Big\}\vec{F} = 0. \tag{2.93}$$

Returning to the basis of Kohn-Sham molecular orbitals, the matrix representation of $\Omega(\omega)$ is

$$\Omega_{ijkl}(\omega) = \delta_{ik}\delta_{jl}(\epsilon_l - \epsilon_k)^2 + 4\sqrt{(f_i - f_j)(\epsilon_j - \epsilon_i)}K_{ijkl}(\omega)\sqrt{(f_k - f_l)(\epsilon_l - \epsilon_k)}. \quad (2.94)$$

We see that the values of ω^2 for which Eq. 2.93 is satisfied are precisely the squares of the excitation frequencies of the system. The oscillator strengths are obtained from the eigenvectors $\vec{F}$ according to:

$$f_i = \frac{2}{3}\left[|\vec{x}^\dagger S^{-\frac{1}{2}}\vec{F}_i|^2 + |\vec{y}^\dagger S^{-\frac{1}{2}}\vec{F}_i|^2 + |\vec{z}^\dagger S^{-\frac{1}{2}}\vec{F}_i|^2\right], \quad (2.95)$$

where f_i is the oscillator strength of the ith transition, $\vec{F}_i$ is the corresponding eigenvector and $\vec{x}^\dagger$, $\vec{y}^\dagger$ and $\vec{z}^\dagger$ are row vectors composed of the matrix elements of the cartesian position operators in the basis of KS molecular orbitals. Eq. 2.93 is called a "pseudo-eigenvalue" equation, because the matrix $\Omega(\omega)$ itself is frequency dependent and thus depends on its own eigenvalues, which is not the case for usual linear eigenvalue problems. As we will discuss in Chapter 6, this creates additional numerical difficulties beyond ordinary matrix diagonalization when solving Eq. 2.93.

The "small-matrix" and "single-pole" approximations

An exact diagonalization of the operator $\Omega(\omega)$ can often be performed to obtain an exact numerical solution to the Casida equations with modest computational effort [67]. However, it will often prove useful to consider approximate solutions to the Casida equations which offer physical insight.

Inspecting Eq. 2.79, we see that the coupling matrix elements K_{ijkl} will tend to decrease with increasing distance from the diagonal, as the transition densities

$\phi_i^*(\mathbf{r})\phi_j^*(\mathbf{r})$ and $\phi_k(\mathbf{r})\phi_l(\mathbf{r})$ will tend to have smaller overlap as they become more separated in energy [14]. In the limit that the off-diagonal elements in Casida's equations can be neglected, we obtain the "small-matrix approximation" [14, 141, 250]. More precisely, if we have a single transition $i \to j$, whose off diagonal matrix elements with all other transitions are negligible, the small matrix approximation holds for this transition and yields:

$$\Omega_{ijij}(\omega_{ij}^{ks})F_{ij} = \omega^2 F_{ij}, \tag{2.96}$$

where $\omega_{ij}^{ks} = \epsilon_i - \epsilon_j$ is the bare KS frequency of the transition $i \to j$. Even though $\Omega_{ijij}(\omega)$ is frequency-dependent, it is evaluated at the bare KS frequency since corrections involve higher-order terms in the off diagonal matrix elements as explained in [14]. Eq. 2.96 can be solved exactly analytically to yield the transition frequencies:

$$\omega_{ij}^{SMA} = \pm\sqrt{(\omega_{ij}^{ks})^2 + 4\omega_{ij}^{ks}K_{ijij}(\omega_{ij}^{ks})}. \tag{2.97}$$

A further approximation known as the "single-pole approximation" results when the corrections due to the coupling matrix element K_{ijij} are much smaller than the bare KS transition frequency ω_{ij}^{ks} [14, 181]. In this limit, $\omega_{ij}^{ks} \gg K_{ijij}$ and we can Laurent expand Eq 2.97 to arrive at the single-pole approximation to the transition frequency,

$$\omega_{ij}^{SPA} = \pm(\omega_{ij}^{ks} + 2K_{ijij}(\omega_{ij}^{ks})). \tag{2.98}$$

Interestingly, we see that the small-matrix and single-pole approximations provide no corrections to the bare KS eigenvectors, which implies that the oscillator strengths retain their bare KS values. As we will discuss in Chapter 6, obtaining corrections

to the oscillator strengths requires inclusion of off-diagonal matrix elements in the Casida equations.

2.4 Approximate functionals in TDDFT

Thus far in this chapter we have presented TDDFT as a formally exact reformulation of time-dependent many-body quantum mechanics. However, in practical implementations of TDDFT the unknown exchange-correlation potential, $v_{xc}[n, \psi_0, \Phi_0](\mathbf{r}, t)$, must be approximated. The exchange-correlation potential of TDDFT is a much more complicated object than that of ground state DFT, since it is a functional of the initial states ψ_0 and Φ_0 of the interacting and KS systems respectively, as well as the history of the density at earlier times $t' < t$ [144, 142]. In contrast, the exchange-correlation potential of ground state DFT is a functional only of the ground state density. As a result, far fewer exact conditions are known about the TDDFT exchange-correlation functional and functional development in TDDFT is at a more immature stage. In this section, we will discuss several widely used approximations to the exchange-correlation potential of TDDFT.

The adiabatic approximation

The simplest and most widely used approximation in TDDFT is the "adiabatic approximation" [11, 12, 280, 281, 20], in which the exchange-correlation potential of TDDFT is approximated by a ground-state DFT functional. i.e.

$$v_{xc}^{adia}[n](\mathbf{r}, t) = v_{xc}^{GS}[n(t)](\mathbf{r}), \tag{2.99}$$

where v_{xc}^{GS} is a ground state approximation to the exchange-correlation potential. Because the adiabatic approximation consists of plugging the instantaneous time-dependent density into a ground state functional, it entirely neglects the initial-state and history dependence of the true TDDFT functional [144, 142]. Furthermore, the adiabatic approximation becomes exact in the limit of slowly varying densities, where the system remains in its instantaneous ground state [37]. Since TDDFT is typically concerned with dynamics which does not necessarily remain close to the ground state, one might expect the adiabatic approximation to be rather crude. However, despite some notorious failures [147, 141, 82, 61, 145] the adiabatic approximation works far beyond its expected domain of validity, and due to its simplicity is used in virtually all applications of TDDFT [40].

In the adiabatic local density approximation (ALDA) [280, 281], one uses the exchange-correlation potential of the local density approximation (LDA) [115, 177, 176] as the ground state functional. The LDA approximates the exchange-correlation potential of an inhomogeneous system by that of a uniform electron gas evaluated on the local density at each point in space. As a result, the ALDA exchange-correlation potential is not only temporally local, but spatially local as well. Explicitly, it is given by:

$$v_{xc}^{ALDA}[n](\mathbf{r},t) = v_{xc}^{hom}(n(\mathbf{r},t)) = \frac{d}{dn}\left[ne_{xc}^{hom}(n)\right]|_{n=n(\mathbf{r},t)}, \tag{2.100}$$

where $e_{xc}^{hom}(n)$ is the exchange-correlation energy per particle of a uniform electron gas, which can be obtained numerically exactly from diffusion Monte-Carlo simulations [45]. The ALDA is often too crude for molecular applications, due to the incorrect asymptotic behavior of the LDA exchange-correlation potential [249] and one

often employs adiabatic approximations based on hybrid functionals such as B3LYP or PBE0 which are far more accurate [21, 3].

Implications of the adiabatic approximation for linear response TDDFT

In section 2.3 we mentioned that the exchange-correlation kernel is the central object that must be approximated in a TDDFT linear response calculation. If one uses an adiabatic approximation to the exchange-correlation potential, the resulting exchange-correlation kernel is proportional to a delta function in time. i.e.

$$f_{xc}^{adia}[n_0](\mathbf{r},\mathbf{r}';t-t') = \frac{\delta v_{xc}^{GS}[n(t)](\mathbf{r})}{\delta n(\mathbf{r}',t')}|_{n_0} = \delta(t-t')\frac{\delta^2 E_{xc}[n]}{\delta n(\mathbf{r})\delta n(\mathbf{r}')}|_{n_0}, \tag{2.101}$$

where $E_{xc}[n]$ is the exchange-correlation energy functional of the ground-state approximation used. If one further uses the ALDA, the resulting exchange-correlation kernel,

$$f_{xc}^{ALDA}[n_0](\mathbf{r},\mathbf{r}';t-t') = \delta(t-t')\delta(\mathbf{r}-\mathbf{r}')\frac{d^2}{dn^2}\left[ne_{xc}^{hom}(n)\right]|_{n=n_0}, \tag{2.102}$$

is proportional to a delta function in space as well. Performing a Fourier-transform to the frequency domain, one finds that the adiabatic approximation always yields a *frequency-independent* kernel. i.e.

$$f_{xc}^{adia}[n_0](\mathbf{r},\mathbf{r}';\omega) = f_{xc}^{adia}[n_0](\mathbf{r},\mathbf{r}';\omega=0). \tag{2.103}$$

As a result, the Casida operator Ω is no longer frequency-dependent and Eq. 2.93 becomes an ordinary eigenvalue equation. In this case, the number of solutions to

Eq. 2.93 is equal to the dimensionality of Ω, which is the number of KS single-excitations included in the calculation. Therefore, excitations which require a strong contribution from double or higher-multiple KS excitations are not well captured within the adiabatic approximation [147]. This has led to the failure of adiabatic TDDFT for several important situations, such as charge-transfer excitations involving widely separated subsystems [141, 61, 82, 145, 225] or potential energy surfaces with conical intersections [222].

Beyond the adiabatic approximation - time-dependent current density functional theory

As we have mentioned, there are several notable shortcomings of the adiabatic approximation and attempts to go beyond it have emerged as a very active area of research. Throughout this thesis, we will see that the adiabatic approximation is often insufficient to capture relaxation and dephasing due to environmental effects in OQS-TDDFT and the development of non-adiabatic functionals will be important [226, 224].

One promising alternative to TDDFT is time-dependent current density functional theory (TDCDFT) [254, 255, 240, 241, 265]. In TDCDFT, one uses the paramagnetic current density $\mathbf{j}(\mathbf{r}, t)$ as the basic variable instead of the density $n(\mathbf{r}, t)$. The current has a temporally and spatially non-local dependence on the density, since the current "flowing" through a given volume element gives information about density that has reached that volume element from distant points in space and time. Therefore,

functionals in TDCDFT are inherently non-adiabatic in terms of the density and also spatially non-local. Another important feature of TDCDFT is that it is possible to construct non-adiabatic functionals in terms of gradients of the current, which is in general not possible in terms of the density due to "ultra-nonlocal" dependence on the density [84]. Furthermore, TDCDFT functionals inherently include dissipation and decoherence [52] and for this reason are promising candidates for OQS-TDDFT. In this section we give a very brief overview of the aspects of TDCDFT that will be relevant later in this thesis, but do not attempt an exhaustive review.

In the TDCDFT generalization of the RG and VL theorems [253], one considers a more general class of Hamiltonians than in Eq. 2.1:

$$\hat{H}(t) = \frac{1}{2}\sum_{i=1}^{N}\left\{ -\imath\nabla_i + \frac{1}{c}\mathbf{A}_{ext}(\mathbf{r}_i,t)\right\}^2 + \sum_{i<j}^{N}\frac{1}{|\mathbf{r_i}-\mathbf{r_j}|} + \sum_i v_{ext}(\mathbf{r_i},t), \qquad (2.104)$$

where $\mathbf{A}_{ext}(\mathbf{r},t)$ is an external vector potential. Since the scalar potential v_{ext} can always be gauge-transformed into a vector potential $\mathbf{A}_{ext}$, there is actually no loss of generality in including only a vector potential and furthermore, the Hamiltonian in Eq. 2.104 includes the additional case of externally applied magnetic fields, which cannot be described by a scalar potential alone. It has been proven that for a given initial state, there is a one-to-one mapping between the paramagnetic current density $\mathbf{j}(\mathbf{r},t)$ and the vector and scalar potentials $\mathbf{A}_{ext}(\mathbf{r},t)$ and $v_{ext}(\mathbf{r},t)$, which establishes the RG theorem of TDCDFT [253]. A VL construction has also been established, which proves that one can construct an auxiliary non-interacting Hamiltonian,

$$\hat{H}^{ks}(t) = \frac{1}{2}\sum_{i=1}^{N}\left\{ -\imath\nabla_i + \frac{1}{c}\mathbf{A}_{ks}(\mathbf{r}_i,t)\right\}^2 + \sum_i v_{ks}(\mathbf{r_i},t), \qquad (2.105)$$

which reproduces the same density and paramagnetic current of the original many-body Hamiltonian in Eq. 2.104 [253]. As in TDDFT, one then partitions $\mathbf{A}_{ks}$ into the external, Hartree and exchange-correlation vector potentials:

$$\mathbf{A}_{ks}(\mathbf{r},t) = \mathbf{A}_{ext}(\mathbf{r},t) + \mathbf{A}_{H}(\mathbf{r},t) + \mathbf{A}_{xc}(\mathbf{r},t). \tag{2.106}$$

The central point of TDCDFT is that one can construct simple approximations to $\mathbf{A}_{xc}$ as spatially local functionals of the current $\mathbf{j}(\mathbf{r},t)$, that are inherently spatially and temporally non-local in terms of the density $n(\mathbf{r},t)$ and therefore go beyond the adiabatic approximation. One such functional due to Vignale, Ullrich and Conti (VUC) [255] constructs the ith component of the exchange-correlation vector potential as the divergence of a stress tensor according to:

$$\frac{1}{c}\frac{\partial}{\partial t}A^{VUC}_{xc,i}(\mathbf{r},t) = -\frac{\partial}{\partial r_i}v^{ALDA}_{xc}(\mathbf{r},t) + \frac{1}{n(\mathbf{r},t)}\sum_j \frac{\partial \sigma_{xc,ij}(\mathbf{r},t)}{\partial r_j}, \tag{2.107}$$

where the exchange-correlation stress tensor is:

$$\sigma_{xc,ij}(\mathbf{r},t) = \int_{-\infty}^{t}\left\{\eta(\mathbf{r},t-t')\left[\frac{\partial u_i(\mathbf{r},t')}{\partial r_j} + \frac{\partial u_j(\mathbf{r},t')}{\partial r_i} - \frac{2}{3}\nabla\cdot\mathbf{u}(\mathbf{r},t')\delta_{ij}\right] + \zeta(\mathbf{r},t-t')\nabla\cdot\mathbf{u}(\mathbf{r},t')\delta_{ij}\right\}. \tag{2.108}$$

In Eq. 9.24, $\mathbf{u}(\mathbf{r},t) = \frac{\mathbf{j}(\mathbf{r},t)}{n(\mathbf{r},t)}$ is the local velocity field and η and ζ are "visco-elastic" coefficients of the uniform electron gas, for which accurate parameterizations are known [71]. $\mathbf{A}^{VUC}_{xc}(\mathbf{r},t)$ in Eq. 2.107 is clearly non-adiabatic, as it depends on the currents and densities at earlier times $t < t'$. It is also spatially local in terms of the current, while being highly non-local as a functional of the density. The VUC functional is velocity dependent and gives rise to relaxation and dephasing due to electron-electron interactions, which is an intrinsic feature of extended systems [52,

71, 265]. As discussed later, the relaxation and dephasing in OQS-TDDFT due to a bosonic bath of phonons or photons is very different, but there will be similarities between the VUC functional and functionals in OQS-TDDFT [224].

In this chapter we have presented a very brief overview of TDDFT, with emphasis on the formal aspects of the theory that will be used later when discussing extensions of TDDFT to open quantum systems and quantum computation. For a more extensive discussion of applications of TDDFT, see ref. [40] and the references contained within. We now turn to our second background chapter, where we provide a brief overview of the theory of open quantum systems.

Chapter 3

The theory of open quantum systems

3.1 Introduction

In Chapter 2 we discussed TDDFT as a formally exact reformulation of the time-dependent Schrödinger equation, which describes isolated systems evolving unitarily with reversible dynamics. In reality, no system is truly isolated and it inevitably interacts with the rest of the universe which induces irreversibility due to dissipation and decoherence. If the interaction of a system with its surroundings is sufficiently weak, unitary dynamics may be a valid approximation, but in many situations in electronic structure theory it is necessary to include the effects of an environment. The theory of open quantum systems (OQS) deals with precisely this situation, in which the bath exchanges energy and momentum with the system, but particle number is typically conserved [36]. In this chapter we will set the stage for generalizing TDDFT to OQS (OQS-TDDFT) by highlighting several important topics in the theory of open quantum systems. Section 3.2 introduces the system-bath partitioning scheme,

while section 3.3 introduces the formally exact generalized quantum master equation derived microscopically from first principles. We then discuss several approximations to the generalized quantum master equation, which will reappear later in the thesis.

3.2 The system-bath partitioning

The formal development of the theory of OQS [36, 156, 170] begins with the full unitary dynamics of the coupled system and reservoir (we will use the terms "reservoir" and bath" interchangeably), described by the Von Neumann equation for the density operator

$$\frac{d\hat{\rho}(t)}{dt} = -\imath[\hat{H}(t), \hat{\rho}(t)]\,. \tag{3.1}$$

Here,

$$\hat{H}(t) = \hat{H}_{\rm S}(t) + \epsilon\hat{V} + \hat{H}_{\rm R} \tag{3.2}$$

is the full Hamiltonian for the coupled system and bath and

$$\hat{H}_{\rm S}(t) = -\frac{1}{2}\sum_{i=1}^{N}\nabla_i^2 + \sum_{i<j}^{N} v_{ee}(\mathbf{r_i}, \mathbf{r_j}) + \sum_i v_{ext}(\mathbf{r_i}, t) \tag{3.3}$$

is the Hamiltonian of the electronic system of interest in an external potential $v_{ext}(\mathbf{r}, t)$. This potential generally consists of a static external potential due to the nuclei and an external driving field coupled to the system such as a laser field. For an interacting electronic system, $v_{ee}(\mathbf{r}, \mathbf{r}') = 1/|\mathbf{r} - \mathbf{r}'|$ is the two-body Coulomb repulsion. The system-bath coupling, $\hat{V}$, acts in the combined Hilbert space of the system and bath and so it couples the two subsystems. Typically, for a single dissipation channel, the

system-bath coupling is taken to have a bilinear form,

$$\hat{V} = -\hat{S} \otimes \hat{R}\,, \tag{3.4}$$

where $\hat{R}$ is an operator in the bath Hilbert space which generally couples to a local one-body operator $\hat{S} = \left[\sum_{i=1}^{N} \hat{s}(\hat{\mathbf{p}}_i, \hat{\mathbf{r}}_i)\right]$ in the system Hilbert space [156]. Implicit in OQS is a weak interaction between the system and bath, so that one can treat the system-bath coupling perturbatively by introducing the small parameter ϵ as in Eq. (3.2). $\hat{H}_R$ is the Hamiltonian of the bath, whose spectrum will typically consist of a dense set of bosonic modes such as photons or phonons. As we discuss later, the density of states of $\hat{H}_R$ determines the structure of reservoir correlation functions, whose time-scale in turn determines the reduced system dynamics.

The goal of the theory of open quantum systems is to arrive at a reduced description of the dynamics of the electronic system alone, by integrating out the bosonic modes of the bath. In this way, one arrives at the quantum master equation, which describes the non-unitary evolution of the reduced system in the presence of its environment. To achieve this, in the next section we derive the generalized many-electron quantum master equation using the Nakagima-Zwanzig projection operator formalism [164, 288, 289].

3.3 The generalized quantum master equation

We begin this section by deriving the formally exact many-electron quantum master equation using the Nakagima-Zwanzig projection operator formalism [164, 288, 289]. Using projection operators, the master equation can be systematically de-

rived from first principles starting from the microscopic Hamiltonian in Eq. (3.2) (i.e. without phenomenological parameters). This is particularly amenable to TDDFT, in which the electronic degrees of freedom are treated using first principles as well.

Our starting point is Eq. (3.1) for the evolution of the full density operator of the coupled system and bath,

$$\frac{\mathrm{d}\hat{\rho}(t)}{\mathrm{d}t} = -\imath[\hat{H}(t), \hat{\rho}(t)] \equiv -\imath\breve{L}(t)\hat{\rho}(t)\,, \tag{3.5}$$

where $\breve{L}(t)$ is the Liouvillian superoperator for the full evolution defined by Eq. (3.5). It may be separated into a sum of Liouvillian superoperators as

$$\breve{L}(t) = \breve{L}_{\mathrm{S}}(t) + \breve{L}_{\mathrm{SB}} + \breve{L}_{\mathrm{B}}\,, \tag{3.6}$$

where each term acts as a commutator on the density matrix with its respective part of the Hamiltonian. Our goal is to derive an equation of motion for the reduced density operator of the electronic system,

$$\hat{\rho}_{\mathrm{S}}(t) = Tr_{\mathrm{R}}\{\hat{\rho}(t)\}, \tag{3.7}$$

defined by tracing the full density operator over the reservoir degrees of freedom. To achieve this formally, we introduce the projection superoperators $\breve{P}$ and $\breve{Q}$. The operator $\breve{P}$ is defined by projecting the full density operator onto a product of the system density operator with the equilibrium density operator of the bath,

$$\breve{P}\hat{\rho}(t) = \hat{\rho}_{\mathrm{B}}^{\mathrm{eq}}\hat{\rho}_{\mathrm{S}}(t)\,. \tag{3.8}$$

$\breve{Q} = 1 - \breve{P}$ projects on the complement space. In this sense, $\breve{P}$ projects onto the degrees of freedom of the electronic system we are interested in, while $\breve{Q}$ projects onto irrelevant degrees of freedom describing the bath dynamics.

Using projection operators, Eq. (3.5) can be written formally as two coupled equations:

$$\frac{d}{dt}\breve{P}\hat{\rho}(t) = -\imath\breve{P}\breve{L}\hat{\rho}(t) = -\imath\breve{P}\breve{L}\breve{P}\hat{\rho}(t) - \imath\breve{P}\breve{L}\breve{Q}\hat{\rho}(t) \tag{3.9}$$

and

$$\frac{d}{dt}\breve{Q}\hat{\rho}(t) = -\imath\breve{Q}\breve{L}\hat{\rho}(t) = -\imath\breve{Q}\breve{L}\breve{P}\hat{\rho}(t) - \imath\breve{Q}\breve{L}\breve{Q}\hat{\rho}(t). \tag{3.10}$$

If Eq. (3.10) is integrated and substituted into Eq. (3.9), one obtains

$$\begin{aligned}\frac{d}{dt}\breve{P}\hat{\rho}(t) &= -\imath\breve{P}\breve{L}\breve{P}\hat{\rho}(t) \\ - &\int_0^t d\tau\ \breve{P}\breve{L}e^{-\imath\int_\tau^t \mathrm{d}\tau'\ \breve{Q}\breve{L}(\tau')}\breve{Q}\breve{L}\breve{P}\hat{\rho}(\tau) - \imath\breve{P}\breve{L}e^{-\imath\int_0^t d\tau\ \breve{Q}\breve{L}(\tau)}\breve{Q}\hat{\rho}(0).\end{aligned} \tag{3.11}$$

By performing a partial trace of both sides of Eq. (3.11) over the bath degrees of freedom, one arrives at the formally exact quantum master equation

$$\frac{d\hat{\rho}_{\mathrm{S}}(t)}{dt} = -\imath[\hat{H}_{\mathrm{S}}(t), \hat{\rho}_{\mathrm{S}}(t)] + \int_0^t dt'\breve{K}(t,\tau)\hat{\rho}_{\mathrm{S}}(\tau) + \Xi(t)\,. \tag{3.12}$$

Here,

$$\breve{K}(t,\tau) = Tr_{\mathrm{R}}\left\{\breve{P}\breve{L}e^{-\imath\int_\tau^t d\tau'\breve{Q}\breve{L}(\tau')}\breve{Q}\breve{L}\hat{\rho}_{\mathrm{R}}^{\mathrm{eq}}\right\} \tag{3.13}$$

is the memory kernel.

$$\Xi(t) = Tr_{\mathrm{R}}\left\{-\imath\breve{P}\breve{L}e^{-\imath\int_0^t d\tau\breve{Q}\breve{L}(\tau)}\breve{Q}\hat{\rho}(0)\right\} \tag{3.14}$$

arises from initial correlations between the system and its environment [157]. Equation (3.12) is still formally exact, as $\hat{\rho}_{\mathrm{S}}(t)$ yields the exact expectation value of any operator depending on the electronic degrees of freedom. In practice, approximations to the memory kernel and initial correlation term are needed, which we now discuss.

3.4 Separation of timescales and the Born-Markov limit

While Eq. 3.1 describing the unitary evolution of the full system and bath is local in time, once we trace over bath degrees of freedom the resulting master equation (Eq 3.12) yields an evolution that is non-local in time. Furthermore, we see from Eq.s 3.13 and 3.14 that the memory kernel and initial correlations contain the Liouvillian $\breve{L}$ in an exponential and therefore contain infinite powers of the system-bath interaction. In contrast, the full dynamics in Eq. 3.1 contains the Liouvillian only to first order. For these reasons, without approximations, Eq 3.12 is certainly not easier (and may even be more difficult) to solve than the full system-bath dynamics.

To deal with the fact that Eq 3.12 contains infinite orders of the system-bath interaction, one often invokes the second-Born approximation [203]. In the second-Born approximation, one assumes a weak system-bath interaction and expands the memory kernel to second order in $\hat{H}_{\mathrm{SB}}$. In this case, the memory kernel takes the simpler form:

$$\int_0^t dt' \breve{K}(t,\tau)\hat{\rho}_{\mathrm{S}}(\tau) = -\epsilon^2 \int_0^t d\tau Tr_{\mathrm{R}} \left\{ [\hat{V}^I(t), \breve{Q}[\hat{V}^I(\tau), \hat{\rho}_{\mathrm{R}}^{\mathrm{eq}} \hat{\rho}_{\mathrm{S}}^I(\tau)]] \right\}, \tag{3.15}$$

where

$$\hat{V}^I(t) = e^{\imath \int_{t_0}^t d\tau (\hat{H}_S(\tau)+\hat{H}_R)} \hat{V} e^{-\imath \int_{t_0}^t d\tau (\hat{H}_S(\tau)+\hat{V})} \tag{3.16}$$

is the system-bath interaction in the interaction picture and $\hat{\rho}_{\mathrm{S}}^I(t)$ is the system density operator in the interaction picture.

To further simplify calculations and make the memory kernel local in time, one of-

ten invokes the Markov approximation in addition to the second-Born approximation. These two approximations together are collectively referred to as the "Born-Markov" approximation [36, 156, 170]. From Eq. 3.4 and a little bit of algebra, we see that the memory kernel in Eq. 3.15 contains two-time correlation functions of bath operators of the form:

$$g(\tau - t) = Tr_{\mathrm{R}} \left\{ \hat{R}^I(\tau) \hat{R}^I(t) \hat{\rho}_{\mathrm{R}}^{\mathrm{eq}} \right\}, \tag{3.17}$$

where $\hat{R}^I(t) \equiv e^{\imath \hat{H}_R t} \hat{R} e^{-\imath \hat{H}_R t}$. If the density of states of $\hat{H}_R$ is extremely dense and approaches the continuum limit, the correlation functions decay exponentially and $g(\tau, t) \sim e^{(\tau - t)/\tau_c}$, where τ_c is the correlation time of the bath [170]. If we denote the characteristic timescale of evolution of the system due to coupling with the bath by τ_S, then in the limit that $\tau_S \gg \tau_c$, there will be negligible error on the evolution of the system by making the replacement $g(\tau, t) \to 0$ when $t \neq \tau$ [36]. In this case the memory kernel becomes time-local, which yields the Born-Markov approximation. i.e. $\breve{K}(t, \tau) \sim \breve{D} \delta(t - \tau)$, where $\breve{D}$ is a time-independent superoperator. Since in the second-Born approximation τ_s is inversely proportional to ϵ^2, the validity of the Born-Markov approximation is determined by the condition $\frac{1}{\epsilon^2 \tau_c} \gg 1$ [162].

3.5 The Lindblad master equation

In making the Born-Markov approximation, there are several different approaches that one can take to construct the Markovian superoperator $\breve{S}$. One approach is derive it microscopically starting from a system-bath Hamiltonian, which leads to the Redfield equations [194, 195] discussed in section 3.6. Another approach is to derive

it by imposing certain exact conditions on the density matrix that one would like it to satisfy during its evolution. One obvious condition is positivity. i.e. if we decompose the density matrix in terms of its eigenvalues and eigenvectors at each time-step as $\hat{\rho}_S(t) = \sum_j p_j|\xi_j(t)\rangle\langle\xi_j(t)|$, one would like to ensure that $p_j > 0$ at each time-step so that the eigenvalues can be interpreted as legitimate occupation probabilities. Secondly, one would like the density matrix to remain normalized at each time-step i.e. $\sum_j p_j = 1$. The most general mathematical form of a Markovian master equation that preserves these two conditions is the Lindblad equation [73, 117, 131]:

$$\frac{d\hat{\rho}_S}{dt} = \breve{D}^{lind}(\hat{\rho}_S) \equiv -i[\hat{H}_S, \hat{\rho}_S(t)] + \hat{L}\hat{\rho}_S(t)\hat{L}^\dagger - \frac{1}{2}\hat{L}\dagger\hat{L}\hat{\rho}_S(t) - \frac{1}{2}\hat{\rho}_S(t)\hat{L}^\dagger\hat{L}, \quad (3.18)$$

where $\hat{L}$ is an arbitrary operator. Furthermore, if $\hat{L}$ is taken to be linear in $\hat{S}$ from Eq. 3.4, the dissipative operator in Eq. 3.18 is second-order in the system-bath interaction and the Lindblad equation is within the Born-Markov approximation. There are numerous ways to derive the Lindblad operators $\hat{L}$ microscopically and in section 3.6 we will discuss the secular Redfield theory, which is microscopically derived and can be written in the Lindblad form [132].

Positivity of the Lindblad master equation for time-dependent Hamiltonians

In its original formulation, the Lindblad master equation was derived for time-independent Hamiltonians $\hat{H}_S$ and Lindblad bath operators $\hat{L}$. In TDDFT, the Hamiltonian is always time-dependent and one might wish to consider time-dependent bath operators as well. Therefore, later in the thesis when we discuss OQS-TDDFT, it will

be very important that the Lindblad master equation preserves positivity and normalization even if the Hamiltonian and bath operators depend on time. As there has been some confusion about this point in the literature, here we prove that the Lindblad form of the master equation *always* ensures preservation of trace and positivity throughout the time-evolution.

Let us begin by generalizing Eq. 3.18 to include N dissipation operators, which may be time-dependent as well as an explicitly time-dependent Hamiltonian:

$$\begin{aligned}\frac{d\hat{\rho}_S}{dt} &= \breve{D}^{lind}(\hat{\rho}_S) \\ &\equiv -i[\hat{H}_S(t), \hat{\rho}_S(t)] + \sum_{i=1}^{N} \hat{L}_i(t)\hat{\rho}_S(t)\hat{L}_i^\dagger(t) - \frac{1}{2}\hat{L}_i^\dagger(t)\hat{L}_i(t)\hat{\rho}_S(t) \\ &- \frac{1}{2}\hat{\rho}_S(t)\hat{L}_i^\dagger(t)\hat{L}_i(t). \end{aligned} \tag{3.19}$$

We now show that this master equation preserves the positivity and trace of the density matrix under its evolution, *irrespective* of the time-dependence of $\hat{H}_S$ and $\hat{L}_i$. To verify this, we expand $\hat{\rho}_S(t + \Delta t)$ for small Δt:

$$\begin{aligned}\hat{\rho}_S(t + \Delta t) &= \hat{\rho}_S(t) + \frac{\partial \hat{\rho}_S}{\partial t}\Delta t + O(\Delta t^2) \\ &\approx \sum_{i=0}^{N} M_i(\Delta t)\hat{\rho}_S(t)M_i(\Delta t)^\dagger. \end{aligned} \tag{3.20}$$

Using eqn (3.18), we can define the so-called Kraus operators $M_i(\Delta t)$ by:

$$M_0(\Delta t) \equiv I + \left(-i\hat{H} - \frac{1}{2}\sum_{i=1}^{N}\hat{L}_i^\dagger\hat{L}_i\right)\Delta t, \tag{3.21}$$

and

$$M_i(\Delta t) \equiv \hat{L}_i\sqrt{\Delta t}, \tag{3.22}$$

for $i > 0$ [36]. An important property of the Kraus operators is that they satisfy

$$\sum_{i=0}^{N} M_i(\Delta t)^\dagger M_i(\Delta t) = I, \tag{3.23}$$

as can be easily checked from eqns (3.22) and (3.21). Notice that, in general, $M_i(\Delta t)$ are time dependent if $\hat{L}_i$ are as well.

Let us write $\hat{\rho}_S(t) = \sum_j p_j |\xi_j(t)\rangle\langle\xi_j(t)|$, where $\{|\xi_i(t)\rangle\}$ is the basis that diagonalizes $\hat{\rho}_S(t)$ at each instant in time and $p_j \geq 0$ for all j. Notice that up to $O(\Delta t)$,

$$\hat{\rho}_S(t+\Delta t) = \sum_j \sum_{i=0}^{N} p_j \left(M_i(\Delta t)|\xi_j(t)\rangle\right) \left(\langle\xi_j(t)|M_i(\Delta t)^\dagger\right), \tag{3.24}$$

which shows that $\hat{\rho}_S(t+\Delta t)$ is positive semidefinite if $\hat{\rho}_S(t)$ is. The preservation of the trace can also be readily shown, i.e.

$$Tr(\hat{\rho}_S(t+\Delta t)) = Tr\left(\sum_{i=0}^{N} M_i(\Delta t)\hat{\rho}_S(t)M_i(\Delta t)^+\right) = Tr(\hat{\rho}_S(t)). \tag{3.25}$$

The proofs above are an adaptation of the discussion of the Lindblad equation in the textbook by Schumacher and Westmoreland [212] [1].

For completeness, we now introduce the concept of a *semigroup*. Consider the integrated form of the equation of motion for $\hat{\rho}_S(t)$ in the form of a dynamical map, $\hat{\rho}_S(t) = \Phi_{t,0}\hat{\rho}_S(0)$, where $\Phi_{t,0}$ is a dynamical map that propagates the density matrix from the initial time 0 to the final time t. The semigroup property is expressed as the following identity for the composition map [36]:

$$\Phi_{s,0}\Phi_{t,0} = \Phi_{s+t,0}. \tag{3.26}$$

[1] The authors discuss the derivation of the Lindblad equation as the generator of a completely positive map.

Notice that, on the one hand, the semigroup property will not be satisfied in general for time-dependent $\hat{H}_S$ or $\hat{L}_i$. On the other hand, for the case where both types of operators are time-independent, it can be shown that $\mathcal{L}$ is the most general form of the generator of a quantum dynamical semigroup, with the dynamical map being the exponential map: $\Phi_{s,0} = e^{\mathcal{L}s}$ [73]. However, it is clear from the above discussion that although the semigroup property may not hold, neither positivity nor trace-preservation are contingent upon the time-independence of $\hat{H}_S$ or $\hat{L}_i$.

3.6 The Redfield master equation

Due to its simplicity, the Redfield equation is one of the most widely employed microscopically-derived master equations [194, 195]. It was originally used to describe spin-environment interactions in nuclear magnetic resonance (NMR) spectroscopy, but more recently has been applied to multi-level molecular systems in condensed phase chemistry [170, 156]. The Redfield equation is derived using the Born-Markov approximation starting from a full system-bath Hamiltonian (Eq. 3.2), and while it is always trace preserving, it is not automatically in the Lindblad form and therefore does not necessarily preserve positivity [132]. As we discuss below, by making the additional secular approximation, the Redfield equation can be brought into the Lindblad form. We now present a brief outline of the derivation of the Redfield equation as it will be widely used throughout this thesis. For a more detailed derivation we refer the reader to [170].

The derivation begins by making the second-Born approximation to the full Nakagima-

Zwanzig equation, which yields the memory kernel given in Eq. 3.15. The first-order term in the system-bath interaction, $Tr_R\left\{\hat{V}\hat{\rho}_{\rm R}^{\rm eq}\right\}$, can simply be absorbed into the system Hamiltonian and we do not consider it further here, since it renormalizes the unitary evolution. Then, the equation of motion for the system density operator in the interaction picture, within the second-Born approximation is (setting $\epsilon = 1$):

$$\frac{d}{dt}\hat{\rho}_{\rm S}^I(t) = -\int_0^t d\tau Tr_{\rm R}\left\{[\hat{V}^I(t), \breve{Q}[\hat{V}^I(\tau), \hat{\rho}_{\rm R}^{\rm eq}\hat{\rho}_{\rm S}^I(\tau)]]\right\}. \tag{3.27}$$

By assuming the bilinear form of the system-bath interaction written in Eq. 3.4, we can explicitly write Eq. 3.27 as:

$$\frac{d}{dt}\hat{\rho}_{\rm S}^I(t) = -\int_0^t d\tau\left\{g(t-\tau)[\hat{S}^I(t), \hat{S}^I(\tau)\hat{\rho}_{\rm S}^I(\tau)] - g^*(t-\tau)[\hat{S}^I(t), \hat{\rho}_{\rm S}^I(\tau)\hat{S}^I(\tau)]\right\}, \tag{3.28}$$

where $\hat{S}^I(t) = e^{\imath\hat{H}_S t}\hat{S}e^{-\imath\hat{H}_S t}$ is the system part of the system-bath interaction in the interaction picture and $g(t)$ is the bath correlation function defined in Eq. 3.17. Returning to the Schrödinger picture, Eq. 3.28 becomes:

$$\frac{d}{dt}\hat{\rho}_{\rm S}(t) = -\imath[\hat{H}_S, \hat{\rho}_{\rm S}(t)] - \int_0^t d\tau\left\{g(\tau)[\hat{S}, e^{-\imath\hat{H}_S t}\hat{S}\hat{\rho}_{\rm S}(t-\tau)e^{\imath\hat{H}_S t}] - g^*(\tau)[\hat{S}, e^{-\imath\hat{H}_S t}\hat{\rho}_{\rm S}(t-\tau)\hat{S}e^{\imath\hat{H}_S t}]\right\}. \tag{3.29}$$

At this point, it is useful to express 3.29 in a basis of eigenstates of the system Hamiltonian. i.e. solutions to the time-independent Schrödinger equation $\hat{H}_S|a\rangle = E_a|a\rangle$. Then, the equations of motion for the matrix elements $\rho_{ab}(t) \equiv \langle a|\hat{\rho}_{\rm S}(t)|b\rangle$ are,

$$\begin{aligned}
&\frac{d}{dt}\rho_{ab}(t) = -\imath\omega_{ab}\rho_{ab}(t) \\
-\ &\sum_{cd}\int_0^t d\tau\left\{M_{ac,cd}(\tau)e^{\imath\omega_{bc}\tau}\rho_{db}(t-\tau) + M_{cd,db}(-\tau)e^{\imath\omega_{da}\tau}\rho_{ac}(t-\tau)\right\} \\
+\ &\sum_{cd}\int_0^t d\tau\left\{M_{db,ac}(\tau)e^{\imath\omega_{da}\tau} + M_{db,ac}(-\tau)e^{\imath\omega_{bc}\tau}\right\}\rho_{cd}(t-\tau),
\end{aligned} \tag{3.30}$$

where we have defined $M_{ab,cd}(t) \equiv g(t)S_{ab}S_{cd}$, with $S_{ab} \equiv \langle a|\hat{S}|b\rangle$ and $\omega_{ab} = E_a - E_b$. At this point we invoke the Markov approximation, which assumes that $g(t)$ decays on a timescale much faster than the evolution of the system due to its coupling to the bath. This corresponds to making approximations of the form

$$\int_0^t d\tau M_{ac,cd}(\tau)e^{\imath\omega_{bc}\tau}\rho_{db}(t-\tau) \approx \rho_{db}(t)\int_0^\infty d\tau M_{ac,cd}(\tau)e^{\imath\omega_{dc}\tau} \tag{3.31}$$

in Eq. 3.30. There are actually two steps in making the approximation in Eq. 3.31. Firstly, one replaces $\rho_{db}(t-\tau)$ under the integral by $e^{\imath\omega_{db}\tau}\rho_{db}(t)$. The reason one needs to keep the exponential factor $e^{\imath\omega_{db}\tau}$ under the integral is that the evolution of the system density matrix is only slow relative to $g(t)$ when considered in the interaction picture. i.e. the time for the system to relax to equilibrium must be much longer than the bath correlation time, but the Bohr frequencies of the system need not be. The second approximation in Eq.. 3.31 is to extend the upper limit of the integral to ∞. This can be done with impunity if $g(t)$ decays sufficiently fast that the long-time contribution of the integrand to the integral in Eq. 3.31 will be negligible [170]. Substituting the approximation in Eq. 3.31 into Eq. 3.30 yields the Redfield equations:

$$\begin{aligned} &\frac{d}{dt}\rho_{ab}(t) = -\imath\omega_{ab}\rho_{ab}(t) \\ -\ &\sum_{cd}\Big\{R_{ac,cd}(\omega_{dc})\rho_{db}(t) + R^*_{bd,dc}(\omega_{cd})\rho_{ac}(t) \\ -\ &\left[R_{bd,ac}(\omega_{ca}) + R^*_{ca,bd}(\omega_{db})\right]\rho_{cd}(t)\Big\}, \end{aligned} \tag{3.32}$$

where we have defined $R_{ab,cd}(\omega) \equiv \int_0^\infty d\tau M_{ab,cd}(\tau)e^{\imath\omega\tau}$.

The Redfield equations consist of a unitary part given by the first term in Eq. 3.32,

$-\imath\omega_{ab}\rho_{ab}(t)$, and a dissipative part given by the second term. We see that there are several different types of contributions to the Redfield tensor $R_{ab,cb}$. Terms of the form $R_{ab,ab}$ describe pure dephasing, while terms of the form $R_{aa,bb}$ describe population relaxation. As discussed in [156], terms of the form $R_{ab,cc}$ which describe population to coherence transfer are responsible for destroying positivity of the density matrix. If these terms are neglected, one arrives at the "secular" Redfield equations, which can be shown to be of the Lindblad form and therefore preserve positivity. The secular Redfield equations are generally valid when the system does not exhibit a degenerate spectrum of transition frequencies (anharmonic potentials). For a detailed discussion of the validity of the secular approximation we refer the reader to [156].

Chapter 4

Theorems of time-dependent density functional theory for open quantum systems

4.1 Introduction

In the first two chapters we have presented TDDFT and OQS as two separate theories. While the theory of OQS treats the bath degrees of freedom in an approximate way to simplify calculations, traditional OQS treats the system degrees of freedom exactly. However, if the system consists of interacting electrons described by the Hamiltonian in Eq. 2.1, this will not be possible and one must treat the system degrees of freedom approximately as well. By treating the electronic system degrees of freedom using TDDFT and the bath degrees of freedom using OQS, we arrive at an entirely new theory (OQS-TDDFT) which allows for a computationally tractable description of electronic systems interacting with an environment.

Before discussing approximate functionals or applications, we will need to prove theorems analogous to those presented in section 2.2 in order to establish OQS-TDDFT as a formally exact theory. In the next section we will establish an analogous VL construction and RG theorem for OQS-TDDFT. In contrast to usual TDDFT, we will see that in OQS-TDDFT there are several different KS schemes one can use which will be useful in different situations. We will see that it is possible to construct an open KS system of non-interacting electrons interacting with a bath, but we will also see that it is possible to construct a closed system of non-interacting electrons as in usual TDDFT, that reproduces the density of an interacting OQS. In Chapter 5 we will discuss exact properties of functionals for this closed KS scheme by investigating an exactly solvable model system and in Chapter 6 we will formulate the linear response version of OQS-TDDFT using the open KS scheme, which gives rise to environmentally broadened absorption spectra. We now present the theorems of OQS-TDDFT, starting with the VL construction.

4.2 The Van Leeuwen construction for generalized quantum master equations

In order to formally establish an OQS-TDDFT starting from the many-body quantum master equation in Eq. 3.12, we must first establish the open-systems version of the van Leeuwen construction [247]. This proves a one-to-one mapping between densities and potentials for non-unitary dynamics, as well as the existence of several different KS schemes [277, 278].

Our starting point is the master equation of Eq. 3.12, which evolves under the many-electron Hamiltonian in Eq. 2.1. We may now state a theorem concerning the construction of an auxiliary system.

Theorem: Let the original system be described by the density matrix $\hat{\rho}_{\rm S}(t)$, which starting as $\hat{\rho}_{\rm S}(0)$ evolves according to Eq. 3.12. Consider an auxiliary system associated with the density matrix $\hat{\rho}'_{\rm S}(t)$ and initial state $\hat{\rho}'_{\rm S}(0)$, which is governed by the master equation

$$\frac{\partial\hat{\rho}'_{\rm S}(t)}{\partial t} = -\imath[\hat{H}'_{\rm S}(t),\hat{\rho}'_{\rm S}(t')] + \int_0^t dt'\breve{K}'(t,t')\hat{\rho}'_{\rm S}(t') + \Xi'(t) \tag{4.1}$$

and with $\breve{K}'(t,t')$ and $\Xi'(t)$ fixed. Here,

$$\hat{H}'_{\rm S}(t) = -\frac{1}{2}\sum_{i=1}^{N}\nabla_i^2 + \sum_{i<j}^{N} v'_{ee}(\mathbf{r}_i,\mathbf{r}_j) + \sum_i v'_{ext}(\mathbf{r}_i,t), \tag{4.2}$$

is the Hamiltonian of an auxiliary system with a different two-particle interaction $v'_{ee}(\mathbf{r},\mathbf{r}')$. Under conditions discussed below, there exists a unique external potential $v'_{ext}(\mathbf{r},t)$ which drives the system in such a way that the particle densities in the original and the auxiliary systems are the same, i.e. $\langle\hat{n}(\mathbf{r})\rangle' = \langle\hat{n}(\mathbf{r})\rangle$ is satisfied for all times, where $\langle\hat{n}(\mathbf{r})\rangle \equiv Tr\{\hat{\rho}_{\rm S}(t)\hat{n}(\mathbf{r})\} = n(\mathbf{r},t)$.

Proof: The method we use closely parallels the van Leeuwen construction given for unitary evolution [247]. By using Eq. 3.12 we can find an equation of motion for the second derivative of the particle density of the original system. This is done by first deriving the equation of motion for the particle density

$$\frac{\partial\langle\hat{n}(\mathbf{r})\rangle_t}{\partial t} = -\nabla\cdot\langle\hat{\mathbf{j}}(\mathbf{r})\rangle_t + Tr\left\{\hat{n}(\mathbf{r})\left[\int_0^t dt'\breve{K}(t,t')\hat{\rho}_{\rm S}(t') + \Xi(t)\right]\right\}, \tag{4.3}$$

as well as for the current density,

$$\frac{\partial\langle\hat{\mathbf{j}}(\mathbf{r})\rangle_t}{\partial t} = -\frac{\langle\hat{n}(\mathbf{r})\rangle_t}{m}\nabla v_{ext}(\mathbf{r},t) + \vec{\mathcal{D}}(\mathbf{r},t) + \frac{\vec{\mathcal{F}}(\mathbf{r},t)}{m} + \vec{\mathcal{G}}(\mathbf{r},t). \tag{4.4}$$

We then differentiate both sides of Eq. 4.3 with respect to time and use Eq. 4.4 to eliminate the current. One thus arrives at,

$$\frac{\partial^2\langle\hat{n}(\mathbf{r})\rangle_t}{\partial t^2} = \nabla\cdot\{\langle\hat{n}(\mathbf{r})\rangle_t\nabla v_{ext}(\mathbf{r},t)/m - \vec{\mathcal{D}}(\mathbf{r},t) - \vec{\mathcal{F}}(\mathbf{r},t)/m - \vec{\mathcal{G}}(\mathbf{r},t)\} + \mathcal{J}(\mathbf{r},t), \tag{4.5}$$

subject to the initial conditions

$$\langle\hat{n}(\mathbf{r})\rangle'_{t=0} = \langle\hat{n}(\mathbf{r})\rangle_{t=0}, \tag{4.6a}$$

$$\left.\frac{\partial\langle\hat{n}(\mathbf{r})\rangle'_t}{\partial t}\right|_{t=0} = \left.\frac{\partial\langle\hat{n}(\mathbf{r})\rangle_t}{\partial t}\right|_{t=0}. \tag{4.6b}$$

i.e. we demand that the densities and their first derivatives be the same at the initial time as in the usual VL construction. In Eq. 4.5, each term has a clear physical interpretation. The quantity $\nabla v_{ext}(\mathbf{r},t)$ is proportional to the external electric field acting on the system,

$$\vec{\mathcal{D}}(\mathbf{r},t) = -\frac{1}{4}\sum_{\alpha,\beta}\hat{\beta}\frac{\partial}{\partial\alpha}\langle\sum_i\{\hat{v}_{i\alpha},\{\hat{v}_{i\beta},\delta(\mathbf{r}-\hat{\mathbf{r}}_i)\}\}\rangle \tag{4.7}$$

is the divergence of the stress tensor, where $\alpha,\beta = x,y,z$ label Cartesian indices, and

$$\vec{\mathcal{F}}(\mathbf{r},t) = -\langle\sum_i\delta(\mathbf{r}-\hat{\mathbf{r}}_i)\sum_{j\neq i}\nabla_{\mathbf{r}_i}v_{ee}(\mathbf{r}_i-\mathbf{r}_j)\rangle \tag{4.8}$$

is the internal force density caused by the pairwise potential. In addition to these quantities which arise in usual TDDFT, we have defined two new quantities,

$$\vec{\mathcal{G}}(\mathbf{r},t) = \quad Tr\left\{\hat{\mathbf{j}}(\mathbf{r})\left[\int_0^t dt'\breve{K}(t,t')\hat{\rho}_{\mathrm{S}}(t') + \Xi(t)\right]\right\} \tag{4.9a}$$

$$\mathcal{J}(\mathbf{r},t) = \frac{\partial}{\partial t}Tr\left\{\hat{n}(\mathbf{r})\left[\int_0^t dt'\breve{K}(t,t')\hat{\rho}_{\mathrm{S}}(t') + \Xi(t)\right]\right\}, \tag{4.9b}$$

which are unique to OQS-TDDFT and arise from forces induced by the bath.

We can now repeat the same procedure in the primed system, to arrive at the equation of motion for the second derivative of the density in terms of primed quantities,

$$\frac{\partial^2\langle\hat{n}(\mathbf{r})\rangle'_t}{\partial t^2} = \nabla\cdot\{\langle\hat{n}(\mathbf{r})\rangle'_t\nabla v'_{ext}(\mathbf{r},t)/m - \vec{\mathcal{D}}'(\mathbf{r},t) - \vec{\mathcal{F}}'(\mathbf{r},t)/m - \vec{\mathcal{G}}'(\mathbf{r},t)\} + \mathcal{J}'(\mathbf{r},t). \tag{4.10}$$

If we subtract Eq. 4.5 from Eq. 4.10 and *demand* that $\langle\hat{n}(\mathbf{r})\rangle'_t = \langle\hat{n}(\mathbf{r})\rangle_t$, we arrive at the equation

$$\begin{aligned} -\nabla\cdot[\frac{\langle\hat{n}(\mathbf{r})\rangle_t}{m}\nabla(\Delta v'_{ext}(\mathbf{r},t))] = &-\nabla\cdot[\vec{\mathcal{D}}'(\mathbf{r},t) + \frac{\vec{\mathcal{F}}'(\mathbf{r},t)}{m} + \vec{\mathcal{G}}'(\mathbf{r},t)] + \mathcal{J}'(\mathbf{r},t) \\ &+\nabla\cdot[\vec{\mathcal{D}}(\mathbf{r},t) + \frac{\vec{\mathcal{F}}(\mathbf{r},t)}{m} + \vec{\mathcal{G}}(\mathbf{r},t)] - \mathcal{J}(\mathbf{r},t), \end{aligned} \tag{4.11}$$

where we have defined $\Delta v'_{ext}(\mathbf{r},t) \equiv v'_{ext}(\mathbf{r},t) - v_{ext}(\mathbf{r},t)$. We now expand both sides of Eq. 4.11 in a Taylor series with respect to time to arrive at

$$\begin{aligned} -\nabla\cdot\left[n_0(\mathbf{r})\nabla v'_{ext;l}(\mathbf{r})\right] = &-\nabla\cdot[n_0(\mathbf{r})\nabla v_{ext;l}(\mathbf{r})] \\ &-\nabla\cdot\left[m\vec{\mathcal{D}}'_l(\mathbf{r}) + \vec{\mathcal{F}}'_l(\mathbf{r}) + m\vec{\mathcal{G}}'_l(\mathbf{r})\right] + m\mathcal{J}'_l(\mathbf{r},t) \\ &+\nabla\cdot\left[m\vec{\mathcal{D}}_l(\mathbf{r}) + \vec{\mathcal{F}}_l(\mathbf{r}) + m\vec{\mathcal{G}}_l(\mathbf{r})\right] - m\mathcal{J}_l(\mathbf{r},t) \\ &+\nabla\cdot\sum_{k=1}^{l} n_k(\mathbf{r})\nabla\left[\Delta v'_{ext;l-k}(\mathbf{r})\right]. \end{aligned} \tag{4.12}$$

The left-hand side of Eq. 4.12 contains Taylor coefficients of $v'_{ext}(\mathbf{r},t)$ of order l, while the right-hand side depends only on Taylor coefficients of $v'_{ext}(\mathbf{r},t)$ of order $k < l$ and known quantities. Equation 4.12 can therefore be regarded as a *unique* recursion relation for constructing the Taylor coefficients of the auxiliary potential

$v'_{ext}(\mathbf{r},t)$, once a suitable boundary condition is specified. We assume that $v'_{ext;l}(\mathbf{r}) \to 0$ sufficiently quickly as $|\mathbf{r}| \to \infty$ for all l as in usual TDDFT. A more detailed discussion of this boundary condition is given in [247].

Several different KS schemes are now evident. If one sets $v'_{ee}(\mathbf{r},\mathbf{r}') = 0$, but keeps the system open by setting $\breve{K}'(t) = \breve{K}^{KS}(t)$ and $\Xi'(t) = \Xi^{KS}(t)$, the auxiliary system is a non-interacting, but open KS system. This is similar to the construction used in [38], but encompasses the non-Markovian case as well. However, one may also choose $v'_{ee}(\mathbf{r},\mathbf{r}') = 0$ and $\breve{K}'(t) = \Xi'(t) = 0$, whereby the density of the original open system is reproduced with a *closed* (unitarily evolving) and non-interacting KS system.

The OQS-TDDFT version of the Runge-Gross theorem, which is proven by setting $v'_{ee}(\mathbf{r},\mathbf{r}') = v_{ee}(\mathbf{r},\mathbf{r}')$, $\breve{K}'(t) = \breve{K}(t)$ and $\Xi'(t) = \Xi(t)$ in Eq. 4.12, requires only that the potential be time-analytic as in usual TDDFT. However, once one considers an auxiliary system with a different electron-electron interaction and/or system-bath coupling, all quantities appearing in Eq. 4.12 must be time-analytic, including the density, memory kernel and initial correlation terms in both the primed and unprimed systems. As discussed in [146], it is possible for time-analytic potentials to generate densities that are not time-analytic. It seems plausible that a similar situation could arise in OQS-TDDFT, where certain potentials, initial states or memory kernels could produce densities that are not time-analytic and so the OQS-TDDFT van Leeuwen theorem might not hold. However, this still needs to be investigated more extensively. Also, as stated, the theorem assumes that the memory kernel and initial correlations do not depend on the external potential. In fact, this restriction is not essential as discussed in detail in [278].

4.3 The closed Kohn-Sham scheme of OQS-TDDFT

In the previous section, we saw that it is possible to take the KS system to be a non-interacting system evolving unitarily under a time-dependent driving field that will reproduce the density of the original interacting OQS. In this scheme, the KS potential v'_{ext} can be partitioned as

$$v'_{ext} = v_{ext} + v_h + v_{xc} + v_{\text{bath}}. \tag{4.13}$$

Here, v_{ext} is the original external potential acting on the real system. The electron-electron interaction is replaced by the sum of a Hartree term

$$v_h = \int d^3r' \frac{\langle \hat{n}(\mathbf{r}') \rangle_t}{|\mathbf{r} - \mathbf{r}'|}, \tag{4.14}$$

and a standard approximation to the exchange-correlation (xc) potential v_{xc}, such as an adiabatic functional [67]. Finally, v_{bath} is a new term which represents a driving field that mimics the interactions of the system with the bath. This KS scheme places electron-electron and system-bath interactions on the same footing, so real-time TDDFT computer codes could in principle be easily modified to include the dissipative effects of an environment [43]. Such a scheme is computationally desirable, since one would only need to propagate N orbital equations for an N-electron system as in usual TDDFT. This is in contrast to a density matrix approach, where one would need to propagate $M^2 - 1$ equations for the elements of the density matrix, with M being the (in principle infinite) dimensionality of the Hilbert space.

In usual TDDFT, the KS potential is a functional of the density and therefore the KS equations can be regarded as nonlinear Schrodinger equations (NLSE). In OQS,

equations of motion for systems coupled to heat baths are often described by Langevin equations, where frictional forces are introduced through velocity-dependent potentials (Stokes law) [288]. These frictional forces also give rise to a nonlinear Schrodinger equation, since velocity-dependent potentials can be regarded as functionals of the current or of time-derivatives of the density. Therefore, the search for approximations to $v_{\rm bath}$ could start by investigating work already done in the field of dissipative nonlinear Schrödinger equations [118, 119, 30, 86] and time-dependent self consistent field (TD-SCF) methods [149, 137, 154]. In this section, we describe a simple Markovian bath functional (MBF) inspired by a NLSE suggested by Kostin [118].

Consider a single particle in one dimension whose evolution is given by the NLSE,

$$\imath\frac{\partial\psi}{\partial t} = H\psi, \tag{4.15}$$

where

$$H = \frac{p^2}{2m} + v_{ext} + v_{\rm bath}, \tag{4.16}$$

and p and v_{ext} are the momentum of the particle and the external potential respectively. The dissipative potential is chosen to have the form

$$v_{\rm bath}(z,t) = \frac{\lambda}{2\imath}\ln\left[\frac{\psi(z,t)}{\psi^*(z,t)}\right]. \tag{4.17}$$

This NLSE has the very interesting property that it satisfies the zero-temperature Langevin equation for the expectation values of the particle's position and momentum. i.e.

$$\langle \dot{z} \rangle = \frac{\langle p \rangle}{M}, \tag{4.18}$$

$$\langle \dot{p} \rangle = -\left\langle \frac{\partial v_{ext}(z,t)}{\partial z} \right\rangle - \lambda \langle p \rangle. \tag{4.19}$$

Interestingly, $v_{\rm bath}$ in Eq. 4.17 can be written as a functional of the density and current as

$$v_{\rm bath}[\langle \hat{n}(z') \rangle_t, \langle \hat{j}(z') \rangle_t] = \lambda \int_{-\infty}^{z} dz' \frac{\langle \hat{j}(z') \rangle_t}{\langle \hat{n}(z') \rangle_t}. \tag{4.20}$$

This identification is very appealing, since the frictional force is proportional to the space integral of the velocity field of the particle, $\langle \hat{j}(z') \rangle_t / \langle \hat{n}(z') \rangle_t$. Furthermore, the friction coefficient λ can be derived from a microscopic model of harmonic bath modes [170, 232]. Note that $v_{\rm bath}$ at a given time only depends on the momentum of the particle at the same instant, implying that this NLSE is Markovian. This situation can be obtained in the limit where the dynamics of the bath can be described as white noise [179].

Although the discussion above has been given for a single particle, we can heuristically propose Eq. 4.20 as a MBF for TDDFT. In practice, we can re-express $v_{\rm bath}$ in terms of the orbitals of a time-dependent single Slater determinant KS wavefunction (orbital-dependent functional), $\Phi(t) = \frac{1}{\sqrt{N!}} \det[\phi_i(z_j, t)]$ as

$$v_{\rm bath}(z,t) = \lambda \int_{-\infty}^{z} dz' \frac{\sum_i |\phi_i(z',t)|^2 \nabla \alpha_i(z',t)}{\sum_i |\phi_i(z',t)|^2}, \tag{4.21}$$

where $\alpha_i(z',t)$ is the phase of the ith orbital. The extension of the functional to more dimensions follows analogously, although the limits of integration must be studied with care. In the higher dimensional case, the Kohn-Sham current may differ from

the physical current by a purely transverse term and one must resort to a formulation in terms of vector potentials using TDCDFT. Equation 4.21 is easy to implement in a real-time propagation, and has been implemented for a model Helium system interacting with a heat bath [278]. Non-Markovian extensions, as well as functionals where several timescales of relaxation and dephasing exist, are currently under development.

Neuhauser and Lopata [167] have recently reported an important result, which could also be considered a MBF in our formalism. Their functional is inspired by an optimal control approach, where they demand that the energy in the KS system decays monotonically. They show that

$$v_{\rm bath}[\langle\hat{j}(z')\rangle_t] = \int dz' a(z') \frac{\partial\langle\hat{j}(z')\rangle_t}{\partial t}\hat{j}(z) \tag{4.22}$$

achieves such goal. This functional couples the time-derivative of the current density to the current operator with a spatially dependent proportionality constant $a(z')$. Their studies of a jellium cluster also show numerical robustness and provide a practical scheme to include dissipation in a real-time KS calculation. In Chapter 5 we will discuss properties of the exact $v_{\rm bath}$ for a model system and compare with the approximate MBF of Eq. 4.20.

4.4 The open Kohn-Sham scheme of OQS-TDDFT

In section 4.2 we mentioned that one can construct a KS scheme by setting $v'_{ee}(\mathbf{r},\mathbf{r}') = 0$, but keeping the system open by setting $\breve{K}'(t) = \breve{K}^{KS}(t)$ and $\Xi'(t) = \Xi^{KS}(t)$. In this scheme, the density of an interacting open system is reproduced

by a system of non-interacting electrons interacting with a different auxiliary bath described by the memory kernel $\breve{K}^{KS}(t)$ and initial correlation term $\Xi^{KS}(t)$. This scheme has the advantage that dissipation is already accounted for in the KS system, and the approximate functionals do not need to account for the entire effect of the environment as in the closed KS scheme discussed in section 4.3 [226]. We will see in Chapter 6 that the open KS scheme is well suited to linear response theory, while for real-time propagation it has the disadvantage that one must propagate a density matrix rather than a set of orbitals, which as we have mentioned is computationally more demanding [277, 278].

In section 6.2 we will discuss the exact conditions that $\breve{K}^{KS}(t)$ should satisfy for the open KS scheme to be computationally useful, so we will only mention one important property here. The KS Hamiltonian is a sum of single-particle terms since it describes non-interacting electrons. i.e. $\hat{H}^{KS}(t) = \sum_{i=1}^{N} \hat{h}(\hat{\mathbf{r}}_i, \hat{\mathbf{p}}_i; t)$. This means that in the absence of interactions with an environment, the KS one-particle reduced density matrix $\hat{\gamma}(t) \equiv Tr_{2,\ldots N}[\hat{\rho}(t)]$ has a closed equation of motion because the Hamiltonian cannot induce two-particle or higher-order correlations. In the language of time-dependent reduced density matrix theory, this arises from the fact that the BBGKY hierarchy closes at first-order if the Hamiltonian is non-interacting [110, 29, 31]. In order for the open KS scheme to be useful practically, this property must be preserved, because if one needed to propagate higher-order KS density matrices just to reproduce the density, the scheme would not be computationally useful. This

implies that the KS memory kernel should be a sum of single-electron terms. i.e.

$$\breve{K}^{KS}(t) = \sum_{i=1}^{N} \breve{k}(\hat{\mathbf{r}}_i, \hat{\mathbf{p}}_i; t). \tag{4.23}$$

In this case, one can trace both sides of Eq. 4.1 over $N-1$ electron coordinates to arrive at a closed equation of motion for $\hat{\gamma}(t)$. In [38] a Lindblad equation for the KS one-particle density matrix was derived using a Markovian superoperator of the form in Eq. 4.23, while in chapter 6 we will derive an analogous KS Redfield equation [226, 173].

4.5 Görling-Levy perturbation theory and the double adiabatic connection

The content of the proof presented in section 4.2 is conveniently summarized by parametrizing the auxiliary system's master equation with two coupling constants λ and β as,

$$\frac{d}{dt}\hat{\rho}'_{\mathrm{S}}(\lambda,\beta,t) = -\imath[\hat{H}'_{\mathrm{S}}(\lambda,\beta,t), \hat{\rho}'_{\mathrm{S}}(\lambda,\beta,t)] + \beta\Big\{\int_0^t d\tau\ \breve{K}'(t,\tau;\lambda)\hat{\rho}'_{\mathrm{S}}(\lambda,\beta,\tau) + \Xi'(t;\lambda)\Big\}, \tag{4.24}$$

where

$$\hat{H}'_{\mathrm{S}}(\lambda,\beta,t) = -\frac{1}{2}\sum_{i=1}^{N}\nabla_i^2 + \lambda\sum_{i<j}^{N} v_{ee}(\mathbf{r}_i,\mathbf{r}_j) + \sum_i v'_{ext}(\lambda,\beta,\mathbf{r}_i,t). \tag{4.25}$$

Here, λ scales the electron-electron interaction and lies in the range $0 \leqslant \lambda \leqslant 1$. When $\lambda = 1$, we have a fully interacting system, while when $\lambda = 0$ we have a system of

non-interacting electrons. The memory kernel and initial correlations are functions of λ as well. Similarly, β scales the non-unitary terms in the master equation and lies in the range $0 \leqslant \beta \leqslant 1$. When $\beta = 1$, we have a fully open system while when $\beta = 0$ the system evolves unitarily. The simple linear parameterization of Eq. 4.24 in terms of β is not unique, and one could consider a more complicated parameterization where $\breve{K}'$ and Ξ' depend on β as well. For instance, if one set $\beta = \epsilon$ from Eq. 3.2, then the right hand side of Eq. 4.24 would contain all orders in β.

The theorem of section 4.2 guarantees the existence and uniqueness of a potential $v'_{ext}(\lambda, \beta, \mathbf{r}, t)$ for all λ and β, which drives the auxiliary system in such a way that the true density is obtained independent of the values of λ and β. This can be viewed as a two-dimensional extension of the usual electron-electron adiabatic connection in closed-systems TDDFT [75]. It is depicted graphically in Figure 4.1. At the coordinate (1,1), we have the original fully interacting and open system, while at the coordinate (0,0) we have the non-interacting and closed KS scheme. Defining $\breve{K}'(\lambda = 0) \equiv \breve{K}^{KS}$ and $\Xi'(\lambda = 0) \equiv \Xi^{KS}$ as the memory kernel and initial correlations of an open system of non-interacting electrons, we see that the point (1,0) describes the open KS scheme. In the remainder of the thesis, we will focus on the points (0,0) and (1,0). However, our proof shows that any coordinate lying within the double adiabatic connection square represents a viable KS scheme.

In traditional Görling-Levy (GL) perturbation theory, one perturbs about the limit that the electron-electron interaction parameter λ is small [77, 75, 76, 78, 74]. This corresponds to performing perturbation theory about the line $(\beta, 0)$ in the double adiabatic connection square. In OQS-TDDFT one can also perturb about the limit

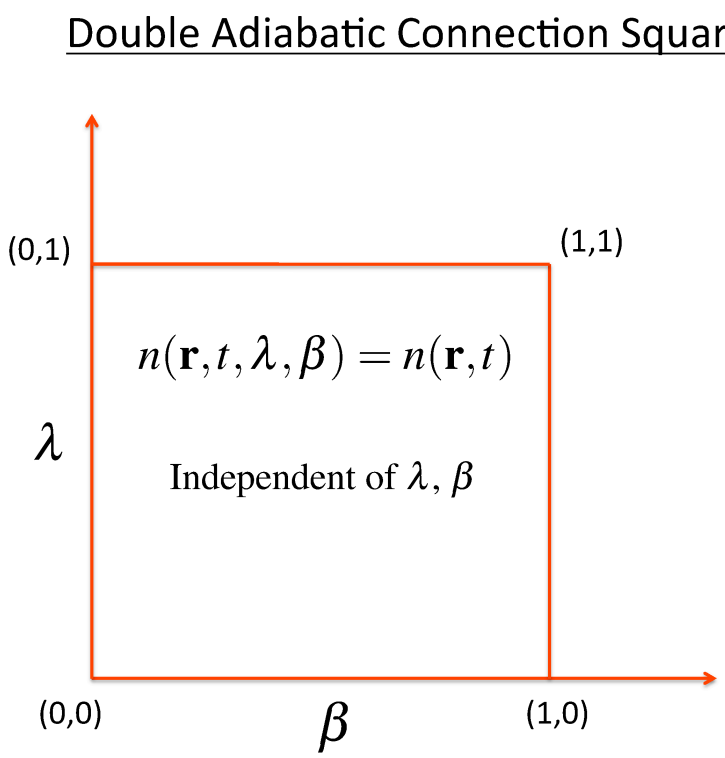

Figure 4.1: The relevant points on the double adiabatic connection square are: **(1,1)**: The original interacting OQS; **(1,0)**: The non-interacting yet open Kohn-Sham scheme; **(0,0)**: The non-interacting and closed Kohn-Sham scheme.

of small system-bath interaction in which the parameter β is small. This corresponds to performing perturbation theory about the line $(0, \lambda)$. In this way, one can derive a variety of different functionals from this generalized GL perturbation theory scheme. In Chapter 6 we will derive an approximate frequency dependent exchange-correlation kernel by perturbing about the point $(1, 0)$, which describes the open KS scheme. As in DFT and TDDFT, the double adiabatic connection provides a powerful tool for deriving exact conditions on OQS-TDDFT functionals and is currently being explored

in more detail.

Having discussed the fundamental theorems of OQS-TDDFT, we now turn to a detailed study of the closed KS scheme presented in section 4.3.

Chapter 5

Relaxation and dephasing in open quantum systems time-dependent density functional theory: Properties of exact functionals from an exactly-solvable model system

5.1 Introduction

In Chapter 4 we showed that the time-dependent density of an interacting OQS can be reproduced with a non-interacting and closed (unitarily evolving) Kohn-Sham system. In principle, the closed Kohn-Sham scheme is remarkably useful for real-time dynamics, since it allows one to calculate any property of a many-body OQS by unitarily propagating a set of one-particle orbital equations evolving in a local potential. With suitable functionals, such a scheme could readily be implemented

in existing real-time TDDFT codes [43, 152, 13]. In practice, the OQS-TDDFT exchange-correlation potential is very complicated object. Not only does it have initial-state and memory dependence as in usual TDDFT [144, 142, 140, 122], but it must also be a functional of bath quantities such as the bath spectral density. As a result, very few exact conditions are known about the exchange-correlation potential of OQS-TDDFT.

In the present chapter, we study exact features of the OQS-TDDFT closed Kohn-Sham scheme using an exactly-solvable one-electron model system: A single electron in a one-dimensional harmonic potential evolving under the Lindblad master equation. We study two representative limits of the dissipative dynamics: Pure dephasing and relaxation with no pure dephasing. By focusing on a single electron, we are able to isolate the part of the exact functional arising solely from interaction with the bath, without the need to describe electron-electron interaction effects within the system.

The chapter is organized as follows. In section 5.2, we review the theory of OQS for a many-electron system and the closed Kohn-Sham scheme presented in previous work [278, 277]. Much of section 5.2 was discussed in previous chapters, but we repeat it here so that the chapter is self-contained. Section 5.3 presents the model system to be analyzed and discusses the procedure used to obtain exact Kohn-Sham quantities. Section 5.4 presents results and an analysis. The chapter concludes with an outlook and discussion of future challenges for the development of OQS-TDDFT functionals in section 5.5.

5.2 OQS-TDDFT using a unitary propagation

The formally exact many-body master equation

The starting point of many-body OQS is the unitary evolution for the full density matrix of the system and the reservoir (we use the terms "reservoir" and "bath" interchangeably throughout) ,

$$\frac{d}{dt}\hat{\rho}(t) = -\imath[\hat{H}(t), \hat{\rho}(t)]. \tag{5.1}$$

The full Hamiltonian is given by

$$\hat{H}(t) = \hat{H}_S(t) + \hat{H}_R + \hat{V}. \tag{5.2}$$

Here,

$$\hat{H}_S(t) = -\frac{1}{2}\sum_{i=1}^{N}\nabla_i^2 + \sum_{i<j}^{N}\frac{1}{|\mathbf{r}_i - \mathbf{r}_j|} + \sum_i v_{ext}(\mathbf{r}_i, t), \tag{5.3}$$

is the Hamiltonian of the electronic system of interest in an external potential $v_{ext}(\mathbf{r}, t)$. This potential generally consists of a static external potential due to the nuclei and an external time-dependent driving field. The system-bath coupling, $\hat{V}$, is generally assumed to be weak and is treated using perturbation theory in most applications. $\hat{V}$ acts in the combined Hilbert space of the system and reservoir and so it couples the two subsystems. $\hat{H}_R$ is the Hamiltonian of the reservoir, which typically has a dense spectrum of eigenstates relative to the system. The density of states of $\hat{H}_R$ determines the decay rate of reservoir correlation functions, whose time-scale in turn determines the reduced system dynamics.

Defining the reduced density operator for the electronic system alone by tracing

over the reservoir degrees of freedom,

$$\hat{\rho}_S(t) = Tr_R\{\hat{\rho}(t)\}, \tag{5.4}$$

one arrives at the formally-exact quantum master equation,

$$\frac{d}{dt}\hat{\rho}_S(t) = -\imath[\hat{H}_S(t), \hat{\rho}_S(t)] + \int_{t_0}^{t} d\tau \breve{K}(t-\tau)\hat{\rho}_S(\tau) + \Xi(t). \tag{5.5}$$

Here, $\breve{K}(t-\tau)$ is the memory kernel and $\Xi(t)$ arises from initial correlations between the system and its environment. It is referred to as the inhomogeneous term. The above equation is still formally exact, as $\hat{\rho}_S(t)$ gives the exact expectation value of any observable depending only on the electronic degrees of freedom. In practice, however, approximations to $\breve{K}$ and Ξ are required. Of particular importance in TDDFT is the time-dependent electronic density,

$$n(\mathbf{r}, t) = Tr_S\{\hat{\rho}_S(t)\hat{n}(\mathbf{r})\}, \tag{5.6}$$

where $\hat{n}(\mathbf{r}) = \sum_i^N \delta(\mathbf{r} - \hat{\mathbf{r}}_i)$ is the number density operator for the electronic system. For OQS, the continuity equation is not strictly satisfied and is modified to

$$\begin{aligned} \frac{\partial}{\partial t} n(\mathbf{r}, t) &= -\nabla \cdot Tr_S\{\hat{\rho}_S(t)\hat{\mathbf{j}}_p(\mathbf{r})\} \\ + \quad & Tr\{\hat{n}(\mathbf{r}) \left(\int_{t_0}^{t} d\tau \breve{K}(t-\tau)\hat{\rho}_S(\tau) + \Xi(t) \right)\}. \end{aligned} \tag{5.7}$$

Here, the first term is the divergence of the usual current arising in closed systems, and is referred to as the "Hamiltonian current". The second term is a contribution to the current due to scattering of electrons with particles in the bath and arises from the non-unitary part of the evolution. One may define a "Dissipative current"

by [69, 28],

$$-\nabla \cdot \mathbf{j}_{disp}(\mathbf{r},t) = Tr\{\hat{n}(\mathbf{r})\left(\int_{t_0}^{t} d\tau \breve{K}(t-\tau)\hat{\rho}_S(\tau) + \Xi(t)\right)\}. \tag{5.8}$$

It will be seen later that the functional dependence of the Kohn-Sham potential on $\mathbf{j}_{disp}(\mathbf{r},t)$ plays an important role in OQS-TDDFT.

The Markov approximation and Lindblad master equation

Without suitable approximations to the memory kernel $\breve{K}(t)$, solving eq. 6.5 is not easier than solving the full system-bath dynamics described in eq. 5.1. One often invokes the Markov approximation, in which the memory kernel is local in time, i.e.

$$\int_{t_0}^{t} d\tau \breve{K}(t-\tau)\hat{\rho}_S(\tau) = \breve{D}\hat{\rho}_S(t). \tag{5.9}$$

The Markov approximation is valid when $\tau_S \gg \tau_B$ is satisfied, where τ_S is the time-scale for the system to relax to thermal equilibrium and τ_B is the longest correlation time of the bath. Roughly speaking, the memory of the bath can be neglected when describing the reduced system dynamics, because the bath decorrelates from itself before the system has had a chance to evolve appreciably. τ_S is inversely related to the magnitude of system-bath coupling, and so a weak interaction between the electrons and the environment is implicit in this condition as well.

The Lindblad form of the Markovian master equation,

$$\breve{D}\hat{\rho}_S(t) = \sum_{mn}\left\{L_{mn}\hat{\rho}_S(t)L_{mn}^{\dagger} - \frac{1}{2}L_{mn}^{\dagger}L_{mn}\hat{\rho}_S(t) - \frac{1}{2}\hat{\rho}_S(t)L_{mn}^{\dagger}L_{mn}\right\}, \tag{5.10}$$

is constructed to guarantee complete positivity of the density matrix [36]. This is desirable, since the populations of any physically sensible density matrix should remain

positive during the evolution.

As written in eq. 5.10, the Lindblad equation is simply a mathematical construction which is guaranteed to give a positive density matrix. However, the bath operators L_{nm} can be derived microscopically starting from a system-bath Hamiltonian of the form given in eq. 5.2 [132]. In general, the operators L_{nm} will describe "jumps" between eigenstates of $\hat{H}_S$ induced by scattering of electrons with bath particles. We will discuss specific forms of the L_{nm} in subsequent sections.

Open-interacting to closed-noninteracting mapping

In this section, we briefly outline the proof given in [278], whereby the density of an interacting and open electronic system is reproduced using a closed and non-interacting Kohn-Sham system.

Starting from the many-body master equation given in eq. 5.5, one considers an auxiliary "primed" system described by a density matrix $\hat{\rho}'_S(t)$, evolving with a different Hamiltonian

$$\hat{H}'_S(t) = -\frac{1}{2}\sum_{i=1}^{N}\nabla_i^2 + \sum_{i<j}^{N}\frac{\alpha}{|\mathbf{r}_i - \mathbf{r}_j|} + \sum_i v'(\alpha, \mathbf{r}_i, t), \tag{5.11}$$

at interaction strength α, and with different memory kernel $\breve{K}'(t)$ and initial correlations $\Xi'(t)$. This auxiliary system evolves under the master equation

$$\frac{d}{dt}\hat{\rho}'_S(t) = -\imath[\hat{H}'_S(t), \hat{\rho}'_S(t)] + \int_{t_0}^{t} d\tau \breve{K}'(t-\tau)\hat{\rho}'_S(\tau) + \Xi'(t). \tag{5.12}$$

Following a construction similar in spirit to [247], one is able to prove that there *exists* a *unique* local potential $v'(\alpha, \mathbf{r}, t)$ for the auxiliary system, at any interaction

strength α, and for arbitrary $\breve{K}'(t-t')$ and $\Xi'(t)$ (with some restrictions discussed in [278]), such that

$$n(\mathbf{r},t) = Tr_S\{\hat{\rho}_S(t)\hat{n}(\mathbf{r})\} = Tr_S\{\hat{\rho}'_S(t)\hat{n}(\mathbf{r})\} \tag{5.13}$$

is satisfied for all times. This means that for a fixed open and interacting system, one can always construct an auxiliary system with different electron-electron and system-bath interactions, such that the potential $v'(\alpha,\mathbf{r},t)$ enforces the correct density evolution. If one sets $\alpha = 0$, but keeps $\breve{K}'(t) = \breve{K}(t)$ and $\Xi'(t) = \Xi(t)$ then the auxiliary system is a non-interacting, but open Kohn-Sham system. This is similar to the construction used in [38, 226], but encompasses the non-Markovian case as well. However, one may also choose $\alpha = 0$ and $\breve{K}'(t) = \Xi'(t) = 0$, whereby the density of the original open system is reproduced with a closed and non-interacting Kohn-Sham system. In this case, the density matrix in the auxiliary system is a pure state given by

$$\hat{\rho}'_S(t) = \Phi^*(t)\Phi(t), \tag{5.14}$$

where $\Phi(t)$ is a single Slater determinant. This determinant is constructed by propagating a set of single-particle orbital equations,

$$\imath\frac{\partial}{\partial t}\phi_i(\mathbf{r},t)\left\{-\frac{1}{2}\nabla^2 + v_{ks}(\mathbf{r},t)\right\}\phi_i(\mathbf{r},t) \tag{5.15}$$

as in usual TDDFT. The density of the original interacting and open system is then simply obtained by square-summing the orbitals. i.e.

$$n(\mathbf{r},t) = \sum_i |\phi_i(\mathbf{r},t)|^2 = Tr_S\{\hat{\rho}_S(t)\hat{n}(\mathbf{r})\}. \tag{5.16}$$

In analogy to usual TDDFT, the Kohn-Sham potential is partitioned as

$$v_{ks}(\mathbf{r},t) = v_{ext}(\mathbf{r},t) + v_h(\mathbf{r},t) + v_{xc}^{open}(\mathbf{r},t), \tag{5.17}$$

where $v_h(\mathbf{r},t)$ is the Hartree potential and the unknown functional $v_{xc}^{open}(\mathbf{r},t)$ accounts for electron-electron interaction within the system as well as interaction between the system and bath. Ideally, these two contributions well be additive, so that one may use standard adiabatic functionals to account for electron-electron interaction within the system and construct dissipative bath functionals to account for system-bath coupling. In general,

$$v_{xc}^{open}(\mathbf{r},t) = v_{xc}^{open}(\mathbf{r},t)[n, \breve{K}, \Xi, \hat{\rho}_S(0), \Phi(0)]. \tag{5.18}$$

Formally, the open-systems exchange-correlation potential is a functional not only of the density, but also of the memory kernel, inhomogeneous term and initial state of the interacting open system, as well as the initial state of the closed Kohn-Sham system.

5.3 An exactly solvable model system

In this section, we construct the exact OQS-TDDFT Kohn-Sham potential for an exactly-solvable model system: one electron in a harmonic well evolving under the Lindblad equation. Our analysis focuses on two limiting cases of the Lindblad master equation. The first limit is that of pure dephasing without relaxation in which the bath decoheres the system, but no energy is exchanged. The second limit is that of relaxation with no pure dephasing.

Construction of the exact OQS functional

With the system Hamiltonian given by

$$\hat{H}_S = -\frac{1}{2}\frac{d^2}{dx^2} + \frac{1}{2}\omega^2 x^2, \tag{5.19}$$

the Lindblad equation

$$\begin{aligned} \frac{d}{dt}\hat{\rho}_S(t) &= -\imath[\hat{H}_S, \hat{\rho}_S(t)] \\ &+ \sum_{mn}\Big\{ L_{mn}\hat{\rho}_S(t)L_{mn}^\dagger \\ &- \frac{1}{2}L_{mn}^\dagger L_{mn}\hat{\rho}_S(t) - \frac{1}{2}\hat{\rho}_S(t)L_{mn}^\dagger L_{mn}\Big\} \end{aligned} \tag{5.20}$$

can be solved exactly to obtain $\hat{\rho}_S(t)$. The exact time-dependent OQS density can then be constructed using eq. 5.6. With an exact OQS density, it is a simple exercise to construct the closed Kohn-Sham system which reproduces this density using a unitary evolution. In this section we work in one dimension, but the formulas apply to higher dimensions as well.

For one electron, there is a single occupied Kohn-Sham orbital given by [92, 91, 10]

$$\phi(x,t) = \sqrt{n(x,t)}e^{\imath\alpha(x,t)}. \tag{5.21}$$

By construction, this orbital must evolve under the time-dependent Kohn-Sham equation

$$\imath\frac{\partial}{\partial t}\phi(x,t) = \big\{ -\frac{1}{2}\frac{d^2}{dx^2} + v_s(x,t)\big\}\phi(x,t), \tag{5.22}$$

in such a way that the true OQS density is reproduced for all times, i.e.

$$n(x,t) = |\phi(x,t)|^2 = Tr_S\{\hat{\rho}_S(t)\hat{n}(\mathbf{x})\}. \tag{5.23}$$

Here,

$$v_{ks}(x,t) = v_{ext}(x) + v_h(x,t) + v_{xc}^{open}(x,t) \tag{5.24}$$

is the OQS-TDDFT Kohn-Sham potential. We now substitute eq. 5.21 in eq. 5.22 and use the fact that for one electron, the exchange potential exactly cancels the self interaction in the Hartree potential. The result is an exact expression for the OQS-TDDFT correlation potential in terms of known quantities,

$$\begin{aligned} v_c^{open}(x,t) &= -\frac{\partial}{\partial t}\alpha(x,t) - \frac{1}{2}\left[\frac{\partial}{\partial x}\alpha(x,t)\right]^2 \\ &+ \frac{1}{4n(x,t)}\frac{\partial^2}{\partial x^2}n(x,t) \\ &- \frac{1}{8n(x,t)^2}\left[\frac{\partial}{\partial x}n(x,t)\right]^2 - v_{ext}(x). \end{aligned} \tag{5.25}$$

As in [238, 91], it is instructive to separate $v_c^{open}(x,t)$ into an adiabatic and dynamical part,

$$v_c^{open}(x,t) = v_c^{dyn}(x,t) + v_c^{ad}(x,t). \tag{5.26}$$

Here,

$$v_c^{ad}(x,t) = \frac{1}{4n(x,t)}\frac{\partial^2}{\partial x^2}n(x,t) - \frac{1}{8n(x,t)^2}\left[\frac{\partial}{\partial x}n(x,t)\right]^2 - v_{ext}(x), \tag{5.27}$$

is the exact functional of ground-state DFT for one electron, or two electrons in a spin-singlet evaluated on the instantaneous OQS density [66] . The dynamical part,

$$v_c^{dyn}(x,t) = -\frac{\partial}{\partial t}\alpha(x,t) - \frac{1}{2}\left[\frac{\partial}{\partial x}\alpha(x,t)\right]^2, \tag{5.28}$$

is a strictly-dynamical contribution which vanishes when the system is in thermal equilibrium. From the generalized continuity equation, eq. 5.7, one finds that the

phase of the Kohn-Sham orbital is given by

$$-\frac{\partial}{\partial x}\alpha(x,t) = \frac{j(x,t)}{n(x,t)} + \frac{j_{disp}(x,t)}{n(x,t)}. \tag{5.29}$$

We see that for OQS, the dynamical correlation potential $v_c^{dyn}(x,t)$ contains a contribution from the Hamiltonian current that is also present in usual TDDFT. In addition, there is a new contribution from the bath arising through $\mathbf{j}_{disp}$. Therefore, the OQS correlation potential is a functional not only of the Hamiltonian current, but the dissipative current as well. In the following, we will consider the two limiting cases mentioned above: Pure dephasing without relaxation and relaxation without pure dephasing.

Pure dephasing without relaxation

We first consider a situation in which the OQS evolves under a Lindblad master equation which induces pure dephasing, but no relaxation [156, 48, 36, 192]. In this case, the Lindblad operators are diagonal in a basis of eigenstates of eq. 5.19 and given by

$$L_{mn} = \delta_{mn}\sqrt{\frac{\gamma_m}{2}}|m\rangle\langle m|, \tag{5.30}$$

where $|m\rangle$ is the mth eigenstate of the oscillator. Since the operators L_m are diagonal, the populations $\rho_{mm}(t)$ remain unchanged as the system evolves. This implies that energy is conserved during the evolution, as the bath cannot drain energy away from the system. However, the coherences given by the off-diagonal density matrix elements, $\rho_{nm}(t)$, decay exponentially with a rate given by

$$\tau^{mn}_{decoherence} = \frac{1}{2}(\gamma_m + \gamma_n). \tag{5.31}$$

Pure dephasing describes a situation in which system-bath collisions are elastic, so that the bath decoheres the system without exchanging energy.

Relaxation without pure dephasing

Next, we consider the case of relaxation without pure dephasing, in which the Lindblad operators are strictly off-diagonal [156]. i.e.

$$L_{mn} = \sqrt{\gamma_{mn}}|m\rangle\langle n|, \quad m \neq n$$
$$L_{mn} = 0, \quad m = n. \tag{5.32}$$

In order to ensure that the populations of the equilibrium solution obey detailed balance, one also requires that

$$\gamma_{mn} = e^{\beta\omega_{mn}}\gamma_{nm}, \tag{5.33}$$

where $\beta = \frac{1}{k_B T}$ is the inverse temperature. With the Lindblad operators given by eq. 5.32, the populations evolve according to

$$\frac{d}{dt}\rho_{nn}(t) = \sum_m \gamma_{nm} e^{-\beta\omega_{nm}}\rho_{mm}(t) - \rho_{nn}(t)\sum_m \gamma_{mn}e^{-\beta\omega_{mn}}. \tag{5.34}$$

The first term in eq. 5.34 expresses the rate at which population is transferred to ρ_{nn} from all other populations $m \neq n$, while the second term expresses the rate at which population leaves ρ_{nn}. It can be readily verified that the right hand side of eq. 5.34 vanishes at equilibrium where $\rho^{eq}_{nn} = \frac{e^{-\beta E_n}}{\sum_m e^{-\beta E_m}}$ and these two rates balance.

The coherences evolve according to

$$\frac{d}{dt}\rho_{nm}(t) = \left\{ -\frac{1}{2}\sum_l \gamma_{ln}e^{-\beta\omega_{ln}} - \frac{1}{2}\sum_l \gamma_{lm}e^{-\beta\omega_{lm}} \right\}\rho_{nm}(t). \tag{5.35}$$

This shows that even in the absence of pure dephasing, relaxation still necessarily implies decoherence. For the special case of a two-level system, one can readily see from eq's. 5.34 and 5.35 that the decoherence rate is exactly half of the relaxation rate. This is analogous to the ubiquitous phenomenological formula from NMR spectroscopy

$$\frac{1}{T_2} = \frac{1}{2T_1} + \frac{1}{T_2^*}, \tag{5.36}$$

relating the time-scale for decoherence T_2, to that of relaxation T_1 and pure dephasing T_2^* [156, 194]. In the absence of pure dephasing, the time-scale for decoherence is twice that of relaxation, which is confirmed by eq's. 5.34 and 5.35.

5.4 Results and analysis

We now present and analyze the results of the inversion procedure mentioned in the previous section for obtaining the exact Kohn-Sham quantities. For all calculations, we choose the initial state of the OQS to be the pure state

$$|\psi(0)\rangle = \frac{1}{\sqrt{2}}(|0\rangle + |1\rangle), \tag{5.37}$$

which corresponds to a density matrix with initial elements $\rho_{00}(0) = \rho_{11}(0) = \rho_{10}(0) = \rho_{01}(0) = \frac{1}{2}$ and all other entries equal to zero. The frequency of the oscillator is taken to be $\omega = 1$.

For the pure dephasing case, we choose the parameters $\gamma_0 = \gamma_1 = 0.15$ a.u., leading to a decay of the initial coherence between $|0\rangle$ and $|1\rangle$ at a rate of $\tau^{01}_{decoherence} = 0.15$ a.u. as given by eq. 5.31.

For the case of relaxation without pure dephasing, we choose the population transfer rate from $|1\rangle$ to $|0\rangle$ to be $\gamma_{01} = 0.3$ a.u. and the inverse temperature to be $\beta = 1$. Using eq. 5.33, this gives $\gamma_{10} = \frac{\gamma_{01}}{e} \approx 0.11$ a.u. and $\gamma_{20} = \frac{\gamma_{01}}{e^2} \approx 0.04$ a.u. At this relatively low temperature, the transfer rates to excited states higher than $|2\rangle$ are sufficiently small that they can be neglected. Using eq. 5.35, the decay of the initial coherence between $|0\rangle$ and $|1\rangle$ is found to be $\tau^{01}_{decoherence} = \frac{\gamma_{01}}{2}(1 + \frac{1}{e}) \approx 2.1$ a.u. These parameters all correspond to underdamped motion in which the decay to equilibrium occurs on a much longer time-scale than the oscillation period of the system. This condition is implicit in the assumption of weak system-bath coupling.

The density, current and dissipative current

In Figures 5.1 and 5.2, we plot the density, current density and dissipative current density as a function of time for the pure dephasing and relaxation without pure dephasing master equations respectively. Since we have chosen parameters corresponding to weak system-bath coupling, the dissipative current $j_{disp}(x,t)$ is significantly smaller than the Hamiltonian current $j(x,t)$, by approximately a factor of $\tau^{01}_{decoherence}$ for the pure dephasing case. In the figures, we have multiplied $j_{disp}(x,t)$ by a factor of 5 to make it more visible.

In Figure 5.1, we see that the coherences decay exponentially in time as the density oscillates in the harmonic well, while the populations remain unchanged, as expected for pure dephasing. In the absence of coupling to the bath, time translational invariance would imply that the snapshots in the right hand column would be the same as those on the left, which occur at a time $t = 2\pi$ earlier. The loss of coherence

manifests itself in the decay of the currents and changing density profile as the system evolves toward the fully mixed state $\rho_{00} = \rho_{11} = \frac{1}{2}$, $\rho_{10} = \rho_{01} = 0$ at equilibrium, which is an incoherent sum of the ground and first excited states. One can also see that the dissipative current is proportional to the spatial integral of the real part of the coherence, and lags the hamiltonian current by a phase of $\frac{\pi}{2}$ which is proportional the spatial integral of the imaginary part. Only the real part of the coherence contributes to the density evolution.

The contribution to the density from the coherences is antisymmetric about the origin, while the contribution from the populations is symmetric. When these two contributions are superposed, the density acquires an asymmetric profile, which can be seen at integer multiples of π where the coherent contribution is a maximum. At half integer multiples of π, the contribution from the real part of the coherences instantaneously vanishes and the density becomes symmetric. In contrast, the currents are always perfectly symmetric about the origin since they are proportional only to the spatial integral of the antisymmetric coherences.

In Figure 5.2, we see that in addition to decoherence there is population transfer, since we have included energy relaxation in the master equation. By $t = \frac{7\pi}{2}$, the system has already nearly approached the equilibrium state

$$\hat{\rho}_S(t = \infty) = \frac{1}{1 + e^{-\beta\omega}}|0\rangle\langle 0| + \frac{e^{-\beta\omega}}{1 + e^{-\beta\omega}}|1\rangle\langle 1|, \tag{5.38}$$

which for the parameters we have chosen corresponds to $\rho_{00}(t = \infty) \approx 0.73$ and $\rho_{11}(t = \infty) \approx 0.27$. Since the equilibrium density is dominated by the ground-state, it is nearly gaussian, but slightly flattened due to a mixing in of the first excited state.

The dissipative current has a similar profile to that seen in [69], which results from the fact that population transfer generates no Hamitonian current, but does give rise to a change in the density which must be compensated by $j_{disp}(x,t)$.

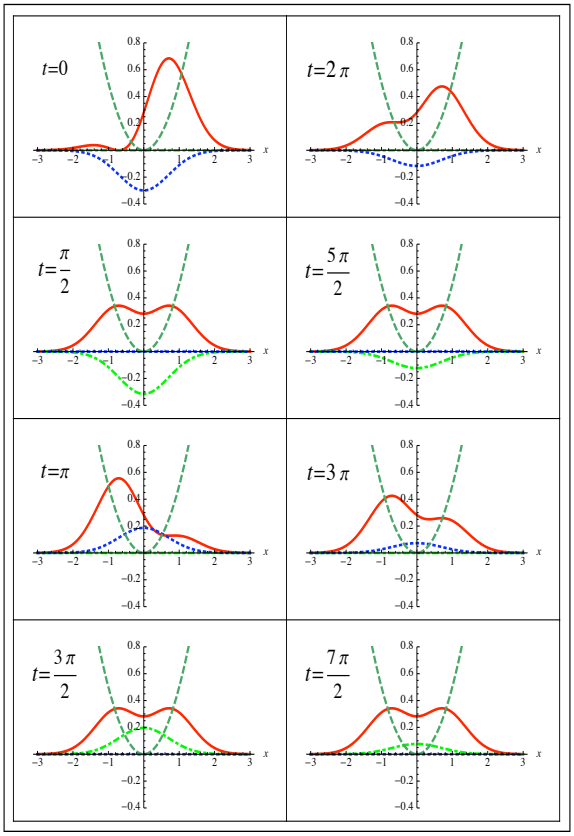

Figure 5.1: Time evolution of the density $n(x,t)$ (red-solid), the Hamiltonian current $j(x,t)$ (green-dot-dashed) and the dissipative current $j_{disp}(x,t)$ (blue-dotted), for the pure dephasing master equation. $j_{disp}(x,t)$ has been scaled by a factor of 5 to make it more visible in the figure. $v_{ext}(x) = \frac{1}{2}\omega^2 x^2$ (green-dashed) is shown for reference as well.

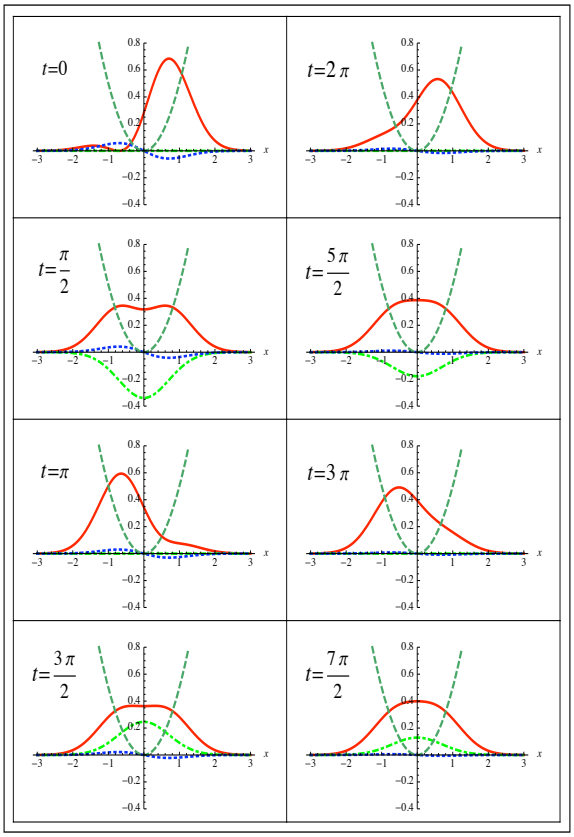

Figure 5.2: Time evolution of the density $n(x,t)$ (red-solid), the Hamiltonian current $j(x,t)$ (green-dot-dashed) and the dissipative current $j_{disp}(x,t)$ (blue-dotted), for the master equation including relaxation with no pure dephasing. $j_{disp}(x,t)$ has been scaled by a factor of 5 to make it more visible in the figure. $v_{ext}(x) = \frac{1}{2}\omega^2 x^2$ (green-dashed) is shown for reference as well.

The exact Kohn-Sham potential, Kohn-Sham orbitals and density matrices

In Figures 5.3 and 5.4, we show the full Kohn-Sham potential and its dynamical contribution (eq. 5.28) for the density evolution presented in Figures 5.1 and 5.2 respectively. In Figure 5.5, we plot the density and dynamical potential $v_c^{dyn}(x,t)$ as a function of space and time for the pure dephasing case as well. Examining Figures 5.3 and 5.5, we see that for pure dephasing, the dynamical potential becomes extremely repulsive in regions where the contribution to the density arising from the coherences in the OQS density matrix is large. For instance, at $t = \pi$, the contribution to the density from the coherences is positive for $x < 0$ and negative for $x > 0$. Likewise, $v_c^{dyn}(x,t)$ is positive for $x < 0$ and negative for $x > 0$, which corresponds to a field which will tend to suppress the coherent part of the density. For $t = 2\pi$, the sign of the coherent part of the density is reversed and $v_c^{dyn}(x,t)$ is as well, again corresponding to a potential which redistributes the density so as to suppress its coherent contribution. This behavior gives us some insight into how the Kohn-Sham system is able to use a unitary evolution to mimic the effect of the bath. In the Kohn-Sham system, decoherence is effectively converted into a control problem, in which the local time-dependent field $v_c^{dyn}(x,t)$ drives the density in the same way that collisions with the bath would in the true open system. This is a complicated task, since not only must $v_c^{dyn}(x,t)$ drive down the coherences, but it must do so without affecting the contribution to the density from the populations. The situation is somewhat different in Figure 5.4, since now the potential not only suppresses the

coherent density evolution, but it also transfers population from the first excited state to the groundstate to reach the thermal equilibrium density distribution.

At $t = 0$, the Kohn-Sham potentials appear to be extremely large, however this occurs in a region of space where the density vanishes and has little effect on the dynamics. At long times, one sees that the dynamical potential decays, while in the pure dephasing case, the full Kohn-Sham potential acquires a double well structure. This corresponds to the adiabatic Kohn-Sham potential (eq. 5.27) evaluated on the fully mixed, equilibrium-state density. In Figure 5.4, the double well structure is less pronounced, since the equilibrium state is dominated by the ground state for which the adiabatic potential reduces to v_{ext} (up to a constant), which is parabolic. In Figures 5.6 and 5.7, the Kohn-Sham orbital corresponding to the two different master equations is shown. The imaginary part of the orbital arises from the Hamitonian current as in usual TDDFT, but also has a contribution from the dissipative current. At long times, the currents decay and so the imaginary part vanishes while the real part is simply given by $\sqrt{n(x,t)}$. In the long-time limit, this orbital must reduce to an eigenstate of the adiabatic Kohn-Sham potential evaluated on the equilibrium OQS density. In this way, the Kohn-Sham system reproduces the correct equilibrium density of a mixed-state density matrix using a pure-state wavefunction. In principle, this wavefunction need not be the ground state, but it is in the cases studied here.

Lastly, we show the real part of the real-space density matrices for both the Kohn-Sham system and the true OQS in Figures 5.8 and 5.9. In the Kohn-Sham case, this is simply the pure-state density matrix

$$\rho_{ks}(x, x', t) = \phi^*(x, t)\phi(x't), \tag{5.39}$$

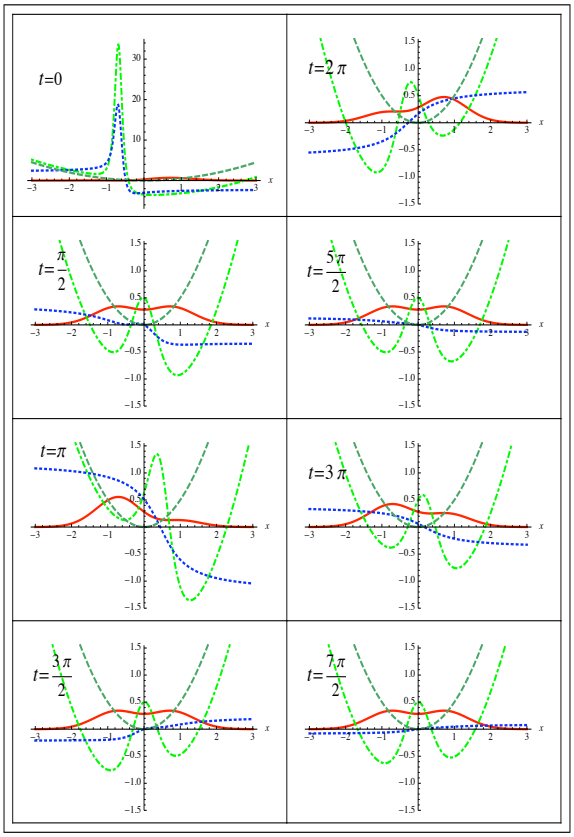

Figure 5.3: Time evolution of the density $n(x,t)$ (red-solid), the full Kohn-Sham potential $v_{ks}(x,t) = v_c^{open}(x,t) + v_{ext}(x)$ (green-dot-dashed) and the dynamical correlation potential $v_c^{dyn}(x,t)$ (blue-dotted) for the pure dephasing master equation. Note the change of scale for the $t = 0$ frame. $v_{ext}(x) = \frac{1}{2}\omega^2 x^2$ (green-dashed) is shown for reference as well.

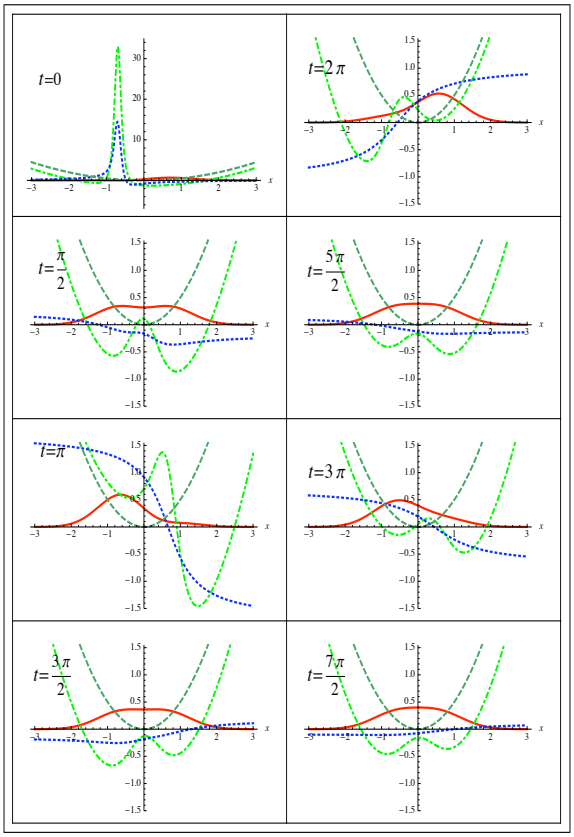

Figure 5.4: Time evolution of the density $n(x,t)$ (red-solid), the full Kohn-Sham potential $v_{ks}(x,t) = v_c^{open}(x,t) + v_{ext}(x)$ (green-dot-dashed) and the dynamical correlation potential $v_c^{dyn}(x,t)$ (blue-dotted) for the master equation including relaxation with no pure dephasing. Note the change of scale for the $t = 0$ frame. $v_{ext}(x) = \frac{1}{2}\omega^2 x^2$ (green-dashed) is shown for reference as well.

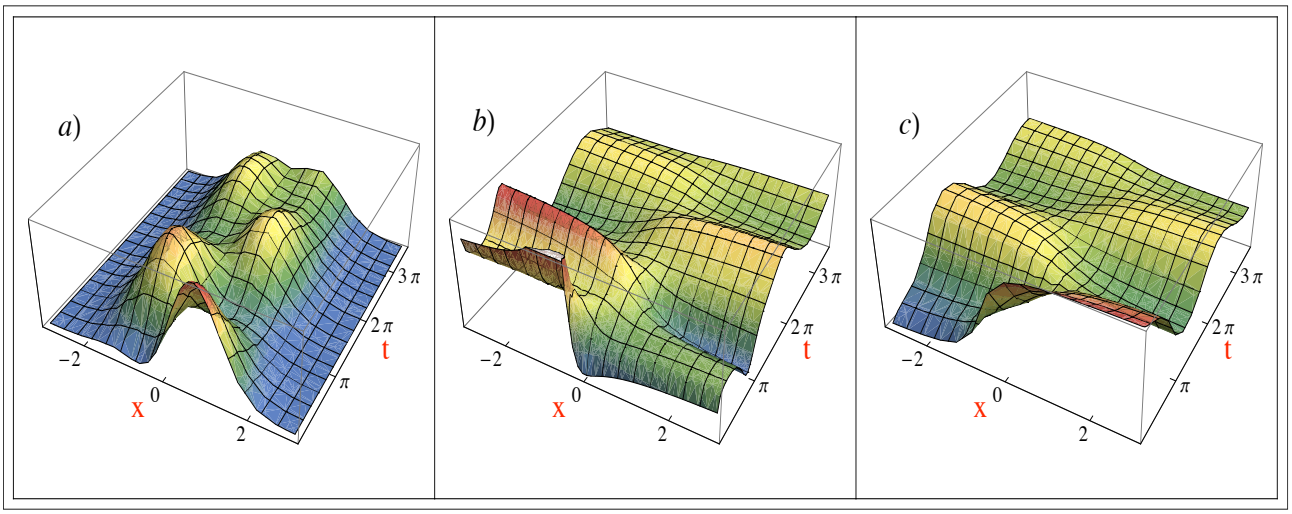

Figure 5.5: a) The density n(x,t), b) the exact dynamical correlation potential $v_c^{dyn}(x,t)$ and c) the Markovian bath functional (MBF), $v_c^{dyn,MBF}(x,t)$ for the pure dephasing master equation during the entire duration of the simulation shown as a function of space and time.

while in the OQS case it is the position representation of the solution to eq. 5.20,

$$\rho_{open}(x,x',t) = \langle x|\hat{\rho}_S(t)|x'\rangle. \tag{5.40}$$

Since we start in a pure-state at $t = 0$, the Kohn-Sham density matrix coincides with that of the true OQS. As the system evolves, the two begin to differ as the true density matrix looses purity while that of the Kohn-Sham system does not. However, it can be seen that at all times $\rho_{ks}(x,x,t) = \rho_{open}(x,x,t) = n(x,t)$ and the Kohn-Sham system reproduces the true OQS density on its diagonal.

In both Figure 5.8 and Figure 5.9, we see that the Kohn-Sham density matrix has large off-diagonal support which is not present in the true density matrix. This is consistent with the fact that the Kohn-Sham density matrix must remain idempotent.

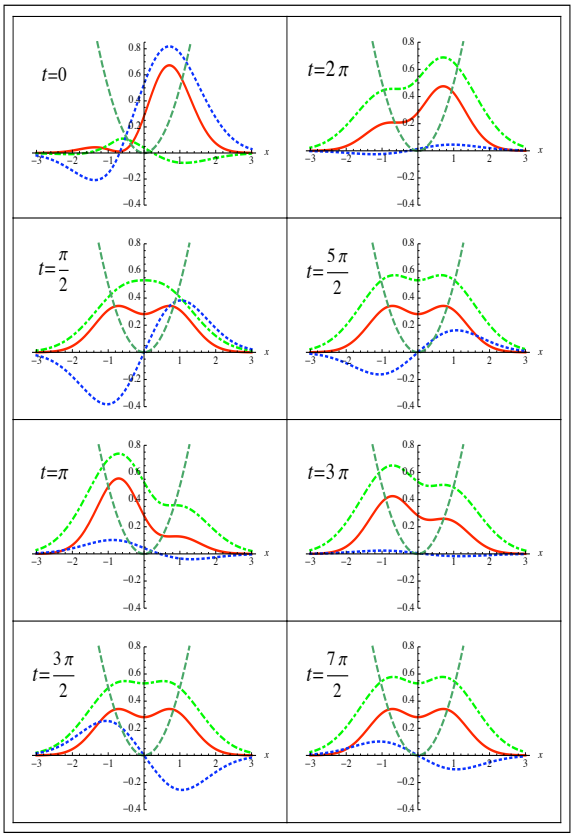

Figure 5.6: Time evolution of the density $n(x,t)$ (red-solid), the real part of the Kohn-Sham orbital $\Re e\phi(x,t)$ (green-dot-dashed) and the imaginary part of the Kohn-Sham orbital $\Im m\phi(x,t)$ (blue-dotted), for the pure dephasing master equation. $v_{ext}(x) = \frac{1}{2}\omega^2 x^2$ (green-dashed) is shown for reference as well.

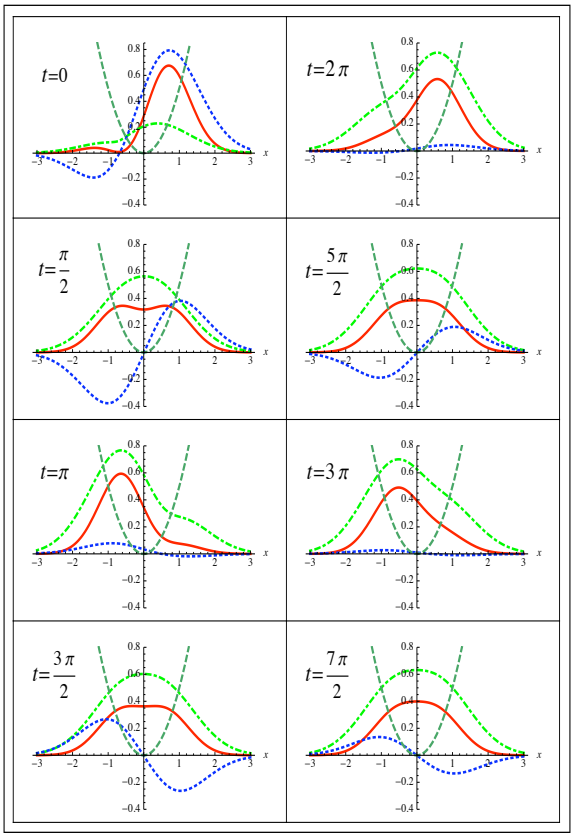

Figure 5.7: Time evolution of the density $n(x,t)$ (red-solid), the real part of the Kohn-Sham orbital $\Re e\phi(x,t)$ (green-dot-dashed) and the imaginary part of the Kohn-Sham orbital $\Im m\phi(x,t)$ (blue-dotted), for the master equation including relaxation with no pure dephasing. $v_{ext}(x) = \frac{1}{2}\omega^2 x^2$ (green-dashed) is shown for reference as well.

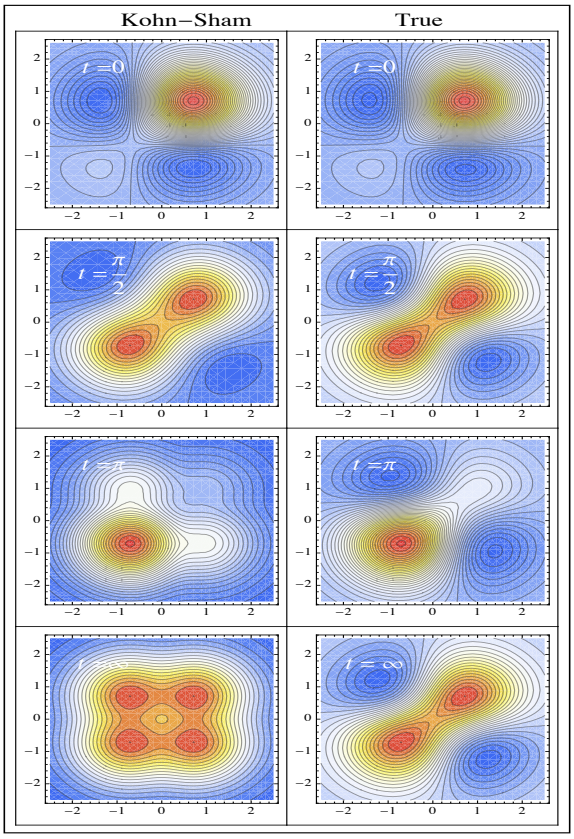

Figure 5.8: Time evolution of the real part of the Kohn-Sham density matrix $\Re e\rho_{ks}(x, x', t)$ (left column) and true OQS density matrix $\Re e\rho_{open}(x, x', t)$ (right column) for the pure dephasing master equation.

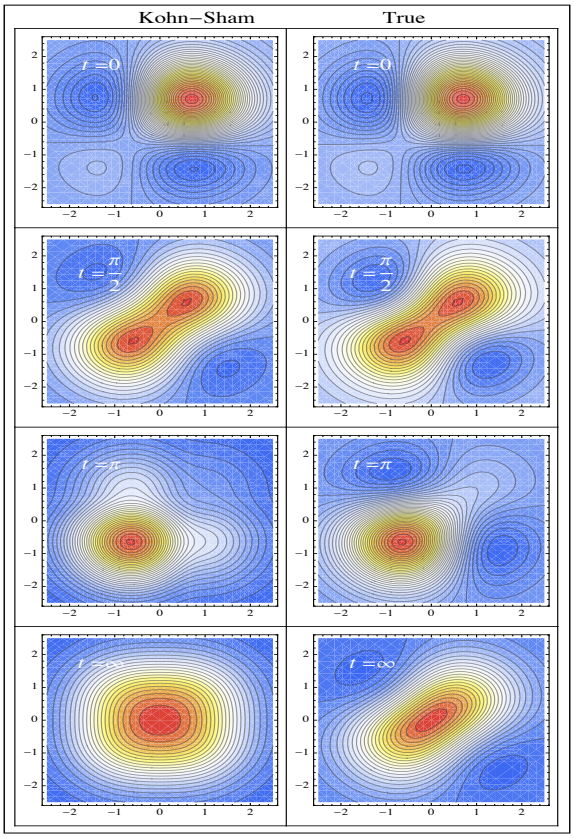

Figure 5.9: Time evolution of the real part of the Kohn-Sham density matrix $\Re e\rho_{ks}(x, x', t)$ (left column) and true OQS density matrix $\Re e\rho_{open}(x, x', t)$ (right column) for the master equation including relaxation with no pure dephasing.

i.e.

$$\int dx \int dx' |\rho_{ks}(x, x', t)|^2 = 1, \tag{5.41}$$

while for the true system,

$$\int dx \int dx' |\rho_{open}(x, x', t)|^2 < 1. \tag{5.42}$$

The Kohn-Sham density matrix is able to satisfy eq. 5.41 by increasing the off-diagonal regions and thus compensating for the lost volume in the true density matrix without affecting the density.

The Markovian bath functional

Our analysis of the exact OQS-TDDFT functional also sheds some light on the Markovian bath functional (MBF) that we first presented in [278]. In the MBF, one approximates the dynamical correlation potential as

$$v_c^{dyn}(x, t) \approx v_c^{dyn,MBF}(x, t) \equiv \lambda \int_{-\infty}^{x} \frac{j(x', t)}{n(x', t)} dx', \tag{5.43}$$

where λ is a fitted parameter. In this approximation, one neglects the contribution to $v_c^{dyn}(x, t)$ arising from the second term in eq. 5.28 involving gradients of the phase *and* one also neglects the contribution from the dissipative current. The first approximation is valid when the phases are spatially slowly varying, while the second approximation is valid if the coupling to the bath is weak. Lastly, one assumes

$$\frac{d}{dt}\alpha(x, t) \propto -\lambda\alpha(x, t). \tag{5.44}$$

i.e. the phase of the orbital is exponentially damped, which is valid in the Markovian limit. The MBF is a simple yet practical functional as it only involves knowledge of the Hamiltonian current and density at each instant in time. It can readily be implemented in real-time codes with existing propagation schemes [167]. Numerical simulations of dissipation of excited states of a model Helium atom show promising results, notwithstanding the simplicity of the MBF [278].

In Figure 5.5, we show a comparison of the MBF $v_c^{dyn,MBF}(x,t)$ and the exact functional $v_c^{dyn}(x,t)$ for the pure dephasing master equation of the model system presented in the previous sections. The fitted decay parameter is taken to be the decoherence rate in the master equation. i.e. $\lambda = \tau^{01}_{decoherence} = 0.15$. This is natural since it is the only decoherence timescale in the problem. The MBF is seen to reproduce the long-time behavior of the exact dissipative potential reasonably well, however it deviates significantly for short times. This arises from the fact that the Markov approximation only provides an adequate description of the dynamics for times longer than the decoherence time. At much shorter times it is not in general valid. In Figure 5.5, we see that this is roughly the timescale for the MBF to become accurate. Also, because the MBF neglects the dissipative current which is out of phase with the Hamiltonian current, there is a slight phase shift in the MBF with respect to the exact dissipative functional which contains both current contributions.

5.5 Conclusion and outlook

In summary, in this chapter we have explored the behavior of the exchange-correlation potential for dissipative open quantum systems using an exactly-solvable one-electron system. The two limiting cases (pure dephasing and relaxation) provided insights into the time-dependence and form of the dissipative potential that will need to be described in OQS-TDDFT functionals. We explored the behavior of the closed auxiliary Kohn-Sham system, as the system evolves under decoherence and relaxation. This is valuable information for the development of many-body, realistic bath functionals for OQS-TDDFT.

We have seen that the Kohn-Sham system mimics the effect of a bath by unitarily evolving with a dynamical potential, which depends on both the Hamitonian and dissipative currents. For a pure dephasing master equation, this potential tends to suppress the coherent part of the density evolution in a delicate way so that energy is still conserved and populations remain unchanged. When relaxation is also present, the potential drains energy away from the system and reaches an equilibrium distribution which satisfies detailed balance.

When dealing with a many-electron system, one expects that the functionals should retain some of the same features as in the one-electron case studied here, however, there are some fundamental differences. Firstly, one does not know the many-electron eigenstates *a priori* and so it is generally not possible to explicitly write down Lindblad operators in terms of these eigenstates as was done in eq. 5.20. Instead, one should start from a master equation written in terms of effective single-

particle eigenstates, such as a basis of orbitals from an equilibrium-state Kohn-Sham-Mermin calculation [115, 38, 226].

Secondly, the simple form of the dynamical functional expressed in eq. 5.28 no longer holds. In the simulation we have considered here, there are only two relevant levels involved in the dynamics. In general, for a many-level system the bath will induce different relaxation and dephasing rates for different eigenfrequencies of the system, depending on the bath spectral density [156, 244, 36]. Rather than simply coupling to the currents in a semi-time-local manner as in eq. 5.28, the exact functional will need to damp different Fourier components of the current at different rates. In the time-domian, this corresponds to a complicated memory-dependence on both the Hamiltonian and dissipative currents at earlier times. The form of this memory-dependence should clearly depend on the bath spectral density, but its exact structure will need to be investigated in future work.

In some respects, OQS-TDDFT functionals are similar to existing current-dependent functionals in TDCDFT, where frequency-dependent dissipation arises due to coupling to currents at earlier times via a stress tensor [254, 255, 52, 265]. However, the physical origin of the dissipation is very different in the two theories. In TDCDFT, the frequency dependence of the stress tensor depends on viscoelastic coefficients derived from the uniform electron gas. In contrast, the OQS-TDDFT functional depends on the spectral density of a bosonic bath such as phonons or photons.

Chapter 6

Time-dependent density functional theory of open quantum systems in the linear response regime

6.1 Introduction

Due to its attractive balance between accuracy and efficiency, time-dependent density functional theory (TDDFT) has seen a tremendous growth of applications in recent years. These range from optical properties of molecules, clusters and solids, to optimal control theory and real-time dynamics of species in intense laser fields [201, 153, 40, 143, 190, 128]. TDDFT has been particularly successful at calculating optical response properties of electronic systems in the linear response regime [181]. In most quantum chemical codes, excitation energies and oscillator strengths are extracted by solving a pseudo-eigenvalue equation, originally formulated by Casida [42]. The Casida equations are derived by considering the linear

density response of an interacting system and corresponding non-interacting Kohn-Sham system, both undergoing unitary evolution. If the Casida equations are solved using the ubiquitous adiabatic approximation (ATDDFT) within a discrete basis set, the resulting eigenvalues are real. This gives rise to a discrete absorption spectrum of delta function peaks.

In experimentally observed spectra, line broadening arises from a variety of different mechanisms, several of which have been explored already within LR-TDDFT. In extended systems, relaxation and dephasing due to electron-electron scattering is well captured using non-adiabatic and current-density dependent functionals [254, 255, 52, 238]. In finite systems, decay of resonant states due to coupling with the continuum gives rise to finite linewidths. The ability of DFT and TDDFT to capture lineshape parameters and widths of resonances has been discussed in [120, 90, 257].

Another important broadening mechanism arises from relaxation and dephasing of electronic degrees of freedom by a classical or bosonic bath such as photons, phonons or impurities. For extended systems, this situation was considered in [240, 237, 241], where linewidths of intersubband plasmon excitations were well captured by combining the Vignale-Kohn functional [254] to account for electron-electron scattering with the memory function formalism for electron-phonon and electron-impurity scattering. For atomic and molecular systems, the theory of open quantum systems within the master equation approach is often used [164, 288, 36, 117, 244, 131, 73]. Several important examples include vibrational relaxation of molecules in liquids and solid impurities [161, 80, 171, 55] , cavity quantum electrodynamics (QED) [89, 4, 5, 6], photoabsorption of chromophores in a protein bath [209, 210, 197, 230], single-molecule

transport [38, 70, 69, 283, 284] and exciton transport [178, 193, 191, 192, 2]. In all of these examples, even with simple system-bath models, the exact solution of the master equation for the reduced dynamics of the many-body electronic system is computationally intractable. Therefore, open quantum systems TDDFT (OQS-TDDFT) offers an attractive approach to the many-body open-systems problem.

Several important steps toward the formulation of OQS-TDDFT have recently been made, with the focus on real-time dynamics. In [38], a Runge-Gross theorem was established for Markovian master equations of the Lindblad form. A scheme in which the many-body master equation is mapped onto a non-interacting Kohn-Sham master equation was proposed for application to single-molecule transport. In [277, 278], the Runge-Gross theorem was extended to arbitrary non-Markovian master equations and a Van Leeuwen construction was established, thereby proving the existence of an OQS-TDDFT Kohn-Sham scheme [247]. In [278], it was shown that the original interacting open system dynamics can be mapped onto either a non-interacting open Kohn-Sham system, or a non-interacting closed (unitarily evolving) Kohn-Sham system. A different formulation of OQS-TDDFT based on the stochastic Schrödinger equation has also been developed [251, 16, 51].

The goal of the present chapter is to formulate the linear response version of (OQS-TDDFT) within the master equation approach. This provides a framework in which environmentally broadened spectra of many-body electronic systems can be accessed in an *ab initio* way using TDDFT, especially when combined with microscopically derived master equations. We use the scheme discussed in [278, 38] and section 4.4, in which the interacting OQS can be mapped onto a non-interacting open Kohn-Sham

system, yielding the same density response. This scheme is better suited to response theory than the closed Kohn-Sham scheme also discussed in [278] and Chapter 5, since relaxation and dephasing is already accounted for in the Kohn-Sham system. The unknown (OQS-TDDFT) exchange-correlation functional only needs to correct the relaxation and dephasing in the Kohn-Sham system to that of the interacting system, rather than needing to explicitly account for the entire effect of the environment. However, the closed Kohn-Sham scheme is better suited for real-time dynamics, since one only needs to propagate a set of equations for the Kohn-Sham orbitals as in usual TDDFT. This is in contrast to the open Kohn-Sham scheme, in which $N^2 - 1$ equations are propagated for the elements of the density matrix, with N being the dimensionality of the Hilbert space.

The chapter is organized as follows. In section 6.2, we formulate the most general OQS-TDDFT linear response equations for arbitrary non-Markovian master equations with initial correlations. In section 6.3, we make the treatment more specific by focusing on the Redfield master equation. We also derive Casida-type equations whose solution yields the environmentally broadened absorption spectrum. The solutions to these equations are complex, with the real part of the frequency yielding the location of absorption peaks and the imaginary part yielding the linewidths. In section 6.4, we apply the formalism developed in section 6.3 to a C^{2+} atom evolving under the Redfield master equation, interacting with the vacuum modes of the electromagnetic field. Section 6.5 analyzes the performance of using an adiabatic functional (OQS-ATDDFT) in solving the OQS-TDDFT Casida equations derived in section 6.3. To a large degree, OQS-ATDDFT is seen to provide a reliable correc-

tion to the location of absorption peaks while leaving the linewidths unchanged. A frequency-dependent functional yielding a correction to the OQS-ATDDFT linewidth based on Görling-Levy (GL) perturbation theory is then calculated and analyzed. In section 6.6 a discussion and outlook is provided.

For generality, we have formulated most of the theory by considering linear response from an equilibrium state at finite temperature. For atoms and molecules, it will generally be sufficient to take the zero temperature limit and consider linear response from the ground state.

6.2 General formulation of OQS-TDDFT linear response theory

A. Linear response of interacting open quantum systems

Our formulation of the interacting OQS density-density response function parallels that used in [236] for calculating spin susceptibilities (see also [53, 273, 235]). The starting point is the unitary evolution for the full density matrix of the system and the reservoir (we use the terms "reservoir" and "bath" interchangeably throughout) ,

$$\frac{d}{dt}\hat{\rho}(t) = \frac{1}{\imath}[\hat{H}(t), \hat{\rho}(t)] \equiv -\imath\breve{L}(t)\hat{\rho}(t), \tag{6.1}$$

where $\breve{L}(t)$ is the Liouvillian superoperator for the full system and reservoir dynamics. The full Hamiltonian is given by

$$\hat{H}(t) = \hat{H}_S(t) + \hat{H}_R + \hat{V}. \tag{6.2}$$

Here,

$$\hat{H}_S(t) = -\frac{1}{2}\sum_{i=1}^{N}\nabla_i^2 + \sum_{i<j}^{N}\frac{1}{|\mathbf{r}_i - \mathbf{r}_j|} + \sum_i v_{ext}(\mathbf{r}_i, t), \tag{6.3}$$

is the Hamiltonian of the electronic system of interest in an external potential $v_{ext}(\mathbf{r}, t)$. This potential generally consists of a static external potential due to the nuclei and an external driving field coupled to the system such as a laser field. The system-bath coupling, $\hat{V}$, is at this point arbitrary, but we will discuss specific forms later. $\hat{V}$ acts in the combined Hilbert space of the system and reservoir and so it couples the two subsystems. $\hat{H}_R$ is the Hamiltonian of the reservoir, assumed to have a dense spectrum of eigenstates. The density of states of $\hat{H}_R$ determines the structure of reservoir correlation functions, whose time-scale in turn determines the reduced system dynamics.

Defining the reduced density operator for the electronic system alone by tracing over the reservoir degrees of freedom,

$$\hat{\rho}_S(t) = Tr_R\{\hat{\rho}(t)\}, \tag{6.4}$$

one arrives at the formally exact quantum master equation,

$$\frac{d}{dt}\hat{\rho}_S(t) = -\imath[\hat{H}_S(t), \hat{\rho}_S(t)] + \int_{t_0}^{t} d\tau \breve{K}(t-\tau)\hat{\rho}_S(\tau) + \Xi(t). \tag{6.5}$$

Here, $\breve{K}(t-\tau)$ is the memory kernel and $\Xi(t)$ arises from initial correlations between the system and its environment. It is referred to as the inhomogeneous term. The above equation is still formally exact, as $\hat{\rho}_S(t)$ gives the exact expectation value of any observable depending only on the electronic degrees of freedom. In practice, however, approximations to $\breve{K}$ and Ξ are required. Of particular importance in TDDFT is the

time-dependent electronic density,

$$n(\mathbf{r},t) = Tr_S\{\hat{\rho}_S(t)\hat{n}(\mathbf{r})\}, \tag{6.6}$$

where $\hat{n}(\mathbf{r}) = \sum_i^N \delta(\mathbf{r} - \hat{\mathbf{r}}_i)$. We now assume that for $t < t_0$, the external potential is time-independent while for $t > t_0$ a weak perturbing field is applied. i.e.

$$t \ < t_0, v_{ext}(\mathbf{r},t) = v_{ext}(\mathbf{r}) \tag{6.7}$$

$$t \ > t_0, v_{ext}(\mathbf{r},t) = v_{ext}(\mathbf{r}) + \delta v_{ext}(\mathbf{r},t). \tag{6.8}$$

For $t < t_0$, the entire system and environment is in thermal equilibrium described by the canonical density operator

$$\hat{\rho}^{eq} = \frac{e^{-\beta\hat{H}}}{Tr_{S+R}\{e^{-\beta\hat{H}}\}}, \tag{6.9}$$

where $\beta = \frac{1}{K_B T}$ is the inverse temperature. The reduced equilibrium density operator of the electronic system is then given by

$$\hat{\rho}_S^{eq} = \frac{Tr_R\{e^{-\beta\hat{H}}\}}{Tr_{S+R}\{e^{-\beta\hat{H}}\}}. \tag{6.10}$$

In Eq. 6.9 and Eq. 6.10, $\hat{H} = \hat{H}_S + \hat{H}_R + \hat{V}$ is the full Hamiltonian for $t < t_0$ and $\hat{H}_S = -\frac{1}{2}\sum_{i=1}^N \nabla_i^2 + \sum_{i<j}^N \frac{1}{|\mathbf{r}_i - \mathbf{r}_j|} + \sum_i v_{ext}(\mathbf{r}_i)$ is the static Hamiltonian of the electrons in the absence of the external perturbation.

For $t > t_0$, the perturbing field is switched on and the system density operator subsequently evolves under the master equation given in Eq. 6.5. The electronic density evolution to first-order in the perturbing field is then given by

$$t \ < t_0, n(\mathbf{r},t) = n^{eq}(\mathbf{r}) \tag{6.11}$$

$$t \ > t_0, n(\mathbf{r},t) = n^{eq}(\mathbf{r}) + \delta n(\mathbf{r},t). \tag{6.12}$$

Here, $n^{eq}(\mathbf{r}) = Tr_S\{\hat{\rho}_S^{eq}\hat{n}(\mathbf{r})\}$ is the equilibrium electron density and

$$\delta n(\mathbf{r},t) = \int d^3\mathbf{r}' \int dt' \chi_{nn}(\mathbf{r},t;\mathbf{r}',t')\delta v_{ext}(\mathbf{r}',t') \tag{6.13}$$

is the linear density response. $\chi_{nn}(\mathbf{r},t;\mathbf{r}',t')$ is the density-density response function. Its Fourier transform to the frequency domain is given by

$$\chi_{nn}(\mathbf{r},\mathbf{r}';\omega) = \lim_{\epsilon\to+0} \imath \int_0^\infty dt e^{-\imath\omega t-\epsilon t} Tr_{S+R}\{[\hat{n}(\mathbf{r},t),\hat{n}(\mathbf{r}')]\hat{\rho}^{eq}\}, \tag{6.14}$$

where

$$\hat{n}(\mathbf{r},t) = e^{\imath\hat{H}t}\hat{n}(\mathbf{r})e^{-\imath\hat{H}t} \tag{6.15}$$

is the operator generating the electronic charge density in the Heisenberg picture with respect to the full Hamiltonian for $t < t_0$. Rearranging terms under the trace operation in Eq. 6.14, the density-density response function can be written as

$$\chi_{nn}(\mathbf{r},\mathbf{r}';\omega) = \lim_{\epsilon\to+0} \imath \int_0^\infty dt e^{-\imath\omega t-\epsilon t} Tr_S\{\hat{n}(\mathbf{r})\hat{\rho}_S^n(\mathbf{r}',t)\}. \tag{6.16}$$

Here, $\hat{\rho}_S^n(\mathbf{r},t)$ is an operator acting in the electronic system Hilbert space, which obeys the same equation of motion as the reduced system density operator (Eq. 6.5)

$$\frac{d}{dt}\hat{\rho}_S^n(\mathbf{r},t) = -\imath[\hat{H}_S,\hat{\rho}_S^n(\mathbf{r},t)] + \int_{t_0}^t d\tau \breve{K}(t-\tau)\hat{\rho}_S^n(\mathbf{r},\tau) + \Xi(t), \tag{6.17}$$

subject to the initial condition

$$\hat{\rho}_S^n(\mathbf{r},0) = Tr_R\big\{[\hat{n}(\mathbf{r}),\hat{\rho}^{eq}]\big\}. \tag{6.18}$$

Carrying out the Fourier transform in Eq. 6.16, one arrives at the formally exact expression for the open-systems density-density response function in Liouville space,

$$\chi_{nn}(\mathbf{r},\mathbf{r}';\omega) = \imath Tr_S\left\{\hat{n}(\mathbf{r})\frac{1}{\omega+\breve{L}_S-\imath\breve{K}(\omega)}(\hat{\rho}_S^n(\mathbf{r}',0)+\Xi(\omega))\right\}. \tag{6.19}$$

$\breve{L}_S$ is the Liouvillian for the system Hamiltonian for $t < t_0$, defined by its action on an arbitrary operator $\hat{O}$ by $\breve{L}_S\hat{O} = [\hat{H}_S, \hat{O}]$. It is readily verified that Eq. 6.19 reduces to the usual expression for the density-density response function of an isolated system when $\breve{K}(\omega) = 0$, $\Xi(\omega) = 0$ and $\hat{\rho}_S^n(\mathbf{r}, 0) = [\hat{n}(\mathbf{r}), \hat{\rho}_S^{eq}]$. Eq. 6.19 is still formally an exact representation of the full density-density response function of the combined system and reservoir and hence satisfies all of the usual exact conditions and sum rules of closed-systems response functions [71]. Most approximate master equations conserve particle number and so the f-sum rule is generally still satisfied. To the best of our knowledge, higher-moment sum rules of approximate OQS response functions have not been explored in the literature.

The absorption spectrum can be extracted by taking the imaginary part of $\chi_{nn}(\mathbf{r}, \mathbf{r}'; \omega)$ in Eq. 6.19. For an isolated system with a discrete spectrum, this is given by a sum over weighted delta function peaks. For an open system as in Eq. 6.19, $\breve{K}(\omega)$ and $\Xi(\omega)$ in principle give rise to the exact complicated broadened and shifted spectrum, due to relaxation and dephasing of the electronic degrees of freedom by the environment. In practice, however, even with simple approximations to $\breve{K}(\omega)$ and $\Xi(\omega)$, the exact form of $\Im m\left[\chi_{nn}(\mathbf{r}, \mathbf{r}', \omega)\right]$ is not exactly known, since it refers to a many-body response function. In subsections 6.2 B and 6.2 C, we consider an open Kohn-Sham system, formally yielding the exact density response of the original interacting open system. In an open-systems TDDFT framework, the exact spectrum of Eq. 6.19 is obtained by correcting the open Kohn-Sham spectrum via an exchange-correlation kernel. The kernel must take into account not only the electron-electron interaction contained in $\breve{L}_S$, but must also correct the interaction of the system with the bath,

described by $\breve{K}(\omega)$ and $\Xi(\omega)$.

B. The open Kohn-Sham system

It was proven in [278], that for a master equation of the form given in Eq. 6.5, there exists a unique, non-interacting and open Kohn-Sham system, whose system density operator evolves under the master equation

$$\frac{d}{dt}\hat{\rho}_S^{ks}(t) = -\imath[\hat{H}^{ks}(t), \hat{\rho}_S^{ks}(t)] + \int_{t_0}^{t} d\tau \breve{K}^{ks}(t-\tau)\hat{\rho}_S^{ks}(\tau) + \Xi^{ks}(t), \tag{6.20}$$

such that the time-dependent density is obtained from

$$n(\mathbf{r}, t) = Tr\{\hat{\rho}_S^{ks}(t)\hat{n}(\mathbf{r})\} \tag{6.21}$$

for all times. $\hat{H}^{ks}(t) = \sum_{i=1}^{N} \hat{h}_i^{ks}(t)$, where the Kohn-Sham Hamiltonian is given by

$$h^{ks}(\mathbf{r}, t) = -\frac{1}{2}\nabla^2 + v_{ks}(\mathbf{r}, t). \tag{6.22}$$

Here, v_{ks} is a local, multiplicative, one-body potential which drives the open Kohn-Sham system in such a way that the true density of the original interacting open system is reproduced for all times. In analogy to usual TDDFT, the Kohn-Sham potential is partitioned as

$$v_{ks}(\mathbf{r}, t) = v_{ext}(\mathbf{r}, t) + v_h(\mathbf{r}, t) + v_{xc}^{open}(\mathbf{r}, t), \tag{6.23}$$

where $v_h(\mathbf{r}, t)$ is the Hartree potential and the unknown functional $v_{xc}^{open}(\mathbf{r}, t)$ accounts for electron-electron interaction within the system as well as interaction between the system and bath. In general,

$$v_{xc}^{open}(\mathbf{r}, t) = v_{xc}^{open}(\mathbf{r}, t)[n, \breve{K}, \breve{K}^{ks}, \Xi, \Xi^{ks}, \hat{\rho}_S(0), \hat{\rho}^{ks}(0)]. \tag{6.24}$$

Formally, the open-systems exchange-correlation potential is a functional not only of the density, but also of the memory kernel, inhomogeneous term and initial state of both the interacting and Kohn-Sham systems. It has been shown in usual TDDFT of closed systems, that initial state dependence can be absorbed as dependence on the history of the density and vice versa [144]. Interestingly, in the theory of open quantum systems, it is possible to absorb the inhomogeneous term Ξ, into the memory kernel $\breve{K}$ [157]. This raises the possibility that v_{xc}^{open} may be a functional only of n, $\breve{K}$ and $\breve{K}^{ks}$, but a more rigorous study of this will be done in future work. For notational convenience, we suppress the explicit functional dependence of v_{xc}^{open} on these quantities, although it is implied unless otherwise stated. In general, $\breve{K}^{ks}$ and Ξ^{ks} can be chosen to simplify $v_{xc}^{open}(\mathbf{r},t)$ as much as possible, although with some restrictions [278] and consistency conditions between $\breve{K}^{ks}$ and Ξ^{ks} [157].

If the system is started in an equilibrium state, as is typically the case in linear response theory, the initial state dependence in Eq. 6.24 is automatically removed. The equilibrium density, $n^{eq}(\mathbf{r})$, is obtained by solving the Kohn-Sham-Mermin equations [115]

$$\left[-\frac{1}{2}\nabla^2 + v_{ks}^{eq}[n](\mathbf{r})\right]\phi_i(\mathbf{r}) = \epsilon_i\phi_i(\mathbf{r}). \tag{6.25}$$

The Kohn-Sham-Mermin potential is partitioned as

$$v_{ks}^{eq}[n](\mathbf{r}) = v_{ext}[n](\mathbf{r}) + v_h[n](\mathbf{r}) + \frac{\delta F_{xc}[n]}{\delta n(\mathbf{r})}, \tag{6.26}$$

where $F_{xc}[n]$ is the exchange-correlation contribution to the free energy. After solving Eq. 6.25, the equilibrium Kohn-Sham-Mermin density operator is obtained by

populating the orbitals according to

$$\hat{\gamma}_{eq}^{ks} = \sum_{i=1}^{\infty} f_i |\phi_i\rangle\langle\phi_i|, \tag{6.27}$$

where f_i are Fermi-Dirac occupation numbers

$$f_i = \frac{1}{e^{\beta(\epsilon_i - \mu)} + 1}. \tag{6.28}$$

Denoting $\langle \mathbf{r}|\phi_i\rangle = \phi_i(\mathbf{r})$, the one-particle Kohn-Sham-Mermin density matrix is

$$\langle \mathbf{r}|\hat{\gamma}_{eq}^{ks}|\mathbf{r}'\rangle \equiv \gamma(\mathbf{r},\mathbf{r}') = \sum_{i=1}^{\infty} f_i \phi_i^*(\mathbf{r})\phi_i(\mathbf{r}'). \tag{6.29}$$

The equilibrium density is then obtained by taking the diagonal elements in real space,

$$n^{eq}(\mathbf{r}) = \gamma(\mathbf{r},\mathbf{r}) = \sum_{i=1}^{\infty} f_i |\phi_i(\mathbf{r})|^2. \tag{6.30}$$

For the open Kohn-Sham scheme to be useful practically, $v_{xc}^{open}[n](\mathbf{r},t)$, $\breve{K}^{ks}$ and Ξ^{ks} should be constructed so that the following conditions are satisfied:

1) $\breve{K}^{ks}$ and Ξ^{ks} should not induce correlations between non-interacting electrons as the Kohn-Sham system evolves. This ensures that the N-body Kohn-Sham density matrix in Eq. 6.20 can be traced over N-1 electron coordinates to arrive at a closed equation of motion for the Kohn-Sham reduced 1-particle density matrix. Physically, this is expected since most reasonable bath models couple to the electronic system through one-body operators [48, 36].

2) The equation of motion for the non-equilibrium open Kohn-Sham reduced 1-particle density matrix should have the Kohn-Sham-Mermin density matrix as its stationary-point solution. This ensures that the system thermalizes to the correct

equilibrium density. This also means that at equilibrium, $v_{xc}^{open}[n](\mathbf{r},t)$ should reduce to $\frac{\delta F_{xc}[n]}{\delta n(\mathbf{r})}$. Although this is automatically satisfied by using $v_{ks}^{eq}[n]$ as an adiabatic approximation, it might not be satisfied by more sophisticated approximations with memory dependence [144, 142, 140, 122].

C. Linear response of the open Kohn-Sham system

Returning to linear response, for $t < t_0$ the Kohn-Sham system is in thermal equilibrium with its environment at inverse temperature β, described by Eq. 6.25. At $t = t_0$, the perturbation $\delta v_{ext}(\mathbf{r},t)$ is switched on and the Kohn-Sham system subsequently evolves according to Eq. 6.20. The Kohn-Sham potential is given by

$$t < t_0, v_{ks}(\mathbf{r},t) = v_{ks}^{eq}[n](\mathbf{r}) \tag{6.31}$$

$$t > t_0, v_{ks}(\mathbf{r},t) = v_{ks}^{eq}[n](\mathbf{r}) + \delta v_{ks}(\mathbf{r},t), \tag{6.32}$$

where $\delta v_{ks}(\mathbf{r},t) = \delta v_{ext}(\mathbf{r},t) + \delta v_h[n](\mathbf{r}) + \delta v_{xc}^{open}[n](\mathbf{r},t)$. Due to Eq. (6.21), the exact linear density response of Eq. (6.12) is obtained through

$$\delta n(\mathbf{r},t) = \int d^3\mathbf{r}' \int dt' \chi_{nn}^{ks}(\mathbf{r},t;\mathbf{r}',t')\delta v_{ks}(\mathbf{r}',t'). \tag{6.33}$$

Here, $\chi_{nn}^{ks}(\mathbf{r},t;\mathbf{r}',t')$ is the density-density response function of the open Kohn-Sham system. Its Fourier transform to the frequency domain is given by

$$\chi_{nn}^{ks}(\omega,\mathbf{r},\mathbf{r}') = \imath Tr_S\left\{\hat{n}(\mathbf{r})\frac{1}{\omega + \breve{L}_{ks} - \imath\breve{K}^{ks}(\omega)}([\hat{n}(\mathbf{r}'),\hat{\rho}_S^{ks}(0)] + \Xi^{ks}(\omega))\right\}, \tag{6.34}$$

where $\breve{L}_{ks}$ is the Liouvillian for the equilibrium Kohn-Sham-Mermin Hamiltonian. Since the system is in the equilibrium state at $t = 0$, $\hat{\rho}_S^{ks}(0)$ must yield the equilibrium

density, implying that it reduces to the Kohn-Sham-Mermin density matrix when traced over N-1 electron coordinates. We now define the open-systems exchange-correlation kernel in analogy to usual TDDFT for closed-systems by,

$$f_{xc}^{open}[n^{eq}](\mathbf{r},\mathbf{r}';\omega) = \frac{\delta v_{xc}^{open}[n](\mathbf{r},\omega)}{\delta n(\mathbf{r}',\omega)}|_{n=n^{eq}}, \tag{6.35}$$

which is a functional of the equilibrium density. As in TDDFT for closed systems, the interacting and Kohn-Sham response functions are related through a Dyson-like equation,

$$\begin{aligned}\chi_{nn}(\omega,\mathbf{r},\mathbf{r}') &= \chi_{nn}^{ks}(\omega,\mathbf{r},\mathbf{r}') \\ &+ \int d^3\mathbf{y}d^3\mathbf{y}'\chi_{nn}^{ks}(\omega,\mathbf{r},\mathbf{y})\Big\{\frac{1}{|\mathbf{y}-\mathbf{y}'|} + f_{xc}^{open}[n^{eq}](\mathbf{y},\mathbf{y}';\omega)\Big\}\chi_{nn}(\omega,\mathbf{y}',\mathbf{r}').\end{aligned} \tag{6.36}$$

χ_{nn}^{ks}, being much simpler then the original interacting χ_{nn}, can readily be constructed from the orbitals and eigenvalues in Eq. 6.25 and approximations to $\breve{K}^{ks}(\omega)$ and $\Xi^{ks}(\omega)$ in terms of these quantities. This will be done explicitly for the Redfield master equation in section 6.3. Since correlation between the open Kohn-Sham system and reservoir is already partially captured through $\breve{K}^{ks}(\omega)$ and $\Xi^{ks}(\omega)$, the bare Kohn-Sham absorption spectrum extracted from $\Im m\left[\chi_{nn}^{ks}(\omega,\mathbf{r},\mathbf{r}')\right]$ is already broadened and shifted. The functional $f_{xc}^{open}[n^{eq}]$ has the task of correcting the spectrum extracted from χ_{nn}^{ks} to that of the interacting χ_{nn}, incorporating both the usual electron-electron correlation in closed-systems TDDFT as well as additional system-bath correlation. We define the part of the kernel arising solely from system-bath interactions by

$$f_{xc}^{bath}[n^{eq}](\mathbf{r},\mathbf{r}';\omega) = f_{xc}^{open}[n^{eq}](\mathbf{r},\mathbf{r}';\omega) - f_{xc}^{closed}[n^{eq}](\mathbf{r},\mathbf{r}';\omega), \tag{6.37}$$

where f_{xc}^{closed} is the exact exchange-correlation kernel of usual closed-systems TDDFT.

In general, the memory kernel $\breve{K}(\omega)$ may give rise to a very complicated non-analytic structure of χ_{nn} in the lower half of the complex plane. However, for Markovian master equations, it will be seen that the pole structure of χ_{nn} in the discrete part of the spectrum consists of simple poles in the lower complex plane, shifted by a finite amount off of the real axis. In such cases, it might be reasonable to use an adiabatic approximation for f_{xc}^{closed}, so that the OQS-TDDFT kernel is given by

$$f_{xc}^{open}[n^{eq}](\mathbf{r},\mathbf{r}';\omega) = \frac{\delta^2 F_{xc}[n]}{\delta n(\mathbf{r})\delta n(\mathbf{r}')}|_{n=n^{eq}} + f_{xc}^{bath}[n^{eq}](\mathbf{r},\mathbf{r}';\omega). \tag{6.38}$$

Here, the first term is just the closed-systems adiabatic contribution to the exchange-correlation kernel and the second term is an in general frequency-dependent and complex-valued correction arising from the bath. This is attractive, since we can take advantage of the usual good performance of adiabatic TDDFT in describing the location of absorption peaks, and attempt to build functionals that go beyond the adiabatic approximation to account for line broadening and lamb shifts. This strategy will be discussed further in section 6.5.

6.3 LR-TDDFT for the redfield master equation.

In section 6.2, we formulated LR-TDDFT for a very general class of master equations. In this section, we make the discussion more specific by invoking the Markov approximation and second Born approximation in the system-bath interaction, to arrive at the microscopically-derived Redfield master equation [209, 48, 156, 244, 195, 194]. Since the Redfield equations are rigorously obtained without phenomenological pa-

rameters, they are amenable to an *ab initio* theory such as TDDFT. Although we focus on Redfield theory here, the generalization of our formalism to other Markovian master equations can be made with small modifications. Finally, we discuss how it is possible to extract the absorption spectrum of a many-body system evolving under the Redfield equations directly within OQS-TDDFT. This is done by formulating Casida-type equations yielding complex eigenvalues due to coupling with the bath.

A. The Markov approximation and the Redfield master equation.

The Markov approximation describes a situation in which the bath correlation functions decay on an infinitely fast time-scale relative to the thermalization time of the system [48, 156]. As a result, the bath has no memory and the memory kernel is time-local

$$\breve{K}(t-\tau) \propto \breve{R}\delta(t-\tau). \tag{6.39}$$

Additionally, this implies that the initial density operator is a tensor product of a density operator in the system space with the equilibrium density operator of the bath

$$\hat{\rho}(0) = \hat{\rho}_s(0) \otimes \left\{ \frac{e^{-\beta \hat{H}_R}}{Tr_R\{e^{-\beta \hat{H}_R}\}} \right\}. \tag{6.40}$$

As a result of Eq. 6.40, the system and environment have no initial correlations, and

$$\Xi(t) = 0. \tag{6.41}$$

The master equation (Eq. 6.5) then takes the simple form,

$$\frac{d}{dt}\hat{\rho}_S(t) = -\imath\breve{L}_S(t)\hat{\rho}_S(t) + \breve{R}\hat{\rho}_S(t). \tag{6.42}$$

If the system Hamiltonian is time-independent, Eq. 6.42 is written in a basis of eigenstates of $\hat{H}_S$ as:

$$\frac{d}{dt}\rho_{ab}(t) = -\imath\omega_{ab}\rho_{ab}(t) + \sum_{abcd} R_{abcd}\rho_{cd}(t). \tag{6.43}$$

Here, $\omega_{ab} = E_a - E_b$ are many-body transition frequencies of $\hat{H}_S$ and R_{abcd} are matrix elements of $\breve{R}$ in this basis. So far our discussion applies to any Markovian master equation. To obtain the Redfield equations, we further assume that the system-bath coupling has a bilinear form

$$\hat{V} = -\hat{S} \otimes \hat{R}, \tag{6.44}$$

where $\hat{R}$ is an operator in the reservoir Hilbert space which couples to a local one-body operator $\hat{S} = \left[\sum_{i=1}^{N} \hat{S}(\hat{\mathbf{p}}_i, \hat{\mathbf{r}}_i)\right]$ in the system Hilbert space. This form of the system-bath coupling is very general and can apply to electron-phonon coupling in molecules and solid impurities, but also momentum dependent couplings which are relevant for instance in laser cooling, Brownian motion in liquids or dissipative strong field dynamics [157, 114, 48]. The Redfield tensor is then derived by performing second-order perturbation theory in $\hat{V}$, and is given explicitly by

$$\begin{aligned} R_{abcd} = &-\int_0^\infty d\tau \left[g(\tau) \left[\delta_{bd} \sum_n S_{an}S_{nc}e^{\imath\omega_{cn}\tau} - S_{ac}S_{db}e^{\imath\omega_{ca}\tau} \right] \right] \\ &- \int_0^\infty d\tau \left[g(-\tau) \left[\delta_{ac} \sum_n S_{dn}S_{nb}e^{\imath\omega_{nd}\tau} - S_{ac}S_{db}e^{\imath\omega_{bd}\tau} \right] \right]. \end{aligned} \tag{6.45}$$

In Eq. 6.45,

$$S_{ab} = N \int d^3\mathbf{r} \int d^3\mathbf{r}_2 ... d^3\mathbf{r}_N \psi_a^*(\mathbf{r}, \mathbf{r}_2, ...\mathbf{r}_N) S(\frac{\nabla}{\imath}, \mathbf{r}) \psi_b(\mathbf{r}, \mathbf{r}_2, ...\mathbf{r}_N) \tag{6.46}$$

are matrix elements of $\hat{S}(\hat{\mathbf{p}}, \hat{\mathbf{r}})$ between system many-body wavefunctions and

$$\omega_{ab} = E_a - E_b \tag{6.47}$$

are system many-body excitation energies. $g(\tau)$ are bath correlation functions given by

$$g(\tau) = Tr_R\{\hat{R}(\tau)\hat{R}(0)\}, \tag{6.48}$$

where

$$\hat{R}(\tau) = e^{\imath \hat{H}_R \tau} \hat{R} e^{-\imath \hat{H}_R \tau}. \tag{6.49}$$

Although the upper limit of the integral in Eq. 6.45 goes to infinity, this arises from the Markov approximation and does not violate causality. The limit is taken on a timescale much longer than that of the bath, but remains much smaller than the timescale for which the system can evolve appreciably. For a detailed discussion of this point and a derivation of the Redfield equations see [156] and section 3.6.

For the simple case of a system with only two-levels, ψ_0 and ψ_1, the Redfield tensor can be related to the ubiquitous phenomenological formula from NMR spectroscopy (with no pure dephasing):

$$\frac{1}{T_2} = \frac{1}{2T_1}. \tag{6.50}$$

Here, $T_2 = \frac{1}{R_{0101}}$ describes the time-scale for decoherence, while $T_1 = \frac{1}{R_{1100} - e^{-\beta\omega_{10}} R_{0011}}$ is that of relaxation [156, 194].

B. Linear response of a many-body system evolving under the Redfield master equation.

Since we consider linear response from the equilibrium state, the initial density matrix for the system is given by

$$\hat{\rho}_S(0) = \frac{e^{-\beta \hat{H}_S}}{Tr_S\{e^{-\beta \hat{H}_S}\}}, \tag{6.51}$$

and the density-density response function in Eq. 6.19 reduces to

$$\chi_{nn}(\mathbf{r}, \mathbf{r}'; \omega) = \imath Tr_S \left\{ \hat{n}(\mathbf{r}) \frac{1}{\omega + \breve{L}_s - \imath \breve{R}} [\hat{n}(\mathbf{r}'), \hat{\rho}_S(0)] \right\}. \tag{6.52}$$

Inserting a complete set of eigenstates of $\hat{H}_S$ in Eq. 6.52, a sum over states expression for the density-density response function is given by,

$$\chi_{nn}(\mathbf{r}, \mathbf{r}'; \omega) = \imath \sum_a [P(E_a)] \sum_b \left\{ \frac{\langle a|\hat{n}(\mathbf{r})|b\rangle\langle b|\hat{n}(\mathbf{r}')|a\rangle}{\omega + \omega_{ab} + \imath R_{abab}} - \frac{\langle a|\hat{n}(\mathbf{r}')|b\rangle\langle b|\hat{n}(\mathbf{r})|a\rangle}{\omega - \omega_{ab} + \imath R^*_{abab}} \right\} \tag{6.53}$$

Here, $P(E_a) = \frac{e^{-\beta E_a}}{\sum_b e^{-\beta E_b}}$ are equilibrium occupation probabilities of the various many-body states.

By hermiticity of the density matrix, it can be readily verified that $R^*_{abab} = R_{baba}$. We can separate the real and imaginary parts of R_{abab} as

$$R_{abab} = \Gamma_{ab} + \imath \Delta_{ab}. \tag{6.54}$$

From the pole structure of Eq. 6.53, we see that Γ_{ab} corresponds to an imaginary part of the energy of the transition ω_{ab}, giving rise to a finite lifetime, while Δ_{ab} is a Lamb shift of the real part of the energy. The effect of the Redfield tensor is to shift the poles of the density-density response function by a finite amount into the lower half of the complex plane.

C. The Markovian Kohn-Sham-Redfield equations

We now discuss the properties of the open Kohn-Sham system for the Redfield master equation. As discussed in subsection 6.2 B, there is some freedom in the construction of the Kohn-Sham dissipative superoperator and corresponding exchange-correlation potential. In this section, we choose a very natural form for the Kohn-Sham superoperator, whose construction is discussed below.

We consider an open Kohn-Sham system evolving under a Markovian master equation

$$\frac{d}{dt}\hat{\rho}_S^{ks}(t) = -\imath[\hat{H}^{ks}(t), \hat{\rho}_S^{ks}(t)] + \breve{R}^{ks}\hat{\rho}_S^{ks}(t), \tag{6.55}$$

which reproduces the exact density evolution of the interacting Markovian master equation in Eq. 6.42. To satisfy condition 1 in subsection 6.2 B, we must have

$$\breve{R}^{ks}(\mathbf{r}_1, \mathbf{r}_2, ...\mathbf{r}_N) \equiv \sum_{i=1}^{N} \breve{r}^{ks}(\mathbf{r}_i), \tag{6.56}$$

i.e. the N-body Kohn-Sham dissipative superoperator is a sum of one-body superoperators acting on each coordinate separately. This also follows very naturally from the assumed one-body nature of the system-bath interaction in Eq. 6.44. Since $\hat{H}^{ks}(t) = \sum_{i=1}^{N} \hat{h}_i^{ks}(t)$ is also a sum of one-body terms, we can trace both sides of Eq. 6.55 over N-1 electron coordinates and arrive at a closed equation of motion for the Kohn-Sham 1-particle reduced density matrix,

$$\frac{d}{dt}\hat{\gamma}(t) = -\imath[\hat{h}^{ks}(t), \hat{\gamma}(t)] + \breve{r}^{ks}\hat{\gamma}(t). \tag{6.57}$$

We can now write Eq. 6.57 in a basis of Kohn-Sham-Mermin orbitals as

$$\frac{d}{dt}\gamma_{ij}(t) = -\imath \sum_k \left\{ h^{ks}(t)_{ik}\gamma_{kj}(t) - \gamma_{ik}(t)h^{ks}(t)_{kj} \right\} + \sum_{ijkl} r^{ks}_{ijkl}\gamma_{kl}(t). \tag{6.58}$$

We choose r^{ks}_{ijkl} to have the form of the Redfield tensor, but written in terms of Kohn-Sham-Mermin orbitals and eigenvalues,

$$\begin{aligned} r^{ks}_{ijkl} = &- \int_0^\infty d\tau \left[g(\tau) \left[\delta_{jl} \sum_m S_{im}S_{mk}e^{\imath\omega^{ks}_{km}\tau} - S_{ik}S_{lj}e^{\imath\omega^{ks}_{ki}\tau} \right] \right] \\ - &\int_0^\infty d\tau \left[g(-\tau) \left[\delta_{ik} \sum_m S_{lm}S_{mj}e^{\imath\omega^{ks}_{ml}\tau} - S_{ik}S_{lj}e^{\imath\omega^{ks}_{jl}\tau} \right] \right]. \end{aligned} \tag{6.59}$$

Here,

$$\omega^{ks}_{ij} = \epsilon_i - \epsilon_j \tag{6.60}$$

are bare Kohn-Sham-Mermin transition frequencies and

$$S_{ij} = \int d^3\mathbf{r}\phi^*_i(\mathbf{r})S(\frac{\nabla}{\imath}, \mathbf{r})\phi_j(\mathbf{r}) \tag{6.61}$$

are matrix elements of the system-bath coupling operator between Kohn-Sham-Mermin orbitals.

Eq. 6.58 has a number of desirable properties. First, its stationary point solution is the Kohn-Sham-Mermin density matrix, Eq. 6.27, if $\hat{h}^{ks}(t)$ reduces to the Kohn-Sham-Mermin Hamiltonian when evaluated on the equilibrium density. This ensures that condition 2 in subsection 6.2 B is satisfied. It also satisfies detailed balance as well as most other properties of the usual many-body Redfield equations, but in terms of Kohn-Sham-Mermin quantities. Also, the tensor r^{ks}_{ijkl} has a simple form and can be constructed explicitly in terms of orbitals and eigenvalues obtained in an equilibrium-state Kohn-Sham calculation. The potential $v^{open}_{xc}(t)$ contained in $\hat{h}^{ks}(t)$

will in general be a functional of $\breve{r}^{ks}$ and $\breve{R}$ as well as the time evolving density. We emphasize that the Kohn-Sham-Redfield system reproduces only the exact density of the original interacting system, while expectation values of other observables will in general be different.

D. Linear response of the Kohn-Sham-Redfield system and the open-systems Casida equations

We now consider the open-systems LR-TDDFT formalism developed in section 6.2, but applied to the Redfield master equation. The density-density response function of the Kohn-Sham-Redfield system is given by

$$\chi^{ks}_{nn}(\mathbf{r},\mathbf{r}';\omega) = \imath Tr_S\left\{\hat{n}(\mathbf{r})\frac{1}{\omega+\breve{L}_{ks}-\imath\breve{R}^{ks}}[\hat{n}(\mathbf{r}'),\hat{\rho}^{ks}_S(0)]\right\}. \tag{6.62}$$

Using Eqs. 6.53-6.56 and inserting a complete set of Kohn-Sham-Mermin states, one obtains the sum-over-states expression,

$$\chi^{ks}_{nn}(\mathbf{r},\mathbf{r}',\omega) = \sum_i f_i \sum_j \left\{\frac{\langle i|\hat{n}(\mathbf{r})|j\rangle\langle j|\hat{n}(\mathbf{r}')|i\rangle}{\omega+\omega^{ks}_{ij}+\imath r^{ks}_{ijij}} - \frac{\langle i|\hat{n}(\mathbf{r}')|j\rangle\langle j|\hat{n}(\mathbf{r})|i\rangle}{\omega-\omega^{ks}_{ij}+\imath r^{ks\ *}_{ijij}}\right\}. \tag{6.63}$$

Eq. 6.53 and Eq. 6.63 are related through the Dyson-like relation given in Eq. 6.36. To extract the poles of the interacting density-density response function in Eq. 6.53 from that of the Kohn-Sham system in Eq. 6.63, a pseudo-eigenvalue equation must be solved for the squares of the complex transition frequencies,

$$\left\{\omega^2-\bar{\Omega}(\omega)\right\}\vec{F}=0. \tag{6.64}$$

The operator $\bar{\Omega}(\omega)$ can be written as a matrix in a basis of Kohn-Sham molecular orbitals (assuming a closed shell system) as

$$\bar{\Omega}_{ijkl}(\omega) = \delta_{ik}\delta_{jl}\Big\{(\omega_{lk}^{ks} + \Delta_{kl}^{ks})^2 + (\Gamma_{kl}^{ks})^2 - 2\imath\omega\Gamma_{kl}^{ks}\Big\} + 4\sqrt{(f_i - f_j)(\omega_{ji}^{ks} + \Delta_{ij}^{ks})}K_{ijkl}(\omega)\sqrt{(f_k - f_l)(\omega_{lk}^{ks} + \Delta_{kl}^{ks})}. \tag{6.65}$$

The explicit derivation of Eq. 6.64 and Eq. 6.65 is given in appendix A. In Eq. 6.65,

$$K_{ijkl}(\omega) = \int d^3\mathbf{r}\int d^3\mathbf{r}'\phi_i^*(\mathbf{r})\phi_j^*(\mathbf{r})\left\{\frac{1}{|\mathbf{r}-\mathbf{r}'|} + f_{xc}^{open}[n^{eq}, \breve{R}, \breve{r}^{ks}](\mathbf{r},\mathbf{r}';\omega)\right\}\phi_k(\mathbf{r}')\phi_l(\mathbf{r}') \tag{6.66}$$

and the bare Kohn-Sham linewidths and Lamb shifts are given by the relation

$$r_{ijij}^{ks} = \Gamma_{ij}^{ks} + \imath\Delta_{ij}^{ks}, \tag{6.67}$$

as in Eq 6.54. In principle, with the exact functional $f_{xc}^{open}[n^{eq}, \breve{R}, \breve{r}^{ks}]$, the exact poles of Eq. 6.53 are recovered by solving Eq. 6.64. The operator $\bar{\Omega}(\omega)$ is non-Hermitian, giving rise to complex eigenvalues corresponding to broadened excitation spectra. $\bar{\Omega}(\omega)$ is also frequency-dependent and complex-valued, both explicitly through the third term in Eq. 6.65 and implicitly through f_{xc}^{open} in the coupling matrix $K_{ijkl}(\omega)$. The explicit frequency-dependence arises because the bare Kohn-Sham transitions are already broadened, even in the absence of Hartree-exchange-correlation effects. This is most easily seen by setting $K_{ijkl}(\omega) = 0$ in Eq. 6.65. $\bar{\Omega}_{ijkl}$ is then diagonal and Eq. 6.64 reduces to a set of uncoupled equations given by

$$\Big\{(\omega_{ij}^{ks} + \Delta_{ij}^{ks})^2 + (\Gamma_{ij}^{ks})^2 - 2\imath\omega\Gamma_{ij}^{ks}\Big\}F_{ij} = \omega^2 F_{ij}. \tag{6.68}$$

These are solved with the quadratic formula to yield

$$\omega = -\imath\Gamma_{ij}^{ks} \pm (\omega_{ij}^{ks} + \Delta_{ij}^{ks}), \tag{6.69}$$

which are precisely the poles of Eq. 6.63.

6.4 Application - spectrum of a C^{2+} atom from the Redfield master equation

As a simple demonstration, in this section we calculate the absorption spectrum of a C^{2+} atom in vacuum, including natural linewidths due to spontaneous emission using the Redfield master equation [48, 36]. We also compare the OQS-TDDFT results to a numerically exact spectrum constructed using experimental data [189].

A. Spontaneous emission from the Redfield master equation

For a single atom with zero center of mass velocity contained in vacuum, the system-bath interaction is

$$\hat{V} = -\imath\hat{\vec{\mu}} \cdot \sum_i \vec{\epsilon}_i \sqrt{\frac{\omega_i}{2V}} (a_i - a_i^\dagger). \tag{6.70}$$

Here, $\hat{\vec{\mu}}$ is the dipole operator for the atom, $\vec{\epsilon}_i$ and ω_i are respectively the polarization vector and frequency of the ith mode of the radiation field and V is the quantization volume. a_i and $a_i^\dagger$ respectively destroy and create a photon in the ith vacuum mode. The photon reservoir Hamiltonian is

$$\hat{H}_R = \sum_i \omega_i a_i^\dagger a_i. \tag{6.71}$$

With the system-bath interaction and bath hamiltonian specified, the Redfield tensor can be explicitly constructed [48].

In general, the modes of the radiation field act as a bosonic bath, leading to decay of the atomic excitations due to spontaneous and stimulated emission [89, 4, 5, 6]. However, if the atom is at sufficiently low temperature, so that it is assumed to be in the ground state, the effect of stimulated emission is absent in the linear spectrum. We then need to only construct the matrix elements R_{a0a0} appearing in Eq. 6.53. For the real part of R_{a0a0} one finds

$$\Gamma_{a0} = \frac{(2\pi)^2}{V} \int\int |\vec{\mu}_{a0} \cdot \vec{\epsilon}_i|^2 \omega_k g(\omega_k, \vec{k}) \delta(\omega_{a0} - \omega_k) d\Omega_k d\omega_k. \tag{6.72}$$

The imaginary part of R_{0a0a} is given by

$$\Delta_{a0} = \frac{2\pi}{V} \sum_n \mathcal{P} \int\int |\vec{\mu}_{an} \cdot \vec{\epsilon}_i|^2 \frac{\omega_k}{\omega_{an} - \omega_k} g(\omega_k, \vec{k}) d\Omega_k d\omega_k, \tag{6.73}$$

where $\mathcal{P}$ denotes the principle value integral [48]. ω_k is the frequency of a photon whose wave-vector magnitude is $k = |\vec{k}|$. $\omega_{an} = E_a - E_n$ is the difference in atomic energy levels and $\vec{\mu}_{an}$ are matrix elements of the dipole operator between atomic wavefunctions. $g(\omega)$ is the density of field modes, which in free-space takes the form $g(\omega) = \frac{V\omega^2}{(2\pi)^2 c^3}$. This gives rise to the natural linewidth,

$$\Gamma_{a0} = \frac{4\mu_{a0}^2 \omega_{a0}^3}{3c^3}, \tag{6.74}$$

which holds for interacting as well as non-interacting electrons [203].

Using experimental data for the atomic energy levels and the transition dipole matrix elements of C^{2+} taken from [189], we can explicitly construct Eq. 6.74. We include in our calculation the 3 lowest dipole allowed transitions of C^{2+}, which are $1s^2 2s^2 \rightarrow 1s^2 2s(2p, 3p, 4p)$. The numerical values of the linewidths (imaginary part of the frequency) calculated in Eq. 6.74 are given in the fourth column of Table 6.2. In

vacuum, the integral in 6.73 formally diverges, however when mass renormalization is taken into account the observed Lamb shifts are several orders of magnitude smaller and will be neglected in the following analysis [26]. From the transition dipole matrix elements we can also construct the oscillator strengths. The "exact" response function constructed with these parameters is included in Figures 1-3. The natural linewidths are very small due to the factor of c^{-3} in Eq. 6.74. We have therefore multiplied the linewidths by c^3 in the figures to make comparison of the relative magnitudes easier.

B. OQS-ATDDFT calculation of the spectrum of C^{2+}

As a first step, we solve Eq. 6.64 using only an adiabatic approximation to the exchange-correlation kernel. This corresponds to including the first term in Eq. 6.38, but entirely neglecting $f_{xc}^{bath}(\mathbf{r}, \mathbf{r}'; \omega)$.

For our calculations, we obtain the Kohn-Sham parameters of C^{2+} to be inputted in Eq. 6.65 using the real-space TDDFT package Octopus [43, 152, 13]. First, a ground state DFT calculation is performed using the local density approximation (LDA) with the modified Perdew-Zunger (PZ) parameterization of the correlation energy [177]. For all calculations, the $1s^2$ core is replaced by a Troullier-Martins pseudopotential [231]. The Kohn-Sham eigenvalues and dipole matrix elements between Kohn-Sham orbitals are computed, and substituted into Eq. 6.74 to obtain the bare Kohn-Sham linewidths, Γ_{ij}^{ks}. These correspond to the real part of the Kohn-Sham-Redfield tensor (imaginary part of the bare Kohn-Sham frequency) of Eq. 6.59 and are given in the second column of Table 6.2. From the dipole matrix elements between Kohn-Sham orbitals, the bare Kohn-Sham oscillator strengths can be con-

structed. The real and imaginary parts of the bare Kohn-Sham response function constructed with these quantities are plotted in Figures 6.1-6.3.

Next, we perform a standard LR-ATDDFT calculation to obtain the matrix elements of the adiabatic Hartree-exchange-correlation kernel to be inputted in Eq. 6.65. The matrix elements of the kernel obtained are given in table 6.4. We also include the energies obtained from the standard LR-ATDDFT calculation in column 4 of Table 6.1. For consistency, we use the LDA with modified PZ functional for the exchange-correlation kernel as well.

Since the operator in Eq. 6.65 is explicitly frequency-dependent even when using an adiabatic kernel, Eq. 6.64 represents a non-linear eigenvalue problem. We solve it using the generalized eigenvalue algorithm presented in [180, 200]. The real part of the solutions to Eq. 6.64 are given in column 3 of Table 6.1, while the imaginary part is given in column 3 of Table 6.2. The real and imaginary parts of the response function obtained are plotted in figures 6.1-6.3.

Table 6.1: Real part of the 3 lowest transition frequencies for C^{2+} in vacuum in a.u.

Transition	Bare Kohn-Sham	OQS-ATDDFT	ATDDFT	Exact
2s $\rightarrow$ 2p	0.3110	0.4428	0.4427	0.4664
2s $\rightarrow$ 3p	1.1164	1.1069	1.1069	1.1798
2s $\rightarrow$ 4p	1.3680	1.3631	1.3631	1.4690

Table 6.2: Imaginary part of the 3 lowest transition frequencies for C^{2+} in vacuum in a.u. The last column includes the GL perturbation correction to the 2s $\rightarrow$ 2p transition.

Transition	Bare Kohn-Sham	OQS-ATDDFT	Exact	OQS-ATDDFT + GL
2s $\rightarrow$ 2p	9.4587×10^{-9}	9.4347×10^{-9}	1.2833×10^{-7}	2.3907×10^{-8}
2s $\rightarrow$ 3p	3.3812×10^{-8}	3.3788×10^{-8}	2.5118×10^{-7}	
2s $\rightarrow$ 4p	1.9581×10^{-8}	1.9581×10^{-8}	4.7670×10^{-8}	

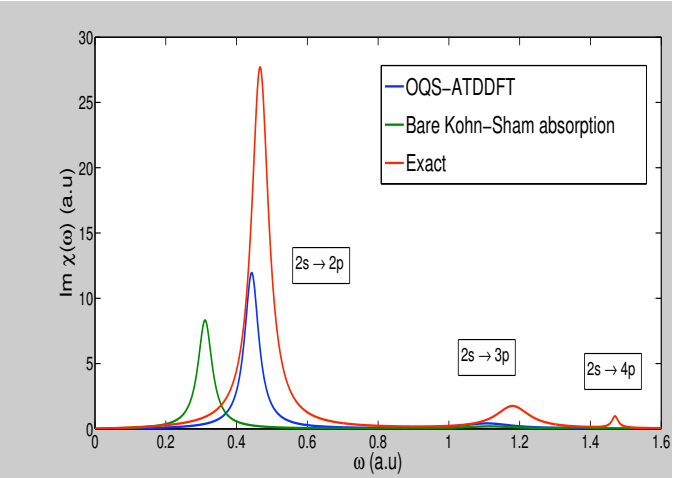

Figure 6.1: Absorption Spectrum of C^{2+} including the 3 lowest dipole allowed transitions. The curves shown are: a) The bare Kohn-Sham spectrum. b) The spectrum obtained by solving Eq. 6.64 with an adiabatic exchange-correlation kernel. c) The numerically exact spectrum obtained using experimental data. All linewidths have been scaled by a factor of c^3 (unscaled values are in table 6.2).

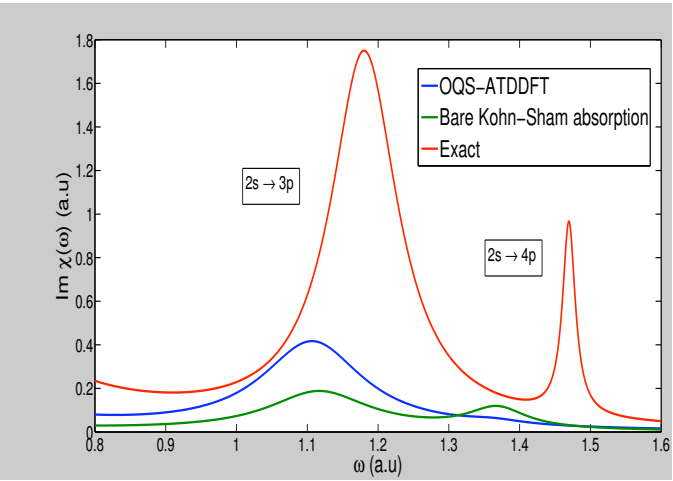

Figure 6.2: Same as Figure 1, but with a close-up view of the $2s \rightarrow 3p$ and $2s \rightarrow 4p$ transitions.

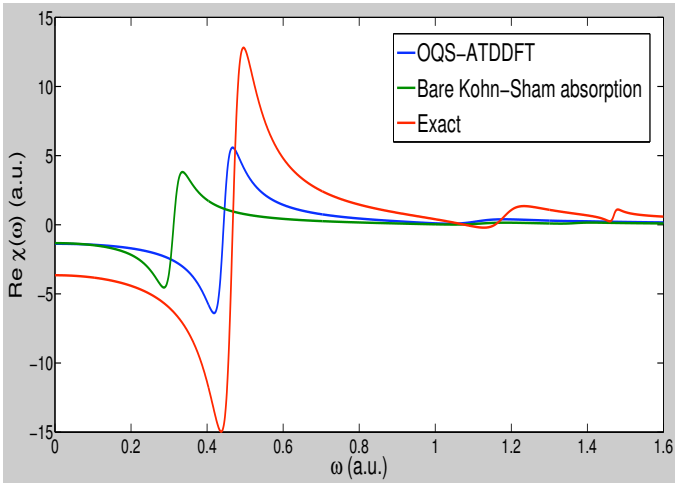

Figure 6.3: Real part of the density-density response function of C^{2+} including the 3 lowest dipole allowed transitions. The effect of the photon bath is to broaden the dispersion over multiple frequencies. The curves shown are: a) The bare Kohn-Sham dispersion. b) The dispersion relation obtained by solving Eq. 6.64 with an adiabatic exchange-correlation kernel. c) The dispersion relation obtained using experimental data.

6.5 Analysis - beyond the adiabatic approximation in OQS-TDDFT linear response theory

A. Effect of using an adiabatic approximation to f_{xc}^{open}

From Tables 6.1 and 6.2, it is clear that using an adiabatic kernel in Eq. 6.64 gives essentially the same corrections to the real part of the energy as usual LR-ATDDFT, while leaving the imaginary part changed by a relatively small amount, especially for the higher transitions. This means that using an adiabatic kernel in linear response OQS-TDDFT is expected to give the same correction to the location of absorption peaks as usual LR-ATDDFT, while correcting the bare Kohn-Sham

linewidths requires an additional frequency-dependent functional. This justifies *a posteriori* our separation of the exchange-correlation kernel in Eq. 6.38 into an adiabatic part for f_{xc}^{closed} and a part due exclusively to bath effects which must have frequency-dependence.

To understand this situation better, we consider a "small matrix approximation" (SMA), in which a single occupied to unoccupied Kohn-Sham transition, $i \to j$, is completely isolated from all other transitions [14, 239, 140, 15]. This is valid when the transition of interest is weakly coupled to all other excitations. In this case, Eq. 6.64 reduces to

$$\bar{\Omega}(\omega)_{ij,ij} F_{ij} = \omega^2 F_{ij}, \tag{6.75}$$

which is equivalent to the polynomial equation

$$\omega^2 + 2\imath\Gamma_{ij}^{ks}\omega - \left[(\omega_{ij}^{ks} + \Delta_{ij}^{ks})^2 + (\Gamma_{ij}^{ks})^2 + 4(\omega_{ij}^{ks} + \Delta_{ij}^{ks})K_{ij,ij}(\omega)\right] = 0. \tag{6.76}$$

If one assumes the adiabatic approximation, the coupling matrix is frequency independent. i.e.

$$K_{ij,ij}(\omega) \approx K_{ij,ij}. \tag{6.77}$$

Eq. 6.76 then reduces to a simple quadratic equation, with solutions given by

$$\omega = -\imath\Gamma_{ij}^{ks} \pm \sqrt{(\omega_{ij}^{ks} + \Delta_{ij}^{ks})^2 + 4(\omega_{ij}^{ks} + \Delta_{ij}^{ks})K_{ij,ij}}. \tag{6.78}$$

This shows that the eigenvalues retain their bare Kohn-Sham linewidths. Therefore, provided the SMA holds, an adiabatic functional is expected to have no effect on the linewidths. In Table 6.3 we compare the real parts of the energies obtained within the SMA with those of the full diagonalization of the Casida matrix in the space of

the 3 lowest dipole-allowed transitions. It is seen that the SMA agrees quite well with the full diagonalization, differing by only 0.8, 0.6, 0.2 mhartree for the $2s \to 2p$, $2s \to 3p$ and $2s \to 4p$ transitions respectively. A rigorous criterion for the validity of the SMA is given in Eq. (11) of [14]. It can be shown that this criterion does in fact hold to a large degree for the 3 lowest transitions of C^{2+} which we have included in our calculation. The SMA is increasingly more accurate for the higher-lying transitions, which explains why the OQS-ATDDFT linewidths for the higher transitions are progressively closer to their bare Kohn-Sham values (see table 6.2).

In table 6.3 we also show the results of using a "single pole approximation" (SPA), which has been studied extensively in the literature for Be [181, 243, 183, 39]. In the SPA, one further assumes that the diagonal kernel matrix elements are small relative to the bare Kohn-Sham transitions [14]. We see that the SPA differs from the full diagonalization by a large amount and is in fact not valid, especially for the $2s \to 2p$ transition. This can be understood by inspecting the kernel matrix elements given in Table 6.4. We see that the diagonal elements are not small relative to the bare Kohn-Sham transitions, especially for the $2s \to 2p$ transition. For this reason, our analysis of Eq. 6.64 will focus on the SMA rather than SPA.

Table 6.3: Real part of the 3 lowest transition frequencies for C^{2+} in vacuum (a.u.) showing a comparison of the SMA and SPA to the full diagonalization of the Casida matrix. The experimental value is included as well for comparison.

Transition	ATDDFT-SMA	ATDDFT-SPA	ATDDFT-Full	Exact
2s $\to$ 2p	0.4435	0.3610	0.4427	0.4664
2s $\to$ 3p	1.1063	1.1052	1.1069	1.1798
2s $\to$ 4p	1.3629	1.3611	1.3631	1.4690

Table 6.4: Matrix elements of the adiabatic Hartree-exchange-correlation kernel (Eq. 6.66) used in solving Eq. 6.64 (a.u.).

Kernel matrix element	Numerical value
$K_{2s2p,2s2p}$	8.0350 $\times 10^{-2}$
$K_{2s3p,2s3p}$	-4.8271 $\times 10^{-3}$
$K_{2s4p,2s4p}$	-2.5278 $\times 10^{-3}$
$K_{2s2p,2s3p}$	1.0305 $\times 10^{-2}$
$K_{2s2p,2s4p}$	1.9445 $\times 10^{-3}$
$K_{2s3p,2s4p}$	-4.7298 $\times 10^{-4}$

B. Additional sources of error in the Calculation

It is evident from Table 6.2 that the bare Kohn-Sham and OQS-ATDDFT linewidths differ from the exact values by a large amount, especially for the $2s \rightarrow 2p$ transition, where this difference is more than an order of magnitude. In addition to the neglect of f_{xc}^{bath}, several other sources of error enter into the calculation which we now address [243, 183, 39]. i) The virtual orbital space is truncated to the 3 lowest transitions. ii) The bare Kohn-Sham linewidths are calculated using orbitals and frequencies of an LDA ground-state Kohn-Sham potential rather than the exact Kohn-Sham ground-state potential. iii) The adiabatic LDA (ALDA) kernel is approximate even for closed-systems since it is local in both space and time.

We have already shown in subsection 6.4 A that the SMA holds and becomes increasingly accurate for the higher-lying transitions, implying that these transitions mix relatively weakly. As a result, we have found very small errors introduced by truncating the virtual space to the 3 lowest-lying transitions. We conclude that the truncation is not an appreciable source of error in our calculations.

To address point ii), in Table 6.5 we have compared the bare Kohn-Sham eigenvalues from our LDA calculation with those obtained using exact-exchange within

Table 6.5: Comparison of the bare Kohn-Sham eigenvalues using LDA and exact-exchange within the localized Hartree-Fock approximation (EXX-LHF) (a.u.).

Eigenvalue	LDA	EXX-LHF
2s	-1.4701	-1.6940
2p	-1.1591	-1.3754
3p	-0.3537	-0.5527
4p	-0.1020	-0.3044

the localized Hartree-Fock approximation (EXX-LHF) [204]. The calculation was performed with the DSCF module of the program package Turbomole [234] using the d-aug-cc-pV6Z basis set with g and higher basis functions removed [266, 267]. Exact-exchange has been shown to be much more accurate for Be than LDA [243], as it is self interaction free and possesses the correct $-\frac{1}{r}$ asymptotic behavior [182]. Being a cation, the LDA potential for C^{2+} possesses more bound states than Be, but it is evident from table 6.5 that the LDA potential decays far too quickly. The differences between the LDA and the exact-exchange bare Kohn-Sham frequencies are 7.6, 24.9, 21.6 mhartree for the $2s \to 2p$, $2s \to 3p$ and $2s \to 4p$ transitions respectively. Since these bare Kohn-Sham frequencies are used in Eq. 6.74 to construct the bare Kohn-Sham linewidths, we see a that large error is already introduced from the approximate nature of the ground-state LDA potential.

Lastly, we mention that in [243], an ALDA kernel was found to be satisfactory for the $s \to p$ transitions of Be and we expect a similar conclusion to hold for C^{2+}. Naturally, going beyond an ALDA kernel will improve the real-part of the energies. However, the analysis of subsection 6.4 A suggests that if one improves the kernel by including spatial non-locality, but still uses the adiabatic approximation, the linewidths will remain largely unchanged.

We can conclude that the largest source of error in our calculation arises from the approximate nature of the LDA ground-state Kohn-Sham potential. As in usual TDDFT, an OQS-TDDFT linear response calculation uses the bare Kohn-Sham orbitals and eigenvalues as input. In OQS-TDDFT, these are used to construct the bare Kohn-Sham linewidths, which must be a good starting point. Reliable approximations to the Kohn-Sham ground-state potential are therefore needed. As mentioned earlier, even with an accurate ground-state functional, one also needs frequency-dependent approximations to f_{xc}^{bath} to correct the bare Kohn-Sham linewidths. We turn to this point now.

C. Beyond an adiabatic approximation to f_{xc}^{open}

In subsection 6.4 A, we discussed the effect of approximating $f_{xc}^{open}(\mathbf{r}, \mathbf{r}'; \omega)$ with an adiabatic (frequency independent) kernel. We now investigate what the frequency-dependent contribution to $f_{xc}^{bath}(\mathbf{r}, \mathbf{r}'; \omega)$ must be to correct the bare Kohn-Sham linewidths. To formulate our construction rigorously, we examine the difference between the Kohn-Sham-Redfield tensor in Eq. 6.59 and the interacting Redfield tensor in Eq. 6.45. The bath correlation functions in both expressions are the same. The difference lies in the eigenenergies and wavefunctions of the system Hamiltonian used to construct the Redfield tensor. These are Kohn-Sham quantities in the first case and many-body quantities in the latter case. This suggests that the interacting Redfield tensor can be expanded in a Görling-Levy (G-L) perturbation series in the electron-electron interaction coupling constant α, with the Kohn-Sham-Redfield tensor entering as the zeroth-order term in the series [74, 75, 76, 77, 78]:

$$R_{abcd}(\alpha) \approx R_{abcd}(0) + \alpha R^1_{abcd} + \alpha^2 R^2_{abcd} + ... \tag{6.79}$$

For linear response from the ground-state as we consider here, we need only construct the quantities $\{R_{a0a0}(\alpha)\}$. This is done by first expanding the ground-state and excited-state wavefunctions in a G-L perturbation series in α,

$$|a(\alpha)\rangle = \sum_{i=1}^{\infty} \alpha^i |a^i\rangle, \tag{6.80}$$

as well as the corresponding energies

$$E_a(\alpha) = \sum_{i=1}^{\infty} \alpha^i E^i_a. \tag{6.81}$$

These expansions are then substituted into the general expression for the Redfield tensor to construct an expansion of the Redfield tensor at coupling constant α. For $\alpha = 1$, we recover the interacting Redfield tensor in Eq. 6.45, since Eq. 6.80 and Eq. 6.81 then refer to wavefunctions and energies of the interacting system. For $\alpha = 0$, we obtain a Redfield tensor $R_{a0a0}(0)$ written in terms of Kohn-Sham ground-state and excited Slater determinants, $\{|a(0)\rangle\}$, and corresponding energies $\{E_a(0)\}$, which lie on the adiabatic connection with the interacting wavefunctions $\{|a(1)\rangle\}$ and energies $\{E_a(1)\}$. Due to the one-body nature of the system-bath coupling, only matrix elements of the tensor $R_{a0a0}(0)$ containing singly-excited Kohn-Sham Slater determinants are non-zero. The zeroth-order term in the expansion of Eq. 6.79 then reduces to,

$$R_{a0a0}(0) = R^{ks}_{ijij}. \tag{6.82}$$

Here, the indices i, j label a pair of Kohn-Sham orbitals, in which an orbital ϕ_i occupied in the Kohn-Sham groundstate is replaced by an orbital ϕ_j occupied in the

singly excited determinant $|a(0)\rangle$. With the G-L expansion of the Redfield tensor well formulated, one can rigorously construct a G-L expansion of $f_{xc}^{open}(\mathbf{r},\mathbf{r}';\omega)$ using the same general procedure outlined in [76].

For the specific example of C^{2+} we consider here with the Lamb shifts neglected, Eq. 6.79 amounts to expanding Γ_{a0}, in a G-L series as

$$\Gamma_{a0}(\alpha) \approx \Gamma_{ij}^{ks} + \alpha\Gamma_{a0}^{1} + ..., \tag{6.83}$$

and determining the corresponding corrections to the bare Kohn-Sham linewidth. This is done explicitly in Appendix B for the $1s^2 2s^2 \rightarrow 1s^2 2s 2p$ transition within the SMA. The first-order correction $\Gamma_{2p,2s}^{1}$ is found to be

$$\begin{aligned} \Gamma_{2p,2s}^{1} &= -\frac{4}{c^3}(\epsilon_{2s}-\epsilon_{2p})^2 \\ \times &\left[\int d^3\mathbf{r}\phi_{2s}(\mathbf{r})\mathbf{r}\phi_{2p}(\mathbf{r})\right]^2 \\ \times &\left[(2s2s|2s2s)-(2s2s|2p2p)-(2s2p|2s2p)\right], \end{aligned} \tag{6.84}$$

where ϕ_{2s} and ϕ_{2p} are ground-state Kohn-Sham orbitals and

$$(ij|kl) = \int d^3\mathbf{r}\int d^3\mathbf{r}'\frac{\phi_i(\mathbf{r})\phi_j(\mathbf{r})\phi_k(\mathbf{r}')\phi_l(\mathbf{r}')}{|\mathbf{r}-\mathbf{r}'|}. \tag{6.85}$$

The frequency-dependent matrix element of the kernel $f_{xc}^{bath}(\mathbf{r},\mathbf{r}';\omega)$ to first-order in G-L perturbation theory is found to be (see appendix B):

$$K_{2s2p,2s2p}^{bath}(\omega) = -\frac{\imath}{2(\epsilon_{2s}-\epsilon_{2p})}(\omega+\imath\Gamma_{2p,2s}^{ks})(\Gamma_{2p,2s}^{1}). \tag{6.86}$$

Due to the simple system-bath coupling, the linewidth formula of Eq. 6.74 depends only on the atomic energies and oscillator strengths, both of which can easily be expanded in a G-L series. The bath kernel must simply yield the difference between

the linewidth calculated using energies and oscillator strengths of the Kohn-Sham system and those of the true system. By construction, the bath kernel matrix element in Eq. 6.86 yields precisely this difference to first-order in G-L perturbation theory. In the general case, the bath will not simply couple to the system through the dipole operator and the G-L expansion of the Redfield tensor will be more complicated. For instance, for a phonon bath one needs the G-L expansion of the electron-phonon coupling matrix elements.

To calculate the numerical value of Eq. 6.84, we evaluated the Coulomb integrals of Eq. 6.85 using the spectral-element code previously presented in [258], taking the orbitals from Octopus as input. The Octopus orbitals were obtained on a uniform mesh with a grid-spacing of 0.1 a.u. The spectral-element code projects the orbitals onto a tensorial Chebyshev basis for the efficient evaluation of Eq. 6.85, and we chose all parameters conservatively such that the main source of error is in the original representation of the orbitals.

The imaginary part of the frequency of the $2s \rightarrow 2p$ transition obtained by solving Eq. 6.64 with Eq. 6.86 included is given in column 5 of Table 6.2. In Figure 6.4, the imaginary part of the density-density response function with Eq. 6.86 included is plotted in the vicinity of the $2s \rightarrow 2p$ transition. Because we have derived Eq. 6.86 within the SMA, there is no correction to the oscillator strength [14, 15] and the entire effect seen in Figure 6.4 is due to a change in the linewidth. The contribution from $f_{xc}^{bath}(\mathbf{r}, \mathbf{r}'; \omega)$ provides significant improvement to the linewidth, but is still far from the exact value.

The kernel matrix element in Eq. 6.86 and coulomb integrals in Eq. 6.85 are

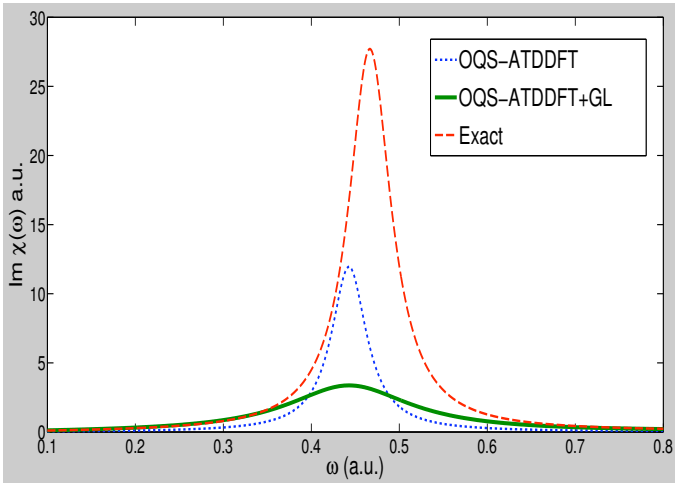

Figure 6.4: Correction to the bare Kohn-Sham linewidth to first-order in GL perturbation theory. All linewidths have been scaled by a factor of c^3 (unscaled values are in table 6.2).

calculated using LDA orbitals and eigenvalues, which as we have mentioned already contain a large degree of error. If instead we were to construct Eq. 6.86 using orbitals and eigenvalues of the exact Kohn-Sham ground-state, the frequency-dependent bath correction would yield a far better linewidth. Also, we have only gone to first order in G-L perturbation theory in deriving Eq. 6.84 and Eq. 6.86, while in principle the SMA contains all orders. However, neglect of higher-order corrections is a far smaller source of error (see appendix B).

6.6 Conclusion and outlook

We have formulated a general framework of LR-TDDFT for many-body open quantum systems, which in principle gives access to environmentally broadened spectra in a strictly *ab initio* manner. Our treatment is most applicable to microscopically

derived master equations, in which the system and bath are both treated by starting from an underlying microscopic Hamiltonian. As an example, we analyzed the microscopically derived Redfield master equation for an atom interacting with a photon bath. In this case, the bath correlation functions were very well characterized since they depended only on the free radiation field density of states, which is analytically known. In some cases, the bath correlation functions may be more complicated and need to be treated in an approximate way. In the case of a phonon bath, one would need to be able to calculate the phonon density of modes as well as electron-phonon couplings. This could be done by obtaining the vibrational normal modes with a usual DFT calculation, and feeding the couplings and phonon density of states into an open-systems LR-TDDFT calculation for the broadened spectrum. This would be particularly applicable to describing the absorption spectrum of impurity molecules imbedded in a lattice. Similarly, for the case of chromophores in a protein environment, one could simulate the protein using classical molecular dynamics to obtain the spectral density and then feed it into an open-systems LR-TDDFT calculation to compute the absorption spectrum of the chromophore. A similar treatment could be applied to molecules in liquid environments. These directions will be explored in our future work.

The Redfield master equation is Markovian and as a result, the pole structure of the OQS response functions are simple. For Markovian master equations, there are only two parameters characterizing the absorption spectrum; the location of the peaks and their width. As a result, the OQS Casida equations have relatively simple frequency-dependence. For non-Markovian master equations, the memory kernel is

non-local in time, which corresponds to a frequency-dependent self-energy in the OQS response functions. The resulting lineshapes are asymmetric and may have many non-zero moments. This is expected to give rise to much more complicated frequency dependence in the exchange-correlation kernel, since it must correct all of these moments. A simple step would be to investigate the first-order non-Markovian correction derived from the cumulant expansion of the memory kernel [162]. This will be investigated in future work.

This paper has focused on homogeneous broadening of the spectrum, which arises when the time-scale of the bath is much faster than that of the electrons. This is the case of interest in OQS-TDDFT, since it implies that the bath can induce relaxation and dephasing of the electronic degrees of freedom. In the other limit of inhomogeneous broadening, the bath is static relative to the time-scale of the electrons. In this case, the external potential due to the nuclei is distributed in different configurations due to the local environment, but no relaxation and dephasing takes place. Inhomogeneous broadening can be well captured by performing usual closed LR-TDDFT calculations for different static nuclear configurations and then ensemble averaging. A realistic spectrum usually consists of both broadening mechanisms. This can be well captured by performing an open systems LR-TDDFT calculation for each static nuclear configuration and then ensemble averaging over the different configurations afterwards.

To perform an open-systems LR-TDDFT calculation using modern electronic structure codes, the greatest challenge is probably the implementation of the algorithm in [180, 200] for solving the complex and non-linear eigenvalue problem. This

algorithm becomes expensive for a large occupied-unoccupied space of Kohn-Sham orbitals and a self consistent procedure becomes more efficient. Work towards implementing these capabilities in a numerical library is currently under investigation.

6.7 Appendix A - derivation of the Casida equations for the Redfield master equation

In this appendix we derive Eq. 6.64 and Eq. 6.65 for the open-systems Casida equations. In keeping with the original derivation by Casida [42], we introduce second quantized creation and annihilation operators, $a_i^\dagger$ and a_i, for a one-particle orbital basis. In what follows, this will be taken to be a basis of real molecular orbitals from a ground or equilibrium-state Kohn-Sham calculation. An arbitrary one-particle operator $\hat{O}$ is represented in this basis as

$$\hat{O} = \sum_{ij} a_i^\dagger a_j \langle i|\hat{O}|j\rangle. \tag{6.87}$$

The interacting density-density response function in Eq. (6.53) is given by

$$\chi_{nn}(\mathbf{r},\mathbf{r}';\omega) = \sum_{ijkl} \phi_i(\mathbf{r})\phi_j(\mathbf{r})\chi_{ijkl}(\omega)\phi_k(\mathbf{r}')\phi_l(\mathbf{r}'), \tag{6.88}$$

where

$$\chi_{ijkl}(\omega) = \sum_a [P(E_a)] \sum_b \left\{ \frac{\langle a|a_j^\dagger a_i|b\rangle\langle b|a_k^\dagger a_l|a\rangle}{\omega + \omega_{ab} + \imath R_{abab}} - \frac{\langle a|a_k^\dagger a_l|b\rangle\langle b|a_j^\dagger a_i|a\rangle}{\omega - \omega_{ab} + \imath R^*_{abab}} \right\}. \tag{6.89}$$

In this basis, the linear response of the interacting 1-particle reduced density matrix at frequency ω is

$$\delta\rho_{ij}(\omega) = \sum_{kl} \chi_{ijkl}(\omega)\delta v_{ext}(\omega)_{kl}, \tag{6.90}$$

and the linear density response is given by

$$\delta n(\mathbf{r},\omega) = \sum_{ij} \delta\rho_{ij}(\omega)\phi_j(\mathbf{r})\phi_i(\mathbf{r}). \tag{6.91}$$

In the Kohn-Sham-Redfield system, the same density response is produced from

$$\delta n(\mathbf{r},\omega) = \sum_{ij} \delta\gamma_{ij}(\omega)\phi_j(\mathbf{r})\phi_i(\mathbf{r}), \tag{6.92}$$

where

$$\delta\gamma_{ij}(\omega) = \sum_{kl} \chi^{ks}_{ijkl}(\omega)\delta v_{ks}(\omega)_{kl}, \tag{6.93}$$

is the response of the Kohn-Sham-Redfield one-particle reduced density matrix and

$$\chi^{ks}_{ijkl}(\omega) = \delta_{ik}\delta_{jl}\left\{\frac{f_j - f_i}{\omega - \omega_{ij} + \imath r^{ks}_{jiji}}\right\}. \tag{6.94}$$

Eq. (6.93) can then be written as

$$\delta\gamma_{ij}(\omega) = \left\{\frac{f_j - f_i}{\omega - \omega_{ij} + \imath r^{ks}_{jiji}}\right\}(\delta v_{ext}(\omega)_{ij} + \delta v_h(\omega)_{ij} + \delta v^{open}_{xc}(\omega)_{ij}). \tag{6.95}$$

We now write

$$\delta v_h(\omega)_{ij} + \delta v^{open}_{xc}(\omega)_{ij} = \sum_{kl} K_{ijkl}(\omega)\delta\gamma_{kl}(\omega), \tag{6.96}$$

where

$$K_{ijkl}(\omega) = \int d^3\mathbf{r}\int d^3\mathbf{r}'\phi^*_i(\mathbf{r})\phi^*_j(\mathbf{r})\left\{\frac{1}{|\mathbf{r}-\mathbf{r}'|} + f^{open}_{xc}[n^{eq}](\mathbf{r},\mathbf{r}';\omega)\right\}\phi_k(\mathbf{r}')\phi_l(\mathbf{r}'). \tag{6.97}$$

We can then re-write Eq. 6.95 as

$$\sum_{kl}^{f_k\neq f_l}\left[\delta_{ik}\delta_{jl}\frac{\omega - \omega_{kl} + \imath r^{ks}_{lklk}}{f_l - f_k} - K_{ijkl}(\omega)\right]\delta\gamma_{kl}(\omega) = \delta v_{ext}(\omega)_{ij}. \tag{6.98}$$

We separate the Kohn-Sham-Redfield matrix into real and imaginary parts

$$r^{ks}_{klkl} = \Gamma^{ks}_{kl} + \imath\Delta^{ks}_{kl}, \tag{6.99}$$

and separate particle-hole and hole-particle contributions as in [42]

$$\sum_{kl,f_k>f_l}\left[\delta_{ik}\delta_{jl}\frac{\omega-\omega_{kl}+\Delta^{ks}_{kl}}{f_l-f_k}+\imath\frac{\delta_{ik}\delta_{jl}\Gamma^{ks}_{kl}}{f_l-f_k}-K_{ijkl}(\omega)\right]\delta\gamma_{kl}(\omega))$$
$$-\sum_{kl,f_k>f_l}K_{ijlk}(\omega)\delta\gamma_{lk}(\omega=\delta v_{ext}(\omega)_{ij} \tag{6.100}$$

$$\sum_{kl,f_k>f_l}\left[\delta_{ik}\delta_{jl}\frac{\omega-\omega_{lk}-\Delta^{ks}_{kl}}{f_k-f_l}+\imath\frac{\delta_{ik}\delta_{jl}\Gamma^{ks}_{kl}}{f_k-f_l}-K_{jilk}(\omega)\right]\delta\gamma_{lk}(\omega)$$
$$-\sum_{kl,f_k>f_l}K_{jikl}(\omega)\delta\gamma_{kl}(\omega)=\delta v_{ext}(\omega)_{ji}. \tag{6.101}$$

We now define the following matrices:

$$A_{ijkl}(\omega)=\delta_{ik}\delta_{jl}\frac{\omega_{kl}-\Delta^{ks}_{kl}}{f_k-f_l}-K_{ijkl}(\omega), \tag{6.102}$$

$$\Gamma_{ijkl}=\frac{\delta_{ik}\delta_{jl}\Gamma^{ks}_{kl}}{f_k-f_l}, \tag{6.103}$$

$$B_{ijkl}(\omega)=-K_{ijlk}(\omega), \tag{6.104}$$

and

$$C_{ijkl}=\frac{\delta_{ik}\delta_{jl}}{f_k-f_l}. \tag{6.105}$$

The matrices B_{ijkl} and C_{ijkl} have the same form as in [42]. A_{ijkl} is similar, but includes a contribution due to the Lamb shift and Γ_{ijkl} is a new term.

We can combine Eq. 6.100 and Eq. 6.101 into a single matrix equation,

$$\left\{\begin{pmatrix}\bar{A}-\imath\bar{\Gamma} & \bar{B}\\ \bar{B} & \bar{A}+\imath\bar{\Gamma}\end{pmatrix}-\omega\begin{pmatrix}\bar{C} & 0\\ 0 & \bar{C}\end{pmatrix}\right\}\begin{pmatrix}\vec{\delta\gamma}(\omega)\\ \vec{\delta\gamma}^{\,*}(\omega)\end{pmatrix}=\begin{pmatrix}\vec{\delta v_{ext}}(\omega)\\ \vec{\delta v_{ext}}^{\,*}(\omega)\end{pmatrix}, \tag{6.106}$$

or by applying the unitary transformation

$$\frac{1}{\sqrt{2}}\begin{pmatrix} 1 & 1 \\ -1 & 1 \end{pmatrix}, \tag{6.107}$$

$$\begin{pmatrix} \bar{A}+\bar{B} & \imath\bar{\Gamma}+\omega\bar{C} \\ \imath\bar{\Gamma}+\omega\bar{C} & \bar{A}-\bar{B} \end{pmatrix}\begin{pmatrix} \Re e(\vec{\delta\gamma}(\omega)) \\ -\imath\Im m(\vec{\delta\gamma}(\omega)) \end{pmatrix} = \begin{pmatrix} \Re e(\vec{\delta v_{ext}})(\omega) \\ -\imath\Im m(\vec{\delta v_{ext}}(\omega)) \end{pmatrix}. \tag{6.108}$$

Without loss of generality we assume the applied perturbation to be real. Since the molecular orbitals are taken to be real, the density response can be calculated from $\Re e(\vec{\delta\gamma}(\omega))$ alone. From Eq. 6.108, we obtain

$$\left[(\bar{A}+\bar{B})-(\imath\bar{\Gamma}+\omega\bar{C})\left[\bar{A}-\bar{B}\right]^{-1}(\imath\bar{\Gamma}+\omega\bar{C})\right]\Re e(\vec{\delta\gamma}(\omega)) = \Re e(\vec{\delta v_{ext}})(\omega). \tag{6.109}$$

We introduce the matrices

$$\bar{S} = -\bar{C}\left[\bar{A}-\bar{B}\right]^{-1}\bar{C}, \tag{6.110}$$

and

$$\Omega(\omega) = -\bar{S}^{-\frac{1}{2}}\left[\bar{A}+\bar{B}\right]\bar{S}^{-\frac{1}{2}}, \tag{6.111}$$

which have the same form as in the usual Casida equations presented in chapter 2. Eq. 6.109 can then be inverted to obtain

$$\begin{aligned} \Re e(\vec{\delta\gamma}(\omega)) &= S^{-\frac{1}{2}}\Big\{\omega^2-\Omega(\omega)+\bar{S}^{-\frac{1}{2}}\bar{\Gamma}\left[\bar{A}-\bar{B}\right]^{-1}\bar{\Gamma}\bar{S}^{-\frac{1}{2}} \\ + \quad & \imath\omega(\bar{S}^{-\frac{1}{2}}\bar{\Gamma}\bar{C}^{-1}\bar{S}^{\frac{1}{2}}+\bar{S}^{\frac{1}{2}}\bar{C}^{-1}\bar{\Gamma}\bar{S}^{-\frac{1}{2}})\Big\}^{-1}S^{-\frac{1}{2}}\Re e(\vec{\delta v_{ext}})(\omega) \end{aligned} \tag{6.112}$$

The poles of the density-density response function are obtained when the operator in brackets vanishes. Defining

$$\bar{\Omega}(\omega) = \Omega(\omega)-\bar{S}^{-\frac{1}{2}}\bar{\Gamma}\left[\bar{A}-\bar{B}\right]^{-1}\bar{\Gamma}\bar{S}^{-\frac{1}{2}}-\imath\omega(\bar{S}^{-\frac{1}{2}}\bar{\Gamma}\bar{C}^{-1}\bar{S}^{\frac{1}{2}}+\bar{S}^{\frac{1}{2}}\bar{C}^{-1}\bar{\Gamma}\bar{S}^{-\frac{1}{2}}), \tag{6.113}$$

this is equivalent to solving the pseudo-eigenvalue equation

$$\Big\{\omega^2 - \bar{\Omega}(\omega)\Big\}\vec{F} = 0. \tag{6.114}$$

Returning to the basis of Kohn-Sham molecular orbitals, the matrix representation of $\bar{\Omega}(\omega)$ is

$$\begin{aligned}\bar{\Omega}_{ijkl}(\omega) = \delta_{ik}\delta_{jl}\Big\{(\omega_{lk}^{ks} + \Delta_{kl}^{ks})^2 + (\Gamma_{kl}^{ks})^2 - 2\imath\omega\Gamma_{kl}^{ks}\Big\} + \\ 4\sqrt{(f_i - f_j)(\omega_{ji}^{ks} + \Delta_{ij}^{ks})}K_{ijkl}(\omega)\sqrt{(f_k - f_l)(\omega_{lk}^{ks} + \Delta_{kl}^{ks})}.\end{aligned} \tag{6.115}$$

6.8 Appendix B - first-order Görling-Levy perturbation correction to the linewidth of the 2s $\rightarrow$ 2p transition of C^{2+}

In this appendix, we derive the first-order correction to the bare Kohn-Sham linewidth in Eq. 6.84 as well as the frequency-dependent functional which gives rise to this correction. Our treatment closely parallels that used by Görling in deriving the exact-exchange kernel in [76]. In what follows, the Lamb shifts are neglected. We also make the assumption that the two electrons in the $1s^2$ core are frozen, and their effect on the two valence electrons is taken into account with an effective potential. This is in fact the case for our numerical calculations, since we replace the $1s^2$ core by a pseudopotential. We then effectively have a two-electron singlet in which the interacting ground-state is

$$\psi_{2s^2}(\mathbf{r}, \mathbf{r}') \equiv \langle \mathbf{r}, \mathbf{r}' | 2s^2(\alpha = 1)\rangle, \tag{6.116}$$

and the first excited state is

$$\psi_{2s2p}(\mathbf{r},\mathbf{r}') \equiv \langle \mathbf{r},\mathbf{r}'|2s2p(\alpha=1)\rangle. \tag{6.117}$$

We denote the respective energies of these two states by $E_{2s^2} \equiv E_{2s^2}(\alpha=1)$ and $E_{2s2p} \equiv E_{2s2p}(\alpha=1)$. The corresponding Kohn-Sham ground-state is

$$\Phi_{2s^2}(\mathbf{r},\mathbf{r}') \equiv \langle \mathbf{r},\mathbf{r}'|2s^2(\alpha=0) = \phi_{2s}(\mathbf{r})\phi_{2s}(\mathbf{r}'), \tag{6.118}$$

and Kohn-Sham first excited state is

$$\Phi_{2s2p}(\mathbf{r},\mathbf{r}') \equiv \langle \mathbf{r},\mathbf{r}'|2s2p(\alpha=0) = \frac{1}{\sqrt{2}}(\phi_{2s}(\mathbf{r})\phi_{2p}(\mathbf{r}') + \phi_{2s}(\mathbf{r}')\phi_{2p}(\mathbf{r})). \tag{6.119}$$

The respective energies are $2\epsilon_{2s} \equiv E_{2s^2}(\alpha=0)$ and $\epsilon_{2s}+\epsilon_{2p} \equiv E_{2s2p}(\alpha=0)$.

Our starting point is the linear density response at coupling constant α, in the subspace spanned by the $1s^22s^2 \rightarrow 1s^22s2p$ transition,

$$\begin{aligned}\delta n(\alpha,\mathbf{r},\omega) = & \frac{2(E_{2s}(\alpha)-E_{2p}(\alpha))}{(E_{2s}(\alpha)-E_{2p}(\alpha))^2-(\omega+\imath\Gamma_{2p,2s}(\alpha))^2} \\ \times & \ \langle 2s^2(\alpha)|\hat{n}(\mathbf{r})|2s2p(\alpha)\rangle\langle 2s2p(\alpha)|\delta\hat{v}(\alpha,\omega)|2s^2(\alpha)\rangle.\end{aligned} \tag{6.120}$$

For $\alpha=1$, this expression refers to the density response of the interacting system, while for $\alpha=0$, it describes that of the Kohn-Sham system. In particular, $\delta\hat{v}(\alpha=1,\omega)=\delta\hat{v}_{ext}(\omega)$ while $\delta\hat{v}(\alpha=0,\omega)=\delta\hat{v}_s(\omega)$. $\delta n(\alpha,\omega,\mathbf{r})=\delta n(\mathbf{r},\omega)$ is invariant with respect to the coupling constant α. We now expand both sides of Eq. 6.120 in a taylor series in α and equate coefficients of equal powers of α on both sides. At zeroth-order in α, we recover the Kohn-Sham response equation

$$\begin{aligned}\delta n(\mathbf{r},\omega) = & \frac{2(\epsilon_{2p}-\epsilon_{2s})}{(\epsilon_{2p}-\epsilon_{2s})^2-(\omega+\imath\Gamma^{ks}_{2p,2s})^2} \\ \times & \int d^3\mathbf{r}'\langle 2s^2(0)|\hat{\rho}(\mathbf{r})|2s2p(0)\rangle\langle 2s2p(0)|\hat{\rho}(\mathbf{r}')|2s^2(0)\rangle\delta v_s(\mathbf{r}',\omega).\end{aligned} \tag{6.121}$$

To evaluate the first-order terms, we need the expansions of the wavefunctions, energies and linewidths to first order in α. The expansions of the wavefunctions and energies are given by standard GL perturbation theory:

$$|\psi^1_{2s^2}\rangle = \frac{\langle\psi_{2s2p}(0)|\hat{v}_{ee} - \hat{v}_h - \hat{v}_x|\psi_{2s^2}(0)\rangle}{\epsilon_{2s} - \epsilon_{2p}}|\psi_{2s2p}(0)\rangle \tag{6.122}$$

$$|\psi^1_{2s2p}\rangle = \frac{\langle\psi_{2s^2}(0)|\hat{v}_{ee} - \hat{v}_h - \hat{v}_x|\psi_{2s2p}(0)\rangle}{\epsilon_{2p} - \epsilon_{2s}}|\psi_{2s^2}(0)\rangle \tag{6.123}$$

$$E^1_{2s^2} = \langle\psi_{2s^2}(0)|\hat{v}_{ee} - \hat{v}_h - \hat{v}_x|\psi_{2s^2}(0)\rangle \tag{6.124}$$

$$E^1_{2s2p} = \langle\psi_{2s2p}(0)|\hat{v}_{ee} - \hat{v}_h - \hat{v}_x|\psi_{2s2p}(0)\rangle. \tag{6.125}$$

Since the ground-state is a spin singlet, $\hat{v}_x = -\frac{\hat{v}_h}{2}$ and all quantities can be explicitly evaluated. We find

$$\langle\mathbf{r},\mathbf{r}'|\psi^1_{2s^2}\rangle = \frac{3}{4(\epsilon_{2s} - \epsilon_{2p})}(2s2s|2s2p)\left[\phi_{2s}(\mathbf{r})\phi_{2p}(\mathbf{r}') + \phi_{2s}(\mathbf{r}')\phi_{2p}(\mathbf{r})\right] = 0 \tag{6.126}$$

and

$$\langle\mathbf{r},\mathbf{r}'|\psi^1_{2s2p}\rangle = \frac{-3}{2\sqrt{2}(\epsilon_{2s} - \epsilon_{2p})}(2s2s|2s2p)\left[\phi_{2s}(\mathbf{r})\phi_{2s}(\mathbf{r}')\right] = 0. \tag{6.127}$$

i.e. the first-order corrections to the wavefunctions vanish since $(2s2s|2s2p) = 0$.

The first-order G-L correction to the energy is

$$\omega^1_{2s^2,2s2p} \equiv E^1_{2s^2} - E^1_{2s2p} = (2s2s|2s2s) - (2s2s|2p2p) - (2s2p|2s2p). \tag{6.128}$$

We now obtain the first-order correction to the bare Kohn-Sham linewidth. The linewidth for the $2s^2 \to 2s2p$ transition at coupling constant α is

$$\Gamma_{2p,2s}(\alpha) = -\frac{4}{3}(\frac{1}{c})^3(\omega_{2s^2,2s2p}(\alpha))^3|\langle\psi_{2s^2}(\alpha)|\vec{\tilde{\mu}}|\psi_{2s2p}(\alpha)\rangle|^2. \tag{6.129}$$

Expanding in a taylor series in α, at zeroth-order we recover the Kohn-Sham linewidth,

$$\Gamma_{2p,2s}(0) \equiv \Gamma^{ks}_{2p,2s} = -\frac{4}{3}(\frac{1}{c})^3(\epsilon_{2s}-\epsilon_{2p})^3|\langle\psi_{2s^2}(0)|\vec{\hat{\mu}}|\psi_{2s2p}(0)\rangle|^2. \tag{6.130}$$

In terms of Kohn-Sham orbitals this is,

$$\Gamma_{2p,2s}(0) \equiv \Gamma^{ks}_{2p,2s} = -\frac{4}{3}(\frac{1}{c})^3(\epsilon_{2s}-\epsilon_{2p})^3|\int d^3\mathbf{r}\phi_{2s}(\mathbf{r})\mathbf{r}\phi_{2p}(\mathbf{r})|^2. \tag{6.131}$$

At first-order in α we find

$$\begin{aligned}\Gamma^1_{2p,2s} = &-\frac{4}{3}(\frac{1}{c})^3(\epsilon_{2s}-\epsilon_{2p})^3\langle\psi_{2s^2}(0)|\vec{\hat{\mu}}|\psi_{2s2p}(0)\rangle\left[\langle\psi_{2s^2}(0)|\vec{\hat{\mu}}|\psi^1_{2s2p}\rangle + \langle\psi^1_{2s^2}|\vec{\hat{\mu}}|\psi_{2s2p}(0)\rangle\right]\\ - \;& 4(\frac{1}{c})^3(\epsilon_{2s}-\epsilon_{2p})^2\omega^1_{2s^2,2s2p}|\langle\psi_{2s^2}(0)|\vec{\hat{\mu}}|\psi_{2s2p}(0)\rangle|^2\end{aligned} \tag{6.132}$$

Using Eqs. 6.126 - 6.128, we can now evaluate Eq. 6.132. We find that,

$$\begin{aligned}\Gamma^1_{2p,2s} = &-4\left[\frac{1}{137}\right]^3(\epsilon_{2s}-\epsilon_{2p})^2\\ \times\;&\left[\int d^3\mathbf{r}\phi_{2s}(\mathbf{r})\mathbf{r}\phi_{2p}(\mathbf{r})\right]^2\\ \times\;&\left[(2s2s|2s2s)-(2s2s|2p2p)-(2s2p|2s2p)\right].\end{aligned} \tag{6.133}$$

which is the correction to the bare Kohn-Sham linewidth we have included in Eq. 6.84. We can now ask what the frequency-dependent exchange-correlation kernel is which gives rise to this correction. This is in some sense a generalization of the exact-exchange kernel to OQS, in that it is correct to first-order in G-L perturbation theory. However, the form of this functional will now depend on the bath.

To construct the kernel, we now equate coefficients of first-order in α in Eq. 6.120. The result is

$$\int d^3\mathbf{r}'\left[\chi^{ks}_{nn}(\omega,\mathbf{r},\mathbf{r}')\delta v^1(\omega,\mathbf{r}') + h^{open}_1(\omega,\mathbf{r},\mathbf{r}')\delta v_s(\omega,\mathbf{r}')\right] = 0. \tag{6.134}$$

Here, $\delta v^1(\omega, \mathbf{r}')$ is the coefficient of the first-order GL expansion of the potential, obtained from

$$\delta v^1(\alpha, \omega, \mathbf{r}) \approx \delta v_s(\omega, \mathbf{r}) + \alpha \delta v^1(\omega, \mathbf{r}), \tag{6.135}$$

and

$$\begin{aligned} & h_1^{open}(\omega, \mathbf{r}, \mathbf{r}') = \\ & \left\{ \frac{2\omega^1_{2s^2 2s2p}}{(\epsilon_{2s} - \epsilon_{2p})^2 - (\omega + \imath\Gamma^{ks}_{2p,2s})^2} - \frac{4(\epsilon_{2s} - \epsilon_{2p})((\epsilon_{2s} - \epsilon_{2p})\omega^1_{2s^2 2s2p} - \imath\Gamma^1_{2p,2s})((\omega + \imath\Gamma^{ks}_{2p,2s})))}{((\epsilon_{2s} - \epsilon_{2p})^2 - (\omega + \imath\Gamma^{ks}_{2p,2s})^2)^2} \right\} \\ \times \quad & [2\phi_{2s}(\mathbf{r})\phi_{2p}(\mathbf{r})\phi_{2s}(\mathbf{r}')\phi_{2p}(\mathbf{r}')]\,. \end{aligned} \tag{6.136}$$

We now separate out the part of $h_1^{open}(\omega, \mathbf{r}, \mathbf{r}')$ which contains the correction to the Kohn-Sham linewidth $\Gamma^1_{2p,2s}$:

$$h_1^{bath}(\omega, \mathbf{r}, \mathbf{r}') = \imath \frac{8(\epsilon_{2s} - \epsilon_{2p})(\Gamma^1_{2p,2s})(\omega + \imath\Gamma^{ks}_{2p,2s})}{((\epsilon_{2s} - \epsilon_{2p})^2 - (\omega + \imath\Gamma^{ks}_{2p,2s})^2)^2} \left[\phi_{2s}(\mathbf{r})\phi_{2p}(\mathbf{r})\phi_{2s}(\mathbf{r}')\phi_{2p}(\mathbf{r}')\right]. \tag{6.137}$$

The functional arising from this correction is then given by:

$$f_x^{bath}(\omega, \mathbf{r}, \mathbf{r}') = \int d^3\mathbf{r}'' d^3\mathbf{r}''' \chi^{ks^{-1}}(\omega, \mathbf{r}, \mathbf{r}'') h_1^{bath}(\omega, \mathbf{r}'', \mathbf{r}''') \chi^{ks^{-1}}(\omega, \mathbf{r}''', \mathbf{r}'). \tag{6.138}$$

Here, $\chi^{ks^{-1}}$ is the inverse of the Kohn-Sham response function

$$\chi^{ks}(\omega, \mathbf{r}, \mathbf{r}') = \frac{4(\epsilon_{2s} - \epsilon_{2p})}{(\epsilon_{2s} - \epsilon_{2p})^2 - (\omega + \imath\Gamma^{ks}_{2p,2s}))^2} \left[\phi_{2s}(\mathbf{r})\phi_{2p}(\mathbf{r})\phi_{2s}(\mathbf{r}')\phi_{2p}(\mathbf{r}')\right] \tag{6.139}$$

in the restricted space. For the open-systems Casida equations, we need the matrix element of $K^{bath}_{2s2p,2s2p}(\omega)$ of Eq. 6.138, which is given by

$$K^{bath}_{2s2p,2s2p}(\omega) = -\frac{\imath}{2(\epsilon_{2s} - \epsilon_{2p})}(\omega + \imath\Gamma^{ks}_{2p,2s})(\Gamma^1_{2p,2s}). \tag{6.140}$$

This is the matrix element given in Eq. 6.86. The remaining part of Eq. 6.137 we have not separated out changes only the location of the $2s^2 \rightarrow 2s2p$ transition and

not the width. In the calculations of section 6.5, we have replaced this contribution to the kernel with an adiabatic functional in solving Eq. 6.64.

To understand Eq. 6.140 better, we consider the SMA equation in the $2s \rightarrow 2p$ subspace:

$$\omega^2 + 2\imath\Gamma^{ks}_{2s2p}\omega - \left\{(\epsilon_{2s} - \epsilon_{2p})^2 + (\Gamma^{ks}_{2s2p})^2 + 4(\epsilon_{2s} - \epsilon_{2p})K_{2s2p,2s2p}(\omega)\right\} = 0.$$

If we separate out the adiabatic and bath parts as

$$K_{2s2p,2s2p}(\omega) = K_{2s2p,2s2p} - \frac{\imath}{2(\epsilon_{2s} - \epsilon_{2p})}(\omega + \imath\Gamma^{ks}_{2p,2s})(\Gamma^{1}_{2p,2s}) \tag{6.141}$$

and substitute Eq. 6.141 in, we get:

$$\begin{aligned} &\omega^2 + 2\imath(\Gamma^{ks}_{2s2p} + \Gamma^{1}_{2p,2s})\omega - \left\{(\epsilon_{2s} - \epsilon_{2p})^2 + (\Gamma^{ks}_{2s2p})^2 + 2\Gamma^{ks}_{2s2p}\Gamma^{1}_{2p,2s} + 4(\epsilon_{2s} - \epsilon_{2p})K_{2s2p,2s2p}\right\} \\ = \;& 0. \end{aligned} \tag{6.142}$$

The solutions are

$$\omega = -\imath(\Gamma^{ks}_{2s2p} + \Gamma^{1}_{2p,2s}) \pm \sqrt{(\epsilon_{2s} - \epsilon_{2p})^2 - (\Gamma^{1}_{2p,2s})^2 + 4(\epsilon_{2s} - \epsilon_{2p})K_{2s2p,2s2p}} \tag{6.143}$$

Since the term $(\Gamma^{1}_{2p,2s})^2$ is very small relative to the ATDDFT shift, the effect of $K^{bath}_{2s2p,2s2p}(\omega)$ is a simple correction to the bare Kohn-Sham linewidth by $\Gamma^{1}_{2p,2s}$. The term $(\Gamma^{1}_{2p,2s})^2$ is due to higher-order corrections in G-L perturbation theory to the real part of the energy. It arises from the fact that in OQS-TDDFT as in usual TDDFT, the SMA contains all orders in G-L perturbation theory [14]. Furthermore, in OQS-TDDFT, higher orders in G-L perturbation theory mix the real and imaginary parts of the energies, i.e. the real part of the kernel affects the imaginary part of the energy

and vice-versa. This is in contrast to the SPA, which is exact to first-order in G-L perturbation theory for OQS-TDDFT and does not mix the real and imaginary parts of the energy. The SPA has also been shown the be exact to first-order in G-L perturbation theory for usual closed-systems TDDFT [72].

Chapter 7

Coherent resonant energy transfer

7.1 Introduction

In this chapter, we model the coherent energy transfer of an electronic excitation within covalently linked aromatic homodimers from first-principles. We do not directly use OQS-TDDFT discussed in previous chapters, but rather use conventional TDDFT to calculate parameters from first-principles to be used in a Redfield master equation. For the systems we model, the timescales of coherent transport are experimentally known from time-dependent polarization anisotropy measurements, and so we can directly assess whether current techniques are predictive for modeling coherent transport. The coupling of the electronic degrees of freedom to the nuclear degrees of freedom is calculated from first principles rather than assumed, and the fluorescence anisotropy decay is directly reproduced. Surprisingly, we find that although TDDFT absolute energies are routinely in error by orders of magnitude more than the coupling energy between monomers, the coherent transport properties of these dimers can be

semi-quantitatively reproduced from first-principles. Future directions which must be pursued to yield predictive and reliable models of coherent transport are suggested.

7.2 Background

Recent experimental evidence of coherent electronic energy transport at biologically relevant physical scales has spurred studies of the basic dynamics [54] as well as new methods for propagating the quantum system state [98, 99, 286] as it interacts with an environment we cannot fully characterize. However, detailed pictures of how the quantum state couples to the bath are usually absent from these studies, which often assume an environment characterized by a small number of parameters (for example a spectral density of the Drude-Lorentz form [199]). Models for the electronic coupling usually vary in detail [206, 23, 96, 85, 196, 163] between the dipole approximation and the single-particle Coulomb interaction, but quantum many-particle effects are assumed to be negligibly small. It is not clear from the literature [202] at present day how well electronic structure theory can provide all the parameters which are required to accurately predict the timescale of coherence decay. The couplings between chromophores are typically on the order of $300\text{cm}^{-1} \approx 1$ kcal/mol. Excited-state methods which can be afforded for molecules of this size, mainly time-dependent density functional theory (TDDFT), are routinely in error [174, 208] by 1600cm^{-1}.

Recently, an experiment [272] has characterized coherent resonant energy transfer (CRET) in a closely related family of anthracene dimers (Fig. 7.1). In this experiment a femtosecond pulse of linearly polarized light prepared superpositions

of electronic states on a pair of identical chromophores. Then, over the course of roughly a picosecond, the time-dependent fluorescence was detected by upconversion. The oscillations of the fluorescence anisotropy ($r(t)$) measured in these experiments are a marker of coherent transport (as demonstrated in the pioneering work of Hochstrasser [285] and coworkers). The three dimers, [2,2'] dithia-anthracenophane (DTA), 3,5-bis(anthracen-2-yl)-tert-butylbenzene (MDAB) and 1,2-bis-(anthracen-9-yl)benzene (ODAB), are all derivatives of anthracene. Theoretically, DTA has been examined [111] by the groups of Cina [155, 27] and Jang [274], who supported the picture of coherent transport. The latter work provided direct calculations of the Coulomb coupling within a model-Hamiltonian picture of transport, and used DTA as a test-bed for an efficient new theory of CRET [103, 102].

The purpose of our present investigation in this chapter is to theoretically reproduce the experimentally measured fluorescence anisotropy. We do this by forming a master equation using first-principles electronic structure calculations, thereby avoiding empirical or phenomenological input. In this work we employ the Redfield [194, 195] master equation. We will see below that *within our simulations*, the couplings between the electronic states are so much larger than the bath reorganization energies, that Redfield theory is appropriate for this application [112, 108, 109] and can furnish good results. However, the Redfield master equation is perturbative and fails entirely when the electronic couplings are small relative to the bath strength. The main goal of this work is to propagate the Redfield equation using affordable electronic structure methods. To this end, we will test out an inexpensive procedure for producing the system-bath model, combining a recently proposed dia-

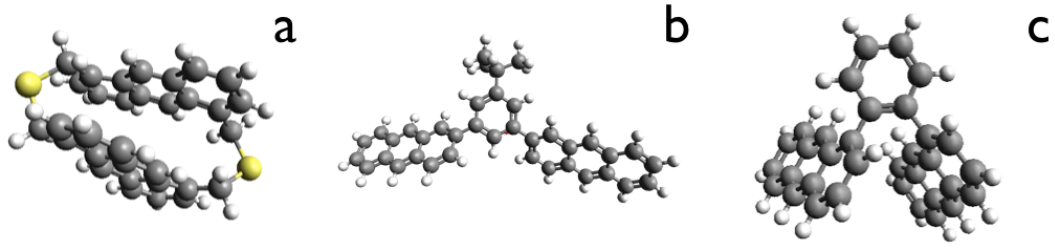

Figure 7.1: Excitonic dimers considered in this study, from left-to-right [2,2'] dithiaanthracenophane (DTA), 3,5-bis(anthracen-2-yl)-tert-butylbenzene (MDAB) and 1,2-bis-(anthracen-9-yl)benzene (ODAB).

batization scheme [219, 256] with the independent mode displaced harmonic oscillator model (IMDHO) for nuclear dephasing.

We should briefly mention that there are many other possible simulation techniques that could be used for modeling coherent transport that we don't use in the present study. Non-Markovian master equations exist which can replace Redfield theory with little additional cost [103, 102]. Moving towards increased accuracy and increased cost, there are several dynamical simulation techniques which can propagate electrons coupled to nuclei [101, 47], such as surface hopping (SH) [233, 50, 160], Ehrenfest dynamics [125, 105, 151], and semi-classical approaches [221, 44]. Sophisticated and sometimes formally-exact master equations which incorporate non-Markovian effects through auxiliary density matrices that propagate along with the system [220, 100, 215, 99, 157] can also be used, but are a difficult starting point for atomistic simulations because the cost which is already significant with model-hamiltonians increases further in a non-linear way as detail is added.

7.3 The electron-phonon Redfield master equation

The starting point of our analysis is the usual Liouville-Von Neumann equation for the full unitary evolution of a molecule linearly coupled [95] to a harmonic phonon bath,

$$\frac{d}{dt}\hat{\rho}(t) = -i\mathcal{L}\hat{\rho}(t) = -i[\hat{H}, \hat{\rho}(t)], \text{ where:} \qquad \hat{H} = \hat{H}_{\text{elec}} + \hat{H}_{\text{ph}} + \hat{H}_{\text{elec-ph}} \tag{7.1}$$

and ρ is the full density matrix describing both electronic and nuclear degrees of freedom. We now introduce fermionic operators a_i and $a_i^\dagger$, which respectively destroy and create an electron in an arbitrary many-electron state i (the exact nature of the electronic states is discussed below). Similarly, we introduce bosonic operators b_α and $b_\alpha^\dagger$, which respectively destroy and create a vibrational excitation in mode α. We expand the terms in the molecular Hamiltonian and density matrix in terms of these basis states as,

$$\hat{H}_{\text{elec}} = \sum_{ij}\sum_{\alpha}(h_{ij} + \delta_{ij}\omega_\alpha d_{i\alpha}^2/2)a_j^\dagger a_i, \tag{7.2}$$

$$\hat{H}_{\text{ph}} = \sum_{\alpha}\omega_\alpha(b_\alpha^\dagger b_\alpha + \frac{1}{2}), \tag{7.3}$$

$$\hat{H}_{\text{elec-ph}} = \sum_{i}\sum_{\alpha}\omega_\alpha d_{i\alpha} a_i^\dagger a_i(b_\alpha^\dagger + b_\alpha), \tag{7.4}$$

$$\sigma = \sum_{ij}\sum_{\alpha\beta}\rho_{ij}a_i^\dagger a_j \times \rho_{\alpha\beta}b_\alpha^\dagger b_\beta. \tag{7.5}$$

In the language of chapter 3, $\hat{H}_{\text{elec}}$ is the reduced system Hamiltonian, $\hat{H}_{\text{elec-ph}}$ is the system-bath coupling (which has the desired bilinear form of eq. 3.4) and $\hat{H}_{\text{ph}}$ is the bath Hamiltonian. Here, $d_{i\alpha}$ is a dimensionless parameter measuring the strength of coupling of the ith electronic state to the vibrational mode α, which is defined

explicitly below (Eq. 7.11). Different choices of electronic states will yield different dimensionless displacements $d_{i\alpha}$. In Eq 7.2, we see that in addition to the usual matrix elements h_{ij} of the electronic Hamiltonian, $\hat{H}_{\text{elec}}$ includes an additional contribution from reorganization energies of the bath [209], $\omega_\alpha d_{i\alpha}^2/2$. The reorganization energies cancel somewhat with the imaginary contribution of the Redfield operator (the Lamb shift), and both are absent from Redfield's original work. In derivations of Redfield's equations from more sophisticated equations of motion [209], neglecting the reorganization energy and Lamb shift is an additional approximation. We opt to include both, since the resulting Hamiltonian can be consistently motivated from first-principles as a linear expansion of $\hat{H}_{\text{elec}}(R)$ in terms of the nuclear coordinates R.

In a more detailed picture, a reorganization Hamiltonian for solvent polarization degrees of freedom which are very slow on the electronic timescale, and have little impact on the dynamics, would localize the adiabatic electronic states of the system. One effective way to incorporate these solvation effects into our simulation is to adopt a recently implemented diabatization [219, 256] procedure invented by Subotnik and coworkers, which mixes the configuration interaction singles (CIS) (or Tamm-Dancoff approximation (TDA)) states with one-another such that their interaction with an implied dielectric is minimized. After this transformation, the electron-phonon coupling is taken to be diagonal in the diabatic electronic basis, although the Hamiltonian now has off-diagonal Coulomb and exchange coupling.

In order to simulate CRET, Eq. 7.1 must be integrated for a few picoseconds, which is prohibitive for these systems with all-electron detail [127, 8]. Instead, we

propagate a limited basis of a few TDDFT states within the TDA [93], which obeys an equation of motion for an auxiliary one-particle density matrix which is the same as the electronic part of Eq. 7.1. We assume that an approximate propagation spanned by the space of adiabatic stationary states (ψ_i) coming from TDDFT/TDA with energies below 6eV (the sum of excitation energy and pulsewidth) is sufficient to represent the combined dynamics. States of the quasi-diabatic model [219, 256] evolve under a non-diagonal Hamiltonian with the off-diagonal Coulomb and exchange matrix elements generating coupling between these energy transfer states. When a field is applied, further coupling between the states will occur via the dipole operator, and also via the Redfield relaxation operator describing coupling to the vibrational modes. Transition moments between states and excitation energies were obtained from the Q-Chem program package [214] and evaluated as expectation values of the dipole operator with TDA density matrices [276] using the functionals and basis sets described below. These add a time-dependent off-diagonal term to $\hat{H}_{elec}$, with matrix elements $V_{ij}(t) = \vec{E}(t) \cdot \mu_{ij}$. Strictly speaking, although the exact Kohn-Sham density matrix reproduces the correct density response, it may not be a valid approximation to the true 1-particle reduced density matrix. Using the Kohn-Sham density matrix as an approximation to the true 1-particle density matrix affects the transition moments most significantly relative to other errors in our calculations arising from this approximation.

To the approximate electronic Liouville equation mentioned above, we add dissipative terms [123, 159] of a Markovian Redfield equation, affording an effective dynamics of the reduced electronic system density matrix in the presence of the vi-

brational bath. The resulting Redfield equation is:

$$\dot{\rho}_{IJ} = i\sum_{K}(H_{elec,IK}(t)\rho_{KJ}(t) - \rho_{IK}(t)H_{elec,KJ}(t)) + \sum_{KL}\mathcal{R}_{IJKL}\rho_{KL}(t), \tag{7.6}$$

$$\mathcal{R}_{IJKL} = \Gamma_{LJIK} + \Gamma^{*}_{KIJL} - \delta_{JL}\Gamma_{IMMK} - \delta_{IK}\Gamma_{JMML}, \tag{7.7}$$

$$\Gamma_{IJKL} = \sum_{\alpha,\beta,i,j}\int_{0}^{\infty} dt e^{i\omega_{KL}t}C_{ij}^{\alpha,\beta}(t)\langle I|a_i^{\dagger}a_i|J\rangle\langle K|a_j^{\dagger}a_j|L\rangle. \tag{7.8}$$

Indices I, J have been capitalized to reflect the possibility that the basis of Eq. 7.8 may be chosen differently than the basis of Eq. 7.1. The lowercase indices refer to the unmixed, purely-electronic TDDFT/TDA states. The capitalized indices may refer to Subotnik's quasi-diabatic states, in which case all the capitalized indices are related to their lowercase counterparts by a simple unitary transformation $\hat{U}$, determined by that model for the localization induced by the solvent, i.e. $\hat{H}_{IJ} = U^{*}_{Ii}\hat{H}_{elec,ij}U_{jJ}$. The correlation functions $C_{ij}^{\alpha,\beta}(t)$ in Eq. 7.8 are explained below.

Structures of [2,2'] dithia-anthracenophane (DTA), meta- Dianthraceneophane(MDAB) and ortho-Dianthraceneophane(ODAB) were optimized using the B3LYP [21] functional and def2-TZVP basis [205] (and auxiliary basis [260]) in the ORCA [165] program package and the harmonic vibrational frequencies and modes were evaluated. These geometries and modes were re-used for excited-state calculations. A local exchange approximation, COSX [166] was also invoked. For the purposes of electronic energy transport in molecules, the classic description of the bath, following Huang [32], is the vibrations which underly the molecule itself. To provide an IMDHO for the correlation function of these bath modes $(\alpha, \beta..)$, a nuclear Hessian calculation was performed which provides mass-weighted normal mode coordinates U_n^{α} and frequencies ω_{α}. The thermal correlation functions of the phonon part of the

electron-phonon interaction Hamiltonian, $\hat{H}_{\text{elec-ph}}$, are given by:

$$C_{i,j}^{\alpha,\beta}(t) = \langle [d_{i\alpha}(b_\alpha^\dagger(t) + b_\alpha(t))][d_{j\beta}(b_\beta^\dagger(0) + b_\beta(0))]\rangle, \tag{7.9}$$

where $b_\alpha(t) = e^{i\hat{H}_{\text{ph}}t} b_\alpha e^{-i\hat{H}_{\text{ph}}t}$ and the expectation value is with respect to the equilibrium phonon density matrix. In the IMDHO model we use in our calculations, one assumes that the correlation functions in Eq. (7.9) vanish unless $\alpha = \beta$. The correlation function of a single nuclear mode is then given explicitly by the expression [162]:

$$C_{ij}^{\alpha}(t) = \omega_\alpha^2 \frac{d_{i\alpha} d_{j\alpha}}{2} [(\bar{n}_\alpha + 1)e^{-i\omega_\alpha t} + (\bar{n}_\alpha)e^{i\omega_\alpha t}], \tag{7.10}$$

where $\bar{n}_\alpha = (e^{(\beta\hbar\omega_\alpha)} - 1)^{-1}$ is the thermal phonon distribution. With the real-time correlation function in Eq. 7.10, we associate the Fourier transform $C_{ij}^{\alpha}(\omega)$ and we will use the notation $\sum_\alpha C_{ij}^{\alpha\alpha}(\omega) = C_{ij}(\omega)$ throughout.

Assuming that the potential surfaces of the lower and upper states are harmonic wells of the same frequency, the dimensionless displacements $d_{i\alpha}$ are given by the gradient of the diagonal electronic matrix element projected onto the mode and the mode frequency [184] via the relation:

$$d_{i\alpha} = \omega_\alpha^{-1} \frac{d}{dQ_\alpha} \langle i|\hat{H}_{\text{elec}}(Q)|i\rangle, \tag{7.11}$$

which can then be used to construct the correlation functions in Eq. 7.10. Equivalently, we compute them by taking finite differences in the nuclear coordinates R_n, using the relation:

$$d_{i\alpha} = \sum_n \frac{d}{dR_n} \langle i|\hat{H}_{\text{elec}}(R)|i\rangle U_n^\alpha (m_n\sqrt{\omega_\alpha})^{-1/2}, \tag{7.12}$$

where the index n labels an atom with mass m_n, and U_n^α is the cartesian mass-weighted normal mode coordinate [116]. The coupling constant between the states

can also be expressed in terms of the so-called Huang-Rhys factor $S_{i\alpha}$, which is simply related to the dimensionless displacements by $S_{i\alpha} = \frac{\omega_\alpha d_{i\alpha}^2}{2}$.

The harmonic correlation functions in Eq. 7.10 were evaluated at 273.15K in our simulations. In a solution of tetrachloroethylene, the redistribution of vibrational quanta in anthracene has been studied at room temperature, with time-resolved Raman techniques and found to occur on timescales between 1-10 ps [79], which would correspond to a homogeneous vibrational linewidth of 5cm^{-1} for one pair of modes. In addition to the approximations mentioned above, we assume a Lorentzian broadening of the harmonic thermal correlation function by $\Gamma = 40cm^{-1}$, due to anharmonicity and collisions with the surrounding medium. Diabatic results are relatively insensitive to choices of this parameter (pure-dephasing lifetimes vary by less than a factor of two for reasonable values). The BLYP/6-31g** pure-dephasing lifetimes of the bright states in DTA and MDAB with $\Gamma = 40$cm^{-1} are .894ps and .566ps respectively. For $\Gamma = 100$cm^{-1} the same two quantities are .900ps and .564ps. The result of this series of approximations are correlation functions between each state which resemble the sum of Lorentzian peaks in (Fig. 7.2). These functions are different for every pair of states. In the direction of further rigor, correlation functions could be collected from classical or semi-classical dynamics calculations, or zero-frequency pure-dephasing contributions may be calculated from anharmonicities [156] of the excited state surface. We do not employ these more sophisticated techniques in the present study.

The experimental observable we seek to reproduce is the fluorescence anisotropy,

$$r(t) \equiv (I_\parallel(t) - I_\perp(t))/(I_\parallel(t) + 2I_\perp(t)). \tag{7.13}$$

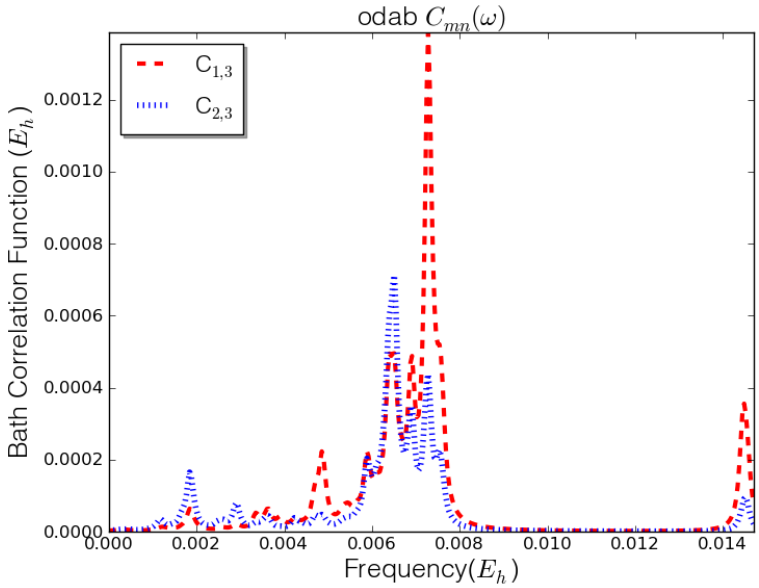

Figure 7.2: An example of the bath correlation functions for ODAB, produced from the approximations discussed in the text. $C_{mn}(\omega)$ is constructed for every pair of states below 6.5eV within the IMDHO model, and used to construct the Redfield tensor.

Here, $I_{\parallel}$ and $I_{\perp}$ are respectively the fluorescence intensity parallel and perpendicular to the stimulation polarization. Factoring out the transition moments of the detector, and making the rotating wave approximations, the fluorescence intensity is given [57] by the dipole-dipole autocorrelation function, $I_{\gamma\delta}(t) \propto Tr(\hat{\rho}_0\hat{\mu}_\gamma e^{-i\mathcal{L}t}\hat{\mu}_\delta)$, where $\rho_0 = |0\rangle\langle 0|$ is the ground state density operator and η, δ are cartesian indices. To spherically average in a numerical propagation of the Redfield equation, we apply an 80fs pulse to three orthogonal directions of the molecule with a carrier frequency that is the average energy of the first four excited states, resulting in a coherent superposition of populated states (Fig. 7.3). The polarization which results in all three directions over time is then used to calculate the tensor $I_{\eta\delta}(t)$. The anisotropy is then evaluated at each time using Eq. 7.13 [282]. Explicitly, one finds that $r(t) = (1 - \rho_{dp})/(1 + 2\rho_{dp})$, where the depolarization ratio $\rho_{dp} = \frac{3\gamma^3}{45\alpha^2+4\gamma^2}$ is determined from the isotropic (α) and anisotropic (γ) tensor invariants of $I_{\eta\delta}(t)$ [245]. The fit of Yamazaki's data with the functional form of Hochstrasser,

$$r(t) = \frac{0.1}{1 + e^{-\frac{2t}{T_2'}}C}\left((1+3C) + 3(1-C)e^{-\frac{t}{T_2'}} * Cos(\omega_{osc}t + \delta) + (3+C)e^{-\frac{2t}{T_2'}}\right)$$
$$\text{where } C = Cos^2\theta \text{ and } \omega_{osc} = 4\beta^2 - (T_2')^{-2}, \tag{7.14}$$

is used to represent the experiment in this work. Since we use a many-state model we interpret β, and T_2' as *effective* couplings and dephasing times respectively. θ is related to the angle between transition moments, and δ is a phase-shift.

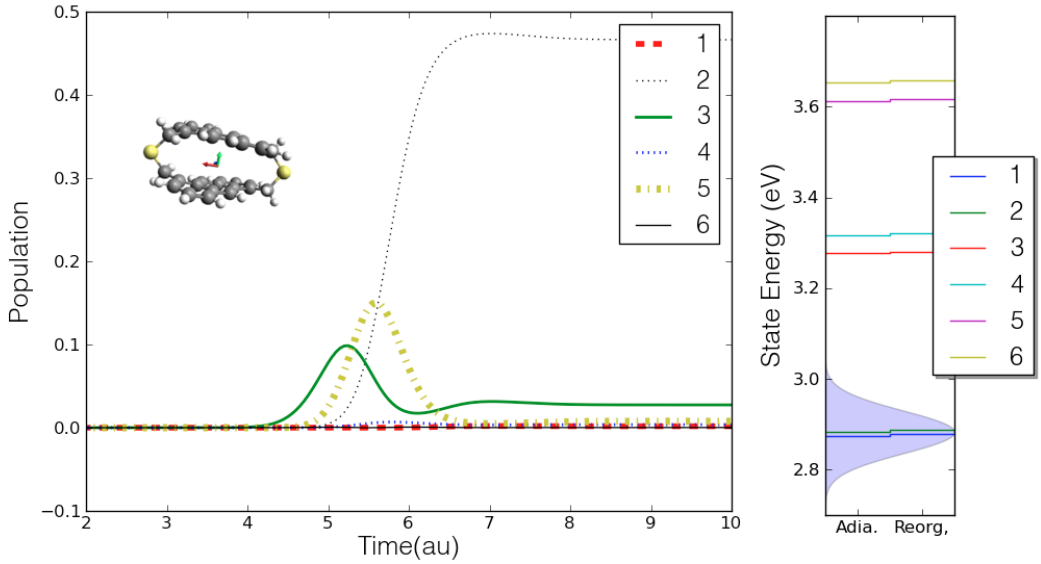

Figure 7.3: An example of how the [2,2'] dithia-anthracenophane(DTA) state populations evolve under the application of an 80fs oscillating electric field of 0.05 au along one of three axes (denoted by the red arrow in the figure). On the right, the corresponding stick spectra are shown, with and without reorganization energy, and in blue the envelope of the exciting pulse.

7.4 Electronic parameters

The vertical (ωB97//6-31g**) [46] TDDFT excitation spectrum of a single anthracene molecule has two poles below 5eV at 4.28, and 4.43 eV, with only the lower state possessing significant oscillator strength. This is a reasonable reproduction [287] of bright $^1B_{1u}$ and dark $^1B_{2u}$ states which occur experimentally at 3.43 and 3.47 eV respectively. For some of the dimers studied, the stick spectrum which results can be rationalized as simple mixtures of these states; with two bright states coming from symmetric and antisymmetric combinations of the bright states amongst themselves. The dark states, whose realism was questioned in previous work [274], appear to have charge-transfer character, and their relative position to the bright states in the spectrum changes depending on whether an asymptotically correct exchange functional is used or not. The TDDFT stick spectra are in good qualitative agreement with a correlated wavefunction based [87, 198] excited state theory (Table 7.1). The low lying dark states are likely real, and indeed in our dynamics simulations they are involved in population relaxation of the bright states.

The semi-quantitative agreement of electronic couplings (β) with the experi-

Method	Species	State 1	State 2	State 3	State 4
RI-SOS-CIS(D_0)	DTA	3.83, f=0.077	3.84, f=0.047	3.89, f=0.104	3.89, f=0.026
	MDAB	3.89, f=0.003	3.90, f=0.004	4.00, f=0.150	4.01, f=0.175
	ODAB	3.93, f=0.023	3.95, f=0.001	3.98, f=0.158	4.05, f=0.266
B3LYP	DTA	2.84 , f=0.002	2.85, f=0.002	3.22, f=0.043	3.26, f=0.069
	MDAB	3.19, f=0.001	3.20, f=0.001	3.37, f=0.153	3.38, f=0.050
	ODAB	3.00, f=0.032	3.07, f=0.021	3.37, f=0.104	3.44, f=0.128

Table 7.1: Singlet excited state energies (eV) and oscillator strengths, f, produced by RI-CIS(D_0)//cc-pvdz follow the same trends as the B3LYP results, although the values of the couplings are more poorly reproduced.

mental oscillation periods is the most difficult aspect of the experiment to reproduce with TDDFT, although it was not the focus of this work. If the Hamiltonian is expressed in a basis of localized degenerate states, β is the off diagonal element between two states. In the basis of adiabatic states which diagonalize the electronic Hamiltonian, it is related to half the gap between the energies of the bright states. The experimental estimate of β from the oscillation period depends on a 2-state model, and the subtraction of a relaxation lifetime. Theoretical models depend on either perturbation theory of monomer densities which have been separated in an ad-hoc way, or a splitting between adiabatic energies. The latter, super-molecule approach is more realistic and can capture whatever electron interaction effects are present in the underlying electronic structure model (although the perfect mixture of the two states is assumed). Because of the uncontrolled nature of the approximations relating the experimental β and electronic state gap, one should view direct comparison of the experimental and calculated β semi-quantitatively. Only the final simulated oscillation should be directly comparable to the experiment. Still if the adiabatic state-splitting is more than an order of magnitude larger than the experimental β no reasonable simulation will be possible, because the reorganization energies will not shift the oscillation into the correct regime.

Cina's previous work [27] introduced a phenomenological 2-state ($J = 22.9$ cm^{-1}) model of DTA coupled explicitly to an intra-chromophore vibration ($\omega_{12} = 385$cm^{-1}, d = .55). It was found that coherent vibrational dynamics could be used to modify the dynamics of excitation transfer, although only weakly in the case of DTA. In the theory of Jang and coworkers [274], the electronic coherence oscillation period is

given by the bare coupling renormalized by a bath contribution which depends on the parameters of a super-ohmic spectral density. Reversing these parameters such that they reproduce the experimental vibrational progression and oscillation period, they estimate a bare (purely electronic) coupling for DTA between 53 and 100cm^{-1}, about 40cm^{-1} less than their B3LYP calculations. The effects of the solvent on the coupling were also calculated (and found to be small ≈7cm^{-1}). A range of values between 44 and 144 cm^{-1} was obtained, and the authors identified the agreement with the experimental values as somewhat fortuitous.

We find that for these covalently bonded dimers, going up-to exchange effects is insufficient (Table 7.2) to reproduce the qualitative trend in coupling energy. In Table 7.2 we calculate the coupling energy with increasingly sophisticated electronic structure models. The basis is held constant, but even in larger bases the conclusions remain the same (see Table 7.3). In the first column the monomers interact mostly via a classical coulomb interaction because the electronic structure lacks long-range exchange. The qualitative trend is correct. In the second and third, more exchange is added and the relative agreement becomes worse. Finally with exchange and a second-order treatment of correlation, good relative agreement is obtained. It seems possible that coulomb only methods (TDC, BLYP, dipole-dipole, etc.) benefit from some cancellation of non-local exchange and correlation errors.

These findings are in keeping with existing work [202, 207] which has found that Forster and Dexter coupling are insufficient for nearby molecules, and are indeed in error by up to a factor of two. It seems likely that for these systems which are separated by less than 5 Angstroms, long-range correlation effects are required to reproduce the

correct trend of energy splittings. Solvation effects on related chromophore pairs have been studied more thoroughly than medium-range correlation, and are known to be meaningful [163]. Roughly twenty percent reductions of the coupling relative to vacuum have been reported for naphthalene dimer in a continuum model of hexane. Ideally, we would fully treat both effects, but unfortunately the costs of these calculations are prohibitive for pursuing them as a means of calculating the decoherence rate.

We do not challenge the validity of the transition dipole, or transition density cube [139] approximations when applied to distant chromophores. Rather we are suggesting that in cases of nearby chromophores where long-range correlation would be considered a prerequisite for ground state thermochemistry [81], it's likely also necessary to reproduce excitonic couplings [133]. Correlated wave-function based models, or double hybrids should be applied to these problems if possible. Simply choosing experimental couplings would be inappropriate, since the basis of adiabatic electronic states from which we calculate the correlation functions $C_{mn}(t)$, and the experimentally accessed states are different. This approach would also have difficulty accessing the dark charge-transfer states. Phenomenological approaches which combine experimental energies with experimental bath parameters are consistent and successful. However, combining calculated electronic spectra with experimental bath correlation functions ignores the difference between the basis states of the experiment and the calculation.

	BLYP	B3LYP	ωB97	RI-SOS-CIS(D)$_0$	Exp.
DTA	64	150	220	4	14
MDAB	88	84	20	18	29
ODAB	266	284	429	273	51

Table 7.2: State couplings $\beta(\mathrm{cm}^{-1})$ as estimated from half the difference of bright excited state energies in the cc-pvdz basis for various methods differing in their treatment of exchange and correlation. The agreement is best with the addition of long-range correlation (last column). The addition of exchange appears to worsen the results. Basis set dependence is addressed below.

	B3LYP	BLYP
DTA	144	93
MDAB	90	80
ODAB	257	246

Table 7.3: State couplings $\beta(\mathrm{cm}^{-1})$ as estimated from half the difference of bright excited state energies in the QZVP basis. With this basis these quantities are nearly converged with respect to basis-set size, but TDDFT is still unable to reproduce the qualitative trend.

7.5 Difficulties of using an adiabatic basis

If one naively choses the excited states of a single electronic structure calculation to prepare a master equation, ie: $h_{ij} = 0$ $(\forall i \neq j)$, there are several problems. In the Markovian case, adiabatic state-derivatives only contribute to the redfield tensor $\mathcal{R}$ via the bath correlation functions $C_{mn}(\omega)$ at $\omega = 0$, where there are no physical vibrational peaks on which the gradient can be projected in Eq. (7.11). Rigorous pure-dephasing contributions at this frequency can be related to anharmonicities [156] which are too expensive to calculate for systems of this size. If fluctuations of non-adiabatic couplings $d_{mn}(R) = \langle m|\frac{d}{dR'}|n\rangle|_{(R'=0)}$ under the equilibrated bath were included this would no longer be the case. The reorganization energy corresponding to d_{mn} would also result in mixed zeroth-order states, which would to some extent be

localized. However, the success of a gradient-based IMDHO model for the spectral density of a non-adiabatic coupling would not be very good, because the non-adiabatic coupling's shape [242] is very far from that of a harmonic oscillator, and near zero at equilibrium.

It is always possible to write a linear system-bath coupling in terms of harmonic oscillator modes [65], but the appropriateness of the IMDHO, or even an oscillator model with frequency changes for a dimer system depends on the strength of the vibronic interaction [22]. The adiabatic states often do not resemble displaced harmonic oscillators (Fig. 7.4), but rather possess a double-well type structure, which means that even a proper Markovian master equation would require dynamics to obtain the bath correlation function. In the case of most modes, this is repaired within the quasi-diabatic states. Some other diabatization [172] procedures directly mix states to eliminate electron nuclear coupling, and along these lines one could construct a basis which leaves the electronic surfaces optimally harmonic which would be useful for a rudimentary model of nuclear motion. In any case, the coherence lifetimes produced (Table 7.4) from our simulations based on adiabatic states are in much poorer agreement with the experimental lifetimes than those using the procedure of Subotnik and co-workers, as discussed further below. This is because only the zero-frequency part of the correlation function is meaningful for work based on an adiabatic basis.

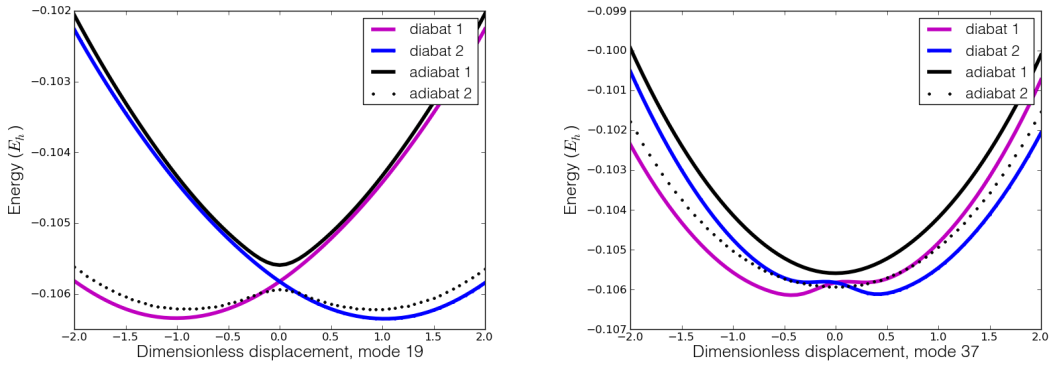

Figure 7.4: Energies of adiabatic, and quasidiabatic transfer states as a function of dimensionless displacement along [2,2'] dithia-anthracenophane's 19^{th}(left), and 37^{th}(right) normal mode. In the figure on the left it's immediately clear by inspection that the diabatic states are more harmonic than the adiabatic states. The figure on the right is an example where the accuracy of using Eq. (7.10) is questionable.

		Adiabatic	Diabatic
Species	Exp.	B3LYP/TZVP	B3LYP/6-31g*
DTA	1.20	2.14	1.40
MDAB	0.73	0.03	1.80
ODAB	1.02	0.12	1.39

Table 7.4: Pure-dephasing time (ps) between the two brightest states ($1/\mathcal{R}_{mnmn}$), as obtained from two different choices of electronic basis, compared to the experimental $T_2^{'}$.

7.6 Quasi-diabatic approach

The Redfield equation (Eq. (7.8)) was integrated with a 0.05 atomic unit timestep, via a basic 4^{th} order Runge-Kutta propagation, after an 80fs gaussian-enveloped 0.05 atomic unit oscillating electric field was applied as a stimulating pulse. The experiments [271, 272] provide noisy oscillating flourescence anisotropy curves, which were fit in that work to Hochstrasser's [285] functional form. We have directly compared the polarization anisotropy decays produced in this work from first principles, to the

experimental data's fit curve. When examining Fig. (7.5), the reader should keep in mind the absence of any rotational relaxation in our simulated anisotropy, and allow for an arbitrary relative phase shift between the coherent oscillations of experiment and theory. A low-pass filter (a step function non-zero below $.07E_h$) has been applied to the calculated signal to remove high frequency components which might be averaged over by the detector response time. The same simulation has been performed Table (7.4) for all three molecules, in the hope that the relative trend of the coherence lifetimes could be reproduced. Although vibronic couplings calculated with a diabatic basis all yield decoherence lifetimes that are within a factor of two of their experimental counterparts, the delicate relative trend of the lifetime isn't reproduced. This isn't surprising given that the relative trend of couplings is also not reproduced. The anisotropy decay can be compared (Fig. 7.5) with the evolution of the coherence between bright states, which largely correspond to the third and fourth states ($\rho_{34}(t)$). This is the picture of decoherence which may come from a less-detailed model of the dynamics. The much more rapid decay of the coherence element signals the breakdown of a two-state model picture of the anisotropy. The anisotropy decays of DTA and mDAB are not shown, because in these cases the oscillations of the anisotropy are more than a factor of 5 too fast (because the couplings are so severely overestimated by TDDFT).

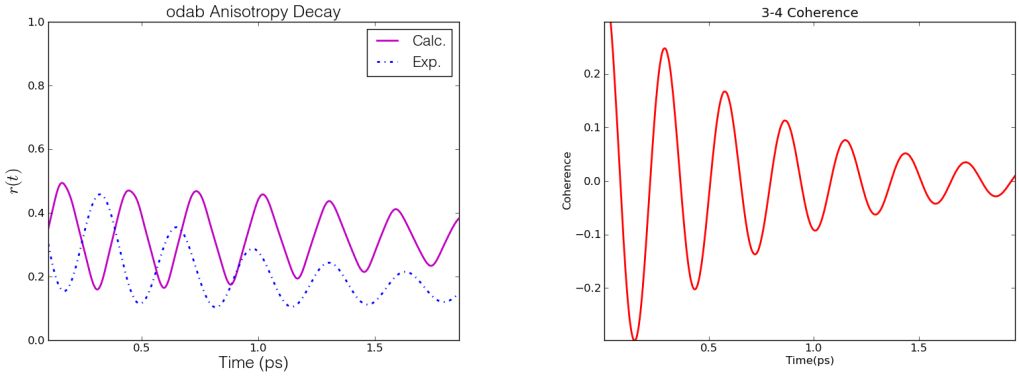

Figure 7.5: (The polarization anisotropy decay of ODAB calculated in this work (ωB97//6-31g**), and compared to the analytically fit experimental decay of Yamazaki. On the right the evolution of the real part of the coherence ($\rho_{34}(t) + \rho_{43}(t)$). The decay of the coherence between these two states is much faster than the decay of the observable.

7.7 Discussion and Conclusions

In this work the ODAB fluorescence anisotropy decay, and the coherence lifetimes of MDAB and DTA are satisfactorily reproduced from a TDDFT/TDA based Redfield model of the electronic system. These results support the existence of electronic coherence between these two chromophores lasting roughly a picosecond, without the assumption of a phenomenological reorganization energy. A picture of the bath as broadened nuclear motion, where solvation serves to localize [219, 256] the electronic states provided reasonable qualitative predictions of the decoherence rate (Table 7.4) based on the electronic structure simulations. This modeling technique is rather inexpensive relative to dynamical simulations, since it requires only a TDDFT frequency calculation and a TDDFT gradient calculation.

The weakest link in this chain of approximations appears to be the adiabatic elec-

tronic energies determined by TDDFT/TDA. The bare electronic couplings of these dimers are overestimated almost systematically, as is the relative trend, with many choices of basis and functional. Table 7.2 implicates long-range correlation as another physical effect which might reduce the bare Coulomb coupling and bring the calculations into closer agreement with experiment. Significant overestimation of the electronic coupling is not only a problem for prediction of the oscillation period, but also the rate of decoherence which depends sensitively on which frequencies the correlation function C_{mn} is sampled in Eq. (8).

The theory of CRET is mature [103, 102] within its assumed model of the system and bath, but deriving those models from first-principles electronic structure calculations is not yet routine. It should be pursued further, because two-state, uncorrelated models of the electronic dynamics are now much less realistic than sophisticated [286, 97] treatments of system-bath correlation. An accurate calculation of the coupling between chromophores separated by less than 5 Angstroms likely requires a treatment of long-range correlation, which is beyond the scope of local TDDFT functionals. However, with available technology, a *single* calculation of excited energies for these molecules which treats long-range electron correlation is a somewhat demanding computation. To provide a fully predictive picture of coherent transport the cost of correlated electronic structure should be further reduced, and the CRET theories should be hybridized with a correlated, many-state Liouville equation.

Part II

Time-dependent density functional theory for quantum computation

Chapter 8

Quantum computation and information theory

8.1 Introduction

Controllable quantum systems offer the possibility of solving problems in quantum chemistry and many-body physics that are intractable to solve on classical computers [1, 17]. This approach is called quantum simulation and was originally proposed by Richard Feynman in 1982 [64]. One key advantage of performing simulations with quantum computers rather than classical computers is the huge Hilbert space available to faithfully represent quantum systems. As mentioned in Chapter 2, the exponential scaling of the Hilbert space of electronic systems makes an exact solution to the time-dependent Schrödinger equation intractable with a classical computer. In this context, TDDFT can be viewed as an approximate method for performing tractable quantum simulations of electronic systems on classical computers.

In Chapters 9 and 10 we will explore the connections between TDDFT and quan-

tum simulation more deeply. In Chapter 9 we will prove that the theorems of TDDFT apply to certain spin Hamiltonians that are universal for quantum computation [223]. This will imply that not only can TDDFT be used to simulate electronic systems on classical computers as it is usually used, but it can in fact be used to simulate any computation that can be performed on a quantum computer. In Chapter 10 we will discuss the quantum complexity of obtaining the exact Kohn-Sham (KS) potential of TDDFT. We will conjecture that it has the complexity characterization "BQP complete", which implies that TDDFT can essentially solve the same set of computational problems that can be solved on a quantum computer in a polynomial amount of time [136].

In the present chapter, we will provide a very brief overview of quantum computation and information theory, with emphasis on only those topics which will be relevant in Chapters 9 and 10. We begin in section 8.2 with a review of universal quantum computation and the concept of universal quantum gates. Then, in section 8.3 we discuss a set of universal spin Hamiltonians for which the Runge-Gross (RG) and van Leeuwen (VL) theorems can be proven. In section 8.4, we discuss different measures of entanglement which will be relevant in Chapter 9 when we discuss the concept of entanglement as a density functional.

8.2 Universal quantum computation

Two models of universal quantum computation are generally employed: The circuit model, also called the "standard" model of quantum computation and the adi-

abatic model of quantum computation (AQC) [169]. In the circuit model, one performs a given computation by applying a set of reversible (unitary) quantum gates to a given quantum system as it evolves in real-time. In the adiabatic model, one prepares the quantum system in the ground state of an easy-to-solve Hamiltonian. Then, the easy-to-solve Hamiltonian is adiabatically transformed to a more difficult Hamiltonian whose ground state encodes the desired answer to the computation [62]. Since the circuit model of quantum computation is performed in real-time and makes no assumptions about the evolution being adiabatic, it is a better starting point for applying TDDFT to quantum computation. Additionally, the adiabatic and circuit models have been shown to be equivalent and thus there is no loss of generality in focusing only on the circuit model [7].

In the circuit model, a computation is performed by applying a unitary transformation to an initial state and then applying a set of measurements on readout qubits which encode the answer to the computation. A set of quantum gates is said to be *universal for quantum computation* if any unitary operation can be approximated to arbitrary accuracy by a quantum circuit involving only those gates [169]. A typical set of universal quantum gates will consist of a two-qubit gate which generates entanglement between qubits and a set of single-qubit gates which perform rotations on individual qubits. One such set of universal gates are the two-qubit CNOT gate, combined with the Hadamard, phase and $\frac{\pi}{8}$ single-qubit gates. In the two-qubit computational basis $\{|00\rangle, |01\rangle, |10\rangle, |11\rangle\}$, the CNOT gate is represented by the following

matrix:

$$U_{CNOT} = \begin{pmatrix} 1 & 0 & 0 & 0 \\ 0 & 1 & 0 & 0 \\ 0 & 0 & 0 & 1 \\ 0 & 0 & 1 & 0 \end{pmatrix}. \tag{8.1}$$

The CNOT operation consists of a control qubit and a readout qubit in an arbitrary state denoted $|\psi\rangle$. If the control qubit is in the state $|0\rangle$ the readout qubit remains unchanged, while if the control qubit is in the state $|1\rangle$ the readout qubit is flipped. In this way, the CNOT gate generates two-qubit entanglement. The CNOT gate is universal when combined with the Hadamard, phase and $\frac{\pi}{8}$ single-qubit gates, which are represented in the single-qubit basis $\{|0\rangle, |1\rangle\}$ as:

$$U_{Hadamard} = \frac{1}{\sqrt{2}} \begin{pmatrix} 1 & 1 \\ 1 & -1 \end{pmatrix}, \tag{8.2}$$

$$U_{phase} = \begin{pmatrix} 1 & 0 \\ 0 & \imath \end{pmatrix} \tag{8.3}$$

and

$$U_{\frac{\pi}{8}} = \begin{pmatrix} 1 & 0 \\ 0 & e^{\imath\frac{\pi}{4}} \end{pmatrix} \tag{8.4}$$

respectively. There are many other possible combinations of universal gates and it has been proven that essentially any two-qubit quantum gate is universal when combined with an appropriate set of single-qubit rotations [134]. Naturally, certain sets of universal gates will be very efficient at performing certain computations while other sets will require many operations. In practice, this distinction will be very important

since whenever a quantum gate is applied to a realistic system, decoherence and errors will be introduced [18].

Hamiltonians which describe an evolution of a quantum system which is able to implement a universal set of quantum gates are said to be "universal Hamiltonians" [169]. In Chapter 9 we will apply TDDFT to a particular class of spin Hamiltonians which have been shown to be universal for quantum computation. We now discuss these Hamiltonians in the next section.

8.3 Universal spin Hamiltonians

In refs. [24, 25] it was proven that Hamiltonians of the form:

$$\hat{H}(t) = \sum_{i=1}^{N-1} J^{\perp}_{i,i+1}(\hat{\sigma}^x_i\hat{\sigma}^x_{i+1} + \hat{\sigma}^y_i\hat{\sigma}^y_{i+1}) + \sum_{i=1}^{N-1} J^{\parallel}_{i,i+1}\hat{\sigma}^z_i\hat{\sigma}^z_{i+1} + \sum_{i=1}^{N} h_i(t)\hat{\sigma}^z_i, \tag{8.5}$$

are universal for quantum computation. Here, $\hat{\sigma}^x_i$, $\hat{\sigma}^y_i$, $\hat{\sigma}^z_i$ are Pauli operators for the ith qubit, $h_i(t)$ are local applied fields arbitrarily chosen along the z-axis and $J^{\parallel}_{i,i+1}$ and $J^{\perp}_{i,i+1}$ are two-qubit interaction terms respectively parallel and perpendicular to the direction of the fields. As we will discuss in more detail in Chapter 9, the general form of the Hamiltonian in Eq. 8.5 describes a variety of physical quantum systems, particularly in solid-state quantum computation.

Upon inspection, we see that the Hamiltonian in Eq. 8.5 bears a striking similarity to the many-electron Hamiltonian (Eq. 2.1). The two-qubit terms $\sum_{i=1}^{N-1} J^{\perp}_{i,i+1}(\hat{\sigma}^x_i\hat{\sigma}^x_{i+1} + \hat{\sigma}^y_i\hat{\sigma}^y_{i+1}) + \sum_{i=1}^{N-1} J^{\parallel}_{i,i+1}\hat{\sigma}^z_i\hat{\sigma}^z_{i+1}$ are fixed and simply serve to generate entanglement, while the local time-dependent fields, $\sum_{i=1}^{N} h_i(t)\hat{\sigma}^z_i$ are externally applied and instruct the quantum system to perform a particular computation. Similarly, in Eq. 2.1 the kinetic

and electron repulsion terms, $-\frac{1}{2}\sum_{i=1}^{N}\nabla_i^2+\sum_{i<j}^{N}\frac{1}{|\mathbf{r_i}-\mathbf{r_j}|}$, are fixed and generate quantum effects and electron-electron correlations respectively, while the time-dependent external potential is particular to each atom, molecule or solid. As we will discuss in Chapter 9, it is dangerous to push this analogy too far, but it suggests that the Hamiltonian in Eq. 8.5 is a good starting point for applying TDDFT to quantum computation.

We now briefly outline the constriction given by Benjamin and Bose in refs. [24, 25], which proves that the Hamiltonian in Eq. 8.5 is universal for quantum computation. The construction begins by partitioning the Hamiltonian into an Ising part:

$$\hat{H}_{Ising}(t)=J^{\parallel}\sum_{i=1}^{N-1}\hat{\sigma}_i^z\hat{\sigma}_{i+1}^z+\sum_{i=1}^{N}h_i(t)\hat{\sigma}_i^z, \tag{8.6}$$

and a part describing the XY two-qubit interaction:

$$\hat{H}_{XY}(t)=J^{\perp}\sum_{i=1}^{N-1}(\hat{\sigma}_i^x\hat{\sigma}_{i+1}^x+\hat{\sigma}_i^y\hat{\sigma}_{i+1}^y), \tag{8.7}$$

where $J^{\parallel}$ and $J^{\perp}$ are uniform couplings (naturally the more general case of non-uniform couplings subsumes this case as well). It is then shown that the evolution operator for this Hamiltonian can be exactly factorized as:

$$\hat{U}(t)=(1-\delta(t)\hat{P}(t))e^{-\imath\int_0^t dt\hat{H}_{Ising}(t)}, \tag{8.8}$$

where $\hat{P}(t)$ is a bounded operator that is independent of the local fields $\{h_1(t),h_2(t),...h_N(t)\}$. The local fields are also constructed to have the same magnitude but alternating sign, so that with the definition $\Delta_j(t)\equiv 2(h_{j+1}(t)-h_j(t))$, we have $\Delta_j(t)\equiv(-1)^j\Delta(t)$. Then, in Eq. 8.8, we defined $\delta(t)\equiv\frac{J^{\perp}}{\Delta(t)}$ which shows that by tuning the local fields

to have a very large magnitude the effective evolution is that of an Ising Hamiltonian. Since $\hat{H}_{Ising}(t)$ contains only $\hat{\sigma}^z$ operators, any state which is an eigenstate of $\hat{\sigma}^z_{total} \equiv \sum_i \hat{\sigma}^z_i$ acquires only a trivial global phase and does not evolve. Therefore, by switching the local fields between large and small values, one can effectively turn on and off the evolution of individual qubits.

The next step is to show that this construction can be used to generate a universal two-qubit quantum gate. In order to achieve this, one uses a construction of three spins, in which the two outermost spins serve as computational qubits and the middle spin is a control qubit that mediates their interaction. The computational basis states are identified as: $|00\rangle \equiv |\downarrow\uparrow\downarrow\rangle$, $|01\rangle \equiv |\downarrow\uparrow\uparrow\rangle$, $|10\rangle = |\uparrow\uparrow\downarrow\rangle$ and $|11\rangle = |\uparrow\uparrow\uparrow\rangle$. Now, the basic idea is to begin with the system in an initial state $|\psi(0)\rangle$ for $t < 0$, which is a superposition of these states and have the local fields initially tuned so that $\delta(t) \ll 1$ and therefore the Hamiltonian is effectively Ising (Eq. 8.8). As a result, the system does not evolve . At $t = 0$, the local fields are tuned so that the parameter $\delta(t) \gg 1$ and the system subsequently evolves. In ref. [25] it is shown that by letting the system evolve for a time $t_R = \pi\hbar \frac{1}{\sqrt{8(J^\perp)^2+(J^\parallel)^2}}$ and then switching the fields so that $\delta(t) \ll 1$ again, one effectively realizes the two-qubit gate:

$$U = \begin{pmatrix} 1 & 0 & 0 & 0 \\ 0 & \imath Qs & Qc & 0 \\ 0 & Qc & \imath Qs & 0 \\ 0 & 0 & 0 & W \end{pmatrix}, \tag{8.9}$$

where the matrix is expressed in the computational basis. In Eq. 8.9, the parameters

are: $Q = -e^{\imath\phi}$, $\frac{s}{c} = \frac{sin\phi}{cos\phi}$, $W = -e^{-2\imath\phi}$ and $\phi = \frac{\pi}{2}\frac{1}{\sqrt{\frac{8(J^{\perp})^2}{(J^{\parallel})^2}+1}}$. This is a two-qubit entangling gate and therefore as discussed in [134] can be used to perform universal quantum computation when combined with single-qubit rotations. In fact, using the procedure described in [60, 34], one can confirm that no more than four uses of the gate in Eq. 8.9 are needed to perform a CNOT operation, with a variety of different possible values of $J^{\parallel}$ and $J^{\perp}$. It is simple to construct the Hadamard, phase and $\frac{\pi}{8}$ gates by allowing single qubits to evolve for the appropriate amount of time, which as mentioned in section 8.2 form a universal set of quantum gates when combined with the CNOT gate. Therefore, the Hamiltonian in Eq. 8.5 is in fact universal for quantum computation, a fact that will be crucial in Chapter 9.

8.4 Entanglement

The principle feature that distinguishes quantum mechanics from classical mechanics is entanglement. Entanglement is the concept that in a quantum mechanical system, it is possible to have complete knowledge of the parts of the system, without complete knowledge of the entire system. In more technical language, for any composite quantum mechanical system, there exist pure states of the system in which the parts do not have pure states of their own. In this way, individual parts of a quantum mechanical system can affect one another in a non-local manner and it is precisely this non-locality which is used as a resource in quantum computation.

Despite this general concept, there is no universally accepted definition of precisely what entanglement is, and many different entanglement measures exist in the litera-

ture. In this section we introduce two widely-used and physically motivated measures of entanglement: The von Neumann entropy and the concurrence [268, 269]. This sets the stage for the next chapter, where we will discuss the possibility of constructing entanglement as a density functional.

The von Neumann entropy

We consider a general quantum system consisting of two parts labeled A and B. Any pure state Ψ of the system can always be written as,

$$|\Psi\rangle = \sum_{i=1}^{n} c_i |\phi_i^A\rangle \otimes |\phi_i^B\rangle, \tag{8.10}$$

where $\{|\phi_1^A\rangle, ..., |\phi_n^A\rangle\}$ and $\{|\phi_1^B\rangle, ..., |\phi_n^B\rangle\}$ are sets of orthonormal states for the subsystems and the c_i's are a set of positive coefficients. The quantity n, which is the number of states in the expansion in Eq. 8.10 is referred to as the Schmidt number. Clearly, for the particular case where the subsystems A and B are unentangled, $|\Psi\rangle = |\phi_i^A\rangle \otimes |\phi_i^B\rangle$ is a tensor product and $n = 1$. Therefore, we see that the Schmidt number and the c_i's characterize the degree of entanglement between subsystems A and B. The von Neumann entropy defined by the expression:

$$S(\Psi) = Tr\left\{ |\Psi\rangle\langle\Psi| \mathrm{Log}(|\Psi\rangle\langle\Psi|) \right\} = -\sum_{i=1}^{n} c_i^2 \mathrm{Log}(c_i^2), \tag{8.11}$$

represents a well chosen measure of entanglement for several reasons. Firstly, it vanishes when $n = 1$ and all the c_i's are zero except for one of them which is equal to one. This is what one would expect for a tensor product state. Secondly, it increases monotonically and reaches a maximum when $c_1 = c_2 = ...c_n = \frac{1}{n}$, which is

what one would expect for a maximally entangled state. Thirdly, it reduces to the conventional definition of thermodynamic entropy if c_i^2 is interpreted as the probability that subsystem A(B) is in the state $|\phi_i^A\rangle(|\phi_i^B\rangle)$. In this way, the von Neumann entropy measures the loss of information about subsystem A by observing B and vice-versa, which is a distinguishing feature of entanglement.

Despite these desirable properties, the von Neumann entropy can only be used to measure entanglement between two subsystems of a pure state. In the more general case, one might want to determine the entanglement between subsystems which are themselves described by a mixed state. For instance, in Chapter 9 we will be interested in determining the entanglement between two qubits which are part of a much larger many-qubit system. If one writes down a reduced density matrix for these two qubits, it will in general be a mixed state due to correlations with the remaining qubits. In the next subsection, we will introduce the entanglement of formation, which generally can be used to describe mixed state entanglement and then we introduce the concurrence, which specifically describes the entanglement of formation for a two-qubit mixed state.

The concurrence

Instead of a pure state considered in the previous section, we now consider systems described by a mixed-state. i.e. a weighted sum of pure states:

$$\hat{\rho} = \sum_{j=1}^{N} P_j |\Psi_j\rangle\langle\Psi_j|, \tag{8.12}$$

where $\sum_i P_j = 1$. In this case, it is immediately clear that the von Neumann entropy is not unambiguous. For if we define the entanglement as a weighted sum of the von

Neumann entropies of the individual pure states,

$$E(\rho) = \sum_j P_j S(\Psi_j), \tag{8.13}$$

we will get a different value depending on the pure state decomposition we choose. For instance, the two-qubit mixed state $\frac{1}{2}(|00\rangle\langle 00| + |11\rangle\langle 11|)$ can be regarded as an equal mixture of $|00\rangle$ and $|11\rangle$ or equivalently as an equal mixture of the states $\frac{1}{\sqrt{2}}(|00\rangle + |11\rangle)$ and $\frac{1}{\sqrt{2}}(|00\rangle - |11\rangle)$. In the first case Eq. 8.13 gives zero entanglement, while for the latter case we get $E(\rho) = 2\text{Log}(2)$. The entanglement of formation gives the unambiguous definition of entanglement as the minimum over all possible pure state decompositions:

$$E_f(\rho) = \inf \sum_j P_j S(\Psi_j). \tag{8.14}$$

In the previous example, the entanglement of formation would be zero.

We now introduce the concurrence and show that it is directly related to the entanglement of formation for two qubits. For a pure state Ψ of two qubits, we define the concurrence $C(\Psi)$ as $C(\Psi) = |\langle\Psi|\tilde{\Psi}\rangle|$, where $|\tilde{\Psi}\rangle = \sigma_y \otimes \sigma_y |\Psi^*\rangle$ and $|\Psi^*\rangle$ is the complex conjugate of $|\Psi\rangle$ in the computational basis $\{|00\rangle, |01\rangle, |10\rangle, |11\rangle\}$. One can show that for a pure state, the entanglement of formation (which is equivalent to the von Neumann entropy for a pure state) and concurrence are related via:

$$E_f(\Psi) = \mathcal{E}(C(\Psi)), \tag{8.15}$$

where

$$\mathcal{E}(C) = h\left[\frac{1 + \sqrt{1 - C^2}}{2}\right], \tag{8.16}$$

and

$$h(x) = -x\text{Log}(x) - (1 - x)\text{Log}(1 - x). \tag{8.17}$$

It can be seen that $\mathcal{E}(C)$ is a monotonically increasing function of C, so the concurrence itself can be regarded as a measure of entanglement.

Analogously, one defines the concurrence of a mixed two-qubit state as:

$$C(\rho) = \inf \sum_j P_j C(\Psi_j). \tag{8.18}$$

Now in addition to being monotonically increasing, the function $\mathcal{E}(C)$ in Eq. 8.16 is also convex. It therefore follows that:

$$\mathcal{E}(C(\rho)) = \inf \mathcal{E}\left[\sum_j P_j C(\Psi_j)\right] \leqslant \inf \sum_j P_j \mathcal{E}\left[C(\Psi_j)\right] = E_f(\rho). \tag{8.19}$$

i.e. $\mathcal{E}(C(\rho))$ is a lower bound on the entanglement of formation. Furthermore, it can be proven [268] that there always exists a decomposition of $\hat{\rho}$ that achieves the minimum in Eq. 8.18 with a set of pure states having the *same* concurrence. This implies that the inequality in Eq. 8.19 is actually an equality and so $\mathcal{E}(C(\rho))$ is actually equal to the entanglement of formation. Therefore, we see that $\mathcal{E}(C(\rho))$ or equivalently $C(\rho)$ itself is a suitable measure for two-qubit mixed state entanglement. In section 9.5 we construct explicit formulas for the concurrence and discuss certain circumstances under which it can be expressed as a density functional.

Having briefly reviewed the fundamentals of universal quantum computation, we now turn to the central topic of Part II of this thesis: TDDFT for universal quantum computation.

Chapter 9

Time-dependent density functional theory for universal quantum computation

9.1 Introduction

The pioneering work of Hohenberg and Kohn [94] in 1964 showed that the properties of a many-body system can be obtained as functionals of the simple electron density rather than the many-body wavefunction. Twenty years later, similar theorems were proven for time-dependent systems [201]. These developments have enabled complex simulations of physical systems at low computational cost using a very simple quantity. Can these ideas be extended to the domain of quantum computation, and therefore enable similar progress in that field? In the present chapter, we prove analogous theorems to those of time-dependent density functional theory (TDDFT) for the domain of universal quantum computation. In a similar spirit to TDDFT for electronic Hamiltonians, the theorems of TDDFT applied to universal Hamiltonians allow us to think of single-qubit expectation values as the basic variables in quantum

computation and information theory, rather than the wavefunction. From a practical standpoint this opens the possibility of approximating observables of interest in quantum computations directly in terms of single-qubit quantities, i.e. as density functionals. Additionally, we demonstrate that TDDFT provides an exact prescription for simulating universal Hamiltonians with other universal Hamiltonians which have different, and possibly easier-to-realize two-qubit interactions. The theorems of TDDFT for universal Hamiltonians establish that TDDFT can in principle be used to simplify quantum computations, similar to how it has been applied in revolutionizing the simulation of atomic, molecular and condensed matter electronic structure dynamics. As we discuss below, the development of accurate approximate functionals for quantum simulation will be a necessary second step for the practical application of TDDFT to quantum computation.

9.2 Quantum computing without wavefunctions

We begin by briefly reviewing TDDFT for a system of N-electrons described by the Hamiltonian

$$\hat{H}(t) = \sum_{i=1}^{N} \frac{\hat{p}_i^2}{2m} + \sum_{i<j}^{N} v_{ee}(\hat{\mathbf{r}}_i, \hat{\mathbf{r}}_j) + \int v_{ext}(\mathbf{r}, t)\hat{n}(\mathbf{r})d^3\mathbf{r}, \tag{9.1}$$

where $\hat{\mathbf{p}}_i$ and $\hat{\mathbf{r}}_i$ are respectively the position and momentum operators of the ith electron, $v_{ee}(\hat{\mathbf{r}}_i, \hat{\mathbf{r}}_j)$ is the electron-electron repulsion and $v_{ext}(\mathbf{r}, t)$ is a time-dependent one-body scalar potential which includes the potential due to nuclear charges as well as any external fields. $\hat{n}(\mathbf{r}) = \sum_i^N \delta(\mathbf{r} - \hat{\mathbf{r}}_i)$ is the electron density operator, whose expectation value yields the one-electron probability density. The first basic theorem

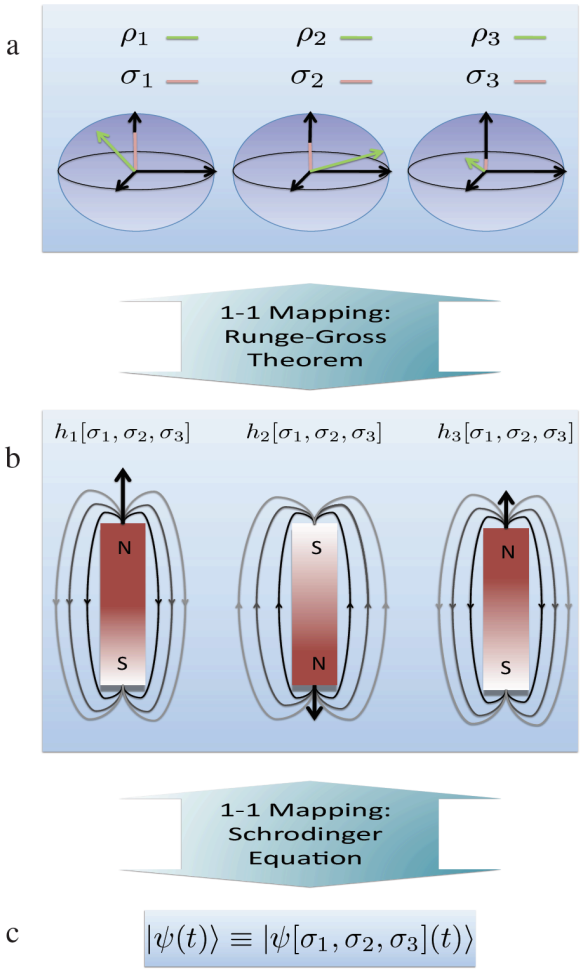

Figure 9.1: **Qubit Runge-Gross theorem for a 3 qubit example** - The set of expectation values $\{\sigma_1^z, \sigma_2^z, ...\sigma_N^z\}$, defined by the the Bloch vector components of each qubit along the z-axis in (a), is uniquely mapped onto the set of local fields $\{h_1, h_2, ...h_N\}$ in (b) through the qRG theorem. Then, through the Schrödinger equation, the set of fields is uniquely mapped onto the wavefunction. These two mappings together imply that the N-qubit wavefunction in (c) is in fact a unique functional of the set of expectation values $\{\sigma_1^z, \sigma_2^z, ...\sigma_N^z\}$.

of TDDFT, known as the "Runge-Gross (RG) theorem" [201] discussed in Chapter 2, establishes a one-to-one mapping between the expectation value of $\hat{n}(\mathbf{r})$ and the scalar potential $v_{ext}(\mathbf{r}, t)$ and therefore through the time-dependent Schrödinger equation, a one-to-one mapping between the density and the wavefunction. The RG theorem implies the remarkable fact that in principle, the one-electron density contains the same information as the many-electron wavefunction. The second basic TDDFT theorem known as the "van Leeuwen (VL) theorem" [247] also discussed in Chapter 2, gives a prescription for constructing an auxiliary system with a different and possibly simpler electron-electron repulsion $v'_{ee}(\hat{\mathbf{r}}_i, \hat{\mathbf{r}}_j)$, which simulates the density evolution of the original Hamiltonian in Eq. 9.1. When $v'_{ee}(\hat{\mathbf{r}}_i, \hat{\mathbf{r}}_j) = 0$, this auxiliary system is referred to as the "Kohn-Sham system" [115] and due to it's simplicity and accuracy, is in practice used in most DFT and TDDFT calculations.

It is not obvious that the RG and VL theorems extend to qubits, which are *distinguishable* spin 1/2 particles. In the results part of this section, we prove analogous RG and VL theorems for a system of N qubits described by the very general universal 2-local Hamiltonian [24, 25] discussed in section 8.3,

$$\hat{H}(t) = \sum_{i=1}^{N-1} J^{\perp}_{i,i+1}(\hat{\sigma}^x_i \hat{\sigma}^x_{i+1} + \hat{\sigma}^y_i \hat{\sigma}^y_{i+1}) + \sum_{i=1}^{N-1} J^{\parallel}_{i,i+1} \hat{\sigma}^z_i \hat{\sigma}^z_{i+1} + \sum_{i=1}^{N} h_i(t) \hat{\sigma}^z_i. \tag{9.2}$$

Here, $\hat{\sigma}^x_i$, $\hat{\sigma}^y_i$, $\hat{\sigma}^z_i$ are Pauli operators for the ith qubit, $h_i(t)$ are local applied fields arbitrarily chosen along the z-axis and $J^{\parallel}_{i,i+1}$ and $J^{\perp}_{i,i+1}$ are two-qubit interaction terms respectively parallel and perpendicular to the direction of the fields. The above Hamiltonian describes an open chain of N qubits arranged in a one-dimensional array, with each qubit interacting with its nearest neighbors. More general geometries are

discussed in sections 9.3 and 9.4. In Refs. [24, 25], it was shown that by appropriately tuning the local fields in Eq. 9.2, one can use the fixed two-qubit interaction alone to realize a set of universal two-qubit and single-qubit quantum gates, which in turn can be employed to perform universal quantum computation. In Eq. 9.2, the case where $J^{\perp}_{i,i+1} = J^{\parallel}_{i,i+1}$ yields the Heisenberg Hamiltonian which describes exchange coupled spins in solid state arrays or quantum dots in heterostructures [59]. The situation $J^{\perp}_{i,i+1} \neq J^{\parallel}_{i,i+1}$ yields the XXZ Hamiltonian, used to model electronic qubits on liquid Helium [186] or solid-state systems with anisotropy due to spin-orbit coupling [129], while the limit $J^{\parallel}_{i,i+1} = 0$ yields the XY model describing superconducting Josephson junction qubits [148]. In the remainder of this section, we will develop the TDDFT theorems for the Hamiltonian in Eq. 9.2 and discuss their implications for quantum computation and information theory.

Results

The qubit Runge-Gross theorem for quantum computation

We now state the equivalent RG theorem for quantum computation with the Hamiltonian in Eq. 9.2, the qubit Runge-Gross (qRG) theorem:

Theorem - For a given initial state $|\psi(0)\rangle$ *evolving to* $|\psi(t)\rangle$ *under the Hamiltonian in Eq. 9.2 and with* $J^{\parallel}_{i,i+1}$ *and* $J^{\perp}_{i,i+1}$ *fixed, there exists a one-to-one mapping between the set of expectation values* $\{\sigma^z_1, \sigma^z_2, ...\sigma^z_N\}$ *and the set of local fields* $\{h_1, h_2, ...h_N\}$ *over a given interval [0 ,t].*

Here, we have defined $\sigma_i^z \equiv \langle\psi(t)|\hat{\sigma}_i^z|\psi(t)\rangle$ as the expectation value of the component of the ith qubit along the field direction (z-axis). A detailed proof together with a more rigorous discussion of the conditions on the theorem are provided in section 9.3. The qRG theorem implies that the set of local fields can be written as unique functionals of the set of expectation values $\{\sigma_1^z, \sigma_2^z, ...\sigma_N^z\}$, as illustrated in the first part of Figure 9.1. Since the solution to the time-dependent Schrödinger equation is unique and $J_{i,i+1}^{\perp}$ and $J_{i,i+1}^{\parallel}$ are fixed, the wavefunction is a unique functional of the local fields, i.e. $|\psi(t)\rangle \equiv |\psi[h_1, h_2, ...h_N](t)\rangle$, where the square brackets denote that ψ is a functional of the set $\{h_1, h_2, ...h_N\}$ over the interval [0,t]. This fact, combined with the qRG theorem allows us to state a corollary, which is the first central result of this communication:

Corollary - There exists a one-to-one mapping between the set of expectation values $\{\sigma_1^z, \sigma_2^z, ...\sigma_N^z\}$*, the initial state* $|\psi(0)\rangle$ *and the N-qubit wavefunction* $|\psi(t)\rangle$ *on the interval [0 ,t].*

The above corollary implies the counterintuitive fact that the full N-qubit wavefunction, which lives in a 2^N dimensional Hilbert space, is a unique functional of only the N components of each qubit along the z-axis and the initial state $|\psi(0)\rangle$, i.e.

$$|\psi(t)\rangle \equiv |\psi[\sigma_1^z, \sigma_2^z, ...\sigma_N^z](t)\rangle. \tag{9.3}$$

This naturally implies that no two wavefunctions can give the same set of expectation values $\{\sigma_1^z, \sigma_2^z, ...\sigma_N^z\}$. Having established the qRG theorem, we now proceed to discuss its implications for quantum computation.

Implications of the qubit Runge-Gross theorem for quantum computation

Although the qRG theorem does not tell us an explicit functional form for ψ, it has profound conceptual implications from a quantum information perspective. At first glance, it might appear that the set $\{\sigma_1^z, \sigma_2^z, ...\sigma_N^z\}$ contains much less information than the full wavefunction, since projective measurements needed to obtain $\{\sigma_1^z, \sigma_2^z, ...\sigma_N^z\}$ would seem to imply that information about non-commuting observables, or observables depending on multi-qubit correlations is lost. However, since the wavefunction completely specifies all properties of the system, Eq. 9.3 implies that even properties depending on non-commuting observables or multi-qubit correlations, such as entanglement and phase information are in fact uniquely determined by the set of expectation values $\{\sigma_1^z, \sigma_2^z, ...\sigma_N^z\}$.

From a practical standpoint, the qRG theorem implies that *all* observables can *directly* be constructed as functionals of single-qubit expectation values, without regard for the wavefunction. Although the qRG theorem proves that the set of expectation values $\{\sigma_1^z, \sigma_2^z, ...\sigma_N^z\}$ in principle contains all of the quantum information in ψ, extracting this information in the form of a functional of $\{\sigma_1^z, \sigma_2^z, ...\sigma_N^z\}$ is not always straightforward. In order to do this, one must either guess the exact functional form of the observable, or try to approximate it. Borrowing an analogy from electronic TDDFT, the time-dependent dipole moment $\mu(t) = \langle\psi(t)|\sum_i \hat{\mathbf{r}}_i|\psi(t)\rangle = \int d^3\mathbf{r} n(\mathbf{r},t)\mathbf{r}$ is a very simple density functional, while the average momentum of the system $\mathbf{p}(t) = \langle\psi(t)|\sum_i \hat{\mathbf{p}}_i|\psi(t)\rangle$ is not simple to construct as an explicit density functional,

since it depends on the density very non-locally in both space and time [188]. A density functional for the average momentum must therefore be approximated in practical applications.

In quantum computation and information theory, a similar situation arises. Often, the observable of interest is simply a subset of $\{\sigma_1^z, \sigma_2^z, ...\sigma_N^z\}$ on designated readout qubits which encode the answer to the computation and this subset is trivially a functional of the entire set. For instance, a simple example is the Deutsch-Jozsa algorithm, where one measures a subset of $\{\sigma_1^z, \sigma_2^z, ...\sigma_N^z\}$ in a query register to determine if a function f(x) is constant or balanced [58]. If one finds the spin density of this subset to be zero everywhere, f(x) is constant, while if it is non-zero, f(x) is balanced. A more challenging observable functional to construct is two-qubit entanglement. We find that an exact entanglement functional can in fact be constructed for a computation involving only one flipped qubit relative to the other $N-1$ qubits having an opposite orientation. The entanglement (as measured by concurrence [268]) between any two qubits labeled k and l can be written as a functional of the set $\{\sigma_1^z, \sigma_2^z, ...\sigma_N^z\}$ as (the derivation is provided in section 9.5)

$$E_{kl}[\sigma_1^z, \sigma_2^z, ...\sigma_N^z](t) = \frac{1}{N-2} \prod_{m=k,l} \left[(N-3)\sigma_m^z + \sum_{i \neq m}^{N} \sigma_i^z \right]^{\frac{1}{2}}. \tag{9.4}$$

Interestingly, this particular entanglement functional is time-local, since it depends only on the set $\{\sigma_1^z, \sigma_2^z, ...\sigma_N^z\}$ at a given instant in time and so $E_{kl}[\sigma_1^z, \sigma_2^z, ...\sigma_N^z](t) = E_{kl}[\sigma_1^z(t), \sigma_2^z(t), ...\sigma_N^z(t)]$. In the more general case, observables may be non-local in time and depend on the set $\{\sigma_1^z, \sigma_2^z, ...\sigma_N^z\}$ over an entire interval [0,t]. Although the functional in Eq. 9.4 is time-local, it is "spatially" non-local, since the entanglement

between qubits k and l depends on the components of all of the other $N-2$ qubits. If one considers two flipped qubits instead of one, the entanglement functional becomes complicated and non-local in both space and time due to dependence on phases in the wavefunction (see section 9.5). Understanding the spatial and temporal non-locality of density functionals in electronic structure theory is a very active research topic [21, 144], and interestingly a similar situation arises here in TDDFT for quantum computation as well.

Thus far we have proven the qRG theorem, which establishes that all observables of an N-qubit system can be obtained directly from the set of single-qubit expectation values $\{\sigma_1^z, \sigma_2^z, ...\sigma_N^z\}$, without needing explicit access to the wavefunction. However, in order to make this fact useful from a practical standpoint, one would like to be able to obtain the set $\{\sigma_1^z, \sigma_2^z, ...\sigma_N^z\}$ by solving an auxiliary problem that is simpler than obtaining $|\psi(t)\rangle$ itself. In the next subsection, we prove that there are in fact infinitely many universal Hamiltonians which can be used to simulate the same set $\{\sigma_1^z, \sigma_2^z, ...\sigma_N^z\}$ and by choosing a Hamiltonian with a simpler evolution, one can in fact make TDDFT a practical tool for quantum computation.

A theorem analogous to the Van Leeuwen theorem for quantum computation

We now turn to the second fundamental theorem of TDDFT for universal computation, a VL-like theorem for qubits, the qubit Van Leeuwen theorem (qVL):

Theorem - Consider a given set of spin components $\{\sigma_1^z, \sigma_2^z, ...\sigma_N^z\}$ *obtained from the*

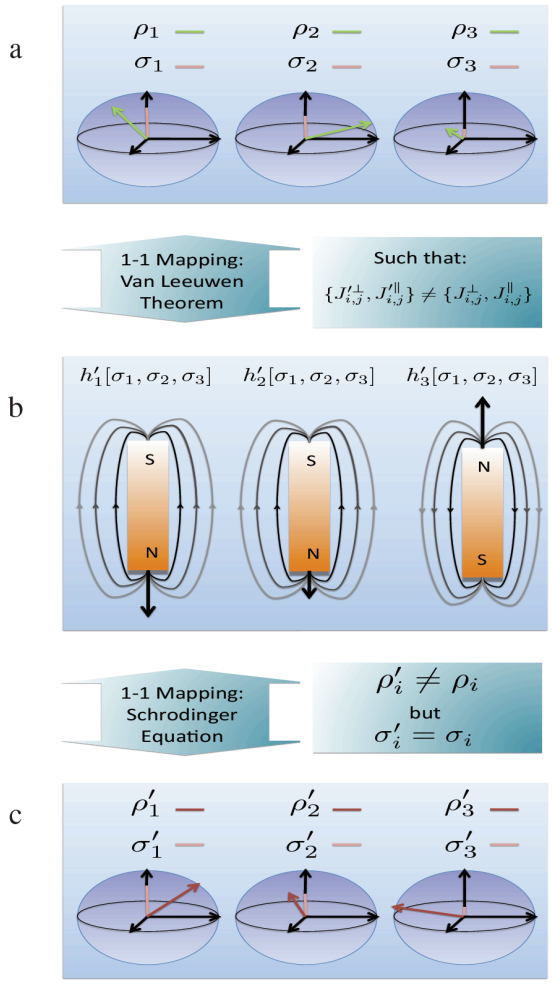

Figure 9.2: **Qubit Van Leeuwen theorem for a 3 qubit example** - The set $\{\sigma_1^z, \sigma_2^z, ...\sigma_N^z\}$ (a) obtained from evolution under Eq. 9.2, is uniquely mapped to a new set of fields $\{h'_1, h'_2, ...h'_N\}$ (b) for a Hamiltonian with different two-qubit interactions. Evolution under this new Hamiltonian returns the same expectation values $\{\sigma_1^z, \sigma_2^z, ...\sigma_N^z\}$, although the wavefunction is different and hence projections of the Bloch vectors along other axes are in general different (c).

wavefunction $|\psi(t)\rangle$ evolved under the Hamiltonian in Eq. 9.2. One can always construct (see section 9.4 for certain conditions) a Hamiltonian with different two-qubit interactions denoted $J'^{\perp}_{i,i+1}$ and $J'^{\parallel}_{i,i+1}$ and different local fields $\{h'_1, h'_2, ...h'_N\}$, which evolves a possibly different initial state $|\psi'(0)\rangle$ to a different final state $|\psi'(t)\rangle$ such that the condition $\{\sigma'^z_1, \sigma'^z_2, ...\sigma'^z_N\} = \{\sigma^z_1, \sigma^z_2, ...\sigma^z_N\}$ is satisfied on the interval [0,t].

Here, we have defined $\sigma'^z_i \equiv \langle\psi'(t)|\hat{\sigma}^z_i|\psi'(t)\rangle$. The qVL theorem allows us to obtain the set $\{\sigma^z_1, \sigma^z_2, ...\sigma^z_N\}$ by simulating the evolution with an auxiliary Hamiltonian having different two-qubit interactions and hence a different (and possibly simpler) wavefunction evolution as illustrated in Figure 9.2. Furthermore, the qVL theorem guarantees that the auxiliary fields $\{h'_1, h'_2, ...h'_N\}$ are unique functionals of the set $\{\sigma^z_1, \sigma^z_2, ...\sigma^z_N\}$. As we discuss in the next subsection, this fact opens the possibility of simplifying computations by constructing simple approximations to the auxiliary fields as functionals of single-qubit expectation values. This is a similar concept to how the exchange-correlation potential of electronic TDDFT is approximated as a functional of the one-body density in the Kohn-Sham scheme.

A numerical demonstration of the qubit Van Leeuwen theorem

Before discussing general approximate functionals for the auxiliary local fields $\{h'_1, h'_2, ...h'_N\}$, in this section we will demonstrate the qVL theorem by constructing the *exact* functional for a simple example where an exact numerical solution is possi-

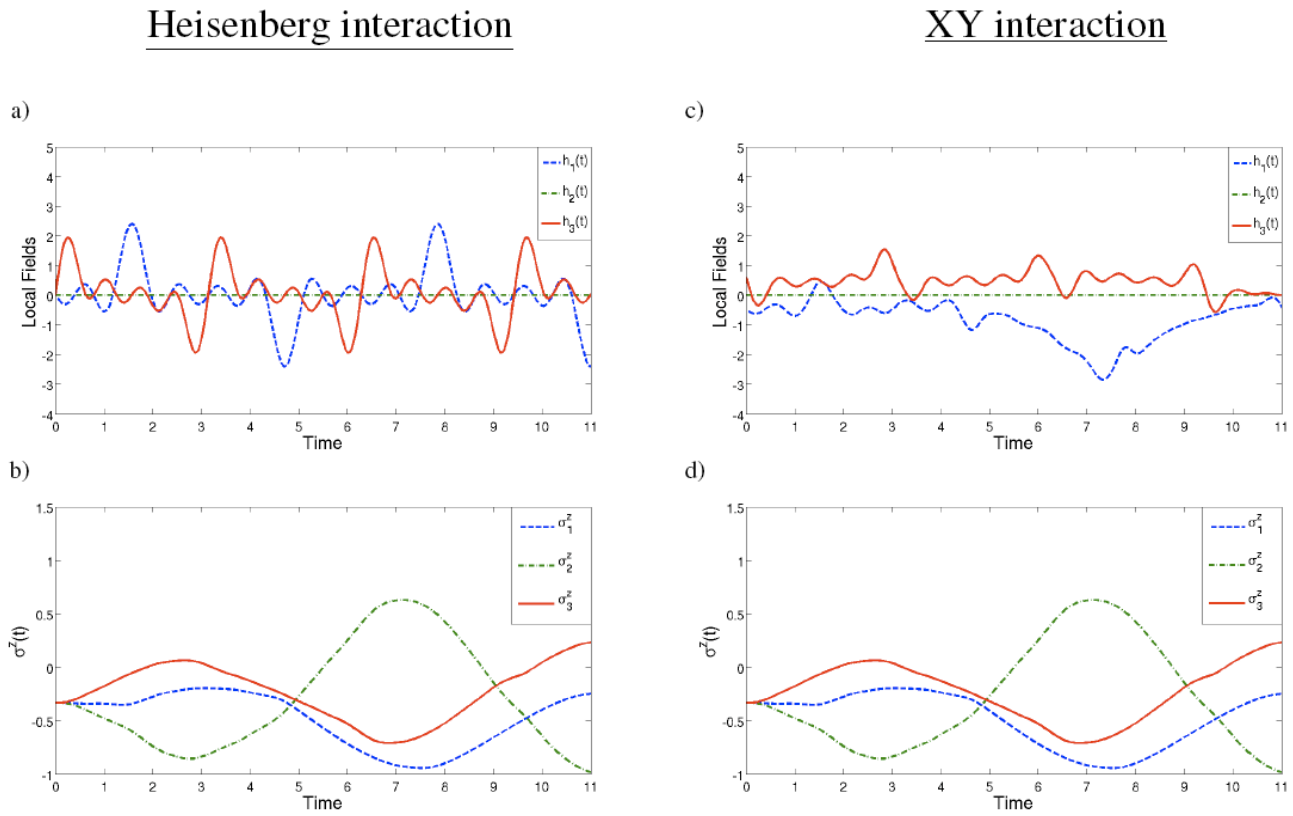

Figure 9.3: **Simulating the Heisenberg Hamiltonian with the XY Hamiltonian** - Pulses of the form $h_1(t) = 0.6\sum_{n=1}^{4}(-1)^{n+1}\sin[(2n-1)t]$ and $h_3(t) = 0.6\sum_{n=1}^{4}(-1)^{2n}\sin[2nt]$ are respectively applied to the first and third qubits of a uniform Heisenberg Hamiltonian (a). The time-dependent Schrödinger equation is then solved exactly numerically and the evolution of the set $\{\sigma_1^z, \sigma_2^z, \sigma_3^z\}$ is read out in (b). The qVL theorem gives us a prescription for constructing different auxiliary fields (c), which simulate the evolution of the set $\{\sigma_1^z, \sigma_2^z, \sigma_3^z\}$ correctly as seen in (d), but using a non-uniform XY interaction instead. (Time is measured in units of $\frac{\hbar}{2J}$)

ble. The proof of the qVL theorem gives a mathematical procedure (see section 9.6) for engineering the *exact* auxiliary fields $\{h'_1, h'_2, ...h'_N\}$ which reproduce a given set $\{\sigma_1^z, \sigma_2^z, ...\sigma_N^z\}$ under a different two-qubit interaction. As a simple demonstration, we use this procedure to numerically simulate a 3-qubit Heisenberg Hamiltonian using an XY Hamiltonian as the auxiliary system (Figure 9.3). For the simulation, the system is prepared in the initial state $|\psi(0)\rangle = \frac{1}{\sqrt{3}}(|011\rangle + |101\rangle + |110\rangle)$, where $|1\rangle$ and $|0\rangle$ are eigenstates of $\hat{\sigma}^z$ with eigenvalues -1 and 1 respectively. In the Heisenberg Hamiltonian, $J^{\perp}_{i,i+1} = J^{\parallel}_{i,i+1} \equiv J_{i,i+1}$ and we choose $J_{12} = J_{23} = 0.5$, which represents a chain with isotropic and uniform antiferromagnetic couplings. We apply a pulse of the form $h_1(t) = 0.6\sum_{n=1}^{4}(-1)^{n+1}\sin[(2\mathrm{n}-1)\mathrm{t}]$ (odd harmonics) to the first qubit and $h_3(t) = 0.6\sum_{n=1}^{4}(-1)^{2n}\sin[2\mathrm{nt}]$ (even harmonics) to the third qubit. The time-dependent Schrödinger equation is solved numerically and the set $\{\sigma_1^z, \sigma_2^z, \sigma_3^z\}$ is read out during the evolution. Details of the simulation are provided in section 9.6.

For the auxiliary XY Hamiltonian, $J'^{\parallel}_{i,i+1} = 0$ and we choose different and non-uniform couplings in which $J'^{\perp}_{12} = 1.2$ and $J'^{\perp}_{23} = -1$. Thus, we have chosen the auxiliary system to be anisotropic, with non-uniform and alternating ferromagnetic and antiferromagnetic couplings. Using the qVL theorem, we engineer the auxiliary local fields $\{h'_1, h'_2, h'_3\}$ which using a this XY interaction, reproduce the set $\{\sigma_1^z, \sigma_2^z, \sigma_3^z\}$ obtained from the original evolution under the uniform Heisenberg Hamiltonian. As seen in Figure 9.3, the auxiliary local fields are quite different from the original local fields applied to the Heisenberg model, but simulate the set of components $\{\sigma_1^z, \sigma_2^z, \sigma_3^z\}$ correctly, i.e. $\{\sigma'^z_1, \sigma'^z_2, \sigma'^z_3\} = \{\sigma_1^z, \sigma_2^z, \sigma_3^z\}$. In the language of electronic TDDFT, the XY model in our simulation is analogous to the "Kohn-Sham system" and the set

$\{h'_1, h'_2, h'_3\}$ play the role of the exact Kohn-Sham potential as a density functional.

In the above example, we have constructed the exact auxiliary fields *a posteriori*, after having already solved the wavefunction evolution of the original system. Although such exact solutions are valuable in guiding functional development, one would ultimately like to develop accurate approximate and generic functionals for the auxiliary fields which can be used to circumvent solving the original problem. Furthermore, one would like to choose the auxiliary system so that its evolution is simpler than that of the original system. Such an approach has proven invaluable in the Kohn-Sham scheme of electronic TDDFT and we now discuss its applicability to TDDFT for quantum computation.

Discussion

The qRG and qVL theorems place TDDFT for universal quantum computation on a firm theoretical footing and open several exciting research avenues. The development of approximate density functionals has been essential for the success of electronic TDDFT and will be in quantum computation and information theory as well. In the Kohn-Sham scheme of electronic TDDFT, one simulates the correlated many-body system evolving under the Hamiltonian of Eq. 9.1, with an uncorrelated non-interacting system in which $v'_{ee}(\hat{\mathbf{r}}_i, \hat{\mathbf{r}}_j) = 0$. The effective "Kohn-Sham" potential $v'_{ext}(\mathbf{r}, t)$ of this non-interacting system must be approximated as a functional of the density. The local density approximation (LDA) [115], was the first density functional to be applied to solid-state systems in the 1960s, but it was not sufficiently accurate

for quantum chemistry. More than 20 years elapsed between the fundamental DFT theorem of Hohenberg and Kohn [94] and the development of density functionals capable of achieving chemical accuracy in the 1980's; the so called generalized gradient approximations (GGA's) [175].

In a similar vein, although we have established the fundamental theorems of TDDFT for quantum computation, the development of accurate approximate functionals will be a future challenge. Additionally, in TDDFT for quantum computation, we expect the path of functional development to be somewhat different. In the electronic Hamiltonian (Eq. 9.1), the kinetic and electron-electron repulsion are always the same operators and similarly the Kohn-Sham system is always non-interacting. Therefore, the Kohn-Sham potential is always the same functional for any electronic system. In contrast, in quantum computation one uses different two-qubit interaction terms depending on which universal Hamiltonian implements a given quantum circuit and therefore the functional will be different for each situation. For instance, if one wants to simulate an antiferromagnetic Heisenberg model using a ferromagnetic Heisenberg model, the functional will be different than a simulation of the same system using an XY model. Therefore, functional development will need to focus on specific implementations of quantum algorithms, rather than a single universal functional for all quantum computations. Typically, one would want to choose the auxiliary system's wavefunction to be less entangled than that of the original system, thereby making it easier to simulate using TDDFT on a classical computer. This is a similar concept to how TDDFT has been applied to electronic systems, where TDDFT provides a tool to approximately simulate quantum many-body systems efficiently on

classical computers.

Naturally, there are systems that will be very hard to simulate using approximate functionals, such as those that are in the complexity class QMA and may require exponentially scaling resources on a quantum computer [211]. The collapse of the computational complexity class hierarchy is of course not expected, and therefore finding functionals that carry out complex quantum computational tasks is extremely unlikely. Nevertheless, understanding how TDDFT functionals can *approximately* simulate efficient quantum algorithms on a classical computer is an open direction. Density functionals for strongly correlated lattice and spin systems have been recently proposed [252, 106, 130, 9] and could be applied to several problems of relevance in quantum computing. In Refs. [252, 106, 130, 9] local density (LDA) and generalized gradient approximations (GGA) for one dimensional Hubbard chains and spin chains were derived from exact Bethe ansatz solutions and could readily be applied to solid-state quantum computing or perfect state transfer protocols in spin networks [33]. Functionals can also be parametrized from numerical simulations of one-dimensional qubit systems using time-dependent density matrix renormalization group methods (TDMRG) [264], in an analogous fashion as quantum Monte Carlo simulations of the uniform electron gas have proven invaluable in electronic DFT [45]. In Figure 9.4, we summarize the analogies between electronic TDDFT and TDDFT for quantum computation, which will necessarily guide development of approximate functionals.

Interestingly, one could also imagine using the qVL theorem as an experimental tool to engineer different physical systems which perform the same computations. For instance, one could simulate an algorithm on an ion trap using a system of super-

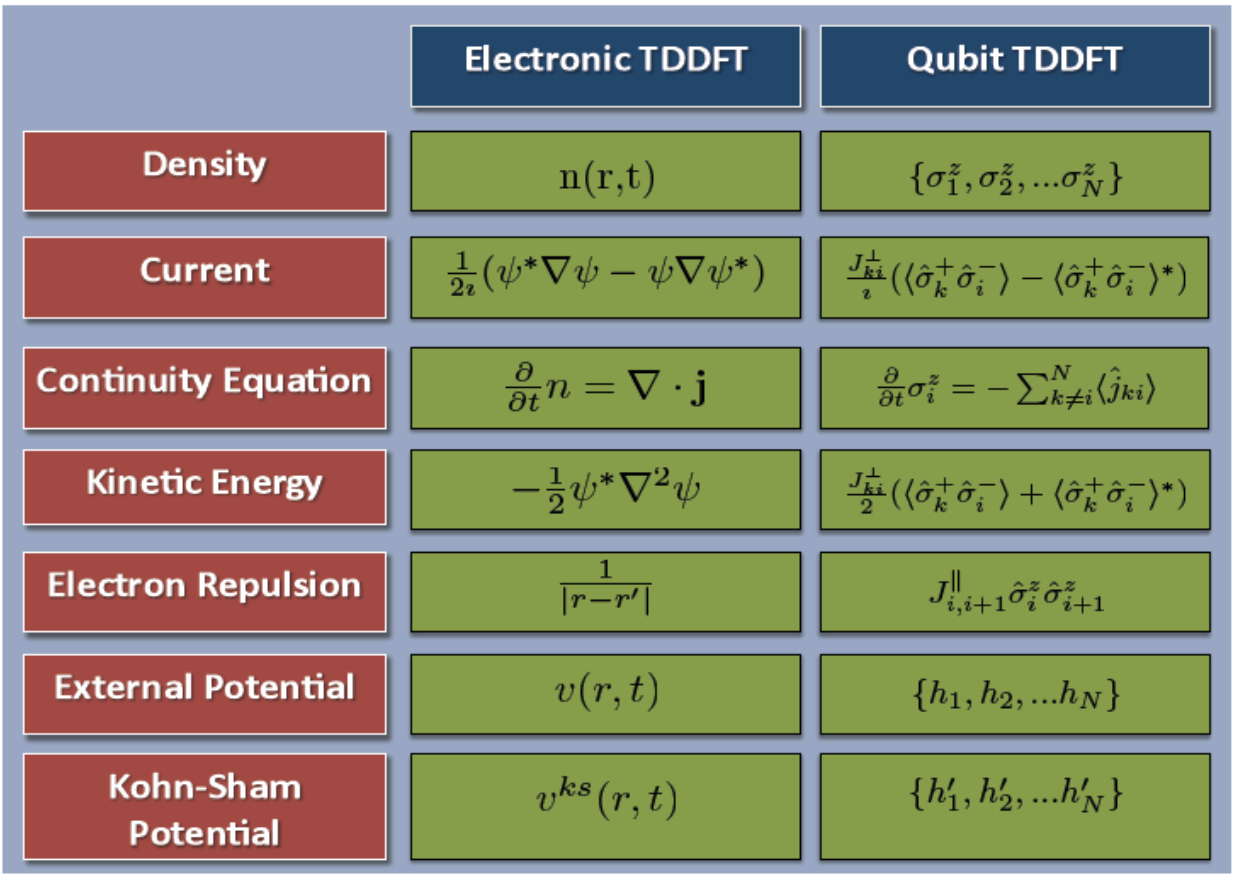

Figure 9.4: **Analogies between electronic TDDFT and TDDFT for quantum computation** - Relevant quantities in electronic TDDFT (left column) and the corresponding quantities in TDDFT for quantum computation (right column). The current and kinetic energy of qubit TDDFT are defined in section 9.3

conducting flux qubits, by using the qVL theorem to engineer the flux qubit Hamiltonian from knowledge of how the algorithm is performed on the ion trap. Another important research direction will be the generalization of DFT and TDDFT to other universal Hamiltonians and models of quantum computation. For instance, Ref. [68] discussed the use of TDDFT for obtaining gaps in adiabatic quantum computation. In [270], groundstate DFT was used to study relationships between entanglement and quantum phase transitions, while Ref. [211] explored DFT from a complexity theory perspective.

9.3 Proof of the qubit Runge-Gross theorem

In this section we will first consider a proof of the qRG theorem for Hamiltonians of the form,

$$\hat{H}(t) = \sum_{i<j}^{N} J_{ij}^{\perp}(\hat{\sigma}_i^x\hat{\sigma}_j^x + \hat{\sigma}_i^y\hat{\sigma}_j^y) + \sum_{i<j}^{N} J_{ij}^{\parallel}\hat{\sigma}_i^z\hat{\sigma}_j^z + \sum_{i=1}^{N} h_i(t)\hat{\sigma}_i^z, \tag{9.5}$$

which reduces to Eq. 9.2 in the limit of a one-dimensional array with nearest-neighbor couplings and open boundary conditions. We will see that it is possible to formulate the qRG theorem of time-dependent current density functional theory (TDCDFT) for the more general class of Hamiltonians in Eq. 9.5, but for TDDFT one must stay with the more restricted form in Eq. 9.2.

The proof begins with the equation of motion for the expectation value of the ith qubit along the field direction (z-axis),

$$\frac{\partial}{\partial t}\sigma_i^z = \imath\langle\Big[\hat{H}(t), \hat{\sigma}_i^z\Big]\rangle, \tag{9.6}$$

where $\langle\hat{O}\rangle \equiv \langle\psi(t)|\hat{O}|\psi(t)\rangle$ denotes the expectation value of an arbitrary operator $\hat{O}$ at time t and $|\psi(t)\rangle$ is the wavefunction evolved on an interval [0,t] from a given initial state $|\psi(0)\rangle$, under the Hamiltonian in Eq. 9.5. Development of the commutator in Eq. 9.6 yields,

$$\begin{aligned}\frac{\partial}{\partial t}\sigma_i^z &= 2\sum_{k\neq i}^{N} J_{ki}^{\perp}(\langle\hat{\sigma}_k^x\hat{\sigma}_i^y\rangle - \langle\hat{\sigma}_k^y\hat{\sigma}_i^x\rangle) \\ &= -\frac{1}{\imath}\sum_{k\neq i}^{N} J_{ki}^{\perp}(\langle\hat{\sigma}_k^+\hat{\sigma}_i^-\rangle - \langle\hat{\sigma}_k^-\hat{\sigma}_i^+\rangle),\end{aligned} \tag{9.7}$$

where we have introduced the Pauli raising and lowering operators $\hat{\sigma}^{\pm} = \hat{\sigma}^x \pm \imath\hat{\sigma}^y$ in the second equality. Defining

$$\hat{j}_{ki} \equiv -2J_{ki}^{\perp}(\hat{\sigma}_k^x\hat{\sigma}_i^y - \hat{\sigma}_k^y\hat{\sigma}_i^x) = \frac{1}{\imath}J_{ki}^{\perp}(\hat{\sigma}_k^+\hat{\sigma}_i^- - \hat{\sigma}_k^-\hat{\sigma}_i^+) \tag{9.8}$$

as the operator that generates the "current" of σ^z flowing from the ith qubit to the kth qubit, Eq. 9.7 takes the form of a local conservation law,

$$\frac{\partial}{\partial t}\sigma_i^z = -\sum_{k\neq i}^{N}\langle\hat{j}_{ki}\rangle. \tag{9.9}$$

This arises from the fact that the Hamiltonian in Eq. 9.5 conserves the total component of all N-qubits along the field direction, i.e. it is readily verified that,

$$\frac{\partial}{\partial t}\sum_{i}^{N}\sigma_i^z = \frac{\partial}{\partial t}\sigma_{total}^z = 0. \tag{9.10}$$

This is analogous to the situation in electronic structure theory, where the local continuity equation

$$\frac{\partial}{\partial t}n(\mathbf{r},t) = -\nabla\cdot\mathbf{j}(\mathbf{r},t) \tag{9.11}$$

implies a global conservation of particle number

$$\frac{\partial}{\partial t}\int n(\mathbf{r},t)d^3\mathbf{r} = \frac{\partial}{\partial t}N = 0, \tag{9.12}$$

where N is the number of electrons in the system.

We now consider a "primed" Hamiltonian

$$\hat{H}'(t) = \sum_{i<j}^{N} J_{ij}^{\perp}(\hat{\sigma}_i^x\hat{\sigma}_j^x + \hat{\sigma}_i^y\hat{\sigma}_j^y) + \sum_{i<j}^{N} J_{ij}^{\parallel}\hat{\sigma}_i^z\hat{\sigma}_j^z + \sum_{i=1}^{N} h_i'(t)\hat{\sigma}_i^z, \tag{9.13}$$

which has the same two-qubit interaction terms as the Hamiltonian in Eq. 9.5, but a different set of local fields $\{h_1', h_2', ...h_N'\}$. Let $|\psi'(t)\rangle$ denote the wavefunction evolved from the *same* initial state $|\psi(0)\rangle$, but under the Hamiltonian in Eq. 9.13. The equation of motion for the expectation value of the ith qubit along the z-axis under this primed Hamiltonian is

$$\frac{\partial}{\partial t}\sigma_i'^z = -\sum_{k\neq i}^{N}\langle\hat{j}_{ki}\rangle', \tag{9.14}$$

where we define $\langle\hat{O}\rangle' \equiv \langle\psi'(t)|\hat{O}|\psi'(t)\rangle$ as the expectation value of an arbitrary operator $\hat{O}$ with respect to the primed wavefunction.

In what follows, we assume that the local fields in both the primed and unprimed systems are equal to their Taylor expansions within a finite radius of convergence around $t = 0$, i.e. $h_i(t) = \sum_{j=0}^{\infty}\left[\frac{1}{j!}\frac{\partial^j}{\partial t^j}h_i(t)\right]_{t=0} t^j$ and similarly $h_i'(t) = \sum_{j=0}^{\infty}\left[\frac{1}{j!}\frac{\partial^j}{\partial t^j}h_i'(t)\right]_{t=0} t^j$ (the assumption of Taylor expandability is discussed below). We will now proceed to show that if the set of fields $\{h_1, h_2, ...h_N\}$ differ from the set of fields $\{h_1', h_2', ...h_N'\}$ by more than a global field which is the same for all N qubits, the set of currents $\{\langle\hat{j}_{12}\rangle, \langle\hat{j}_{13}\rangle, ...\langle\hat{j}_{23}\rangle, ...\langle\hat{j}_{N-1,N}\rangle\}$ and $\{\langle\hat{j}_{12}\rangle', \langle\hat{j}_{13}\rangle', ...\langle\hat{j}_{23}\rangle', ...\langle\hat{j}_{N-1,N}\rangle'\}$ will necessarily be different. The condition that the two sets of fields differ by more than a global field, is equivalent to the statement that there exists a smallest integer

$m \geqslant 0$ such that the set

$$\Big\{\frac{\partial^m}{\partial t^m}(h_1(t)-h_1'(t))|_{t=0}, \frac{\partial^m}{\partial t^m}(h_2(t)-h_2'(t))|_{t=0},$$
$$... \quad \frac{\partial^m}{\partial t^m}(h_N(t)-h_N'(t))|_{t=0}\Big\} \neq \{C\}, \tag{9.15}$$

where here $\{C\}$ is a constant set of N elements that are all the same, i.e. the Taylor coefficients of the local fields in the primed and unprimed systems will differ at some order.

Next, we write down the equation of motion for the difference of the currents between the ith and kth qubits in the primed and unprimed systems:

$$\frac{\partial}{\partial t}(\langle\hat{j}_{ki}\rangle - \langle\hat{j}_{ki}\rangle') = \imath\langle\Big[\hat{H}(t),\hat{j}_{kl}]\Big\rangle - \imath\langle\Big[\hat{H}(t),\hat{j}_{kl}]\Big\rangle'. \tag{9.16}$$

Since both systems evolve from a common initial state $|\psi(0)\rangle$, we have at $t=0$,

$$\frac{\partial}{\partial t}(\langle\hat{j}_{ki}\rangle - \langle\hat{j}_{ki}\rangle')|_{t=0} = \imath\langle\psi(0)|\left[(\hat{H}(0)-\hat{H}'(0)),\hat{j}_{ki}\right]|\psi(0)\rangle$$
$$= \quad 4\langle\psi(0)|\hat{T}_{ki}|\psi(0)\rangle(\Delta h_i(0)-\Delta h_k(0)). \tag{9.17}$$

Here, we have defined $\Delta h_i(t) = h_i(t) - h_i'(t)$ as the difference between the unprimed and primed fields acting on the ith qubit and similarly, $\Delta h_k(t) = h_k(t) - h_k'(t)$.

$$\hat{T}_{ki} \equiv J_{ki}^{\perp}(\hat{\sigma}_k^x\hat{\sigma}_i^x + \hat{\sigma}_k^y\hat{\sigma}_i^y) = \frac{J_{ki}^{\perp}}{2}(\hat{\sigma}_k^+\hat{\sigma}_i^- + \hat{\sigma}_k^-\hat{\sigma}_i^+) \tag{9.18}$$

is similar to a local kinetic energy operator, describing the total transfer of σ^z between the ith and kth qubits. From Eq. 9.17, we see that if the condition in Eq. 9.15 is satisfied for $m=0$, the sets $\{\langle\hat{j}_{12}\rangle, \langle\hat{j}_{13}\rangle, ...\langle\hat{j}_{23}\rangle, ...\langle\hat{j}_{N-1,N}\rangle\}$ and $\{\langle\hat{j}_{12}\rangle', \langle\hat{j}_{13}\rangle', ...\langle\hat{j}_{23}\rangle', ...\langle\hat{j}_{N-1,N}\rangle'\}$

will become different instantaneously later than $t = 0$ (with a restriction on the vanishing of $\langle\psi(0)|\hat{T}_{ki}|\psi(0)\rangle$ discussed below). If the condition in Eq. 9.15 instead holds for some $m > 0$, we differentiate Eq. 9.16 m times to obtain,

$$\begin{aligned} & \frac{\partial^{m+1}}{\partial t^{m+1}}(\langle\hat{j}_{ki}\rangle - \langle\hat{j}_{ki}\rangle')|_{t=0} \\ = \; & 4\langle\psi(0)|\hat{T}_{ki}|\psi(0)\rangle \frac{\partial^m}{\partial t^m}(\Delta h_i(t) - \Delta h_k(t))|_{t=0}. \end{aligned} \tag{9.19}$$

From here we see that if the set of local fields eventually differ at any order, the set of currents must as well. This establishes the qRG theorem of TDCDFT: For a fixed initial state $|\psi(0)\rangle$, there is a one to one mapping between the set of local fields and the set of currents, up to a globally constant field.

We now discuss the three main conditions of the theorem:

1) The expectation values $\langle\psi(0)|\hat{T}_{ki}|\psi(0)\rangle$ must be non-zero for at least one pair of qubits k and i, whose local field differences $\Delta h_i(t)$ and $\Delta h_k(t)$ are different for at least one instant on the interval [0,t]. This is a fairly mild restriction on the set of admissible initial states, $|\psi(0)\rangle$. For instance, consider a worst case scenario, in which all the fields $\{h_1, h_2, ...h_N\}$ and $\{h_1', h_2', ...h_N\}$ differ by a constant field, except for h_1 and h_1' which differ by a different amount from the others at only one instant in time on the interval [0,t]. In this worst case, the restriction means that $\langle\psi(0)|\hat{T}_{1i}|\psi(0)\rangle$ must be non-zero for at least one value of i, where $i = 1, 2, ..., N$. In the more general case, where the sets $\{h_1, h_2, ...h_N\}$ and $\{h_1', h_2', ...h_N\}$ differ for several qubits or on finite time intervals, this restriction is even less severe.

2) The elements of the sets $\{h_1, h_2, ...h_N\}$ and $\{h_1', h_2', ...h_N\}$ must be analytic functions of time, i.e. equal to their Taylor expansions within a finite radius of conver-

gence. In quantum computing, this is not a very severe restriction, as one typically constructs pulses which are well behaved functions. This restriction does not even exclude sudden switching, which is the case when applying idealized pulses to perform single-qubit rotations.

3) The theorem establishes a one-to-one mapping between the set of currents and the set of local fields up to a globally constant field, we will denote $C(t)$, which is the same for all N qubits. Since the global field $C(t)$ is arbitrary, it corresponds to an arbitrary term $C(t)\sum_i^N \hat{\sigma}_i^z \equiv C(t)\hat{\sigma}_{total}^z$ in the Hamiltonian. If one begins in an initial state which is an eigenstate of $\hat{\sigma}_{total}^z$, this term is simply a c-number and adds a trivial global phase to the wavefunction. This is typically the case when one begins in a computational basis state. However, if one starts in a superposition of states with different values of σ_{total}^z, the term C(t) $\hat{\sigma}_{total}^z$ yields a nontrivial coherence between these states. Such coherences would be measurable for observables with non-zero matrix elements between states of different σ_{total}^z. These observables would therefore not be uniquely determined by the current.

We now turn to the qRG theorem of TDDFT, which is discussed in section 9.2. From Eq. 9.9, we see that it is possible for two different sets of currents $\{\langle\hat{j}_{12}\rangle, \langle\hat{j}_{13}\rangle, ...\langle\hat{j}_{23}\rangle, ...\langle\hat{j}_{N-1,N}\rangle$ and $\{\langle\hat{j}_{12}\rangle', \langle\hat{j}_{13}\rangle', ...\langle\hat{j}_{23}\rangle', ...\langle\hat{j}_{N-1,N}\rangle'\}$ to correspond to the same set of spin components $\{\sigma_1^z, \sigma_2^z, ...\sigma_N^z\}$, if there exists a set of current differences

$$\begin{aligned} & \{\delta j_{12}, \delta j_{13}, ...\delta j_{23}, ...\delta j_{N-1,N}\} \\ \equiv\ & \{(\langle\hat{j}_{12}\rangle - \langle\hat{j}_{12}\rangle'), (\langle\hat{j}_{13}\rangle - \langle\hat{j}_{13}\rangle'), \\ ...\ & (\langle\hat{j}_{23}\rangle - \langle\hat{j}_{23}\rangle'), ...(\langle\hat{j}_{N-1,N}\rangle - \langle\hat{j}_{N-1,N}\rangle')\}, \end{aligned} \tag{9.20}$$

such that,

$$\sum_{k\neq i}^{N} \delta j_{ik} = 0 \tag{9.21}$$

for some i. For a one-dimensional chain with open boundary conditions and nearest-neighbor couplings as in Eq. 9.2, such a set *never* exists, as illustrated in Figure 9.5. Thus, for this case, no two sets of currents can yield the same set $\{\sigma_1^z, \sigma_2^z, ...\sigma_N^z\}$, and through the qRG theorem of TDCDFT, no two sets of fields $\{h_1, h_2, ...h_N\}$ and $\{h_1', h_2', ...h_N'\}$ differing by more than a constant can yield the same set $\{\sigma_1^z, \sigma_2^z, ...\sigma_N^z\}$. This establishes the qRG theorem of TDDFT for the Hamiltonian in Eq. 9.2. For more general geometries, such as in Figure 9.6, it is possible to find two different sets of currents such that $\sum_{k\neq i}^{N} \delta j_{ik} = 0$. For these geometries, the qRG theorem of TDCDFT holds, however that of TDDFT does not. From the continuity equation of electronic structure (Eq. 9.11), we see that we can add an arbitrary transverse vector field $\vec{\delta j}$ (such that $\vec{\nabla} \cdot \vec{\delta j} = 0$) to the electronic current, without altering the value of $\frac{\partial}{\partial t} n(\mathbf{r}, t)$. A set $\{\delta j_{12}, \delta j_{13}, ...\delta j_{23}, ...\delta j_{N-1,N}\}$ satisfying the condition in Eq. 9.21 is analogous to a purely transverse current.

9.4 Proof of the qubit van Leeuwen theorem

The proof of the qVL theorem begins with the equation of motion for the current under the evolution of the Hamiltonian in Eq. 9.5,

$$\frac{\partial}{\partial t}\langle \hat{j}_{ki} \rangle = \imath \langle \Big[\hat{H}(t), \hat{j}_{ki} \Big] \rangle. \tag{9.22}$$

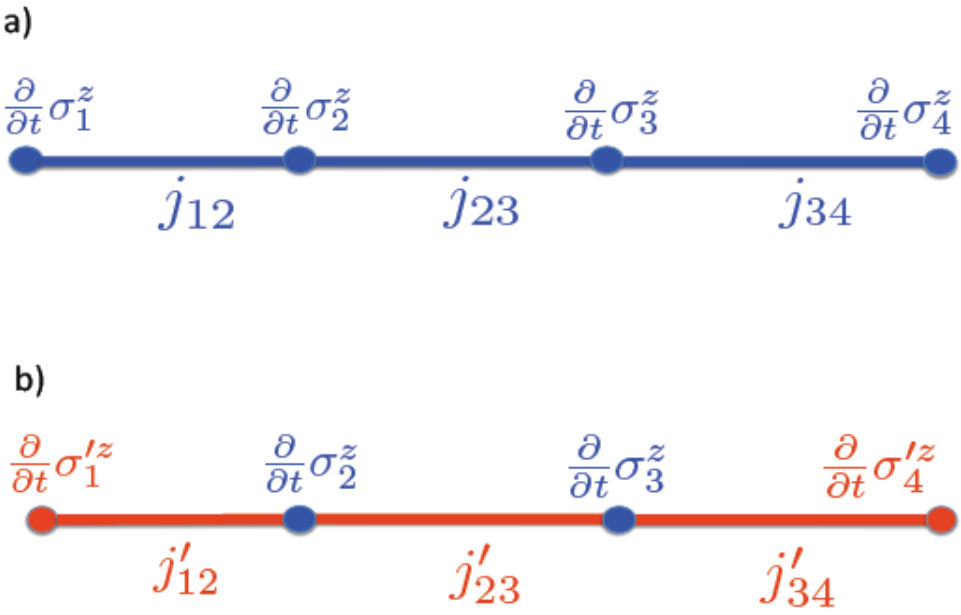

Figure 9.5: **Open Chain of 4 qubits with nearest-neighbor couplings** - If we consider the set of currents shown in a), it will never be possible to find a new set of currents that will yield the same derivatives of σ^z. For instance, as shown in b), we can find a new set of currents that will yield the same derivatives of σ^z on the middle two sites, but the derivatives at the ends of the chain will necessarily be different.

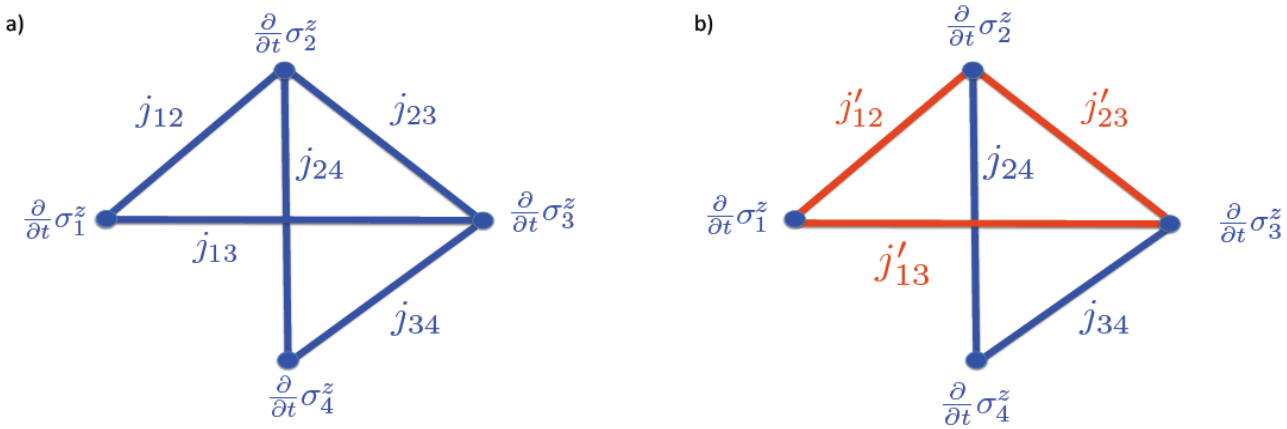

Figure 9.6: **Open chain of 4 qubits with second nearest-neighbor couplings** - If we add second nearest neighbor couplings as well (shown in a)), it will be possible to find two sets of currents that yield the same derivatives of σ^z. For instance, if one considers a new set of currents around the closed loop shown in b), such that $\{\delta j_{12}, \delta j_{13}, \delta j_{23}\}$ = constant, the derivatives of σ^z will remain unchanged. This is equivalent to adding a purely transverse term to the current.

Developing the commutator in Eq. 9.22 yields,

$$\frac{\partial}{\partial t}\langle \hat{j}_{ki} \rangle = \langle \hat{\mathcal{T}}_{ki} \rangle + \langle \hat{\mathcal{F}}_{ki} \rangle + 4\langle \hat{T}_{ki} \rangle \delta h_{ik}(t), \tag{9.23}$$

where $\delta h_{ik}(t) = h_i(t) - h_k(t)$ is the difference between the local fields applied to the ith and kth qubits and we have defined the operators $\hat{\mathcal{T}}_{ki}$ and $\hat{\mathcal{F}}_{ki}$ as:

$$\begin{aligned} \hat{\mathcal{T}}_{ki} \equiv 4J_{ki}^{\perp} \Big\{ & \hat{\sigma}_k^z \left[\sum_{m \neq k} J_{mk}^{\perp} \hat{\sigma}_m^x \right] \hat{\sigma}_i^x + \hat{\sigma}_k^z \left[\sum_{m \neq k} J_{mk}^{\perp} \hat{\sigma}_m^y \right] \hat{\sigma}_i^y \\ - & \hat{\sigma}_k^x \left[\sum_{m \neq i} J_{mi}^{\perp} \hat{\sigma}_m^x \right] \hat{\sigma}_i^z - \hat{\sigma}_k^y \left[\sum_{m \neq i} J_{mi}^{\perp} \hat{\sigma}_m^y \right] \hat{\sigma}_i^z \Big\}, \end{aligned} \tag{9.24}$$

and

$$\begin{aligned} \hat{\mathcal{F}}_{ki} \equiv 4J_{ki}^{\perp} \Big\{ & \hat{\sigma}_k^y \left[\sum_{m \neq i} J_{mi}^{\parallel} \hat{\sigma}_m^z \right] \hat{\sigma}_i^y - \hat{\sigma}_k^x \left[\sum_{m \neq i} J_{mi}^{\parallel} \hat{\sigma}_m^z \right] \hat{\sigma}_i^x \\ + & \hat{\sigma}_k^y \left[\sum_{m \neq k} J_{mk}^{\parallel} \hat{\sigma}_m^z \right] \hat{\sigma}_i^y - \hat{\sigma}_k^x \left[\sum_{m \neq k} J_{mk}^{\parallel} \hat{\sigma}_m^z \right] \hat{\sigma}_i^x \Big\}. \end{aligned} \tag{9.25}$$

$\hat{\mathcal{T}}_{ki}$ arises from the commutator of the current operator with the kinetic energy operator $\sum_{i<j}^{N} \hat{T}_{ij}$ and is similar to the "stress tensor" operator of electronic TDDFT [247]. $\hat{\mathcal{F}}_{ki}$ arises from the commutator of the current operator with the term $\sum_{i<j}^{N} J_{ij}^{\parallel} \hat{\sigma}_i^z \hat{\sigma}_j^z$ in the Hamiltonian and is analogous to the "internal force density" operator due to the electron-electron repulsion in electronic TDDFT. Both the terms $\langle \hat{\mathcal{T}}_{ki} \rangle$ and $\langle \hat{\mathcal{F}}_{ki} \rangle$ in Eq. 9.23 represent "internal forces" due to the two-qubit terms in the Hamiltonian, while the term $4\langle \hat{T}_{ki} \rangle \delta h_{ik}(t)$ represents an "external" driving force due to the applied local fields which couple to the one-qubit operators $\hat{\sigma}_i^z$.

We now consider an auxiliary "primed" system, with the Hamiltonian,

$$\hat{H}'(t) = \sum_{i<j}^{N} J_{ij}'^{\perp} (\hat{\sigma}_i^x \hat{\sigma}_j^x + \hat{\sigma}_i^y \hat{\sigma}_j^y) + \sum_{i<j}^{N} J_{ij}'^{\parallel} \hat{\sigma}_i^z \hat{\sigma}_j^z + \sum_{i=1}^{N} h_i'(t) \hat{\sigma}_i^z, \tag{9.26}$$

having different two-qubit interactions $J'^{\perp}_{ij}$ and $J'^{\parallel}_{ij}$ and a different set of local fields $\{h'_1, h'_2, ...h'_N\}$. We allow the initial state $|\psi'(0)\rangle$ to be different from the initial state $|\psi(0)\rangle$, with the only constraint that the initial currents and the initial expectation values of $\hat{\sigma}^z_i$ must be the same in the primed and unprimed systems, i.e. we only require that,

$$\langle\psi'(0)|\hat{j}'_{ki}|\psi'(0)\rangle = \langle\psi(0)|\hat{j}_{ki}|\psi(0)\rangle \tag{9.27}$$

and

$$\langle\psi'(0)|\hat{\sigma}^z_i|\psi'(0)\rangle = \langle\psi(0)|\hat{\sigma}^z_i|\psi(0)\rangle \tag{9.28}$$

for all k and i. The equation of motion for the current under evolution of this Hamiltonian is,

$$\frac{\partial}{\partial t}\langle\hat{j}'_{ki}\rangle' = \langle\hat{\mathcal{T}}'_{ki}\rangle' + \langle\hat{\mathcal{F}}'_{ki}\rangle' + 4\langle\hat{T}'_{ki}\rangle'\delta h'_{ik}. \tag{9.29}$$

Here, the operators $\hat{j}'_{ki}$, $\hat{T}'_{ki}$, $\hat{\mathcal{T}}'_{ki}$ and $\hat{\mathcal{F}}'_{ki}$ are defined exactly as for the unprimed system in Eq's 9.8, 9.18, 9.24 and 9.25 respectively, but with $J^{\perp}_{ij}$ and $J^{\parallel}_{ij}$ replaced by $J'^{\perp}_{ij}$ and $J'^{\parallel}_{ij}$.

We now assume that *all* quantities in Eq.'s 9.23 and 9.29 are equal to their Taylor series expansions with a finite radius of convergence around $t = 0$. Denoting the Taylor expansion of an arbitrary function $f(t)$ as $f(t) = \sum_{i=0}^{\infty} f^m t^m$ and Taylor expanding both sides of Eq. 9.23, we find after equating coefficients of equal powers of t,

$$(m+1)\langle\hat{j}_{ki}\rangle^{m+1} = \langle\hat{\mathcal{T}}_{ki}\rangle^m + \langle\hat{\mathcal{F}}_{ki}\rangle^m + 4\sum_{s=0}^{m}\langle\hat{T}_{ki}\rangle^{m-s}\delta h^s_{ik}. \tag{9.30}$$

Similarly, for Eq. 9.29 we have,

$$(m+1)\langle\hat{j}'_{ki}\rangle'^{m+1} = \langle\hat{\mathcal{T}}'_{ki}\rangle'^{m} + \langle\hat{\mathcal{F}}'_{ki}\rangle'^{m} + 4\sum_{s=0}^{m}\langle\hat{T}'_{ki}\rangle'^{m-s}\delta h'^{s}_{ik}. \tag{9.31}$$

We now subtract Eq. 9.31 from Eq. 9.30 and *demand* that the set of currents $\{\langle\hat{j}_{12}\rangle, \langle\hat{j}_{13}\rangle, ...\langle\hat{j}_{23}\rangle, ...\langle\hat{j}_{N-1,N}\rangle\}$ and $\{\langle\hat{j}'_{12}\rangle', \langle\hat{j}'_{13}\rangle', ...\langle\hat{j}'_{23}\rangle', ...\langle\hat{j}'_{N-1,N}\rangle'\}$ be the same in the primed and unprimed systems, i.e. we demand that the Taylor coefficients $\langle\hat{j}_{ki}\rangle^m$ and $\langle\hat{j}'_{ki}\rangle'^m$ be the same for all m and for all qubit pairs k and i. This yields

$$\begin{aligned} 4\langle\hat{T}'_{ki}\rangle'^0\delta h'^m_{ik} &= -4\sum_{s=0}^{m-1}\langle\hat{T}'_{ki}\rangle'^{m-s}\delta h'^s_{ik} + 4\sum_{s=0}^{m}\langle\hat{T}_{ki}\rangle^{m-s}\delta h^s_{ik} \\ + \quad &\langle\hat{\mathcal{T}}_{ki}\rangle^m - \langle\hat{\mathcal{T}}'_{ki}\rangle'^m + \langle\hat{\mathcal{F}}_{ki}\rangle^m - \langle\hat{\mathcal{F}}'_{ki}\rangle'^m, \end{aligned} \tag{9.32}$$

for all k and i. We see that the left hand side of Eq. 9.32 contains Taylor coefficients of $\delta h'_{ik}(t)$ of order m, while the right hand side has only Taylor coefficients of $\delta h'_{ik}(t)$ of order less than m and known quantities. Thus, when supplemented with the condition in Eq. 9.27, Eq. 9.32 is a unique recursion relation for the Taylor coefficients of the local field differences $\delta h'_{ik}(t)$, which reproduce the given set of currents $\{\langle\hat{j}_{12}\rangle, \langle\hat{j}_{13}\rangle, ...\langle\hat{j}_{23}\rangle, ...\langle\hat{j}_{N-1,N}\rangle\}$ using different two-qubit interactions $J'^{\perp}_{ij}$ and $J'^{\parallel}_{ij}$. Eq. 9.32 can be used to construct the set of local fields, $\{h'_1, h'_2, ...h'_N\}$ up to an arbitrary constant field, which can be chosen to make the propagation of the auxiliary system as simple as possible (section 9.6).

So far we have established a qVL theorem for TDCDFT. In order to establish the qVL theorem of TDDFT discussed in the text, we simply need to add the condition in Eq. 9.28. With this additional constraint, it is clear from Eq's. 9.9 and 9.14 that if the constructed fields $\{h'_1, h'_2, ...h'_N\}$ force the set $\{\langle\hat{j}'_{12}\rangle', \langle\hat{j}'_{13}\rangle', ...\langle\hat{j}'_{23}\rangle', ...\langle\hat{j}'_{N-1,N}\rangle'\}$ to be the same as $\{\langle\hat{j}_{12}\rangle, \langle\hat{j}_{13}\rangle, ...\langle\hat{j}_{23}\rangle, ...\langle\hat{j}_{N-1,N}\rangle\}$, the sets $\{\sigma'^z_1, \sigma'^z_2, ...\sigma'^z_N\}$ and $\{\sigma^z_1, \sigma^z_2, ...\sigma^z_N\}$ must be the same as well.

We now discuss two main conditions of the theorem:

1) *All* of the quantities appearing in Eq.'s 9.23 and 9.29 as well as the sets $\{\sigma_1^z, \sigma_2^z, ...\sigma_N^z\}$ and $\{\sigma_1'^z, \sigma_2'^z, ...\sigma_N'^z\}$ must be equal to their Taylor expansions within a finite radius of convergence for the theorem to hold. This is a much more restrictive condition than for the qRG theorem, which only requires that the sets of fields $\{h_1, h_2, ...h_N\}$ and $\{h_1', h_2', ...h_N'\}$ be equal to their Taylor series expansions. This restriction arises in the VL theorem of electronic TDDFT as well and approaches to circumvent this condition have begun to be researched [146].

2) For the entire set of fields $\{h_1', h_2', ...h_N'\}$ to exist, $\langle \hat{T}_{ki}' \rangle'^0$ must be non-vanishing for *all* pairs of qubits k and l. This too is a more severe restriction on the class of admissible initial states than in the qRG theorem, which only required that $\langle \hat{T}_{ki} \rangle^0$ be non-vanishing for certain values of k and l. However, since we are free to choose $|\psi'(0)\rangle$ so long as it satisfies the conditions in Eq.'s 9.27 and 9.28, we will often be able to choose an initial state such that $\langle \hat{T}_{ki}' \rangle'^0 \neq 0$. From a practical standpoint, we have also found in our numerical simulations that for vanishing $\langle \hat{T}_{ki}' \rangle'^0$, we can add a small convergence factor to make the fields well behaved at the initial time with little error in the overall propagation. This situation does not arise in electronic TDDFT for continuous systems, but similar problems have been noticed when one defines electronic TDDFT for lattice systems [19, 126, 121, 228]. Since the qubit Hamiltonians we consider in this chapter are also discrete, it is not surprising that a similar situation arises.

9.5 Entanglement as a density functional

In this section, we will discuss the construction of two-qubit entanglement as a functional of the single-qubit expectation values, $\{\sigma_1^z, \sigma_2^z, ...\sigma_N^z\}$. We use the concurrence as a measure of the entanglement between any two qubits in an N-qubit system [268]. Since the concurrence depends on non-commuting two-qubit observables, we expect that it is in general very hard to construct exactly as a functional of the set $\{\sigma_1^z, \sigma_2^z, ...\sigma_N^z\}$, which are simple expectation values of commuting single-qubit observables. We will see that this is indeed the case, but in the spirit of electronic TDDFT, one can hope to develop simple approximations.

The two-qubit reduced density matrix (2RDM) for the kth and lth qubits is obtained by tracing the full N-qubit density matrix over all other $N-2$ qubits in the system. In this letter we consider only pure states, so the 2RDM is simply given by

$$\rho_{kl} = \mathrm{Tr}_{1,...\mathrm{k}-1,\mathrm{k}+1,...\mathrm{l}-1,\mathrm{l}+1,...\mathrm{N}} \left[|\psi(\mathrm{t})\rangle\langle\psi(\mathrm{t})| \right], \tag{9.33}$$

where Tr denotes a partial trace. Defining the "time-reversed" 2RDM as

$$\tilde{\rho}_{kl} = \hat{\sigma}_k^y \otimes \hat{\sigma}_l^y \rho_{kl}^* \hat{\sigma}_k^y \otimes \hat{\sigma}_l^y, \tag{9.34}$$

the concurrence E_{kl} is defined in terms of the eigenvalues λ_i of the matrix $\rho_{kl}\tilde{\rho}_{kl}$ as,

$$E_{kl} = \max(0, \sqrt{\lambda_1} - \sqrt{\lambda_2} - \sqrt{\lambda_3} - \sqrt{\lambda_4}). \tag{9.35}$$

In Eq. 9.35, the eigenvalues λ_i are arranged in decreasing order, i.e. $\lambda_1 > \lambda_2 > \lambda_3 > \lambda_4$.

We first investigate the concurrence for a system which is restricted to the $\sigma_{total}^z = \pm(N-2)$ subspace. There is only one flipped qubit relative to the other $N-1$ qubits.

This is also known as the single-excitation manifold. We denote $|i\rangle = |00...010...00\rangle$ as the computational basis state with the ith qubit in the state $|1\rangle$ and all other qubits in the state $|0\rangle$ (the 0's and 1's can be interchanged without changing any results). The N-qubit density matrix can be expanded in terms of the N computational basis functions as,

$$|\psi(t)\rangle\langle\psi(t)| = \sum_{i,j=1}^{N} a_i^*(t)a_j(t)|j\rangle\langle i|. \tag{9.36}$$

From the above expression, we find the 2RDM for the kth and lth qubits to be

$$\rho_{kl} = \begin{pmatrix} \sum_{i\neq k,l}|a_i(t)|^2 & 0 & 0 & 0 \\ 0 & |a_l(t)|^2 & a_l(t)a_k^* & 0 \\ 0 & a_l^*(t)a_k & |a_k(t)|^2 & 0 \\ 0 & 0 & 0 & 0 \end{pmatrix}. \tag{9.37}$$

In Eq. 9.37, ρ_{kl} is expressed in the 2-qubit computational basis states, $\{|00\rangle, |01\rangle, |10\rangle, |11\rangle\}$. From Eq.'s 9.34 and 9.35, we find the concurrence to be,

$$E_{kl} = 2|a_l(t)||a_k(t)|. \tag{9.38}$$

In order to re-express E_{kl} in terms of $\{\sigma_1^z, \sigma_2^z, ...\sigma_N^z\}$, we need to invert the matrix equation

$$\vec{\sigma^z} = \overleftrightarrow{M}\vec{a}, \tag{9.39}$$

where $\vec{\sigma^z}$ and $\vec{a}$ are column vectors formed from the sets $\{\sigma_1^z, \sigma_2^z, ...\sigma_N^z\}$ and $\{|a_1|^2, |a_2|^2, ...|a_N|^2\}$ respectively and $\overleftrightarrow{M}$ is a square matrix with the diagonal elements equal to -1 and all other elements equal to 1. Carrying out the inversion and substituting the result into Eq. 9.38 yields Eq. 9.4. Thus, we see that in the case of a single flipped qubit, it is very simple to obtain an exact entanglement functional.

As a more complicated example, we consider entanglement in the $\sigma^z_{total} = \pm(N-4)$ subspace, which contains states with two flipped qubits. We denote $|ij\rangle = |00...010...010...00\rangle$ as the computational basis state with the ith and jth qubits in the state $|1\rangle$ and all other qubits in the state $|0\rangle$. Here, we can expand the N-qubit density matrix in terms of these $\frac{N(N-1)}{2}$ computational basis functions as,

$$|\psi(t)\rangle\langle\psi(t)| = \sum_{i<j,k<l} a^*_{ij}(t)a_{kl}(t)|kl\rangle\langle ij|. \tag{9.40}$$

Obtaining the 2RDM as before, we find the eigenvalues of $\rho_{kl}\tilde{\rho}_{kl}$ to be

$$\lambda_1 = \Big\{\sqrt{(\sum_{i\neq k,l}|a_{il}(t)|^2)(\sum_{j\neq k,l}|a_{jk}(t)|^2)} + |\sum_{i\neq k,l} a_{ki}(t)a^*_{li}(t)|\Big\}^2, \tag{9.41}$$

$$\lambda_2 = \lambda_3 = |a_{kl}(t)|^2 \sum_{i<j\neq k,l}|a_{ij}(t)|^2, \tag{9.42}$$

and

$$\lambda_4 = \Big\{\sqrt{(\sum_{i\neq k,l}|a_{il}(t)|^2)(\sum_{j\neq k,l}|a_{jk}(t)|^2)} - |\sum_{i\neq k,l} a_{ki}(t)a^*_{li}(t)|\Big\}^2. \tag{9.43}$$

The terms depending on sums over the coefficients' moduli squared, $|a_{ij}(t)|^2$, can be obtained fairly easily in terms of $\{\sigma^z_1, \sigma^z_2, ...\sigma^z_N\}$ using the expression

$$\sigma^z_i = 1 - \sum_{l\neq i}|a_{il}(t)|^2. \tag{9.44}$$

However, we see that λ_1 and λ_4 also contain the term $|\sum_{i\neq k,l} a_{ki}(t)a^*_{li}(t)|$, which depends explicitly on phases in the wavefunction. The imaginary parts of the coherences can be obtained from the currents, which in turn can be obtained from time derivatives of $\{\sigma^z_1, \sigma^z_2, ...\sigma^z_N\}$. However, the real parts of the coherences depend on expectation values of the kinetic energy operators, $\hat{T}_{kl}$, and in general will need to be approximated. Since the number of computational basis states increases with the

number of flipped qubits, we expect the exact entanglement functional to become progressively more complicated as more qubits are flipped. This highlights the need for constructing simple approximate entanglement functionals and will be explored in future work.

9.6 Numerical propagation of the qubit van Leeuwen construction

In this section we discuss how the proof of the qVL theorem can be used to numerically construct a set of auxiliary fields $\{h'_1, h'_2, ...h'_N\}$, which reproduce a given set $\{\sigma_1^z, \sigma_2^z, ...\sigma_N^z\}$ using a different two-qubit interaction. This procedure was used to simulate a Heisenberg model using an XY model and was demonstrated in Figure 9.3 and Figures 9.7 and 9.8 (below).

In principle, Eq. 9.32 can be used as a recursion relation to construct the Taylor coefficients of $\{h'_1, h'_2, ...h'_N\}$ to arbitrary order, but in practice this proves to be numerically cumbersome. Instead, we use a formulation of the qVL construction based on a non-linear Schrödinger equation. A similar construction was presented in ref. [146] for electronic TDDFT.

We begin by numerically solving the time-dependent Schrödinger equation in the "unprimed system",

$$\frac{\partial}{\partial t}|\psi(t)\rangle = \hat{H}(t)|\psi(t)\rangle, \tag{9.45}$$

for a given initial state $|\psi(0)\rangle$ and a given Hamiltonian $\hat{H}(t)$ which we wish to simulate

(see below for simulation details). From $|\psi(t)\rangle$, we can calculate all relevant observables, and in particular, we can calculate the set of currents $\{\langle\hat{j}_{12}\rangle, \langle\hat{j}_{13}\rangle, ...\langle\hat{j}_{23}\rangle, ...\langle\hat{j}_{N-1,N}\rangle\}$ at each time-step.

We then construct the set of fields $\{h'_1, h'_2, ...h'_N\}$ which reproduce this set of currents, but using a Hamiltonian with different two-qubit interactions $J'^{\perp}_{ij}$ and $J'^{\parallel}_{ij}$,

$$\hat{H}'(t) = \sum_{i<j}^{N} J'^{\perp}_{ij}(\hat{\sigma}^x_i\hat{\sigma}^x_j + \hat{\sigma}^y_i\hat{\sigma}^y_j) + \sum_{i<j}^{N} J'^{\parallel}_{ij}\hat{\sigma}^z_i\hat{\sigma}^z_j + \sum_{i=1}^{N} h'_i(t)\hat{\sigma}^z_i. \tag{9.46}$$

This is done by numerically solving Eq. 9.29 for the set $\{h'_1, h'_2, ...h'_N\}$ at each time-step, with the requirement that $\{\langle\hat{j}_{12}\rangle, \langle\hat{j}_{13}\rangle, ...\langle\hat{j}_{23}\rangle, ...\langle\hat{j}_{N-1,N}\rangle\} = \{\langle\hat{j}'_{12}\rangle', \langle\hat{j}'_{13}\rangle', ...\langle\hat{j}'_{23}\rangle', ...\langle\hat{j}'_{N-1,N}\rangle'\}$ for all k and l, i.e. we solve

$$\frac{\partial}{\partial t}\langle\hat{j}_{ki}\rangle = \langle\hat{\mathcal{T}}'_{ki}\rangle' + \langle\hat{\mathcal{F}}'_{ki}\rangle' + 4\langle\hat{T}'_{ki}\rangle'\delta h'_{ik}(t), \tag{9.47}$$

for all $\delta h'_{ik}(t)$, where on the left hand side $\langle\hat{j}_{ki}\rangle$ are known from the solution to Eq. 9.45. However, since $\langle\hat{\mathcal{T}}'_{ki}\rangle'$, $\langle\hat{\mathcal{F}}'_{ki}\rangle'$ and $\langle\hat{T}'_{ki}\rangle'$ depend on the auxiliary wavefunction $|\psi'(t)\rangle$, to solve Eq. 9.47 we must simultaneously solve the auxiliary system's time-dependent Schrödinger equation,

$$\frac{\partial}{\partial t}|\psi'(t)\rangle = \hat{H}'(t)|\psi'(t)\rangle, \tag{9.48}$$

where $\hat{H}'(t)$ in turn depends on $\delta h'_{ik}(t)$. Thus, Eq. 9.48 is a non-linear Schrödinger equation and Eq.'s 9.47 and 9.48 represent a set of coupled non-linear ordinary differential equations for the auxiliary wavefunction $|\psi'(t)\rangle$ and the set of fields $\{h'_1, h'_2, ...h'_N\}$. To solve this system of equations, we begin with an initial state $|\psi'(0)\rangle$ which satisfies the conditions in Eq.'s 9.27 and 9.28. By enforcing Eq. 9.28, we ensure that our solutions to Eq.'s 9.47 and 9.48 will reproduce the set $\{\sigma^z_1, \sigma^z_2, ...\sigma^z_N\}$ in

addition to the currents. From $|\psi'(0)\rangle$, we can solve Eq. 9.47 at $t = 0$,

$$\frac{\partial}{\partial t}\langle\hat{j}_{ki}\rangle|_{t=0} = \langle\hat{\mathcal{T}}'_{ki}\rangle'|_{t=0} + \langle\hat{\mathcal{F}}'_{ki}\rangle'|_{t=0} + 4\langle\hat{T}'_{ki}\rangle'|_{t=0}\delta h'_{ik}(0), \tag{9.49}$$

for field differences $\delta h'_{ik}(0)$. After making a choice for the arbitrary global field, we can construct the set of fields $\{h'_1(0), h'_2(0), ...h'_N(0)\}$ at $t = 0$ and the Hamiltonian $\hat{H}'(0)$. We then solve

$$\frac{\partial}{\partial t}|\psi'(t)\rangle|_{t=0} = \hat{H}'(0)|\psi'(0)\rangle, \tag{9.50}$$

to obtain $|\psi'(dt)\rangle$ at the next time-step. From $|\psi'(dt)\rangle$, we obtain $\{h'_1(dt), h'_2(dt), ...h'_N(dt)\}$ by solving

$$\frac{\partial}{\partial t}\langle\hat{j}_{ki}\rangle|_{t=dt} = \langle\hat{\mathcal{T}}'_{ki}\rangle'|_{t=dt} + \langle\hat{\mathcal{F}}'_{ki}\rangle'|_{t=dt} + 4\langle\hat{T}'_{ki}\rangle'|_{t=dt}\delta h'_{ik}(dt). \tag{9.51}$$

This procedure is continued at each time-step until we obtain $\{h'_1, h'_2, ...h'_N\}$ and $|\psi'(t)\rangle$ on the entire interval [0,t].

For the simulation presented in section 9.2, $\hat{H}(t)$ is the Heisenberg Hamiltonian and $\hat{H}'(t)$ is an XY Hamiltonian with the chosen parameters. With the initial state $|\psi(0)\rangle = \frac{1}{\sqrt{3}}(|011\rangle + |101\rangle + |110\rangle)$, we solve Eq. 9.45 using the fourth-order Runge-Kutta method. $|\psi(t)\rangle$ is propagated on a uniform grid with 10^4 time-steps, each of duration $dt = 1.5 \times 10^{-4}\frac{\hbar}{2J}$. With $|\psi(t)\rangle$, we can calculate derivatives of the currents between all 3 qubits to be used in Eq. 9.47. We use the procedure outlined in Eq.'s 9.47- 9.51 to obtain $|\psi'(t)\rangle$ and $\{h'_1, h'_2, h'_3\}$ of the auxiliary XY Hamiltonian. For the auxiliary system's initial state, we chose $|\psi'(0)\rangle = |\psi(0)\rangle = \frac{1}{\sqrt{3}}(|011\rangle + |101\rangle + |110\rangle)$, which satisfies the conditions in Eq.'s 9.27 and 9.28 since the initial currents vanish in both the primed and unprimed systems. We also fix the arbitrary global field

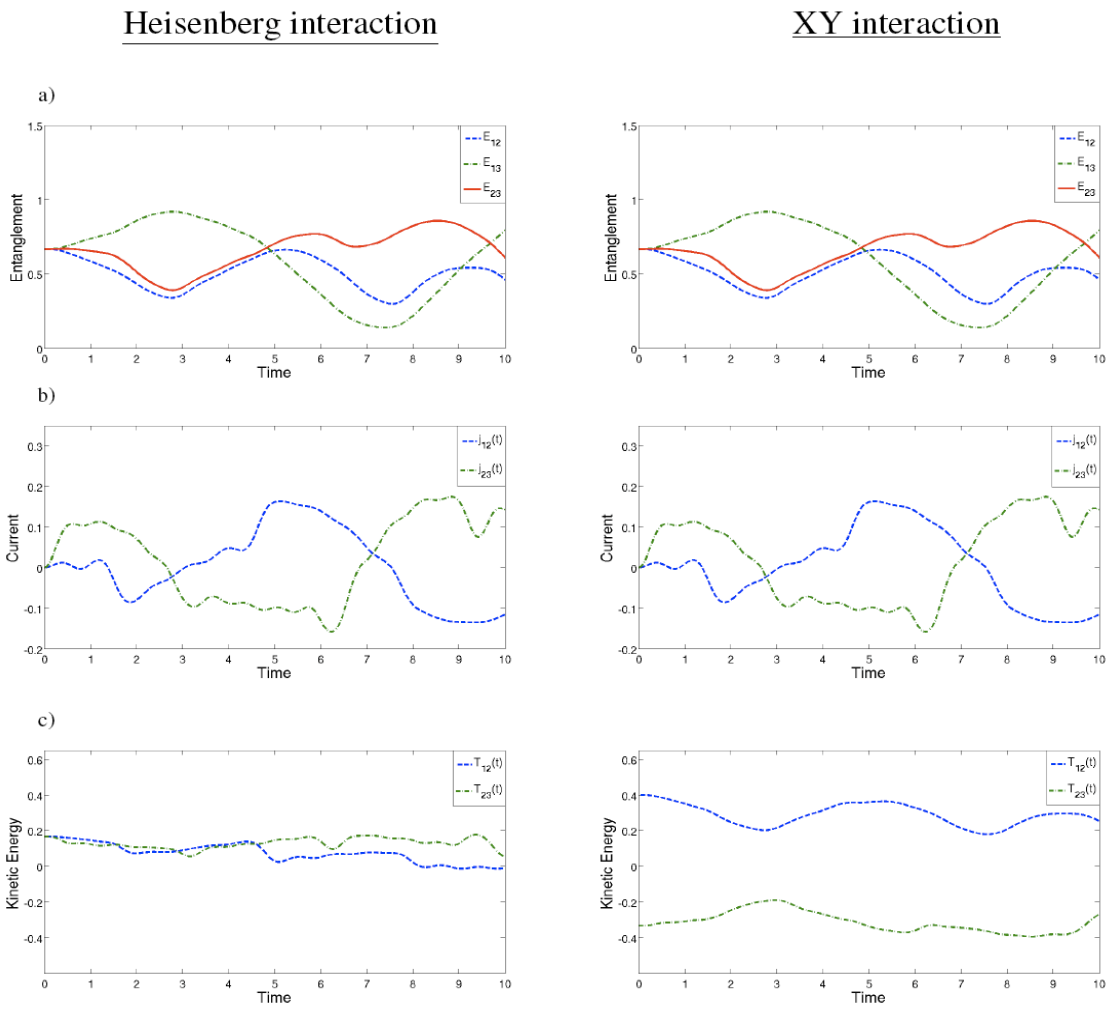

Figure 9.7: **Observables in the Heisenberg Hamiltonian verses the XY Hamiltonian** - a) The entanglement calculated directly with the wavefunctions $|\psi(t)\rangle$ (left column) and $|\psi'(t)\rangle$ (right column) is seen to be the same, as expected since the propagation is restricted to the subspace with one flipped qubit and Eq. 9.4 holds. b) The currents $\{\langle\hat{j}_{12}\rangle, \langle\hat{j}_{23}\rangle\}$ (left column) and $\{\langle\hat{j}'_{12}\rangle', \langle\hat{j}'_{23}\rangle'\}$ (right column) are also the same, as a consequence of the qVL construction. c) The kinetic energies $\{\langle\hat{T}_{12}\rangle, \langle\hat{T}_{23}\rangle\}$ (left column) and $\{\langle\hat{T}'_{12}\rangle', \langle\hat{T}'_{23}\rangle'\}$ (right column) are very different, as is often the case in electronic TDDFT as well.

by choosing $h_2'(t) = h_2(t)$ for all t. Since $|\psi'(0)\rangle$ is an eigenstate of $\hat{\sigma}^z_{total}$, this choice corresponds to trivially fixing the global phase of the auxiliary system's wavefunction and any other choice would yield identical expectation values of observables.

As shown in Figure 9.3, the set $\{\sigma_1^z, \sigma_2^z, \sigma_3^z\}$ is faithfully reproduced by $|\psi'(t)\rangle$. In Figure 9.7 we show expectation values of several other observables calculated with $|\psi(t)\rangle$ in the left column and $|\psi'(t)\rangle$ in the right column. Naturally, observables that depend explicitly on the set $\{\sigma_1^z, \sigma_2^z, \sigma_3^z\}$ are the same in both cases, while those that do not will be different. In particular, we see that the entanglement is the same in both cases, since both $|\psi(t)\rangle$ and $|\psi'(t)\rangle$ remain a superposition of states with one flipped qubit during the evolution. This means that the explicit entanglement functional in Eq. 9.4 holds, and since both wavefunctions produce the same set $\{\sigma_1^z, \sigma_2^z, \sigma_3^z\}$, they necessarily produce the same entanglement. As expected, the currents $\{\langle\hat{j}_{12}\rangle, \langle\hat{j}_{23}\rangle\}$ and $\{\langle\hat{j}'_{12}\rangle', \langle\hat{j}'_{23}\rangle'\}$ are the same for both wavefunctions, while the kinetic terms $\{\langle\hat{T}_{12}\rangle, \langle\hat{T}_{23}\rangle\}$ and $\{\langle\hat{T}'_{12}\rangle', \langle\hat{T}'_{23}\rangle'\}$ are different. The same situation arises in electronic DFT, where the Kohn-Sham wavefunction reproduces the correct density and current, but the kinetic energy is in general different from that of the true correlated wavefunction. In Figure 9.8, we plot the expansion coefficients of $|\psi(t)\rangle$ and $|\psi'(t)\rangle$ in the computational basis $\{|011\rangle, |101\rangle, |110\rangle\}$, which as expected are rather different. It is also interesting to note that in our formalism, the operators for the current and kinetic energy are different in the original and auxiliary systems, since we let all two-qubit parameters in the Hamiltonian differ. This situation is different than in electronic TDDFT, where the kinetic energy and current operators themselves are the same, although expectation values may be different in the case

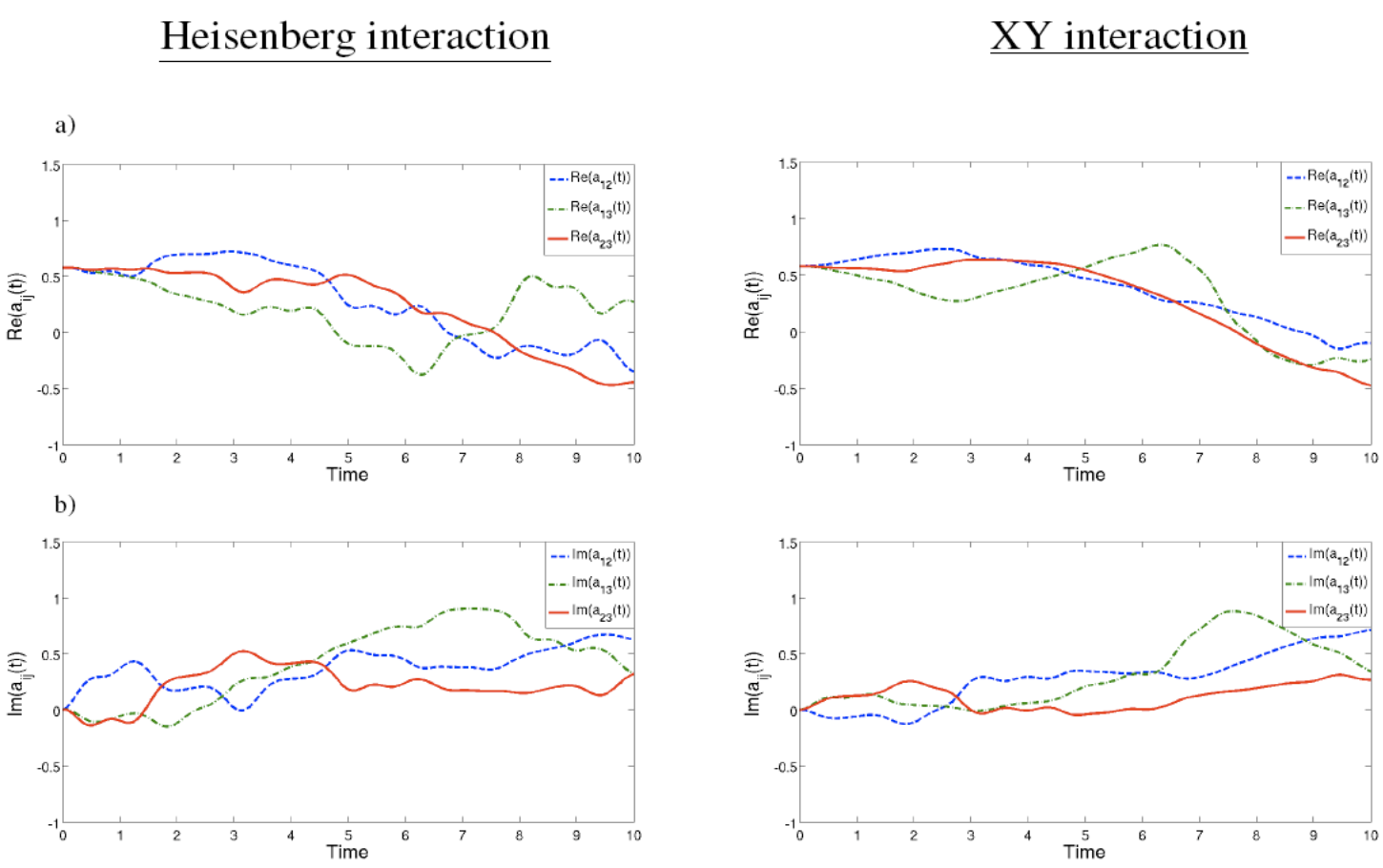

Figure 9.8: **Wavefunctions in the Heisenberg Hamiltonian verses the XY Hamiltonian** - The real parts (a) and the imaginary parts (b) of the expansion coefficients of $|\psi(t)\rangle = \sum_{i<j}^{3} a_{ij}(t)|ij\rangle$ (left column) and $|\psi'(t)\rangle = \sum_{i<j}^{3} a'_{ij}(t)|ij\rangle$ (right column) in the computational basis. Although the wavefunctions are clearly different, they both reproduce the same set $\{\sigma_1^z, \sigma_2^z, \sigma_3^z\}$ throughout the evolution.

of the kinetic energy. This is important in our formalism, especially with regard to the current, since although $\{\langle\hat{j}_{12}\rangle, \langle\hat{j}_{23}\rangle\} = \{\langle\hat{j}'_{12}\rangle', \langle\hat{j}'_{23}\rangle'\}$, one finds that in general $\{\langle\hat{j}_{12}\rangle, \langle\hat{j}_{23}\rangle\} \neq \{\langle\hat{j}_{12}\rangle', \langle\hat{j}_{23}\rangle'\}$.

Chapter 10

The quantum complexity classification of time-dependent density functional theory

10.1 Introduction

In the previous chapter we proved that TDDFT can be used to simulate systems of entangled qubits during quantum computations. In the present chapter, we return to TDDFT as a tool for simulating systems of interacting electrons and investigate its complexity as a method in computational chemistry from a computer science perspective. More specifically, we outline a proof that TDDFT lies in the quantum computational complexity class BQP (bounded-error quantum polynomial), which represents the class of computational problems that can be solved with polynomially many resources on a quantum computer. This is in contrast to ground state DFT, which has been shown to be in the more difficult complexity class QMA (quantum Merlin-Arthur) [211].

Our result is somewhat counterintuitive, as most users and developers of density

functional methods would characterize TDDFT as more difficult than DFT. This is largely due to the fact that TDDFT is at a more immature stage of development than DFT and one often uses DFT functionals as approximations to the true TDDFT functional (adiabatic approximation). Computational complexity theory on the other hand investigates the resources required to solve a given computational problem in the worst-case scenario and "coarse grains" over many issues of practical importance. Nevertheless, complexity theory is useful from a theoretical standpoint, as it allows one to classify general computational problems without needing to consider specifics on a case-by-case basis. Our result also places TDDFT within the hierarchy of computational methods in chemistry such as Hartree-Fock and 2RDM theory (second-order reduced density matrix theory), whose complexity classification has been investigated recently [138, 211].

In the forthcoming sections, we will be more specific about what exactly we mean by "the computational complexity of TDDFT" and what it means to prove that a computational method is in a given complexity class. In section 10.2, we provide a brief overview of computational complexity theory, particularly as it applies to methods in chemistry. Then, in section 10.3 we give a precise definition of the problem we wish to solve and bound the computational resources required to solve it. i.e. we prove that TDDFT is within BQP. Section 10.4 contains concluding remarks and also speculates that TDDFT is not only within BQP, but it is also "BQP complete." We have done our best to maintain mathematical rigor, however, there are most likely parts of our arguments that would not be completely satisfactory to the pure mathematician. Nevertheless, we outline a proof that we believe could serve as a

good starting point for an even more rigorous mathematical treatment.

10.2 Computational complexity in chemistry

In this section, we provide a brief overview of computational complexity theory, particular as it relates to chemistry. The theory of computational complexity studies the scaling of the resources necessary to solve a given problem as a function of the input size. Problems are considered to be "easy," or efficiently solvable, if the time (or number of steps) for solving the problem scales as a polynomial of the input size n. For example, sorting a list of n items will take at most $O(n^2)$ steps. On the other hand, problems are considered "hard" if the scaling is exponential in n. Exponential scaling is the worst case scenario for many-body problems in physics and chemistry [187], for instance performing full configuration interaction on highly frustrated ground states of strongly correlated systems. Fortunately, most problems of practical interest in chemistry and physics do not fall into this worst case scenario.

Computational complexity is often formulated using decision problems, due to the binary nature of the inputs and outputs of logic gates. A decision problem determines if some condition is true or false e.g. is the ground-state energy of the system below a certain critical value? Although the answer to decision problems is either "yes" or "no," one can keep asking questions in a binary search fashion. For instance, one could attempt to determine in this way the ground-state energy to an arbitrarily high accuracy. A complexity class contains a set of computational problems that share some common properties about the computational resources required for solving them.

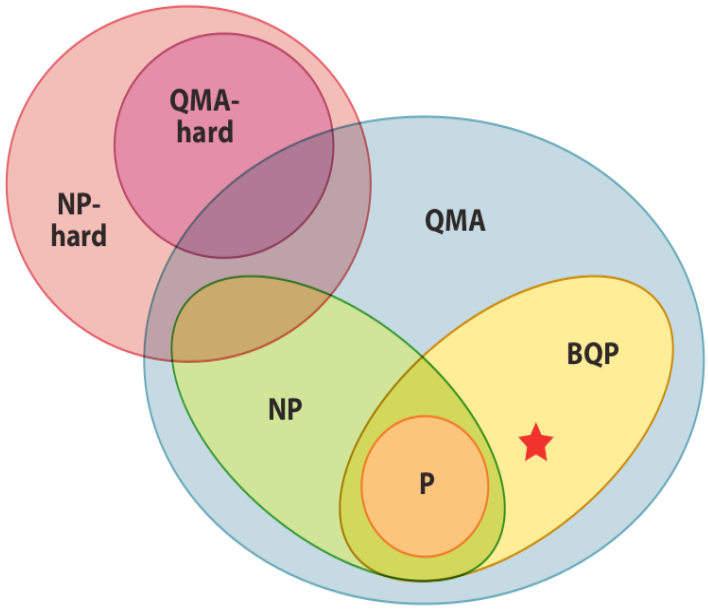

Figure 10.1: **Computational complexity classes** - A schematic Venn diagram of the main classical and quantum complexity classes and their conjectured relationships. Note that the relationships depicted in this diagram are conjectured, but many are not proven. For instance, it is strongly conjectured, but not proven that $P \neq NP$. Figure taken from ref. [279].

A given problem is said to be "Hard" within a given class, if it is at least as hard to solve as any other problem within that class. A problem is said to be "Complete" within a given class if it is Hard and also is contained within that class. Thus, in the next section we will prove that TDDFT is within the class BQP, but to prove that it is "BQP Complete" we will need to additionally prove that it is BQP Hard. We will conjecture, but not prove that TDDFT is BQP complete. Solving a problem that is complete within a given class is equivalent to solving all other problems within that class. Below, we briefly summarize a few important examples of complexity classes of decision problems, which are depicted schematically in Figure 10.1.

The complexity class P contains all decision problems that are solvable in a polynomial time with a classical computer (more precisely, a deterministic Turing machine). Roughly speaking, solving a problem in a polynomial time refers to the cases where the number of steps for solving the problem scales as a polynomial power as opposed to exponentially. This is considered "efficient," but of course from a practical standpoint there could be exceptions. For example, problems that scale as $O(n^{10000})$ may take a very long time to finish, compared with ones that scale exponentially as $O(1.0001^n)$.

Problems that are typically hard to solve on classical computers fall into the complexity class NP, which contains decision problems whose "yes" instances can be efficiently verified to be true with a classical computer given an appropriate solution or "witness". There is no doubt that P is a subclass of NP, i.e.,

$$P \subset NP. \tag{10.1}$$

As an example, finding the prime factors of an integer belongs to an NP problem; once the factors are given, it is easy to check the answer by performing a multiplication. However, finding the factors in the first place is generally difficult. Interestingly, finding the ground state energy of the Ising model

$$H = \sum_{(i,j)\in E} \sigma_z^i \sigma_z^j + \sum_{i\in V} \sigma_z^i \,, \tag{10.2}$$

where (V, E) is a planar graph, is NP-complete. This implies that if a polynomial algorithm for finding the ground state energy of Eq. 10.2 is found, *all* of the problems in NP could be solved in polynomial time. In other words, it would imply that P = NP, a result considered highly unlikely. It is believed, but not known with certainty, that quantum computers are not capable of solving all NP problems efficiently. However, it has been shown using Shor's algorithm that they can solve the integer-factoring problem efficiently. It is believed that the complexity of integer-factoring is intermediate between P and NP [216].

The quantum analog of P and NP problems are, respectively, the complexity classes BQP and QMA. BQP is the class of (decision) problems that are solvable by a quantum computer in polynomial time. QMA is the class of (decision) problems that can be verified by a quantum computer in polynomial time. Like NP, the QMA class covers many problems that are important in physics and chemistry [138, 211, 259]. For example, the ground-state problem of Hamiltonians involving local interactions is known to be QMA-complete [107].

Having discussed the relevant complexity classes, we now outline a proof that TDDFT $\subset$ BQP.

10.3 The computational complexity of TDDFT

Formulation of the problem

Before discussing the computational complexity of TDDFT, we must define the computational problem "TDDFT" more carefully. Broadly speaking, we define this problem to be that of finding a local, multiplicative potential for a given many-electron system, which when applied to a non-interacting system of electrons yields the exact density of the original interacting system. If we can find an algorithm which produces this potential for any many-electron system given a set of inputs, we would have solved the computational problem "TDDFT". To be precise, we define the computational problem of finding the time-dependent Kohn-Sham potential at a fixed time t and with bounded error δ as:

> Given an initial N-electron state, $|\psi(0)\rangle$, a time-dependent N-electron Hamiltonian $H(t) = T + V_{ee} + v_{ext}(t)$ and a wave function $|\Phi(0)\rangle$ from a non-interacting system which reproduces the initial density and its first time-derivative, return an approximation to the time-dependent one-body potential at a given time t, $\tilde{v}_{ks}[v_{ext}, \Phi(0)](t)$ which is δ close to the exact Kohn-Sham potential, $v_{ks}[v_{ext}, \Phi(0)](t)$.

The algorithm for solving this computational problem is efficient, when the computational cost grows polynomially in $1/\delta$ and polynomially in t. This algorithm is depicted schematically in Figure 10.2. The first subroutine involves a quantum computer and its inputs are the initial many-body state $|\psi(0)\rangle$ and the external potential $v_{ext}(t)$ on a given interval $[0, t]$. The quantum computer then evolves the initial state with the given external potential and subsequently outputs the time-evolved wavefunction at a series of discrete time-steps. The wavefunction is then used to measure

the time-dependent density. i.e. construct the expectation value of the density operator. The second subroutine involves only a classical computer, with the inputs being the initial Kohn-Sham state $|\Phi(0)\rangle$ and the density $n(\mathbf{r}, t)$ on the given interval [0,t] which has been provided by the quantum computer. At each time-step, the classical computer solves the VL and KS equations, which represent a set of coupled nonlinear partial differential equations as mentioned in section 9.6. The classical computer then outputs the KS potential at each time-step and uses the evolved KS state as input for the next time-step. This procedure is iterated until the KS potential is obtained on the entire interval [0,t].

For a given initial state, it has been shown that time evolution can be done efficiently on a quantum computer and we don't discuss this point further in the present chapter [135]. Thus, we assume that given the initial many-body state, the first subroutine can be performed efficiently. It is worth mentioning that we make no claims on how easy it is to prepare the initial state. If we insist that the initial state be the ground state of a many-electron Hamiltonian, the problem could become difficult as this in fact belongs to a QMA Hard problem. Our proof only pertains to the time-evolution for a *given* initial state, as is the case in TDDFT.

In the remainder of this chapter, we attempt to bound the errors on the algorithm discussed above to obtain the KS potential. If we can show that these errors increase only polynomially in time and parameters characterizing the input size, we will have succeeded in showing that we have an algorithm which can be performed in a polynomial time using a quantum computer. Therefore, the computational problem we are solving, TDDFT, would be in BQP.

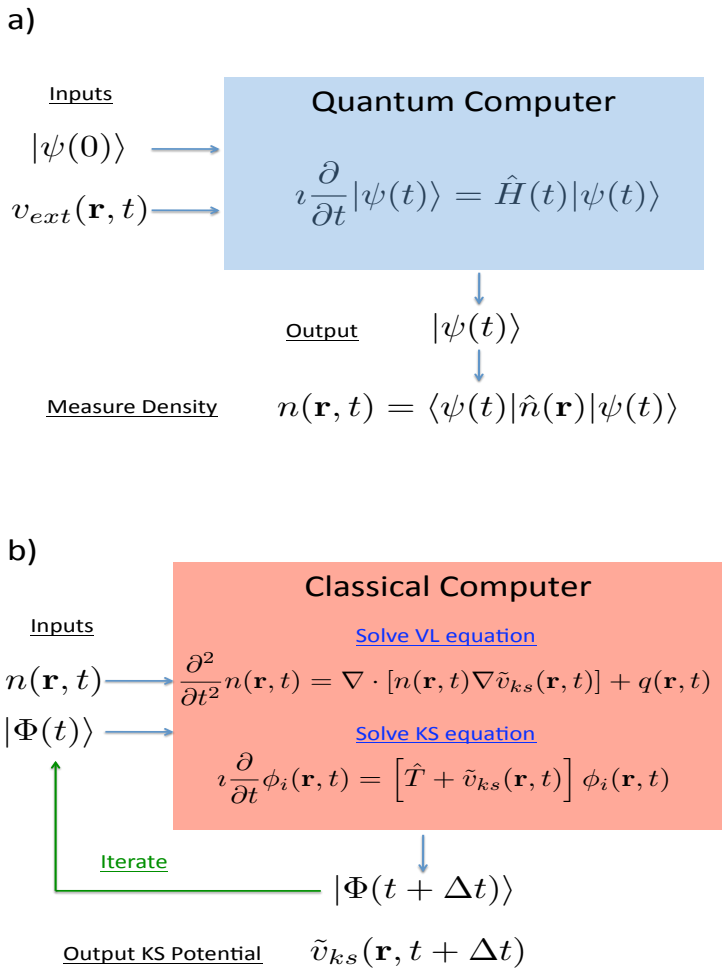

Figure 10.2: **Algorithm for obtaining the Kohn-Sham potential** - a) The many-body wavefunction is evolved on a quantum computer and the density obtained at a series of discrete time-steps. b) The density is then given to a classical computer which solves the VL equation at each time-step and outputs an approximation to the KS potential. The classical computer also evolves the KS equations with the obtained KS potential and uses the orbitals to solve the VL equation at the next time-step. This procedure is iterated until v_{ks} is obtained at each time-step on the entire interval $[0,t]$.

Error bounds on evolving the density on a quantum computer

Our first step is to bound the errors in the first subroutine in Figure 10.2: Evolving the density on the quantum computer. We derive the time-dependent Dyson equation as follows. Let $H(t) = H_0(t) + h(t)$, where $H_0(t)$ and $h(t)$ are arbitrary, possibly time-dependent Hamiltonians. We can write the time-evolution operator for the full Hamiltonian as:

$$\mathcal{T} e^{-i\int_{t_0}^{t_1} H(t)dt} = \mathcal{T} e^{-i\int_{t_0}^{t_1} H_0(t)dt} - i\int_{t_0}^{t_1} \mathcal{T} e^{-i\int_{t'}^{t_1} H_0(t)dt}\, h(t')\, \mathcal{T} e^{-i\int_{t_0}^{t'} H(t)dt} dt' \,. \quad (10.3)$$

This can be proved by checking that the right hand side obeys the defining differential equation,

$$\frac{\partial}{\partial t_1} \mathcal{T} e^{-i\int_{t_0}^{t_1} H(t)dt} = -iH(t_1)\mathcal{T} e^{-i\int_{t_0}^{t_1} H(t)dt} \,. \quad (10.4)$$

Using the Leibniz integral rule we get,

$$\frac{\partial}{\partial t_1}\left(\mathcal{T} e^{-i\int_{t_0}^{t_1} H_0(t)dt} - i\int_{t_0}^{t_1} \mathcal{T} e^{-i\int_{t'}^{t_1} H_0(t)dt}\, h(t')\, \mathcal{T} e^{-i\int_{t_0}^{t'} H(t)dt} dt'\right) \quad (10.5)$$

$$= -iH_0(t_1)\mathcal{T} e^{-i\int_{t_0}^{t_1} H_0(t)dt} - i\int_{t_0}^{t_1} \frac{\partial}{\partial t_1}\left(\mathcal{T} e^{-i\int_{t'}^{t_1} H_0(t)dt}\, h(t')\, \mathcal{T} e^{-i\int_{t_0}^{t'} H(t)dt}\right) dt'$$

$$- ih(t_1)\mathcal{T} e^{-i\int_{t_0}^{t_1} H(t)dt} \quad (10.6)$$

$$= -iH_0(t_1)\left(\mathcal{T} e^{-i\int_{t_0}^{t_1} H_0(t)dt} - i\int_{t_0}^{t_1} \mathcal{T} e^{-i\int_{t'}^{t_1} H_0(t)dt}\, h(t')\, \mathcal{T} e^{-i\int_{t_0}^{t'} H(t)dt} dt'\right)$$

$$- ih(t_1)\mathcal{T} e^{-i\int_{t_0}^{t_1} H(t)dt}, \quad (10.7)$$

and then using Eq. 10.3 we get Eq. 10.4.

We now bound the error made by evolving in discrete time-steps. Assume that we evolve from t_0 to $t_1 = t_0 + \delta t$ with the fixed Hamiltonian $H(t_0)$, instead of using

the time dependent Hamiltonian $H(t)$. Using the time-dependent Dyson equation (Eq. 10.3) we can bound the difference between the corresponding time evolution operators. The unperturbed Hamiltonian is now defined to be $H_0(t) = H(t_0)$, and so the perturbation is $h(t) = H(t) - H(t_0)$. We therefore write, for the operator norm $\|\cdot\|$,

$$\left\|\mathcal{T}e^{-i\int_{t_0}^{t_1} H(t)dt} - e^{-iH(t_0)\delta t}\right\| = \left\|\int_{t_0}^{t_1} e^{-iH_0(t_0)(t_1-t')}\left(H(t') - H(t_0)\right)\mathcal{T}e^{-i\int_{t_0}^{t'} H(t)dt}dt'\right\| \tag{10.8}$$

$$\leq \int_{t_0}^{t_1} \left\|e^{-iH_0(t_0)(t_1-t')}\right\| \left\|H(t') - H(t_0)\right\| \left\|\mathcal{T}e^{-i\int_{t_0}^{t'} H(t)dt}\right\|dt' \tag{10.9}$$

$$\leq \delta t \max_{t'\in[t_0,t_1]} \|H(t') - H(t_0)\| \,. \tag{10.10}$$

If $H(t)$ is Lipschitz continuous, with Lipschitz constant K, we can write,

$$\left\|\mathcal{T}e^{-i\int_{t_0}^{t_1} H(t)dt} - e^{-iH(t_0)\delta t}\right\| \leq K(\delta t)^2 \,, \tag{10.11}$$

and if the evolution is from $t = 0$ to T, we get the bound

$$\left\|\mathcal{T}e^{-i\int_{0}^{T} H(t)dt} - \Pi_j e^{-iH(t_j)\delta t}\right\| \leq \frac{T}{\delta t}K(\delta t)^2 = TK\delta t \,. \tag{10.12}$$

Similarly, we get the bound

$$\left\| \mathcal{T} e^{-i\int_0^T H(t)dt} \rho \mathcal{T} e^{i\int_0^T H(t)dt} - \Pi_j e^{-iH(t_j)\delta t} \rho \Pi_j e^{+iH(t_j)\delta t} \right\|_1 \tag{10.13}$$

$$\leq \frac{T}{\delta t} \max_j \left\| \mathcal{T} e^{-i\int_{t_j}^{t_j+\delta t} H(t)dt} \rho \mathcal{T} e^{i\int_{t_j}^{t_j+\delta t} H(t)dt} - e^{-iH(t_j)\delta t} \rho e^{+iH(t_j)\delta t} \right\|_1 \tag{10.14}$$

$$\leq 2\frac{T}{\delta t} \max_j \left\| \left(\mathcal{T} e^{-i\int_{t_j}^{t_j+\delta t} H(t)dt} - e^{-iH(t_j)\delta t} \right) \rho \right\|_1 \tag{10.15}$$

$$\leq 2\frac{T}{\delta t} \max_j \left\| \mathcal{T} e^{-i\int_{t_j}^{t_j+\delta t} H(t)dt} - e^{-iH(t_j)\delta t} \right\| \|\rho\|_1 \tag{10.16}$$

$$\leq 2\frac{T}{\delta t} K(\delta t)^2 = 2TK\delta t, \tag{10.17}$$

where $\rho = |\psi(t)\rangle\langle\psi(t)|$ is the many-body density operator. The Lipschitz constant K is bounded by the maximum derivative of the external potential. i.e.

$$K \leq \max_{t' \in [0,T]} \left\| \frac{dv_{ext}(t')}{dt} \right\|. \tag{10.18}$$

A clear assumption on the VL theorem is that the first-derivative of the external potential should be finite. Thus, since $n(\mathbf{r}, t) = Tr[\rho \hat{n}(\mathbf{r})]$, we have shown that the error on the density evolution is bounded and grows only polynomially in the number of time-steps ($N = \frac{T}{\delta t}$) and the time-step size δt.

Error bounds on solving the van Leeuwen construction on a classical computer

We now bound the errors on the second subroutine in Figure 10.2, beginning with the solution of the VL equation on a classical computer. The VL equation represents a generalized, elliptic, inhomogeneous partial differential equation which can be solved by the method of finite elements with the boundary condition that $v_{ks}(\mathbf{r}, t) \to 0$ faster than $\frac{1}{r}$ as $r \to \infty$ [262, 261, 263, 35, 229].

We write the VL equation as:

$$\nabla \cdot [n(\mathbf{r},t)\nabla v_{ks}(\mathbf{r},t)] = f(\mathbf{r},t), \tag{10.19}$$

with the inhomogeneous term $f(\mathbf{r},t) = \frac{\partial^2}{\partial t^2} n(\mathbf{r},t) - q(\mathbf{r},t)$. Formulating the solution in terms of Sobolev spaces [218, 88], we can write the VL equation in terms of a complete set of functions $\{p_i(\mathbf{r})\}$ as:

$$a(v_{ks}, p_i) = -(f, p_i), \tag{10.20}$$

for all i in the set. Typically, the set will be chosen to be a set of polynomials representing our grid in the finite element solver [35]. Here,

$$a(v_{ks}, p_i) = \int d^3r n(\mathbf{r},t)(\nabla p_i(\mathbf{r})) \cdot (\nabla v_{ks}(\mathbf{r},t)), \tag{10.21}$$

is the bilinear form characterizing the differential equation and

$$(f, p_i) = \int d^3r p_i(\mathbf{r}) f(\mathbf{r},t). \tag{10.22}$$

Using Cea's lemma [104, 35], we can bound the error in the approximate finite-element solution $\tilde{v}_{ks}$ to the VL equation by:

$$\|v_{ks} - \tilde{v}_{ks}\| \leq \frac{\gamma}{\alpha} \|v_{ks} - p_i\|, \tag{10.23}$$

for all p_i in the Sobolev space. Here, v_{ks} is the exact KS potential and γ and α are positive constants determined by the continuity and coercivity conditions respectively:

$$|a(p_i, p_j)| \leq \gamma \|p_i\| \|p_j\| \tag{10.24}$$

and

$$a(p_i, p_i) \geq \alpha \|p_i\|^2, \tag{10.25}$$

for all p_i in the Sobolev space. This is a very nice lemma, because it tells us that provided we choose our finite element polynomials to represent the exact potential well and thus $\|v_{ks} - p_i\|$ is small, our approximate solution $\tilde{v}_{ks}$ will be close to the exact one v_{ks}. This however, is contingent upon the condition that $\alpha \neq 0$, or at least α is not too close to zero, otherwise the bound in Eq. 10.23 will be very weak. Let us examine the coercivity condition (Eq. 10.25) more carefully, which is explicitly given in real-space by:

$$\frac{\int d^3r n(\mathbf{r},t)|\nabla p_i(\mathbf{r})|^2}{\int d^3r |p_i(\mathbf{r})|^2} \geq \alpha. \tag{10.26}$$

In finite element solvers, one chooses the polynomials to have a finite L^2 norm and so the denominator in Eq. 10.26 will be finite [104, 35]. However, if one or more of the functions $\{p_i(\mathbf{r})\}$ are localized in a region where the density vanishes, the numerator in Eq. 10.26 will vanish and the bound in Eq. 10.23 tells us nothing. This can happen in two circumstances. Firstly, since we will need to place some of the $\{p_i(\mathbf{r})\}$ where $\tilde{v}_{ks}(\mathbf{r},t)$ is non-zero (to get a good representation of the solution), if the density has a node in a region where $\tilde{v}_{ks}$ is not small, the numerator in Eq. 10.26 will become very small. Thus, we must restrict our proof to nodeless densities. Typically, densities of many-electron systems are nodeless and so this is not a major restriction [146]. Secondly, in the asymptotic region of large r the density decays exponentially and the numerator in Eq. 10.26 will become very small if we try to represent $\tilde{v}_{ks}(\mathbf{r},t)$ in this region with some of the functions $\{p_i(\mathbf{r})\}$. However, for a real-time propagation we will only need to be able to represent the Kohn-Sham potential $\tilde{v}_{ks}(\mathbf{r},t)$ where the Kohn-Sham orbitals are non vanishing, which in turn only occurs in regions where the density is non-vanishing. Therefore, we only solve the VL equation in regions

where $n(\mathbf{r},t) > \epsilon$, where epsilon is a finite cutoff. In this case there is no problem in applying Cea's lemma. Of course, if one is interested in ionization energies or response properties it will be essential to sample $\tilde{v}_{ks}(\mathbf{r},t)$ in the asymptotic region, but it will not be necessary for our purposes.

The last step in bounding errors on the solution to the VL equation consists of bounding the errors in the inhomogeneous term $\frac{\partial^2}{\partial t^2}n(\mathbf{r},t) - q(\mathbf{r},t)$. We have already bounded the errors in the evolution of the density on the quantum computer and therefore in $\frac{\partial^2}{\partial t^2}n(\mathbf{r},t)$. We now need to bound errors in:

$$q(\mathbf{r},t) = \langle\Phi(t)|\hat{q}(\mathbf{r})|\Phi(t)\rangle, \tag{10.27}$$

where

$$\hat{q}(\mathbf{r}) = \sum_{\alpha,\beta} \frac{\partial^2}{\partial r_\alpha \partial r_\beta}\hat{T}_{\alpha,\beta} \tag{10.28}$$

and in second quantization the stress tensor is:

$$\hat{T}_{\alpha,\beta} = \frac{1}{2}\Big\{ \frac{\partial}{\partial r_\beta}\hat{\Psi}^\dagger(\mathbf{r})\frac{\partial}{\partial r_\alpha}\hat{\Psi}(\mathbf{r}) + \frac{\partial}{\partial r_\alpha}\hat{\Psi}^\dagger(\mathbf{r})\frac{\partial}{\partial r_\beta}\hat{\Psi}(\mathbf{r}) - \frac{1}{2}\frac{\partial^2}{\partial r_\alpha \partial r_\beta}\left[\hat{\Psi}^\dagger\hat{\Psi}(\mathbf{r})\right]\Big\}. \tag{10.29}$$

Before doing this we need to bound the error between the evolution with $U_{\delta t} = e^{-iH_{ks}\delta t}$ on the true Kohn-Sham density operator $\hat{\rho}_{ks} = |\Phi(t)\rangle\langle\Phi(t)|$ and $\tilde{U}_{\delta t} = e^{-i\tilde{H}_{ks}\delta t}$ on $\hat{\rho}_C$, the approximation to the Kohn-Sham density operator on the classical computer evolved with our approximate solution from finite elements $\tilde{v}_{ks}$. Note that

$$H_{ks}(t) = \sum_j T_j + v_{j,ks}(t) \tag{10.30}$$

is the Kohn-Sham Hamiltonian in many-body first quantization, and $\tilde{H}_{ks}$ is the Hamiltonian with the approximated $\tilde{v}_{ks}$. The proper bound should be for the trace norm

$\|\cdot\|_1$. Let the error from previous time steps be

$$\|\hat{\rho}_{ks} - \hat{\rho}_C\| = \epsilon_1 \ . \tag{10.31}$$

If the error in every step is small, which is what we are trying to prove right now, this error will be small. Then,

$$\|U_{\delta t}\hat{\rho}_{ks}U_{\delta t}^\dagger - \tilde{U}_{\delta t}\hat{\rho}_C\tilde{U}_{\delta t}^\dagger\|_1 \leq \epsilon_1 + \|U_{\delta t}\hat{\rho}_C U_{\delta t}^\dagger - \tilde{U}_{\delta t}\hat{\rho}_C\tilde{U}_{\delta t}^\dagger\|_1. \tag{10.32}$$

We now bound the second term:

$$\|U_{\delta t}\hat{\rho}_C U_{\delta t}^\dagger - \tilde{U}_{\delta t}\hat{\rho}_C\tilde{U}_{\delta t}^\dagger\|_1 = \|(U_{\delta t} - \tilde{U}_{\delta t})\hat{\rho}_C U_{\delta t}^\dagger + U_{\delta t}\hat{\rho}_C(U_{\delta t} - \tilde{U}_{\delta t})^\dagger\|_1 \leq 2\|(U_{\delta t} - \tilde{U}_{\delta t})\hat{\rho}_C\|_1 \ . \tag{10.33}$$

Now, using again the Dyson equation (Eq. 10.3):

$$\|(U_{\delta t} - \tilde{U}_{\delta t})\hat{\rho}_C\|_1 = \left\| \int_0^{\delta t} e^{-iH_{ks}(\delta t - t')} \sum_j (v'_{j,ks} - \tilde{v}'_{j,ks}) e^{-i\tilde{H}_{ks}t'} dt' \hat{\rho}_C \right\|_1 \tag{10.34}$$

$$\leq n \int_0^{\delta t} \left\| (v'_{ks} - \tilde{v}'_{ks}) e^{-i\tilde{H}_{ks}t'} \hat{\rho}_C \right\|_1 dt' \tag{10.35}$$

$$\leq n \int_0^{\delta t} \|\hat{\rho}_C(v'_{ks} - \tilde{v}'_{ks})\|_1 \, dt' \tag{10.36}$$

$$\leq n\,\delta t \|(v'_{ks} - \tilde{v}_{ks})\rho_C\|_1 = n\,\delta t \|\delta Q\|_1, \tag{10.37}$$

where n is the number of electrons, $Q(\mathbf{r},t) = n(\mathbf{r},t)v_{ks}(\mathbf{r},t)$ and $\delta Q(\mathbf{r},t) = n(\mathbf{r},t)(v_{ks}(\mathbf{r},t) - \tilde{v}_{ks}(\mathbf{r},t))$. Using Hölder's inequality [262], we can bound the 1-norm with the 2-norm

$$\|\delta Q\|_1 \leq \|\delta Q\|_2 \sqrt{V} \ , \tag{10.38}$$

where V is the volume of integration. The dominant error will then be,

$$\|\delta Q\|_2 \leq \epsilon_2 \ . \tag{10.39}$$

We can now use this result to bound the errors in $q(\mathbf{r},t)$. The error in $q(\mathbf{r},t)$ over one time-step from using the approximate potential $\tilde{v}_{ks}(\mathbf{r},t)$ from the previous time-step is:

$$\|[U_{\delta t}\hat{\rho}_C U_{\delta t}^\dagger - \tilde{U}_{\delta t}\hat{\rho}_C \tilde{U}_{\delta t}^\dagger][\sum_i \hat{q}_i]\|_1 \tag{10.40}$$

$$= \|[(U_{\delta t} - \tilde{U}_{\delta t})\hat{\rho}_C U_{\delta t}^\dagger + U_{\delta t}\hat{\rho}_C (U_{\delta t} - \tilde{U}_{\delta t})^\dagger][\sum_i \hat{q}_i]\|_1 \tag{10.41}$$

$$\leq 2\|(U_{\delta t} - \tilde{U}_{\delta t})\hat{\rho}_C\|_1 \|[\sum_i \hat{q}_i]\|_1 \ . \tag{10.42}$$

The first term has already been bounded, and so we simply have for the error in the $q(\mathbf{r},t)$ due to the approximate potential, ϵ_3:

$$\epsilon_3 = n\,\delta t \|\delta Q\|_1 \|\hat{q}\|_1. \tag{10.43}$$

The error ϵ_4 due to the time-step is obtained from Eq. 10.17 applied to the Kohn-Sham system:

$$\epsilon_4 = 2TK_{KS}\delta t \|\hat{q}\|_1, \tag{10.44}$$

where K_{KS} is the Lipschitz constant for the Kohn-Sham potential. It can readily be shown from the VL construction that K_{KS} is finite provided K, the Lipschitz constant of v_{ext} is finite as well. So, the total error in $q(\mathbf{r},t)$ for a given time-step is

$$\|\hat{q}\|_1 \delta t(2TK_{KS} + n\|\delta Q\|_1\|). \tag{10.45}$$

For the entire interval, we have

$$(\frac{T}{\delta t})\|\hat{q}\|_1 \delta t(2TK_{KS} + n\|\delta Q\|_1\|) = \|\hat{q}\|_1 T(2TK_{KS} + n\|\delta Q\|_1\|). \tag{10.46}$$

Therefore the error is bounded and grows at most quadratically in T, provided the one-norm of $\hat{q}$ is bounded. If one solves the VL construction on a finite grid in real-space, the one- norm scales as $\|\hat{q}\|_1 \sim \frac{1}{h^2}$, where h is the grid spacing. Thus although it diverges in the continuum limit, this divergence is only polynomial.

10.4 Conclusion and outlook

To summarize, we have demonstrated polynomial bounds at all stages in the quantum algorithm needed to obtain the Kohn-Sham potential given the initial states $|\psi(0)\rangle$, $|\Phi(0)\rangle$ and $v_{ext}(t)$ as inputs. We have shown that all errors scale only polynomially in the number of time-steps N, the time-step size δt (or equivalently the total evolution time $T = N\delta t$), the number of electrons n, the volume of the bounding box V and the number of grid points $\frac{V}{h^3}$. Therefore, the algorithm is efficient and since it requires a quantum computer to perform, the computational problem it solves, "TDDFT" is in the complexity class BQP.

To prove that TDDFT is BQP Complete, we would not only need to prove that it is in BQP as we have done above, but that it is also BPQ Hard, i.e. given the exact Kohn-Sham potential for any electronic system from the algorithm we have presented, one could solve using a classical computer, any problem that could be solved on a quantum computer. This seems plausible, since many quantum computing devices are based on interacting electronic systems (atoms, molecules, quantum dots etc.) and given an efficient algorithm for the exact Kohn-Sham potential, one could efficiently simulate the density evolution of any electronic system. However, a rigorous proof of

this direction remains a work in progress and will hopefully be presented in a future PhD thesis of another student of the Aspuru-Guzik group.

Chapter 11

Concluding remarks

The goal of this thesis has been to explore the fundamentals of TDDFT from a new perspective and extend the basic theory to a new class of problems: The theory of open quantum systems and quantum computation and information theory. Since TDDFT has had such success as an applied method in computational chemistry, my hope is that the work in this thesis will give rise to new applications in these fields as well. Of course, there are several steps that must be taken before the basic theory can be directly applied.

For applications of OQS-TDDFT to become widespread, the first step is to implement the methods of this thesis in existing computational codes. For the real-time closed system Kohn Sham scheme presented in Chapters 4 and 5, the Octopus [152] package is already set up to perform real-time propagation and could be modified to include a routine using a bath functional with little additional effort. Implementation of the algorithm presented in Chapter 6 for solving the open systems Casida equations is more involved, as the exchange-correlation kernel is frequency-dependent and imag-

inary. Casida solvers in existing codes are generally not set up to solve the required complex-valued and non-linear eigenvalue problem, but it can certainly be done with modest effort. Chapter 7 represents a success in implementation, as we were able to explicitly propagate a Kohn-Sham master equation and the code developed for this is a valuable tool.

A second step in applying OQS-TDDFT will be to develop better functionals, which has remained a challenge in ordinary TDDFT as well. This is especially important for the real-time closed system Kohn-Sham scheme, where the functional must account for all of the environmental effects. As we have seen in Chapter 5, it is not difficult to write down a functional such as the MBF, that simply relaxes the system to equilibrium on the correct timescale. However, I have learned that developing sophisticated functionals that capture subtle (even Markovian) system-bath correlations is going to be challenging. As a result, I think it is more feasible to use an open Kohn-Sham system with a Kohn-Sham master equation. In this case, as we have seen in Chapters 6 and 7, although the true functional has complicated frequency dependence, one can get nice results using existing adiabatic functionals. It might also be valuable to develop a framework for treating open quantum systems within time-dependent density matrix functional theory (TDDMFT), and this is something I hope to explore further.

Whether the direct application of TDDFT to quantum computing will be useful remains an open question, as experimentalists have yet to build large-scale quantum computing devices. However, even from a theoretical standpoint, the work of Chapters 9 and 10 fill in a missing piece of the puzzle in understanding the connections

between computational methods in electronic structure and quantum information theory. Most work in this field thus far has focused on wavefunction and density matrix based methods, so it is important to see where density functional theory fits into this picture.

Most importantly, I have learned a great deal during the struggles and successes of my Ph.D., which are documented in the work presented in this thesis. By exploring the connections between TDDFT, open quantum systems and quantum computation, I have had the opportunity to learn about these three very different fields. I am perhaps most happy with the breadth of different, yet related topics covered in this thesis. In this way, my research has definitely been an ideal learning experience.

References

[1] S. Aaronson. Computational complexity: Why quantum chemistry is hard. *Nat. Phys.*, **5**, 707 (2009).

[2] D. Abramavicius and S. Mukamel. Quartic interband exciton couplings in pump-probe spectroscopy of light harvesting complexes. *J. Phys. Chem. B*, **108**, 10295 (2004).

[3] C. Adamo and V. Barone. Accurate excitation energies from time-dependent density functional theory: assessing the pbe0 model for organic free radicals. *Chem. Phys. Lett.*, **314**, 152 (1999).

[4] G. S. Agarwal. Master-equation approach to spontaneous emission. *Phys. Rev. A*, **2**, 2038 (1970).

[5] G. S. Agarwal. Master-equation approach to spontaneous emission. ii. emission from a system of harmonic oscillators. *Phys. Rev. A*, **3**, 1783 (1971).

[6] G. S. Agarwal. Master-equation approach to spontaneous emission. iii. many-body aspects of emission from two-level atoms and the effect of inhomogeneous broadening. *Phys. Rev. A*, **4**, 1791 (1971).

[7] D. Aharonov, W. van Dam, J. Kempe, Z. Landau, S. Lloyd, and O. Regev. Adiabatic quantum computation is equivalent to standard quantum computation. *SIAM J. Comp.*, **37**, 166 (2007).

[8] T. Akama and H. Nakai. Short-time fourier transform analysis of real-time time-dependent hartree fock and time-dependent density functional theory calculations with gaussian basis functions. *J. Chem. Phys.*, **132**, 054104 (2010).

[9] F. C. Alcaraz and K. Capelle. Density functional formulations for quantum chains. *Phys. Rev. B*, **76**, 035109 (2007).

[10] I. D. Amico and G. Vignale. Exact exchange-correlation potential for a time-dependent two electron system. *Phys. Rev. B.*, **59**, 7876 (1999).

[11] T. Ando. Inter-subband optical-absorption in space-charge layers on semiconductor surfaces. *Z. Phys. B*, **26**, 263 (1977).

[12] T. Ando. Inter-subband optical transitions in a surface space-charge layer. *Solid State Commun.*, **21**, 133 (1977).

[13] X. Andrade, S. Botti, M. Marques, and A. Rubio. Time-dependent density functional theory scheme for efficient calculations of dynamic (hyper)polarizabilities. *J. Chem. Phys.*, **126**, 184106 (2007).

[14] H. Appel, E. K. U. Gross, and K. Burke. Excitations in time-dependent density-functional theory. *Phys. Rev. Lett.*, **90**, 043005 (2003).

[15] H. Appel, E. K. U. Gross, and K. Burke. Double-pole approximation in time-dependent density functional theory. *Int. J. Quantum Chem.*, **106**, 2840 (2006).

[16] H. Appel and M. D. Ventra. Stochastic quantum molecular dynamics. *Phys. Rev. B*, **80**, 212303 (2009).

[17] A. Aspuru-Guzik, A. D. Dutoi, P. Love, and M. Head-Gordon. Simulated quantum computation of molecular energies. *Science*, **309**, 1704 (2005).

[18] D. Bacon, J. Kempe, D. A. Lidar, and K. B. Whaley. Universal fault-tolerant quantum computation on decoherence-free subspaces. *Phys. Rev. Lett.*, **85**, 1758 (2000).

[19] R. Baer. On the mapping of time-dependent densities onto potentials in quantum mechanics. *J. Chem. Phys.*, **128**, 044103 (2008).

[20] R. Bauernschmitt and R. Ahlrichs. Treatment of electronic excitations within the adiabatic approximation of time dependent density functional theory. *Chem. Phys. Lett.*, **256**, 454 (1996).

[21] A. D. Becke. Density functional thermochemistry. iii. the role of exact exchange. *J. Chem. Phys.*, **98**, 5648 (1993).

[22] W. J. D. Beenken, M. Dahlbom, P. Kjellberg, and T. Pullerits. Potential surfaces and delocalization of excitons in dimers. *J. Chem. Phys.*, **117**, 5810 (2002).

[23] W. J. D. Beenken and T. Pullerits. Excitonic coupling in polythiophenes: Comparison of different calculation methods. *J. Chem. Phys.*, **120**, 2490 (2004).

[24] S. C. Benjamin and S. Bose. Quantum computing with an always-on heisenberg interaction. *Phys. Rev. Lett.*, **90**, 247901 (2003).

[25] S. C. Benjamin and S. Bose. Quantum computing in arrays coupled by always-on interactions. *Phys. Rev. A*, **70**, 032314 (2004).

[26] H. A. Bethe. The electromagnetic shift of energy levels. *Phys. Rev.*, **72**, 339 (1947).

[27] J. D. Biggs and J. A. Cina. Calculations of nonlinear wave-packet interferometry signals in the pump-probe limit as tests for vibrational control over electronic excitation transfer. *J. Chem. Phys.*, **131**, 224302 (2009).

[28] A. Bodor and L. Diosi. Conserved current in markovian open-quantum systems. *Phys. Rev. A*, **73**, 064101 (2006).

[29] N. N. Bogoliubov. Kinetic equations. *J. Phys. USSR*, **10**, 265 (1946).

[30] A. O. Bolivar. Quantization of non-hamiltonian physical systems. *Phys. Rev. A*, **58**, 4330 (1998).

[31] M. Born and H. S. Green. A general kinetic theory of liquids i. the molecular distribution functions. *Proc. Roy. Soc. A*, **188**, 10 (1946).

[32] M. Born and K. Huang. *Dynamical Theory of Crystal Lattices*. Oxford University Press, 1998.

[33] S. Bose. Quantum communication through an unmodulated spin chain. *Phys. Rev. Lett.*, **91**, 207901 (2003).

[34] M. J. Bremner, C. M. Dawson, J. L. Dodd, A. Gilchrist, A. W. Harrow, D. Mortimer, M. A. Nielsen, and T. J. Osborne. Practical scheme for quantum computation with any two-qubit entangling gate. *Phys. Rev. Lett.*, **89**, 247902 (2002).

[35] S. C. Brenner and L. R. Scott. The mathematical theory of finite elements. *Springer - Texts in Applied Mathematics* (2008).

[36] H. Breuer and F. Petruccione. The theory of open quantum systems. *Oxford University Press, USA* (2002).

[37] K. Burke. Exact conditions. *in* Springer Lecture Notes in Physics, **706**, 181 (2006).

[38] K. Burke, R. Car, and R. Gebauer. Density functional theory of the electrical conductivity of molecular devices. *Phys. Rev. Lett.*, **94**, 146803 (2005).

[39] K. Burke, M. Petersilka, and E. K. U. Gross. A hybrid functional for the exchange-correlation kernel in time-dependent density functional theory. *Recent Advances in Density Functional Methods, vol. III, eds. V. Varone, P. Fantucci, A. Bencini*, World Scientific (2002).

[40] K. Burke, J. Werschnik, and E. K. U. Gross. Time-dependent density functional theory: Past, present, and future. *The Journal of Chemical Physics*, **123**, 062206 (2005).

[41] O. Butriy, H. Ebadi, P. L. de Boeij, R. van Leeuwen, and E. K. U. Gross. Multicomponent density-functional theory for time-dependent systems. *Phys. Rev. A*, **76**, 052514 (2007).

[42] M. E. Casida. Time-dependent density functional response theory for molecules. *Recent Developments and Applications in Density Functional Theory, ed. J.M. Seminario*, Elsevier, Amsterdam (1996).

[43] A. Castro, H. Appel, M. Oliveira, C. Rozzi, X. Andrade, F. Lorenzen, M. Marques, E. K. U. Gross, and A. Rubio. Octopus: A tool for the application of time-dependent density functional theory. *Phys. Stat. Sol. B*, **243**, 2465 (2006).

[44] M. Ceotto, S. Atahan, G. F. Tantardini, and A. Aspuru-Guzik. Multiple coherent states for first-principles semiclassical initial value representation molecular dynamics. *J. Chem. Phys*, **130**, 234113 (2009).

[45] D. M. Ceperley and B. J. Alder. Ground state of the electron gas by a stochastic method. *Phys. Rev. Lett.*, **45**, 566 (1980).

[46] J.-D. Chai and M. Head-Gordon. Systematic optimization of long-range corrected hybrid density functionals. *J. Chem. Phys.*, **128**, 084106 (2008).

[47] C. T. Chapman, W. Liang, and X. Li. Open-system electronic dynamics and thermalized electronic structure. *J. Chem. Phys.*, **134**, 024118 (2011).

[48] C. Cohen-Tannoudji, J. Dupont-Roc, and G. Grynberg. Atom-photon interactions. *Wiley-VCH, Weinheim* (2004).

[49] E. U. Condon. The theory of complex spectra. *Phys. Rev.*, **36**, 1121 (1930).

[50] C. F. Craig, W. R. Duncan, and O. V. Prezhdo. Trajectory surface hopping in the time-dependent kohn-sham approach for electron-nuclear dynamics. *Phys. Rev. Lett.*, **95**, 163001 (2005).

[51] R. D'Agosta and M. D. Ventra. Stochastic time-dependent current-density-functional theory: A functional theory of open quantum systems. *Phys. Rev. B*, **78**, 165105 (2009).

[52] R. D'Agosta and G. Vignale. Relaxation in time-dependent current-density-functional theory. *Phys. Rev. Lett.*, **96**, 016405 (2006).

[53] E. B. Davies and H. Spohn. Open quantum systems with time-dependent hamiltonians and their linear response. *J. Stat. Phys.*, **19**, 511 (1978).

[54] J. M. Dawlaty, D. I. G. Bennett, V. M. Huxter, and G. R. Fleming. Mapping the spatial overlap of excitons in a photosynthetic complex via coherent nonlinear frequency generation. *J. Chem. Phys.*, **135**, 044201 (2011).

[55] P. de Bree and D. A. Wiersma. Application of redfield theory to optical dephasing and line shape of electronic transitions in molecular mixed crystals. *J. Chem. Phys.*, **70**, 790 (1979).

[56] D. de Falco and D. Tamascelli. Time-dependent density functional theory for open spin chains. *Phys. Rev. A*, **85**, 022341 (2012).

[57] Z. Deng and S. Mukamel. Non-markvian dephasing of two-level resonance flourescence in a strong radiation field. *Phys. Rev. A*, **29**, 1914 (1984).

[58] D. Deutsch and R. Jozsa. Rapid solutions of problems by quantum computation. *Proc. R. Soc. London A*, **439**, 553 (1992).

[59] D. P. DiVincenzo, D. Bacon, J. Kempe, G. Burkard, and K. B. Whaley. Universal quantum computation with the exchange interaction. *Nature*, **408**, 339 (2000).

[60] J. L. Dodd, M. A. Nielsen, M. J. Bremner, and R. T. Thew. Universal quantum computation and simulation using any entangling hamiltonian and local unitaries. *Phys. Rev. A*, **65**, 040301(R) (2002).

[61] A. Dreuw, J. L. Weisman, and M. Head-Gordon. Long-range charge-transfer excited states in time-dependent density functional theory require non-local exchange. *J. Chem. Phys.*, **119**, 2943 (2000).

[62] E. Farhi, J. Goldstone, S. Gutmann, and M. Sipser. Quantum computation by adiabatic evolution. arXiv:quant-ph/0001106v1 (2000).

[63] A. L. Fetter and J. D. Walecka. Quantum theory of many-particle systems. *McGraw-Hill, New York* (1971).

[64] R. P. Feynman. Simulating physics with computers. *Int. J. Theo. Phys.*, **21**, 467 (1982).

[65] R. P. Feynman and F. L. Vernon. The theory of a general quantum system interacting with a linear dissipative system. *Ann. Phys.*, **24**, 118 (1963).

[66] C. Filippi, C. J. Umrigar, and M. Taut. Comparison of exact and approximate density functionals for an exactly soluble model. *J. Chem. Phys.*, **100**, 1290 (1994).

[67] F. Furche and R. Ahlrichs. Adiabatic time-dependent density functional methods for excited state properties. *J. Chem. Phys.*, **117**, 7433 (2002).

[68] F. Gaitan and F. Nori. Density functional theory and quantum computation. *Phys. Rev. B*, **79**, 205117 (2009).

[69] R. Gebauer and R. Car. Current in open quantum systems. *Phys. Rev. Lett.*, **93**, 160404 (2004).

[70] R. Gebauer, S. Piccinin, and R. Car. Quantum collision current in electronic circuits. *ChemPhysChem.*, **6**, 1727 (2005).

[71] G. F. Giuliani and G. Vignale. Quantum theory of the electron liquid. *Cambridge University Press* (2005).

[72] X. Gonze and M. Scheffler. Exchange and correlation kernels at the resonance frequency: Implications for excitation energies in density-functional theory. *Phys. Rev. Lett.*, **82**, 4416 (1999).

[73] V. Gorini, A. Kossakowski, and E. Sudarshan. Completely positive dynamical semigroups of n-level systems. *J. Math. Phys.*, **17**, 821 (1976).

[74] A. Görling. Density-functional theory for excited states. *Phys. Rev. A*, **54**, 3912 (1996).

[75] A. Görling. Time-dependent kohn-sham formalism. *Phys. Rev. A*, **55**, 2630 (1997).

[76] A. Görling. Exact exchange-correlation kernel for dynamic response properties and excitation energies in density-functional theory. *Phys. Rev. A*, **57**, 3433 (1998).

[77] A. Görling and M. Levy. Correlation-energy functional and its high-density limit obtained from a coupling-constant perturbation expansion. *Phys. Rev. B*, **47**, 13105 (1993).

[78] A. Görling and M. Levy. Exact kohn-sham scheme based on perturbation theory. *Phys. Rev. A*, **50**, 196 (1994).

[79] N. Gottfried and W. Kaiser. Redistribution of vibrational energy in naphthalene and anthracene studied in liquid solution. *Chem. Phys. Lett.*, **101**, 331 (1983).

[80] D. Grimbert and S. Mukamel. Franck condon approach to collisional dephasing of spectral lines in liquids. *J. Chem. Phys.*, **76**, 834 (1982).

[81] S. Grimme. Semiempirical gga-type density functional constructed with a long-range dispersion correction. *J. Comp. Chem.*, **27**, 1787 (2006).

[82] O. V. Gritsenko, S. J. A. van Gisbergen, A. Grling, and E. J. Baerends. Excitation energies of dissociating h2: A problematic case for the adiabatic approximation of time-dependent density functional theory. *J. Chem. Phys.*, **113**, 8478 (2000).

[83] E. K. U. Gross, J. F. Dobson, and M. Petersilka. Density functional theory of time-dependent phenomena. *in* Density Functional Theory*, ed. R. F. Nalewajski, Springer-Verlag Berlin Heidelberg*, **181**, 81 (1996).

[84] E. K. U. Gross and W. Kohn. Local density-functional theory of frequency-dependent linear response. *Phys. Rev. Lett.*, **55**, 2850 (1985).

[85] J. Guthmuller, F. Zutterman, and B. Champagne. Multimode simulation of dimer absorption spectra from first principles calculations: Application to the 3,4,9,10-perylenetetracarboxylic diimide dimer. *J. Chem. Phys.*, **131**, 154302 (2009).

[86] F. Haas. The damped pinney equation and its applications to dissipative quantum mechanics. *Phys. Scripta*, **81**, 025004 (2010).

[87] M. Head-Gordon, M. Oumi, and D. Maurice. Quasidegenerate second-order perturbation corrections to single excitation configuration interaction. *Mol. Phys.*, **96**, 593 (1999).

[88] S. Heinrich. Quantum integration in sobolev classes. arXiv:quant-ph/0112153 (2001).

[89] D. J. Heinzen and M. S. Feld. Vacuum radiative level shift and spontaneous-emission linewidth of an atom in an optical resonator. *Phys. Rev. Lett.*, **59**, 2623 (1987).

[90] M. Hellgren and U. von Barth. Exact-exchange kernel of time-dependent density functional theory: Frequency dependence and photoabsorption spectra of atoms. *J. Chem. Phys.*, **131**, 044110 (2009).

[91] P. Hessler, N. T. Maitra, and K. Burke. Correlation in time-dependent density-functional theory. *J. Chem. Phys.*, **1**, 72 (2002).

[92] P. Hessler, J. Park, and K. Burke. Several theorems in time-dependent density functional theory. *Phys. Rev. Lett.*, **82**, 378 (1999).

[93] S. Hirata and M. Head-Gordon. Time-dependent density functional theory within the tamm-dancoff approximation. *Chem. Phys. Lett.*, **314**, 291 (1999).

[94] P. Hohenberg and W. Kohn. Inhomogeneous electron gas. *Phys. Rev.*, **136**, B864 (1964).

[95] T. Holstein. Studies of polaron motion-part i: The molecular-crystal model. *Ann. Phys.*, **8**, 325 (1959).

[96] C.-P. Hsu. The electronic couplings in electron transfer and excitation energy transfer. *Acc. Chem. Research*, **42**, 509 (2009).

[97] P. Huo and D. F. Coker. Iterative linearized density matrix propagation for modeling coherent excitation energy transfer in photosynthetic light harvesting. *J. Chem. Phys.*, **133**, 184108 (2010).

[98] A. Ishizaki and G. R. Fleming. On the adequacy of the Redfield equation and related approaches to the study of quantum dynamics in electronic energy transfer. *J. Chem. Phys.*, **130**, 234110 (2009).

[99] A. Ishizaki and G. R. Fleming. Unified treatment of quantum coherent and incoherent hopping dynamics in electronic energy transfer: Reduced hierarchy equation approach. *J. Chem. Phys.*, **130**, 234111 (2009).

[100] A. Ishizaki and Y. Tanimura. Multidimensional vibrational spectroscopy for tunneling processes in a dissipative environment. *J. Chem. Phys.*, **123**, 014503 (2005).

[101] S. S. Iyengar and J. Jakowski. Quantum wave packet ab initio molecular dynamics: An approach to study quantum dynamics in large systems. *J. Chem. Phys*, **122**, 114105 (2005).

[102] S. Jang. Theory of multichromophoric coherent resonance energy transfer: A polaronic quantum master equation approach. *J. Chem. Phys.*, **135**, 034105 (2011).

[103] S. Jang, Y.-C. Cheng, D. R. Reichman, and J. D. Eaves. Theory of coherent resonance energy transfer. *J. Chem. Phys.*, **129**, 101104 (2008).

[104] C. Johnson. Numerical solution of partial differential equations by the finite element method. *Cambridge University Press* (1987).

[105] H. Kamisaka, S. V. Kilina, K. Yamashita, and O. V. Prezhdo. Ultrafast vibrationally-induced dephasing of electronic excitations in pbse quantum dots. *Nano Lett.*, **6**, 2295 (2006).

[106] D. Karlsson, A. Privitera, and C. Verdozzi. Time-dependent density-functional theory meets dynamical mean-field theory: Real-time dynamics for the 3d hubbard model. *Phys. Rev. Lett.*, **106**, 116401 (2011).

[107] J. Kempe, A. Kitaev, and O. Regev. The complexity of the local hamiltonian problem. *SIAM J. Computing*, **35**, 1070 (2006).

[108] D. S. Kilin and D. A. Micha. Relaxation of photoexcited electrons at a nanostructured si(111) surface. *J. Phys. Chem. Lett.*, **1**, 1073 (2010).

[109] D. S. Kilin and D. A. Micha. Modeling the photovoltage of doped si surfaces. *J. Phys. Chem. C*, **115**, 770 (2011).

[110] J. G. Kirkwood. The statistical mechanical theory of transport processes i. general theory. *J. Chem. Phys.*, **14**, 180 (1946).

[111] R. Kishi, M. Nakano, T. Minami, H. Fukui, H. Nagai, K. Yoneda, and H. Takahashi. Theoretical study on exciton recurrence motion in anthracene dimer using the ab initio mo-ci based quantum master equation approach. *J. Phys. Chem. A*, **113**, 5455 (2009).

[112] P. Kjellberg and T. Pullerits. Three-pulse photon echo of an excitonic dimer modeled via redfield theory. *J. Chem. Phys.*, **124**, 024106 (2006).

[113] W. Koch and M. C. Holthausen. A chemist's guide to density functional theory. *Wiley-VCH, Weinheim* (2001).

[114] D. Kohen, C. C. Marston, and D. J. Tannor. Phase space approach to theories of quantum dissipation. *J. Chem. Phys.*, **107**, 5236 (1997).

[115] W. Kohn and L. J. Sham. Self-consistent equations including exchange and correlation effects. *Phys. Rev.*, **140**, A1133 (1965).

[116] I. Kondov, H. Wang, and M. Thoss. Computational study of titanium (IV) complexes with organic chromophores. *Int. J. Quant. Chem.*, **106**, 1291 (2006).

[117] A. Kossakowski. On quantum statistical mechanics of non-hamiltonian systems. *Rep. Math. Phys.*, **3**, 247 (1972).

[118] M. D. Kostin. On the schrödinger-langevin equation. *J. Chem. Phys.*, **57**, 3589 (1972).

[119] M. D. Kostin. Friction and dissipative phenomena in quantum mechanics. *J. Stat. Phys.*, **12**, 145 (1975).

[120] A. J. Krueger and N. T. Maitra. Autoionizing resonances in time-dependent density functional theory. *Phys. Chem. Chem. Phys.*, **11**, 4655 (2009).

[121] S. Kurth and G. Stefanucci. Time-dependent bond-current functional theory for lattice hamiltonians: Fundamental theorem and application to electron transport. *Chem. Phys.*, **391**, 164 (2011).

[122] Y. Kurzweil and R. Baer. Generic galilean-invariant exchange-correlation functionals with quantum memory. *Phys. Rev. B.*, **72**, 035106 (2005).

[123] A. S. Leathers and D. A. Micha. Density matrix treatment of the nonmarkovian dissipative dynamics of adsorbates on metal surfaces. *J. Phys. Chem. A*, **110**, 749 (2006).

[124] H. Lehmann. Uber eigenschaften von ausbreitungsfunktionen und renormierungskonstanten quantisierter felder. *Nuovo Cimento*, **11**, 342 (1954).

[125] X. Li, J. C. Tully, H. B. Schlegel, and M. J. Frisch. Ab initio Ehrenfest dynamics. *J. Chem. Phys.*, **123**, 084106 (2005).

[126] Y. Li and C. A. Ullrich. Time-dependent v-representability on lattice systems. *J. Chem. Phys.*, **129**, 044105 (2008).

[127] W. Liang, C. T. Chapman, and X. Li. Efficient first-principles electronic dynamics. *J. Chem. Phys.*, **134**, 184102 (2011).

[128] W. Liang, C. M. Isborn, A. Lindsay, X. Li, S. M. Smith, and R. J. Levis. Time-dependent density functional theory calculations of ehrenfest dynamics of laser controlled dissociation of no+: Pulse length and sequential multiple single-photon processes. *J. Phys. Chem. A*, **114**, 6201 (2010).

[129] D. A. Lidar and L. A. Wu. Reducing constraints on quantum computer design by encoded selective recoupling. *Phys. Rev. Lett.*, **88**, 017905 (2001).

[130] N. A. Lima, L. N. Olivera, and K. Capelle. Density-functional study of the mott gap in the hubbard model. *Europhys. Lett.*, **60**, 601 (2002).

[131] G. Lindblad. On the generators of quantum dynamical semigroups. *Commun. Math. Phys.*, **48**, 199 (1976).

[132] O. Linden and V. May. Quantum master equation, lindblad-type of dissipation and temperature dependent monte carlo wave-function propagation. *Eur. Phys. J. D*, **12**, 473 (2000).

[133] W. Liu, V. Settels, P. H. P. Harbach, A. Dreuw, R. F. Fink, and B. Engels. Assessment of td-dft- and td-hf-based approaches for the prediction of exciton coupling parameters, potential energy curves, and electronic characters of electronically excited aggregates. *J. Comp. Chem.*, **32**, 1971 (2011).

[134] S. Lloyd. Almost any quantum logic gate is universal. *Phys. Rev. Lett.*, **75**, 346 (1995).

[135] S. Lloyd. Universal quantum simulators. *Science*, **273**, 1073 (1996).

[136] S. Lloyd and D. Abrams. Simulation of many-body fermi systems on a universal quantum computer. *Phys. Rev. Lett.*, **79**, 2586 (1997).

[137] S. Lopez-Lopez and M. Nest. Analysis of the continuous-configuration time-dependent self-consistent field method applied to system-bath dynamics. *J. Chem. Phys.*, **132**, 104103 (2010).

[138] Y. K. Lui, M. Christandl, and F. Verstraete. Quantum computational complexity of the n-representability problem: Qma complete. *Phys. Rev. Lett.*, **98**, 110503 (2007).

[139] M. Madjet, A. Abdurahman, and T. Renger. Intermolecular coulomb couplings from ab initio electrostatic potentials: application to optical transitions of strongly coupled pigments in photosynthetic antennae and reaction centers. *J. Phys. Chem. B*, **110**, 17268 (2006).

[140] N. T. Maitra. Memory formulas for perturbations in time-dependent density functional theory. *Int. Journal of Quant. Chem.*, **102**, 573 (2005).

[141] N. T. Maitra. Undoing static correlation: Long-range charge transfer in time-dependent density-functional theory. *J. Chem. Phys.*, **122**, 234104 (2005).

[142] N. T. Maitra and K. Burke. Demonstration of initial-state dependence in time-dependent density-functional theory. *Phys. Rev. A*, **63**, 042501 (2002).

[143] N. T. Maitra, K. Burke, H. Appel, E. K. U. Gross, and R. van Leeuwen. Ten topical questions in time-dependent density functional theory. *Rev. Mod. Quant. Chem.*, A Celebration of the Contributions of R.G. Parr, ed. K.D. Sen (2002).

[144] N. T. Maitra, K. Burke, and C. Woodward. Memory in time-dependent density functional theory. *Phys. Rev. Lett.*, **89**, 023002 (2002).

[145] N. T. Maitra and D. G. Tempel. Long-range excitations in time-dependent density functional theory. *J. Chem. Phys.*, **125**, 184111 (2006).

[146] N. T. Maitra, T. N. Todorov, C. Woodward, and K. Burke. Density-potential mapping in time-dependent density-functional theory. *Phys. Rev. A*, **81**, 042525 (2010).

[147] N. T. Maitra, F. Zhang, R. J. Cave, and K. Burke. Double excitations within time-dependent density functional theory linear response. *J. Chem. Phys.*, **120**, 5932 (2004).

[148] Y. Makhlin, G. Schön, and A. Shnirman. Josephson-junction qubits with controlled couplings. *Nature*, **398**, 305 (1999).

[149] N. Makri and W. H. Miller. Time-dependent self-consistent field (tdscf) approximation for a reaction coordinate coupled to a harmonic bath: Single and multiple configuration treatments. *J. Chem. Phys.*, **87**, 5781 (1987).

[150] M. P. Marder. Condensed matter physics. *Wiley-VCH, Weinheim* (2000).

[151] C. J. Margulis and D. F. Coker. Nonadiabatic molecular dynamics simulations of the photofragmentation and geminate recombination dynamics in size-selected i2(co2)n cluster ions. *J. Chem. Phys.*, **110**, 5677 (1999).

[152] M. Marques, A. Castro, G. F. Bertsch, and A. Rubio. Octopus: A first-principles tool for excited electron-ion dynamics. *Comput. Phys. Commun.*, **151**, 60 (2003).

[153] M. Marques and E. K. U. Gross. Time-dependent density functional theory. *Annual Review of Physical Chemistry*, **55**, 427 (2004).

[154] R. Martinazzo, M. Nest, P. Saalfrank, and G. F. Tantardini. A local coherent-state approximation to system-bath quantum dynamics. *J. Chem. Phys.*, **125**, 194102 (2006).

[155] A. Matro and J. Cina. Theoretical study of time-resolved fluorescence anisotropy from coupled chromophore pairs. *J. Phys. Chem.*, **99**, 2568 (1995).

[156] V. May and O. Kuhn. Charge and energy transfer dynamics in molecular systems. *Wiley-VCH, Weinheim* (2004).

[157] C. Meier and D. Tannor. Non-markovian evolution of the density operator in the presence of strong laser fields. *J. Chem. Phys.*, **111**, 3365 (1999).

[158] N. D. Mermin. Thermal properties of the inhomogeneous electron gas. *Phys. Rev.*, **137**, A1441 (1965).

[159] D. A. Micha. Time-dependent many-electron treatment of electronic energy and charge transfer in atomic collisions. *J. Phys. Chem. A*, **103**, 7562 (1999).

[160] R. Mitric, J. Petersen, and V. Bonacic-Koutecky. Laser-field-induced surface-hopping method for the simulation and control of ultrafast photodynamics. *Phys. Rev. A*, **79**, 053416 (2009).

[161] S. Mukamel. Non-markovian theory of molecular relaxation. i. vibrational relaxation and dephasing in condensed phases. *Chem. Phys.*, **37**, 33 (1979).

[162] S. Mukamel. Principles of nonlinear optical spectroscopy. *Oxford University Press, New York* (1995).

[163] A. Munoz-Losa, C. Curutchet, I. F. Galvan, and B. Mennucci. Quantum mechanical methods applied to excitation energy transfer: A comparative analysis on excitation energies and electronic couplings. *J. Chem. Phys.*, **129**, 034104 (2008).

[164] S. Nakajima. On quantum theory of transport phenomena — steady diffusion. *Rep. Prog. Phys.*, **20**, 948 (1958).

[165] F. Neese. *ORCA – an ab initio, Density Functional and Semiempirical program package, Version 2.6.* University of Bonn, 2008.

[166] F. Neese, F. Wennmohs, A. Hansen, and U. Becker. Efficient, approximate and parallel hartree-fock and hybrid dft calculations. a chain-of-spheres algorithm for the hartree-fock exchange. *Chem. Phys.*, **356**, 98 (2009).

[167] D. Neuhauser and K. Lopata. Quantum drude friction for time-dependent density functional theory. *J. Chem. Phys.*, **129**, 134106 (2008).

[168] T. K. Ng and K. S. Singwi. Time-dependent density-functional theory in the linear-response regime. *Phys. Rev. Lett.*, **59**, 2627 (1987).

[169] M. A. Nielsen and I. L. Chuang. Quantum computation and quantum information. *Cambridge University Press, New York* (2011).

[170] A. Nitzan. Chemical dynamics in condensed phases. *Oxford University Press, Oxford* (2006).

[171] A. Nitzan, S. Mukamel, and J. Jortner. Some features of vibrational relaxation of a diatomic molecule in a dense medium. *J. Chem. Phys.*, **60**, 3929 (1974).

[172] T. Pacher, L. S. Cederbaum, and H. Köppel. *Adiabatic and Quasidiabatic States in a Gauge Theoretical Framework.* Advances in Chemical Physics. John Wiley and Sons, Inc., 2007.

[173] J. Parkhill, D. G. Tempel, and A. Aspuru-Guzik. Exciton coherence lifetimes from electronic structure. *J. Chem. Phys.*, **136**, 104510 (2012).

[174] M. J. G. Peach, P. Benfield, T. Helgaker, and D. J. Tozer. Excitation energies in density functional theory: An evaluation and a diagnostic test. *J. Chem. Phys*, **128**, 044118 (2008).

[175] J. P. Perdew, K. Burke, and M. Ernzerhof. Generalized gradient approximation made simple. *Phys. Rev. Lett.*, **77**, 3865 (1996).

[176] J. P. Perdew and Y. Wang. Accurate and simple analytic representation of the electron-gas correlation energy. *Phys. Rev. B*, **45**, 13244 (1992).

[177] J. P. Perdew and A. Zunger. Self-interaction correction to density-functional approximations for many-electron systems. *Phys. Rev. B.*, **23**, 5048 (1981).

[178] A. Perdomo, L. Vogt, A. Najmaie, and A. Aspuru-Guzik. Engineering directed excitonic energy transfer. *Appl. Phys. Lett.*, **96**, 093114 (2010).

[179] U. Peskin and M. Steinberg. A temperature-dependent schrödinger equation based on a time-dependent self consistent field approximation. *J. Chem. Phys.*, **109**, 704 (1998).

[180] G. Peters and J. H. Wilkinson. The generalized eigenproblem. *J. Num. Analysis*, **7**, 479 (1970).

[181] M. Petersilka, U. J. Gossmann, and E. K. U. Gross. Excitation energies from time-dependent density-functional theory. *Phys. Rev. Lett.*, **76**, 1212 (1996).

[182] M. Petersilka and E. K. U. Gross. Spin-multiplet energies from time-dependent density functional theory. *Int. J. Quantum Chem. Quantum Biol. Symp.*, **30**, 181 (1996).

[183] M. Petersilka, E. K. U. Gross, and K. Burke. Excitation energies from time-dependent density functional theory using exact and approximate potentials. *Int. J. Quantum Chem.*, **80**, 534 (2000).

[184] T. Petrenko and F. Neese. Analysis and prediction of absorption band shapes, fluorescence band shapes, resonance raman intensities, and excitation profiles using the time-dependent theory of electronic spectroscopy. *J. Chem. Phys.*, **127**, 4319 (2007).

[185] D. Pines and P. Nozieres. The theory of quantum liquids. *W. A. Benjamin, New York* (1966).

[186] P. M. Platzman and M. I. Dykman. Quantum computing with electrons floating on liquid helium. *Science*, **284**, 1967 (1999).

[187] J. Pople. Nobel lecture: Quantum chemical models. *Rev. Mod. Phys.*, **71**, 1267 (1999).

[188] A. K. Rajam, I. Raczkowska, and N. Maitra. Semiclassical electron correlation in density-matrix time propagation. *Phys. Rev. Lett.*, **105**, 113002 (2010).

[189] Y. Ralchenko, A. E. Kramida, and J. Reader. Nist atomic spectra database. *National Institute of Standards and Technology, Gaithersburg, MD*, page http://physics.nist.gov/asd3.

[190] D. Rappoport and F. Furche. Analytical time-dependent density functional derivative methods within the ri-j approximation, an approach to excited states of large molecules. *J. Chem. Phys.*, **122**, 064105 (2005).

[191] P. Rebentrost, R. Chakraborty, and A. Aspuru-Guzik. Non-markovian quantum jumps in excitonic energy transfer. *J. Chem. Phys.*, **131**, 184102 (2009).

[192] P. Rebentrost, M. Mohseni, I. Kassal, S. Loyd, and A. Aspuru-Guzik. Environment-assisted quantum transport. *New J. Phys.*, **11**, 033003 (2009).

[193] P. Rebentrost, M. Stopa, and A. Aspuru-Guzik. Förster coupling in nanoparticle excitonic circuits. *Nano Lett.*, **10**, 2849 (2010).

[194] A. G. Redfield. On the theory of relaxation processes. *IBM J. Res. Dev.*, **1**, 19 (1957).

[195] A. G. Redfield. The theory of relaxation processes. *Adv. Magn. Reson.*, **1**, 1 (1965).

[196] T. Renger. Theory of excitation energy transfer: from structure to function. *Photosynthesis Research*, **102**, 471 (2009).

[197] T. Renger and R. Marcus. On the relation of protein dynamics and exciton relaxation in pigmentprotein complexes: An estimation of the spectral density and a theory for the calculation of optical spectra. *J. Chem. Phys.*, **116**, 9997 (2010).

[198] Y. M. Rhee, D. Casanova, and M. Head-Gordon. Performance of quasi-degenerate scaled opposite spin perturbation corrections to single excitation configuration interaction for excited state structures and excitation energies with application to the stokes shift of 9-methyl-9,10-dihydro-9-silaphenanthrene. *J. Phys. Chem. A*, **113**, 10564 (2009).

[199] J. G. Ritschel, W. Roden, T. Strunz, and A. Eisfeld. An efficient method to calculate excitation energy transfer in light harvesting systems. application to the fmo complex. arXiv:1106.5259v1.

[200] A. Ruhe. Algorithms for the nonlinear eigenvalue problem. *J. Num. Analysis*, **10**, 674 (1973).

[201] E. Runge and E. K. U. Gross. Density-functional theory for time-dependent systems. *Phys. Rev. Lett.*, **52**, 997 (1984).

[202] E. Sagvolden, F. Furche, and A. Köhn. Förster energy transfer and davydov splittings in time-dependent density functional theory: Lessons from 2-pyridone dimer. *J. Chem. Theory and Computation*, **5**, 873 (2009).

[203] J. J. Sakurai. Advanced quantum mechanics. *Addison-Wesley Publishing Company* (1967).

[204] F. D. Sala and A. Görling. Efficient localized hartreefock methods as effective exact-exchange kohnsham methods for molecules. *J. Chem. Phys.*, **115**, 5718 (2001).

[205] A. Schäfer, C. Huber, and R. Ahlrichs. Fully optimized contracted gaussian basis sets of triple zeta valence quality for atoms li to kr. *J. Chem. Phys.*, **100**, 5829 (1994).

[206] G. D. Scholes. Long-range resonance energy transfer in molecular systems. *Annu. Rev. Phys. Chem.*, **54**, 57 (2003).

[207] G. D. Scholes, K. P. Ghiggino, A. M. Oliver, and M. N. Paddon-Row. Through-space and through-bond effects on exciton interactions in rigidly linked dinaphthyl molecules. *J. American Chem. Soc.*, **115**, 4345 (1993).

[208] M. Schreiber, M. R. Silva-Junior, S. P. A. Sauer, and W. Thiel. Benchmarks for electronically excited states: Caspt2, cc2, ccsd, and cc3. *J. Chem. Phys.*, **128**, 134110 (2008).

[209] M. Schröeder, U. Kleinekathöfer, and M. Schreiber. Calculation of absorption spectra for light-harvesting systems using non-markovian approaches as well as modified redfield theory. *J. Chem. Phys.*, **124**, 084903 (2006).

[210] M. Schröeder, M. Schreiber, and U. Kleinekathöfer. A time-dependent modified redfield theory for absorption spectra applied to light-harvesting systems. *J. Lumin.*, **125**, 126 (2007).

[211] N. Schuch and F. Verstraete. Computational complexity of interacting electrons and fundamental limitations of density functional theory. *Nature Phys.*, **5**, 732 (2009).

[212] B. Schumacher and M. Westmoreland. Quantum processes, systems, and information. *Cambridge University Press, Cambridge* (2010).

[213] M. A. Sepulveda and E. J. Heller. Semiclassical analysis of hierarchical spectra. *J. Chem. Phys.*, **101**, 8016 (1994).

[214] Y. Shao, L. Fusti-Molnar, Y. Jung, J. Kussmann, C. Oschsenfeld, S. T. Brown, A. T. B. Gilbert, L. V. Slipchenko, S. V. Levchenko, D. P. O'Neill, R. A. DiStasio Jr., R. C. Lochan, T. Want, G. J. O. Beran, N. A. Besley, J. M. Herbert, C. Y. Lin, T. V. Voorhis, S. H. Chien, A. Sodt, R. P. Steele, V. A. Rassolov, P. E. Maslen, P. P. Korambath, R. D. Adamson, B. Austin, J. Baker, E. F. C. Byrd, H. Dachsel, R. J. Doerksen, A. Dreuw, B. D. Dunietz, A. D. Dutoi, T. R. Furlani, S. R. Gwaltney, A. Heyden, S. Hirata, C.-P. Hsu, G. Kedziora, R. Z. Khalliulin, P. Klunzinger, A. M. Lee, M. S. Lee, W. Liang, I. Lotan, N. Nair, B. Peters, E. I. Proynov, P. A. Pieniazek, Y. M. Rhee, J. Ritchie, E. Rosta, C. D. Sherrill, A. C. Simmonett, J. E. Subotnik, H. L. W. III, W. Zhang, A. T. Bell, A. K. Chakraborty, D. M. Chipman, F. J. Keil, A. Warshel, W. J. Hehre, H. F. Schaefer III, J. Kong, A. I. Krylov, P. M. W. Gill, and M. Head-Gordon.

Advances in methods and algorithms in a modern quantum chemistry program package. *Phys. Chem. Chem. Phys.*, **8**, 3172 (2006).

[215] Q. Shi, L. Chen, G. Nan, R.-X. Xu, and Y. Yan. Efficient hierarchical liouville space propagator to quantum dissipative dynamics. *J. Chem. Phys*, **130**, 084105 (2009).

[216] P. W. Shor. Polynomial-time algorithms for prime factorization and discrete logarithms on a quantum computer. *SIAM J. Computing*, **26**, 1484 (1997).

[217] J. C. Slater. The theory of complex spectra. *Phys. Rev.*, **34**, 1293 (1929).

[218] S. L. Sobolev. On a theorem of functional analysis. *Transl. Amer. Math. Soc.*, **34**, 39 (1963).

[219] J. E. Subotnik, R. J. Cave, R. P. Steele, and N. Shenvi. The initial and final states of electron and energy transfer processes: Diabatization as motivated by system-solvent interactions. *J. Chem. Phys.*, **130**, 234102 (2009).

[220] Y. Tanimura and R. Kubo. Time evolution of a quantum system in contact with a nearly gaussian-markoffian noise bath. *J. Phys. Soc. of Japan*, **58**, 101 (1989).

[221] G. Tao and W. H. Miller. Semiclassical description of electronic excitation population transfer in a model photosynthetic system. *J. Phys. Chem. Lett.*, **1**, 891 (2010).

[222] E. Tapavicza, I. Tavernelli, U. Rothlisberger, C. Filippi, and M. E. Casida. Mixed time-dependent density-functional theory/classical trajectory surface hopping study of oxirane photochemistry. *J. Chem. Phys.*, **129**, 124108 (2008).

[223] D. G. Tempel and A. Aspuru-Guzik. Quantum computing without wavefunctions: Time-dependent density functional theory for universal quantum computation. *Scientific Reports (in press)* (2011).

[224] D. G. Tempel and A. Aspuru-Guzik. Relaxation and dephasing in open quantum systems time-dependent density functional theory: Properties of exact functionals from an exactly-solvable model system. *Chem. Phys.*, **391**, 130 (2011).

[225] D. G. Tempel, T. J. Martinez, and N. T. Maitra. Revisiting molecular dissociation in density functional theory: A simple model. *J. Chem. Theory and Computation*, **5**, 770 (2009).

[226] D. G. Tempel, M. A. Watson, R. Olivares-Amaya, and A. Aspuru-Guzik. Time-dependent density functional theory of open quantum systems in the linear-response regime. *J. Chem. Phys.*, **134**, 074116 (2011).

[227] D. G. Tempel, J. Yuen-Zhou, and A. Aspuru-Guzik. Open quantum systems: density matrix formalism and applications. *in* Springer Lecture Notes in Physics, page 211 (2012).

[228] I. V. Tokatly. Time-dependent current density functional theory on a lattice. *Phys. Rev. B*, **83**, 035127 (2011).

[229] J. F. Traub and A. G. Werschulz. Complexity and information. *Oxford University Press, Oxford* (1998).

[230] S. Tretiak, C. Middleton, V. Chernyak, and S. Mukamel. Bacteriochlorophyll and carotenoid excitonic couplings in the lh2 system of purple bacteria. *J. Phys. Chem. B.*, **104**, 4519 (2000).

[231] N. Troullier and J. L. Martins. Efficient pseudopotentials for plane-wave calculations. *Phys. Rev. B.*, **43**, 1993 (1991).

[232] M. E. Tuckerman. Statistical mechanics: Theory and molecular simulation. *Oxford University Press, Oxford* (2010).

[233] J. C. Tully and R. K. Preston. Trajectory surface hopping approach to nonadiabatic molecular collisions: The reaction of h+ with d2. *J. Chem. Phys.*, **55**, 562 (1971).

[234] TURBOMOLE. *V6.1 2010, a development of University of Karlsruhe and Forschungszentrum Karlsruhe GmbH, 1989-2007, TURBOMOLE GmbH, since 2007; available from: http://www.turbomole.com.*

[235] C. Uchiyama and M. Aihara. Role of initial quantum correlation in transient linear response. *Phys. Rev. A*, **82**, 044104 (2010).

[236] C. Uchiyama, M. Aihara, M. Saeki, and S. Miyashita. Master equation approach to line shape in dissipative systems. *Phys. Rev. E*, **80**, 021128 (2009).

[237] C. A. Ullrich. Semiconductor nanostructures. *Time-Dependent Density Functional Theory, eds. M .A. L. Marques, C. A. Ullrich, F. Nogueira, A. Rubio, K. Burke and E. K. U. Gross*, Springer, Berlin (2006).

[238] C. A. Ullrich. Time-dependent density-functional theory beyond the adiabatic approximation: Insights from a two-electron model system. *J. Chem. Phys.*, **125**, 234108 (2006).

[239] C. A. Ullrich. Excitation energies in time-dependent (current-) density-functional theory: A simple perspective. *J. Chem. Theory Comput.*, **5**, 859 (2009).

[240] C. A. Ullrich and G. Vignale. Theory of the linewidth of intersubband plasmons in quantum wells. *Phys. Rev. Lett.*, **87**, 037402 (2001).

[241] C. A. Ullrich and G. Vignale. Time-dependent current-density-functional theory for the linear response of weakly disordered systems. *Phys. Rev. B*, **65**, 245102 (2002).

[242] R. Valero, D. G. Truhlar, and A. W. Jasper. Adiabatic states derived from a spin-coupled diabatic transformation: Semiclassical trajectory study of photodissociation of hbr and the construction of potential curves for libr+. *J. Phys. Chem. A*, **112**, 5756 (2008).

[243] S. J. A. van Gisbergen, F. Koostra, P. R. T. Schipper, O. Gritsenko, J. Snijders, and E. J. Baerends. Density-functional-theory response-property calculations with accurate exchange-correlation potentials. *Phys. Rev. A*, **57**, 2556 (1998).

[244] N. G. van Kampen. Stochastic processes in physics and chemistry. *North-Holland, Amsterdam* (1992).

[245] E. H. van Kleef. The cartesian rank two representation of spherical tensors with an application to raman scattering. *American J. Phys.*, **63**, 626 (1995).

[246] J. M. J. van Leeuwen, J. Groeneveld, and J. de Boer. New method for the calculation of the pair correlation function. i. *Physica*, **25**, 792 (1959).

[247] R. van Leeuwen. Mapping from densities to potentials in time-dependent density-functional theory. *Phys. Rev. Lett.*, **82**, 3863 (1999).

[248] R. van Leeuwen. Key concepts in time-dependent density functional theory. *Int. J. Mod. Phys. B*, **15**, 1969 (2001).

[249] R. van Leeuwen and E. J. Baerends. Exchange-correlation potential with correct asymptotic behavior. *Phys. Rev. A*, **49**, 2421 (1994).

[250] I. Vasiliev, S. Ogut, and J. R. Chelikowsky. Ab initio excitation spectra and collective electronic response in atoms and clusters. *Phys. Rev. Lett.*, **82**, 1919 (1999).

[251] M. D. Ventra and R. D'Agosta. Stochastic time-dependent current-density-functional theory. *Phys. Rev. Lett.*, **98**, 226403 (2007).

[252] C. Verdozzi. Time-dependent density-functional theory and strongly correlated systems: Insight from numerical studies. *Phys. Rev. Lett.*, **101**, 166401 (2008).

[253] G. Vignale. Mapping from current densities to vector potentials in time-dependent current density functional theory. *Phys. Rev. B*, **70**, 201102(R) (2004).

[254] G. Vignale and W. Kohn. Current-dependent exchange-correlation potential for dynamical linear response theory. *Phys. Rev. Lett.*, **77**, 2037 (1996).

[255] G. Vignale, C. Ullrich, and S. Conti. Time-dependent density functional theory beyond the adiabatic local density approximation. *Phys. Rev. Lett.*, **79**, 4878 (1997).

[256] J. Vura-Weis, M. D. Newton, M. R. Wasielewski, and J. E. Subotnik. Characterizing the Locality of Diabatic States for Electronic Excitation Transfer By Decomposing the Diabatic Coupling . *J. Phys. Chem. C*, **114**, 20449 (2010).

[257] A. Wasserman and N. Moiseyev. Hohenberg-kohn theorem for the lowest-energy resonance of unbound systems. *Phys. Rev. Lett.*, **98**, 093003 (2007).

[258] M. A. Watson and H. Kimihiko. A linear-scaling spectral-element method for computing electrostatic potentials. *J. Chem. Phys.*, **129**, 184107 (2008).

[259] T. C. Wei, M. Mosca, and A. Nayak. Interacting boson problems can be qma hard. *Phys. Rev. Lett.*, **104**, 1 (2010).

[260] F. Weigend. Accurate coulomb-fitting basis sets for h to rn. *Phys. Chem. Chem. Phys.*, **8**, 1057 (2006).

[261] A. G. Werschulz. Average case complexity of elliptic partial differential equations. *J. Complexity*, **5**, 306 (1989).

[262] A. G. Werschulz. The computational complexity of differential and integral equations: An information-based approach. *Oxford University Press, New York* (1991).

[263] A. G. Werschulz. The complexity of multivariate elliptic problems with analytic data. *J. Complexity*, **11**, 154 (1995).

[264] S. R. White and A. E. Feiguin. Real-time evolution using the density matrix renormalization group. *Phys. Rev. Lett.*, **93**, 076401 (2004).

[265] H. O. Wijewardane and C. A. Ullich. Time-dependent kohn-sham theory with memory. *Phys. Rev. Lett.*, **95**, 086401 (2005).

[266] A. K. Wilson, T. V. Mourik, and T. Dunning. Gaussian basis sets for use in correlated molecular calculations. vi. sextuple zeta correlation consistent basis sets for boron through neon. *J. Mol. Struct. (THEOCHEM)*, **388**, 339 (1996).

[267] D. E. Woon and T. H. Dunning. Gaussian basis sets for use in correlated molecular calculations. iv. calculation of static electrical response properties. *J. Chem. Phys.*, **100**, 2975 (1994).

[268] W. K. Wooters. Entanglement of formation of an arbitrary state of two qubits. *Phys. Rev. Lett.*, **80**, 2245 (1998).

[269] W. K. Wootters. Entanglement of formation and concurrence. *Quant. Information and Computation*, **1**, 27 (2001).

[270] L. A. Wu, M. S. Sarandy, D. A. Lidar, and L. J. Sham. Linking entanglement and quantum phase transitions via density-functional theory. *Phys. Rev. A*, **74**, 052335 (2006).

[271] I. Yamazaki, S. Akimoto, T. Yamazaki, S. Sato, and Y. Sakata. Oscillatory Excitation Transfer in Dithiaanthracenophane: Quantum Beat in a Coherent Photochemical Process in Solution. *J. Phys. Chem. A*, **106**, 2122 (2002).

[272] I. Yamazaki, N. Aratani, S. Akimoto, T. Yamazaki, and A. Osuka. Observation of quantum coherence for recurrence motion of exciton in anthracene dimers in solution. *JACS*, **125**, 7192 (2003).

[273] Y. Yan and R. Xu. Quantum mechanics of dissipative systems. *Annu. Rev. Phys. Chem.*, **56**, 187 (2005).

[274] L. Yang, S. Caprasecca, B. Mennucci, and S. Jang. Theoretical Investigation of the Mechanism and Dynamics of Intramolecular Coherent Resonance Energy Transfer in Soft Molecules: A Case Study of Dithia-anthracenophane. *J. Am. Chem. Soc.*, **132**, 16911 (2010).

[275] W. Yang. Thermal proyerties of many-electron systems: An integral formulation of density-functional theory. *Phys. Rev. A*, **38**, 5504 (1988).

[276] D. L. Yeager, M. A. C. Nascimento, and V. McKoy. Some applications of excited-state-excited-state transition densities. *Phys. Rev. A*, **11**, 1168 (1975).

[277] J. Yuen-Zhou, C. Rodríguez-Rosario, and A. Aspuru-Guzik. Time-dependent current-density functional theory for generalized open quantum systems. *Phys. Chem. Chem. Phys.*, **11**, 4509 (2009).

[278] J. Yuen-Zhou, D. G. Tempel, C. Rodríguez-Rosario, and A. Aspuru-Guzik. Time-dependent density functional theory for open quantum systems with unitary propagation. *Phys. Rev. Lett.*, **104**, 043001 (2010).

[279] M.-H. Yung, J. D. Whitfield, S. Boixo, D. G. Tempel, and A. Aspuru-Guzik. Introduction to quantum algorithms for physics and chemistry. *Annual Review of Physical Chemistry (in press)* (2012).

[280] A. Zangwill and P. Soven. Density-functional approach to local-field effects in finite systems: Photoabsorption in the rare gases. *Phys. Rev. A*, **21**, 1561 (1980).

[281] A. Zangwill and P. Soven. Resonant two-electron excitation in copper. *Phys. Rev. B*, **24**, 4121 (1981).

[282] R. Zare. *Angular Momentum*. Wiley-Interscience, 1988.

[283] X. Zheng, G. Chen, Y. Mo, S. Koo, H. Tian, C. Yam, and Y. Yan. Time-dependent density functional theory for quantum transport. *J. Chem. Phys.*, **133**, 114101 (2010).

[284] X. Zheng, F. Wang, C. Yam, Y. Mo, and G. Chen. Time-dependent density-functional theory for open systems. *Phys. Rev. B*, **75**, 195127 (2007).

[285] F. Zhu, C. Galli, and R. Hochstrasser. The realtime intramolecular electronic excitation transfer dynamics of 9 [script'], 9bifluorene and 2 [script'], 2binaphthyl in solution. *J. Chem. Phys.*, **98**, 1043 (1993).

[286] J. Zhu, S. Kais, P. Rebentrost, and A. Aspuru-Guzik. Modified scaled hierarchical equation of motion approach for the study of quantum coherence in photosynthetic complexes. *J. Phys. Chem. B*, **115**, 1531 (2011).

[287] S. Zilberg, Y. Haas, and S. Shaik. Electronic spectrum of anthracene: An ab-initio molecular orbital calculation combined with a valence bond interpretation. *J. Phys. Chem.*, **99**, 16558 (1995).

[288] R. Zwanzig. Ensemble method in the theory of irreversibility. *J. Chem. Phys.*, **33**, 1338 (1960).

[289] R. Zwanzig. Nonequilibrium statistical mechanics. *Oxford University Press, Oxford* (2001).